1972

An exact analysis of two-dimensional radiative transfer in an absorbing and emitting gray medium

William F. Breig

AN EXACT ANALYSIS OF TWO-DIMENSIONAL RADIATIVE TRANSFER IN AN ABSORBING AND EMITTING GRAY MEDIUM

by

WILLIAM FRANCIS BREIG, 1940-

A DISSERTATION

Presented to the Faculty of the Graduate School of the

UNIVERSITY OF MISSOURI-ROLLA

In Partial Fulfillment of the Requirements for the Degree

DOCTOR OF PHILOSOPHY

in

MECHANICAL ENGINEERING

1972

A. L. Crosbie
Advisor

T. S. Chen

L. Pagano

Robert L. Davis

J. R. Barnett

Jerry F. Lehnhoff

ABSTRACT

The exact formulations for the radiative flux and the emissive power are presented for a two-dimensional, finite, planar, absorbing and emitting, gray medium in radiative equilibrium. Exact expressions are obtained for the medium subjected to the following types of boundary conditions: (1) cosine varying diffuse, (2) cosine varying collimated, (3) constant temperature strip, and (4) the strip illuminated by a uniform collimated flux. The solutions for the physically unrealistic cosine varying models are used to construct the solutions for the more practical finite strip models. The two-dimensional equations are reduced to one-dimensional equations by the method of separation of variables. This simplification is made possible by the cosine form of the boundary radiation. The corresponding equations for the semi-infinite medium are obtained from the equations for the finite optical thick medium by letting the optical thickness become infinite. The reduced one-dimensional equations are then solved exactly by techniques from one-dimensional radiative theory for the emissive power and radiative flux at the boundaries for both the finite and semi-infinite models. A wide range of exact numerical data is presented.

The cosine varying collimated boundary condition generates functions which are analogous to the one-dimensional X- and Y-functions of Chandrasekhar for the finite model and the H-function of Chandrasekhar for the semi-infinite model. These generalized functions represent the dimensionless emissive power at the boundaries

and appear in the radiative flux and emissive power at the boundaries for the cosine varying diffuse model as well as for both finite strip models. The generalized H-, X- and Y-functions are tabulated exactly for a wide range of numerical values.

In addition to the generalized H-, X- and Y-functions, a function analogous to the exponential integral function is introduced. Generalized exponential integral functions of the first, second, and third order are defined and the recurrence formulas and series expansions are developed. The generalized exponential integral functions are tabulated for a wide range of numerical values.

ACKNOWLEDGEMENT

The author is grateful to Dr. A. L. Crosbie for the suggestion of the topic and guidance throughout the course of this thesis. Special thanks are also due to Dr. T. S. Chen for his helpful assistance.

Financial support from the Mechanical Engineering and the Engineering Mechanics Departments is also appreciated.

TABLE OF CONTENTS

Table of Contents (continued) Page

Table of Contents (continued) Page

LIST OF ILLUSTRATIONS

List of Illustrations (continued)

List of Illustrations (continued)

List of Illustrations (continued)

List of Illustrations (continued)

Figure Page

LIST OF TABLES

List of Tables (continued)

List of Tables (continued)

List of Tables (continued)

List of Tables (continued)

List of Tables (continued)

LIST OF SYMBOLS

a = Half strip width

B = Dimensionless emissive power for a semi-infinite medium bounded by a uniform collimated strip

B_β = Dimensionless emissive power for a semi-infinite medium illuminated by a collimated flux of cosine magnitude

E_n = Exponential integral function of the n-th order

$\mathcal{E}_n$ = Generalized exponential integral function of the n-th order

F = Dimensionless component of radiative flux in the z-direction for a semi-infinite medium bounded by a constant temperature strip

F_o = Amplitude of the incident collimated radiation

F_β = Dimensionless component of radiative flux in the z-direction for a semi-infinite medium bounded by a diffuse wall radiating in a cosine fashion

f = Dimensionless emissive power for a finite medium bounded by a diffuse wall radiating in a cosine fashion

$\mathcal{F}_A$ = Dimensionless component of radiative flux in the z-direction for a finite medium illuminated by a collimated flux of cosine magnitude

$\overline{\mathcal{F}}_A$ = Dimensionless component of radiative flux in the z-direction for a finite medium illuminated by a collimated flux of cosine magnitude

$\mathcal{F}_C$ = Dimensionless component of radiative flux in the z-direction for a finite medium bounded by a diffuse wall radiating in a cosine fashion

H = Generalized H-function, equation (4.21)

h_n = Moment of the generalized H-function

I = Local intensity

I^+ = Intensity directed in the direction of increasing τ_z

I_o^+ = Boundary condition for intensity at $\tau_z=0$

I^- = Intensity directed in the direction of decreasing τ_z

List of Symbols (continued)

I_o^- = Boundary condition for intensity at $\tau_z=\tau_o$

J = Dimensionless emissive power for a finite medium bounded by a uniform collimated strip

J_β = Dimensionless emissive power for a finite medium illuminated by a collimated flux of cosine magnitude

K_o = Modified Bessel function

L = Thickness of the medium

P = Generalized P-function

Q = Dimensionless component of radiative flux in the z-direction for a semi-infinite medium bounded by a uniform collimated strip

Q_β = Dimensionless component of radiative flux in the z-direction for a semi-infinite medium illuminated by a collimated flux of cosine magnitude

$\bar{Q}_\beta$ = Dimensionless component of radiative flux in the z-direction for a semi-infinite medium illuminated by a collimated flux of cosine magnitude

q_{zA} = Component of radiative flux in the z-direction for a finite medium illuminated by a collimated flux of cosine magnitude

$\bar{q}_{zA}$ = Dimensionless component of radiative flux in the z-direction for a finite medium illuminated by a collimated flux of cosine magnitude

q_{yA} = Component of radiative flux in the y-direction for a finite medium illuminated by a collimated flux of cosine magnitude

q_{zB} = Component of radiative flux in the z-direction for a finite medium bounded by a uniform collimated strip

q_{zC} = Component of radiative flux in the z-direction for a finite medium bounded by a diffuse wall radiating in a cosine fashion

$\bar{q}_{zC}$ = Dimensionless component of radiative flux in the z-direction for a finite medium bounded by a diffuse wall radiating in a cosine fashion

q_{yC} = Component of radiative flux in the y-direction for a finite medium bounded by a diffuse wall radiating in a cosine fashion

List of Symbols (continued)

$\bar{q}_{yC}$ = Dimensionless component of radiative flux in the y-direction for a finite medium bounded by a diffuse wall radiating in a cosine fashion

q_{zD} = Component of radiative flux in the z-direction for a finite medium bounded by a constant temperature strip

R_β = Generalized reflection function

S_β = Generalized transmission function

s = Distance along line of sight in the medium

T = Local temperature

T_A = Local temperature for a finite medium illuminated by a collimated flux of cosine magnitude

T_B = Local temperature for a finite medium bounded by a uniform collimated strip

T_C = Local temperature for a finite medium bounded by a diffuse wall radiating in a cosine fashion

T_D = Local temperature for a finite medium bounded by a constant temperature strip

T_o = Temperature of the medium

T_1 = Temperature of the boundary at $\tau_z=\tau_o$

T_2 = Temperature of the boundary at $\tau_z=0$

X = Generalized X-function, equation (5.25)

x,y,z = Cartesian coordinates

x_n = Moment of generalized X-function, equation (5.49)

Y = Generalized Y-function, equation (5.26)

y_n = Moment of generalized Y-function, equation (5.50)

α_n = Moment of generalized X-function, equation (5.46)

β_n = Moment of generalized Y-function, equation (5.47)

β = Spacial frequency of the incident radiation

List of Symbols (continued)

δ = Dirac delta function

θ = Polar angle

θ_o = Polar angle for the incident collimated radiation

θ_1 = Dimensionless temperature, T_1/T_o

θ_2 = Dimensionless temperature, T_2/T_o

$\theta_x, \theta_y, \theta_z$ = Directional cosines

κ = Absorption coefficient

σ = Secant of the polar angle for the incident radiation

$\overline{\sigma}$ = Stefan-Boltzmann constant

τ_s = Optical thickness, κs

τ_o = Optical thickness of the medium, κL

τ_a = Optical half strip width, κa

τ_x, τ_y, τ_z = Optical coordinates

ϕ = Azimuthal angle

ϕ_o = Azimuthal angle for the incident collimated radiation

ϕ = Dimensionless emissive power for a finite medium bounded by a constant temperature strip

ϕ_β = Dimensionless emissive power for a finite medium bounded by a diffuse wall radiating in a cosine fashion

$\overline{\phi}$ = Dimensionless emissive power for a semi-infinite medium bounded by a constant temperature strip

$\overline{\phi}_\beta$ = Dimensionless emissive power for a semi-infinite medium bounded by a diffuse wall radiating in a cosine fashion

ω = Solid angle

I. INTRODUCTION

The one-dimensional model for radiative heat transfer through a participating medium has been extensively analyzed. In fact, the major portion of the current literature involving radiative heat transfer is concerned with the one-dimensional analysis. This is due to the mathematical simplification and certainly not because the one-dimensional model yields the best physical description. The one-dimensional analysis permits a rigorous mathematical solution as well as gives a first approximation to many two-dimensional problems. However, recent advances in high temperature technology in the areas of gas dynamics, fluid mechanics, and energy exchange between surfaces, indicate that much more precision is needed in calculating heat flux and temperature. The calculation of two-dimensional radiative transfer is also required in many atmospheric problems. Of principal importance in the areas of weather forecasting and meteorology is the calculation of the net radiant energy exchange between the earth and the atmosphere. Typical problems include the prediction of frost and fog, evaporation and melting of snow, and the formation and transport of air masses.

The present investigation is concerned with two-dimensional radiative transfer in a participating medium. The radiative flux and temperature thus depend upon two space variables with the flux having a component in each direction. The integral equation describing the temperature is very complicated and difficult to solve. For this reason, the limited two-dimensional development which appears in the literature is either highly analytical or approximate in nature. The analytical studies have provided only limited numerical results, and

the validity of the approximate analyses is yet unknown. The present analysis offers an exact analytical formulation of a two-dimensional model with a wide range of numerical data which can be utilized to verify the one-dimensional assumption and the validity of various two-dimensional approximate solutions.

The mathematical analysis encountered in solving for temperature and heat flux in a two-dimensional medium in which conduction, convection, and radiation occur simultaneously is very complicated due to the interaction of the various modes of heat transfer. If any one mode can be considered to be negligible, the mathematics is considerably simplified. For this reason, the present investigation is concerned with two-dimensional gray absorbing and emitting media in which energy transport is solely by radiation. A medium under these conditions is said to be in radiative equilibrium and the formulation of the problem reduces to the solution of an integral equation for the temperature distribution.

The two-dimensional radiative equilibrium model can be used as a standard of comparison whereby the results of the one-dimensional radiative equilibrium model can be verified or rejected. A confidence interval for the parameters involved can then be obtained within which the one-dimensional radiative equilibrium assumption can be utilized. Such an error bound is very desirable because of the abundance of practical problems appearing in the current literature which are solved by the one-dimensional radiative equilibrium assumption. The radiative equilibrium model can also be used to construct approximate solutions to more complex models that involve combined modes of heat

transfer. This approximation can be accomplished by regarding the total heat flux to be evaluated through superposition of the separate contributions. Thus, if radiation and conduction occur simultaneously, the radiative heat transfer can be calculated as if the conductive mode is not present and then added to the heat transfer due to the conduction. This procedure has been successful in the one-dimensional case, and would provide useful knowledge of the heat transfer process if they could be extended to cover two-dimensional models.

Exact two-dimensional solutions are presented for the radiative flux and the emissive power for both the finite and semi-infinite media subjected to cosine varying collimated and cosine varying diffuse boundary conditions. The solutions for the radiative flux and emissive power due to the cosine varying boundary conditions are then used to obtain the radiative flux and emissive power due to more realistic boundary conditions. In particular, the emissive power and radiative flux for the constant temperature strip and the strip illuminated by a uniform collimated flux are expressed in terms of the solutions for the cosine varying diffuse boundary and cosine varying collimated boundary, respectively. A wide range of exact numerical solutions are presented for the emissive power and radiative flux at the boundaries.

In addition to being suitable for constructing solutions to problems involving more complex types of boundary conditions, the cosine varying boundary conditions are important since this form enables the two-dimensional equations to be reduced to one-dimensional equations. Hence, the methods of solution which have been successfully applied to the one-dimensional theory can be utilized to solve the reduced

one-dimensional equations. In fact, the cosine varying collimated boundary condition generates functions which are analogous to the one-dimensional X- and Y-functions of Chandrasekhar [1,p.183] for the finite medium and the H-function of Chandrasekhar [1,p.105] for the semi-infinite medium. These generalized functions represent the dimensionless emissive power at the boundaries and are shown to appear in the solutions for the emissive power and flux at the boundaries for the cosine varying diffuse boundary condition and both finite strip models. For this reason, a wide range of numerical data is tabulated for the generalized functions.

Chapter II of this investigation reports the current status of multidimensional radiative transfer and the analogous problem of neutron transport. The formulation of the basic equations for emissive power and radiative flux appears in Chapter III. Chapter IV is devoted to the emissive power and radiative flux at the boundary of a semi-infinite medium. Chapter V is concerned with the finite medium and is followed by concluding remarks and suggested future extensions of the present work.

II. REVIEW OF LITERATURE

INTRODUCTION

The development of the theory of radiant energy transfer in a participating medium has centered around one-dimensional plane geometries due to the complications involved in solving the transport equations. In general, the radiation intensity is a function of position, direction, time, and frequency. The solution to such a general problem is very complicated. The presence of the source function in the transport equation is a contributing factor to the mathematical difficulties encountered in a solution.

For a scattering medium, the source function is an integral over the intensity, making the transport equation an integro-differential equation. If the medium absorbs and emitts radiation and is in local thermodynamic equilibrium, the source function becomes Planck's function which introduces the unknown temperature into the transport equation. Hence, the transport equation is a coupled equation in intensity and temperature. When the participating media emitts, absorbs, and scatters, the transport equation assumes its most complicated form. Various simplifying assumptions are then necessary in order to obtain a solution to the transport equation. The dependence upon the frequency can be eliminated by the gray medium approximation. This approximation means that the absorption coefficient is assumed independent of frequency. The transport equation can then be integrated over all frequency and the spectral quantities replaced by the total integrated quantities. A further mathematical simplification follows if the intensity is considered to be time independent. Most of the papers cited in this review are time independent unless specifically indicated.

In addition to the transport equation, the equation which governs the conservation of energy in the system must be satisfied. For a general conductive, convective, and radiative participating medium, the energy equation relates the temperature to the radiative flux in a very complicated manner. Since the radiative flux is an integral over solid angle of the intensity of radiation, the transport equation and the energy equation are coupled equations. However, neglecting the conductive and convective modes of heat transfer reduces the energy equation to a form which, when solved simultaneously with the transport equation, yields an integral equation for the temperature distribution.

The number of space variables considered in a model contributes significantly to the degree of the mathematical complexity. A large part of the current literature is concerned with the one-dimensional model. This assumption limits the temperature distribution to vary in a single space variable as opposed to two space variables required for the two-dimensional model. Since the one-dimensional model is less difficult to solve, it has found application in the areas of astrophysics and engineering. The astrophysical development can be found in the works of Eddington [2], Rosseland [3], and more recently those of Chandrasekhar [1], Kourganoff [4], and Sobolev [5]. Engineering oriented applications can be found in Love [6], and also Sparrow and Cess [7].

Since the one-dimensional model is a first approximation, a more refined knowledge of the heat transfer process can be obtained from the two-dimensional model. This natural extension has been found necessary due to the requirement for more precise calculations. The

following is a summary of associated works in multidimensional analysis and the order of presentation is according to the type of participating media. The analogous problem of neutron transport is presented last.

ABSORBING AND EMITTING MEDIA

The first attempt to solve multidimensional radiative transfer problems in nonscattering media was done by assuming the gas to be optically thick, thereby permitting the radiation to be thought of as a diffusion process. The problem reduces to solving a modified heat conduction equation. This approach is known as the Rosseland approximation which was first introduced by Rosseland [3]. The Rosseland approximation yields favorable results when applied at locations interior to the optical thick medium. However it fails in the near vicinity of boundaries.

Another approximate method, the differential approximation which replaces the general expression for the radiative flux by a differential equation, has also been used for multidimensional analysis. Cheng [8,9] used the spherical-harmonic approximation to study a two-dimensional radiating, flowing gas. Khosla [10] also applied the differential approximation to a two-dimensional high speed gas dynamics problem. Glicksman [11] developed an approximate method similar to the differential approximation which is referred to as the method of flux summing. Taitel [12] also developed an approximate formulation for the radiative flux for a finite two-dimensional medium bounded by nonisothermal walls. Taitel's formulation is shown to approach the exact solution in the optically thin limit. Lunardini and Chang [13]

used the differential approximation to study the effect of heat conduction.

The only exact integral formulations of radiative transfer in an absorbing and emitting two-dimensional medium were presented by Olfe [14] and Cheng [15]. Olfe considered a semi-infinite medium with a nonuniform wall temperature which varied in a sinusoidal fashion and presented two-dimensional integral expressions for temperature and flux without derivation. The sinusoidal form of the boundary radiation enabled the two-dimensional integral equation for the emissive power to be reduced to a one-dimensional integral equation. This equation was solved numerically by iteration, and graphical results for the emissive power at the boundary were presented. However, numerical solutions were difficult to obtain and the emphasis of this work was on various schemes for an approximate solution, specifically the modified differential approximation.

Cheng [15], unlike Olfe, considered the temperature of the medium to be a known quantity. He formulated exact equations for the radiative flux and intensity for the two-dimensional medium bounded by two parallel walls with arbitrary discontinuous wall radiation over a finite portion of each wall in terms of the assumed temperature of the medium. The principle of superposition was employed to obtain expressions for the radiative flux and intensity for the two-dimensional rectangular medium bounded by four finite discontinuous radiating walls. A similar set of equations were developed by using the differential approximation. A graphical comparison between the exact solution and the differential approximation solution was presented for the case of an isothermal medium and continuous isothermal walls.

SCATTERING MEDIA

The searchlight problem occurs when a narrow pencil of radiation (such as a searchlight beam) is incident on an absorbing and scattering medium. Chandrasekhar [16] considered the searchlight problem for an isotropic scattering semi-infinite medium and obtained with invariance principles a nonlinear integro-differential equation in five variables for the scattering function. This equation was not solved. Bellman, Kalaba, and Ueno [17] treated the searchlight problem for the two-dimensional isotropically scattering finite medium. The integro-differential equation which governs the scattering function was presented with the aid of invariant imbedding techniques. No solutions were provided for the equation. The more general case of a transient searchlight problem was treated by Bellman, Kalaba, and Ueno [18]. The formulation was entirely analytical with no solutions provided. Rybicki [19] formulated the searchlight problem for both finite and semi-infinite media in terms of an integral equation for the source function. Limited results for the source function at the boundary of a semi-infinite medium were calculated by means of the kernel approximation method.

Smith [20] considered the theoretical development for the source function of a two-dimensional, finite thick, isotropically scattering medium illuminated by a collimated flux of cosine magnitude. An integral equation was presented for the source function. The corresponding two-dimensional integral equation for the source function of the semi-infinite medium was reduced to a one-dimensional integral equation in a fashion similar to that of Olfe [14]. The solution to

the reduced one-dimensional equation was then used to construct a solution for the finite strip illuminated by a constant collimated normal flux. The source function for the finite strip problem was expressed in terms of a cosine series the coefficients of which were difficult to obtain. Both of these problems were analytical with no numerical solutions presented.

Smith and Hunt [21] considered a flat beam of constant magnitude incident normally on an isotropically scattering semi-infinite medium of finite width. A Fourier cosine series was obtained for the source function with the use of complex contour integration. The coefficients of the series were very complicated and not easily obtained. Hunt [22] developed the integral equation for the source function for an axially symmetric, isotropically scattering medium illuminated by an incident beam of radiation that varied in the radial direction as the zeroth order Bessel function of the first kind. The source function was approximated by a Fourier cosine series. However, the coefficients were not evaluated. Hunt [23] considered a finite, three-dimensional, isotropically scattering medium illuminated by a beam of radiation obliquely incident on the boundary. The kernel of the integral equation for the source function was expressed in terms of a singular integral equation by utilizing the Green's function. The resulting integral equation for the kernel was not solved.

Only one work is available which treats multidimensional anisotropic scattering of radiation. Hunt [24] considered a finite, three-dimensional slab with anisotropic scattering and used the first three terms in a series of Legendre polynomials for the scattering function.

The boundary radiation was in the form of a general two-dimensional collimated flux incident normally. The intensity of radiation was divided into eight components each of which acted over a separate region of the medium. A complicated set of integral equations was developed which involved each of the components of intensity. No solution to this complex system of equations was proposed.

ABSORBING, EMITTING, AND SCATTERING MEDIA

Bobco [25] developed a closed form approximate solution for the directional emissivity of a finite thick, two-dimensional slab. Solutions were obtained by an approximation based on an iteration of the diffusion solution. Love and Turner [26] used Monte Carlo techniques to solve the same problem and found a close agreement with Bobco's results. Both of these methods are approximate, with the Monte Carlo technique being less practical due to the excessive amount of computer time required.

NEUTRON TRANSPORT

A field of study closely associated with the radiative transfer is neutron transport. Since the transport equations for neutrons and photons have the same mathematical form, methods applied to multidimensional neutron transport can be used in radiative transfer. Thus, a review of two-dimensional neutron transport literature is appropriate.

Elliott [27] considered an isotropically scattering half space and used the Wiener-Hopf technique to obtain a complicated triple integral expression for neutron density due to a point source on the boundary. An approximate solution was presented which was valid for large distances away from the source. Erdmann [28] considered a flux due to a

point source of neutrons in a two-dimensional, semi-infinite medium and solved the transport equation by the Wiener-Hopf technique. The solution for neutron density was left in integral form and not solved.

Williams [29] considered the three-dimensional medium inside a finite rectangular prism and reduced the three-dimensional transport equation to a one-dimensional form. This reduction was accomplished by approximating two of the space variables and treating the remaining one exactly. The Wiener-Hopf technique was applied to the reduced one-dimensional form.

Williams [30] investigated the diffusion of neutrons from a plane source in an infinite slab with the source plane perpendicular to the faces of the slab. An integral equation approach was utilized to formulate the transfer problem with solution by means of Fourier transforms. Fourier inversion by complex contour integration was used to obtain an integral solution for neutron density. Williams [31] also extended the neutron diffusion analysis to an infinite cylinder with source plane perpendicular to the axis of the cylinder. Fourier transform techniques were used to formulate the equation for neutron density, but the equation was not solved.

Kaper [32] reduced the three-dimensional transport equation to an equation of one-dimensional form by treating one of the space variables exactly and approximating the other two. The reduced transport equation was then solved for neutron density in integral form by Fourier inversion techniques. The integral solution was not solved.

Sotoodehnia and Erdmann [33] treated two-dimensional infinite and semi-infinite isotropically scattering media with a line source of

neutrons. The two-dimensional transport equation was reduced to a single dimension by Fourier transform and variable changes. The complicated integrals were not evaluated.

Garrettson and Leonard [34] treated multidimensional neutron transport in an isotropically scattering medium with point, line, or plane sources. The three-dimensional transport equation was reduced to a one-dimensional integral equation with difference kernel by using Fourier and Laplace transforms. Integral solutions were obtained by use of Green's function technique. No numerical results were obtained.

SUMMARY

In comparison to the one-dimensional model, there is a definite lack of two-dimensional analysis in the current literature. This was especially noted for the nongray assumption for which no reference was found. Most of the investigations reported deal with scattering or neutron transport with only two completely rigorous discussions pertaining to an absorbing and emitting medium. Virtually no results were found to verify the usefulness of the highly analytical formulations or the accuracy of the various approximate techniques. All investigations assume the medium to be gray, and none of the investigators attempted to determine the validity of the one-dimensional model.

The present investigation attempts to eliminate some of the above limitations by (1) considering an exact development for the two-dimensional absorbing and emitting gray medium, and (2) supplying numerical data for the radiative flux and the emissive power for a wide range of the parameters τ_o, β, and σ which correspond to the optical thickness, the spacial frequency of the incident radiation, and the angle of the incident collimated radiation, respectively.

III. PHYSICAL MODEL AND GOVERNING EQUATIONS

A. ASSUMPTIONS

The coordinate system and geometry used in calculating radiative heat transfer through a two-dimensional participating medium are shown in Figure 3.1. Both finite and semi-infinite media are considered. The present investigation is based on the following assumptions:

1. two-dimensional transfer
2. steady state temperature and intensity
3. absorbing and emitting, but non-scattering medium
4. gray medium
5. local thermodynamic equilibrium
6. no conduction or convection; no heat generation
7. refractive index of unity

The radiation incident on the boundaries of the medium is either collimated or diffuse. The collimated boundary condition means that radiation is incident upon the boundary from a single direction. This kind of boundary condition is often used to simulate solar energy striking a planetary atmosphere or an air-sea interface. The diffuse boundary condition occurs when the radiation incident on the boundary is independent of direction. This kind of boundary condition is often used to simulate the radiation incident on the sea from the atmosphere. The diffuse boundary condition has many engineering applications since it approximates the radiation leaving an opaque surface.

The present investigation is concerned with two-dimensional radiative transfer produced by spacially varying incident radiation. Figures 3.2 and 3.3 exhibit the physical models for the cosine

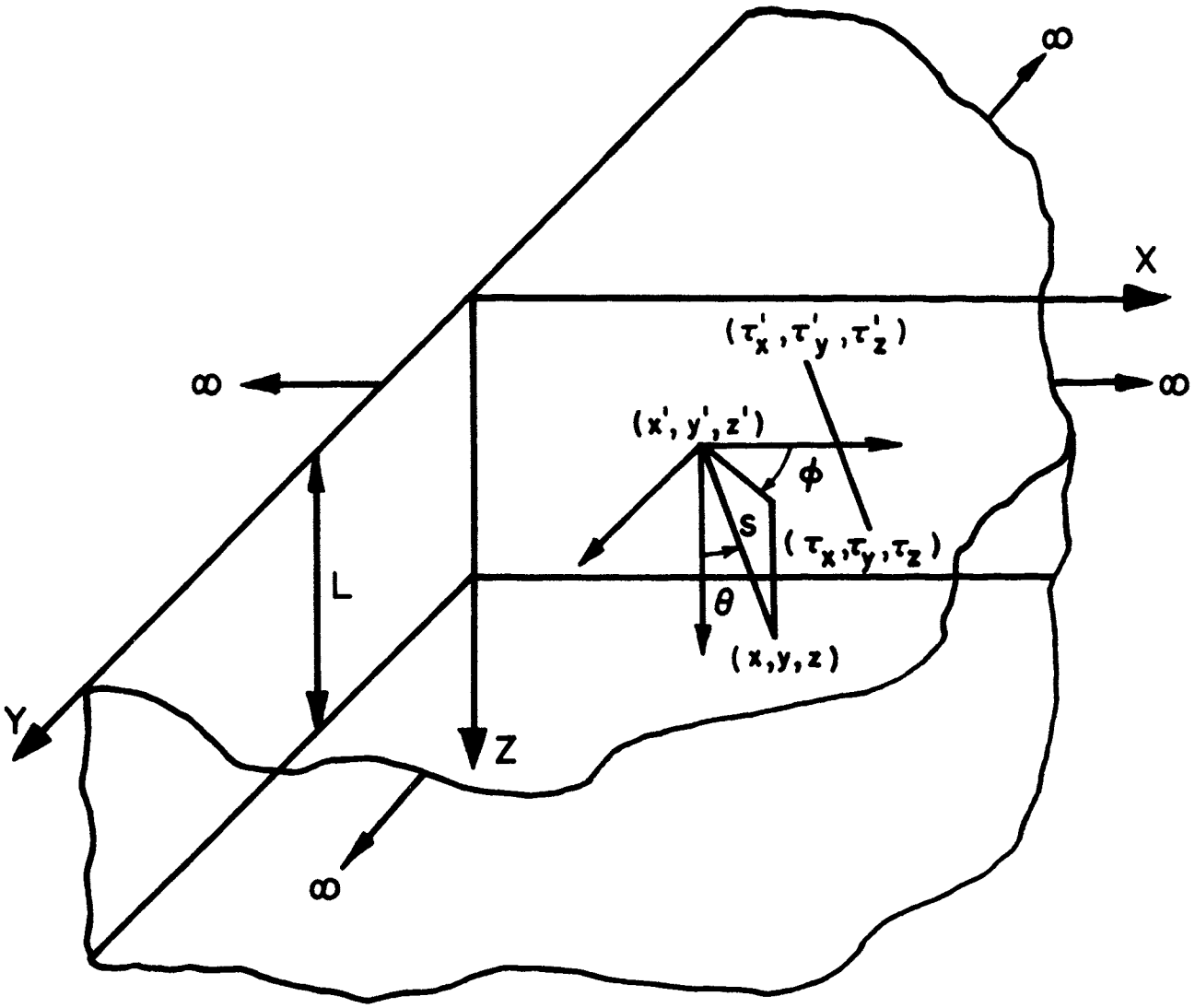

Figure 3.1 Coordinate system

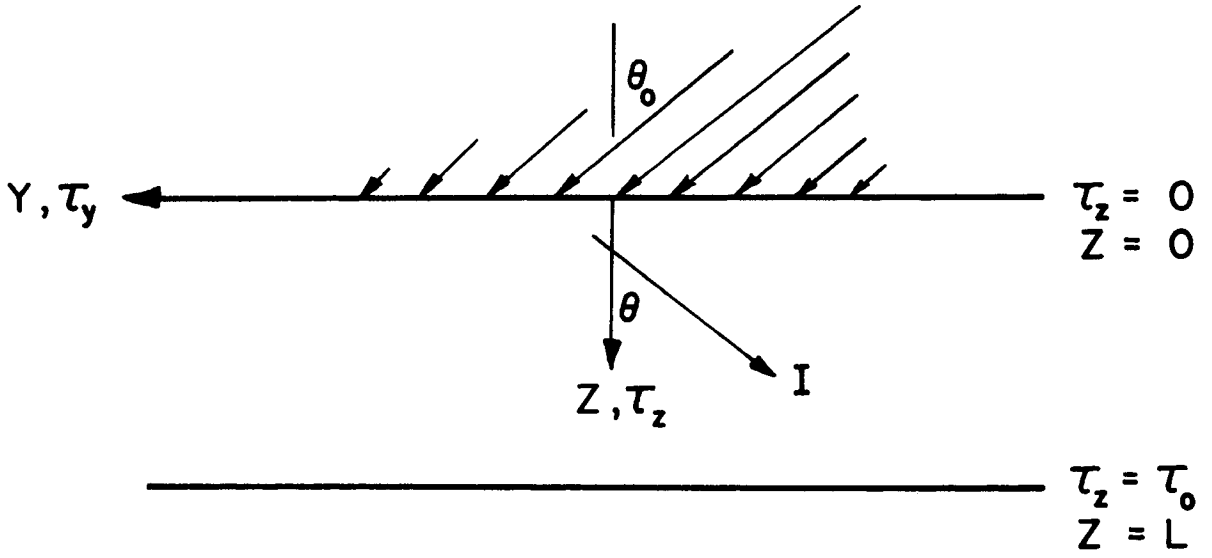

Figure 3.2 Cosine varying collimated model

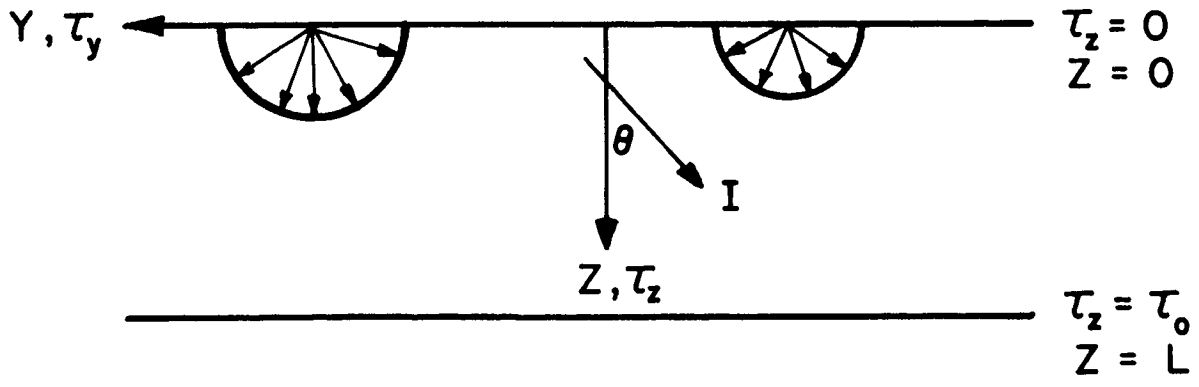

Figure 3.3 Cosine varying diffuse model

collimated and diffuse boundary conditions, respectively. The cosine boundary conditions are not physically realistic. Their usefulness lies in the fact that the solution to other more realistic problems can be expressed in terms of the cosine solutions. This is the case when the incident radiation is uniform over a finite portion of the boundary. Physical models for the finite strip boundary conditions are shown in Figures 3.4 and 3.5 for the strip illuminated by a uniform collimated flux and the constant temperature strip, respectively. Since the boundary radiation is uniform over the entire strip but different from that outside the strip, the finite strip models are two-dimensional. When the strip width becomes infinite, the finite strip models approach the one-dimensional models.

Figure 3.6 outlines the various solutions which are expressed in terms of solutions to other boundary conditions. The notation A→B indicates that A is expressed in terms of B. Figure 3.6 reveals that the cosine varying collimated solution is fundamental to that of the cosine varying diffuse as well as the finite strip solutions. Table 3.1 lists the notation employed throughout this investigation.

B. FUNDAMENTAL EQUATION FOR EMISSIVE POWER

The fundamental equation which governs the transport of radiant energy through a medium which satisfies the assumptions previously listed can be written as [1,pp.8,9]

$$\frac{dI}{ds} + \kappa I = \kappa \frac{\overline{\sigma}}{\pi} T^4 \tag{3.1}$$

where the operator $\frac{d}{ds}$ is defined as

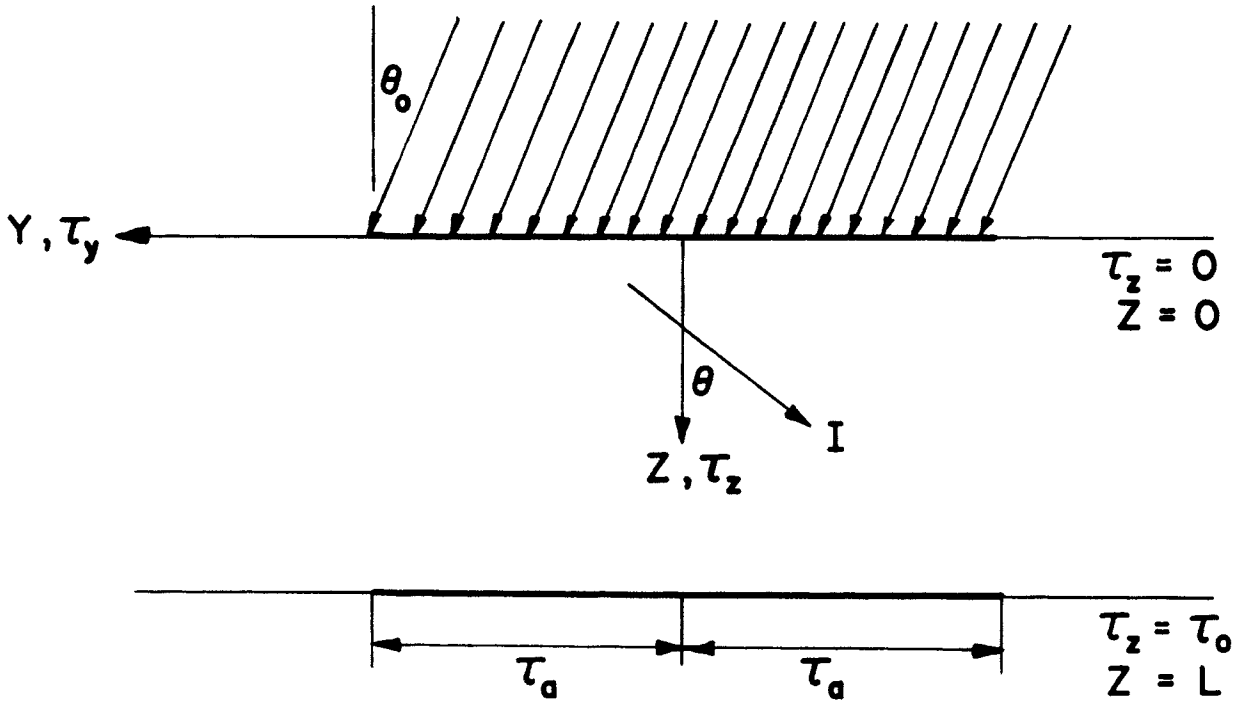

Figure 3.4 Uniform collimated strip model

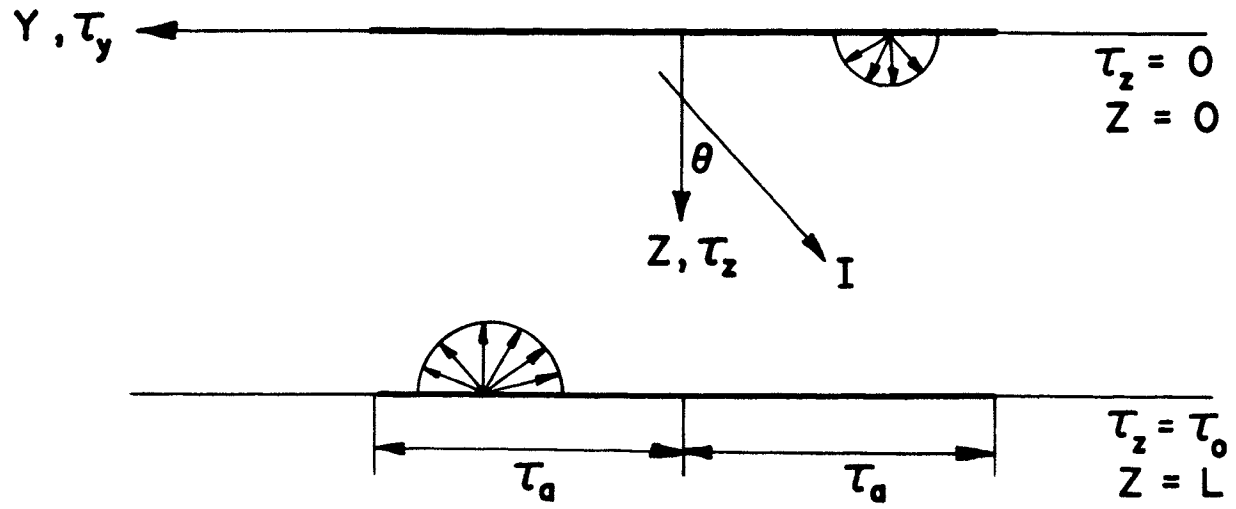

Figure 3.5 Constant temperature strip model

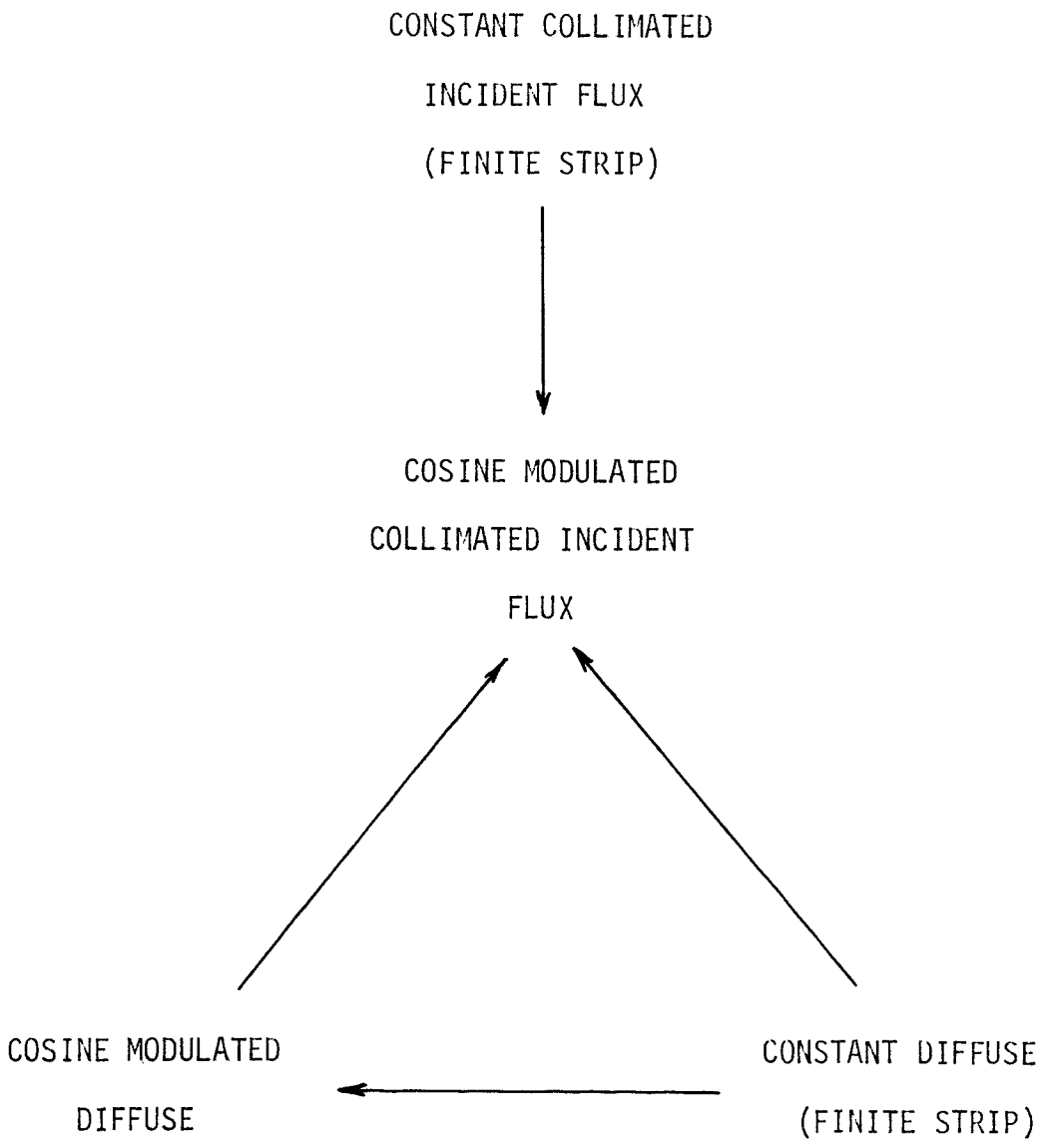

Figure 3.6 Schematic relationship for the emissive power and flux due to collimated and diffuse boundary conditions

Table 3.1 Notation used in calculating flux and emissive power

Type of External Radiation	FINITE MEDIA					SEMI-INFINITE MEDIA	
	Notation	Temperature	Dimensionless Emissive Power	Flux	Dimensionless Flux	Dimensionless Emissive Power	Dimensionless Flux
Variable Collimated	A	T_A	J_β	q_{zA}	$\bar{q}_{zA}, \bar{q}_{yA}, \mathcal{F}_A, \bar{\mathcal{F}}_A$	B_β	$Q_\beta, \bar{Q}_\beta$
Collimated Strip	B	T_B	J	q_{zB}	$\bar{q}_{zB}, \bar{q}_{yB}, \mathcal{F}_B$	B	Q
Variable Diffuse	C	T_C	ϕ_β	q_{zC}	$\bar{q}_{zC}, \bar{q}_{yC}, \mathcal{F}_C$	$\bar{\phi}_\beta$	F_β
Diffuse Strip	D	T_D	ϕ	q_{zD}	$\bar{q}_{zD}, \bar{q}_{yD}, \mathcal{F}_D$	$\bar{\phi}$	F

$$\frac{d}{ds} = \sin\theta\cos\phi \frac{\partial}{\partial x} + \sin\theta\sin\phi \frac{\partial}{\partial y} + \cos\theta \frac{\partial}{\partial z} \quad . \tag{3.2}$$

Equations (3.1) and (3.2) are expressed in terms of the cartesian coordinate system arbitrarily fixed at the point (x,y,z) as shown in Figure 3.1. At every point in the medium, the integration point (x',y',z') is allowed to vary over its entire range of values with z'=0 on the upper boundary. The polar and azimuthal angles θ and ϕ and distance s locate the fixed coordinates (x,y,z) with respect to the integration coordinates (x',y',z').

The steady state conservation of energy requires that

$$\vec{\nabla} \cdot \vec{F} = 0 \tag{3.3}$$

where the radiative flux vector is defined as

$$\vec{F} = \vec{i} \int_{4\pi} I\cos\theta_x d\omega + \vec{j} \int_{4\pi} I\cos\theta_y d\omega + \vec{k} \int_{4\pi} I\cos\theta_z d\omega \tag{3.4}$$

with ω the solid angle and θ_x, θ_y, θ_z the angles that the x, y, and z axes make with the line of sight of the intensity vector.

The quantity $\overline{\sigma}T^4$ appearing in equation (3.1) is the emissive power of the medium. The constant absorption coefficient κ is combined with the distance s by introducing a dimensionless optical depth τ_s between the points s=o and s=s

$$\tau_s = \int_0^s \kappa ds = \kappa s \quad . \tag{3.5}$$

The coordinate systems of Figure 3.1 are converted to optical coordinate systems by considering transformations similar to equation (3.5). The optical coordinates are defined as

$$\tau_x = \kappa x \; ; \quad \tau_y = \kappa y \; ; \quad \tau_z = \kappa z \tag{3.6}$$

and

$$\tau_x' = \kappa x' \; ; \quad \tau_y' = \kappa y' \; ; \quad \tau_z' = \kappa z' \quad . \tag{3.7}$$

The optical thickness is measured in a direction normal to the boundaries and is given by

$$\tau_o = \kappa L \quad . \tag{3.8}$$

When expressed in terms of the optical coordinates, equations (3.1) and (3.2) become

$$\frac{dI}{d\tau_s} + I = \frac{\bar{\sigma}}{\pi} T^4 \tag{3.9}$$

and

$$\frac{d}{d\tau_s} = \sin\theta\cos\phi \frac{\partial}{\partial\tau_x} + \sin\theta\sin\phi \frac{\partial}{\partial\tau_y} + \cos\theta \frac{\partial}{\partial\tau_z} \quad . \tag{3.10}$$

For simplification of the treatment of the boundary conditions, the intensity is divided into two components. The intensity associated with the direction of increasing τ_z is denoted by I^+ and that with the decreasing τ_z direction by I^-. Thus, equation (3.9) can be written as two equations, one for I^+ and one for I^-. The general boundary conditions for equation (3.9) can be written as

$$I^+(\tau_y,o) = I_o{}^+(\tau_y) \tag{3.11}$$

and

$$I^-(\tau_y,\tau_o) = I_o{}^-(\tau_y) \quad . \tag{3.12}$$

Application of integrating factor techniques to equation (3.9) and use of equations (3.11) and (3.12) yields expressions for I^+ and I^- in terms of the unknown emissive power

$$I^{+} = I_o{}^{+}(\tau_y')e^{-\tau_z \sec\theta} + \frac{1}{\pi}\int_0^{\tau_z} \bar{\sigma}\, T^4(\tau_y',\tau_z',\tau_o)e^{-(\tau_z-\tau_z')\sec\theta} \sec\theta d\tau_z' \quad (3.13)$$

with

$$\tau_s = \frac{\tau_z-\tau_z'}{\cos\theta} = \frac{\tau_y-\tau_y'}{\sin\theta\sin\phi} = \frac{\tau_x-\tau_x'}{\sin\theta\cos\phi} \qquad (0 \le \theta \le \frac{\pi}{2}) \quad (3.14)$$

and

$$I^{-} = I_o{}^{-}(\tau_y')e^{(\tau_o-\tau_z)\sec\theta} - \frac{1}{\pi}\int_{\tau_z}^{\tau_o} \bar{\sigma}\, T^4(\tau_y',\tau_z',\tau_o)e^{(\tau_z'-\tau_z)\sec\theta} \sec\theta d\tau_z' \quad (3.15)$$

with

$$\tau_s = \frac{\tau_z-\tau_z'}{\cos\theta} = \frac{\tau_y-\tau_y'}{\sin\theta\sin(\phi+\pi)} = \frac{\tau_x-\tau_x'}{\sin\theta\cos(\phi+\pi)} \qquad (\frac{\pi}{2} \le \theta \le \pi) \quad (3.16)$$

The equation governing the emissive power in the medium is obtained by writing the divergence of the flux in the following form [35,p.22]

$$\vec{\nabla}\cdot\vec{F} = \int_{4\pi} \frac{dI}{d\tau_s} d\omega \quad . \quad (3.17)$$

Substituting equations (3.3) and (3.9) into equation (3.17) yields an expression for the emissive power

$$4\,\bar{\sigma}\, T^4(\tau_y,\tau_z,\tau_o) = \int_{4\pi} I d\omega \quad . \quad (3.18)$$

Dividing intensity into its two components I^{+} and I^{-} reveals

$$4\,\bar{\sigma}\, T^4(\tau_y,\tau_z,\tau_o) = \int_0^{2\pi}\left[\int_0^{\pi/2} I^{+}\sin\theta d\theta + \int_{\pi/2}^{\pi} I^{-}\sin\theta d\theta\right]d\phi \quad . \quad (3.19)$$

Substitution of equations (3.13) and (3.15) into the conservation of energy equation (3.19) then yields

$$4\,\bar{\sigma}\,T^4(\tau_y,\tau_z,\tau_o) = \int_{2\pi} I_o^{+}(\tau_y')e^{-\tau_z\sec\theta}\,d\omega + \int_{2\pi} I_o^{-}(\tau_y')e^{-(\tau_o-\tau_z)\sec\theta}\,d\omega$$

$$+ \frac{1}{\pi}\int_0^{2\pi}\int_0^{\pi/2}\left[\int_0^{\tau_z}\bar{\sigma}\,T^4(\tau_y',\tau_z',\tau_o)e^{-(\tau_z-\tau_z')\sec\theta}\sec\theta\,d\tau_z'\right.$$

$$\left. + \int_{\tau_z}^{\tau_o}\bar{\sigma}\,T^4(\tau_y',\tau_z',\tau_o)e^{-(\tau_z'-\tau_z)\sec\theta}\sec\theta\,d\tau_z'\right]\sin\theta\,d\theta\,d\phi \qquad (3.20)$$

with

$$\tau_y' = \tau_y + (\tau_z'-\tau_z)\tan\theta\sin\phi \quad . \qquad (3.21)$$

Equation (3.20) is of the same form as the emissive power distribution presented by Olfe [14].

For numerical computation, the trigonometric dependence will be replaced by position dependent functions. The standard substitution

$$\bar{\mu} = \cos\theta \qquad (3.22)$$

and the transform pair

$$\bar{\mu}\gamma = 1 \qquad (3.23)$$

and

$$\lambda\bar{\mu} = \sqrt{1-\bar{\mu}^2}\,\sin\phi \qquad (3.24)$$

with Jacobian given by

$$d\bar{\mu}d\phi = d\gamma d\lambda/\gamma^2\sqrt{\gamma^2-\lambda^2-1} \qquad (3.25)$$

along with the integral

$$\int_1^\infty \frac{e^{-zt}dt}{t\sqrt{t^2-1}} = \int_z^\infty K_o(s)ds \tag{3.26}$$

reduces equation (3.20) to the form

$$4\bar{\sigma}T^4(\tau_y,\tau_z,\tau_o) = \int_{2\pi} I_o^+(\tau_y')e^{-\tau_z \sec\theta}d\omega + \int_{2\pi} I_o^-(\tau_y')e^{-(\tau_o-\tau_z)\sec\theta}d\omega$$

$$+ \frac{2}{\pi}\int_1^\infty dt\int_{-\infty}^{\infty} d\tau_y'\int_0^{\tau_o} K_o[t\sqrt{(\tau_z-\tau_z')^2+(\tau_y-\tau_y')^2}]\,\bar{\sigma}T^4(\tau_y',\tau_z',\tau_o)d\tau_z' \tag{3.27}$$

where $K_o(s)$ is the modified Bessel function. Equation (3.27) is a linear integral equation in the emissive power of the medium and agrees with the form given by Smith [20]. Any further reduction in form should be preceded by an assumption regarding the behavior of the boundary conditions.

The following sections (1-5) of this chapter are concerned with assigning specific forms to the incident radiation and formulating general expressions for emissive power. Equation (3.27) is the fundamental equation which will be employed with the notation following from Table 3.1.

1. COLLIMATED FLUX OF COSINE MAGNITUDE

A variable collimated flux of magnitude $I_W^+(\tau_y)$ is incident on the upper boundary $\tau_z=0$ of the medium from a fixed direction. No radiation is incident on the lower boundary $\tau_z=\tau_o$. Mathematically, the boundary conditions are expressed as

$$I_o^+(\tau_y) = I_W^+(\tau_y)\delta(\bar{\mu}-\bar{\mu}_o)\delta(\phi-\phi_o) \qquad \tau_z=0 \tag{3.28}$$

and

$$I_o^-(\tau_y) = 0 \qquad \tau_z=\tau_o \tag{3.29}$$

where δ is the Dirac delta function, and $\bar{\mu}_o$ and ϕ_o specify the fixed direction. Equation (3.27) reduces to the integral equation for the emissive power

$$4\,\bar{\sigma}\,T^4(\tau_y,\tau_z,\tau_o) = I_w^+(\bar{\tau}_y')e^{-\sigma\tau_z}$$

$$+\frac{2}{\pi}\int_1^\infty dt\int_{-\infty}^{\infty} d\tau_y'\int_0^{\tau_o} K_o[t\sqrt{(\tau_z-\tau_z')^2+(\tau_y-\tau_y')^2}]\;\bar{\sigma}\,T^4(\tau_y',\tau_z',\tau_o)d\tau_z' \tag{3.30}$$

where

$$\sigma = \sec\theta_o = 1/\bar{\mu}_o \tag{3.31}$$

and $\bar{\tau}_y'$ represents τ_y' at the boundary $\tau_z'=0$. The product of Dirac delta functions in the integrand of the integral in equation (3.27) selects the specific direction $\phi=\phi_o$ and $\bar{\mu}=\bar{\mu}_o$ so that equation (3.21) reduces to

$$\bar{\tau}_y' = \tau_y - \tau_z\tan\theta_o\sin\phi_o \quad . \tag{3.32}$$

In particular, the incident flux varies in a cosine fashion and is written in exponential form

$$I_w^+(\tau_y) = F_o e^{i\beta\tau_y} \tag{3.33}$$

where F_o and β are the amplitude and spacial frequency of the incident radiation, respectively. Figure (3.2) exhibits the physical system. Equation (3.30) then yields

$$4\,\bar{\sigma}\,T_A^4(\tau_y,\tau_z,\tau_o) = F_o e^{i\beta(\tau_y-\tau_z\tan\theta_o\sin\phi_o)-\sigma\tau_z}$$

$$+\frac{2}{\pi}\int_1^\infty dt\int_{-\infty}^{\infty} d\tau_y'\int_0^{\tau_o} K_o[t\sqrt{(\tau_z-\tau_z')^2+(\tau_y-\tau_y')^2}]\;\bar{\sigma}\;T_A^4(\tau_y',\tau_z',\tau_o)d\tau_z' \qquad (3.34)$$

where T_A is the temperature of the medium. The complicated term arising from the boundary condition is simplified by confining the incident radiation to lie in planes that are perpendicular to the y-z plane, i.e., $\phi_o=0$ and hence $\bar{\tau}_y'=\tau_y$. With this assumption, equation (3.34) reduces to

$$4\,\bar{\sigma}\,T_A^4(\tau_y,\tau_z,\tau_o) = F_o e^{i\beta\tau_y-\sigma\tau_z}$$

$$+\frac{2}{\pi}\int_1^\infty dt\int_{-\infty}^{\infty} d\tau_y'\int_0^{\tau_o} K_o[t\sqrt{(\tau_z-\tau_z')^2+(\tau_y-\tau_y')^2}]\;\bar{\sigma}\;T_A^4(\tau_y',\tau_z',\tau_o)d\tau_z' \quad . \qquad (3.35)$$

The two-dimensional integral equation for the emissive power of the medium can now be reduced to a one-dimensional integral equation by applying the concept of separation of variables. The geometry of the medium permits this reduction since the τ_y-coordinate is unbounded in both positive and negative directions and hence suitable for Fourier integral transform theory. The assumption that the emissive power can be written as

$$\frac{4\,\bar{\sigma}}{F_o}\,T_A^4(\tau_y,\tau_z,\tau_o) = J_\beta(\tau_z,\sigma,\tau_o)e^{i\beta\tau_y} \qquad (3.36)$$

reduces equation (3.35) to an integral equation for $J_\beta(\tau_z,\sigma,\tau_o)$

$$J_\beta(\tau_z,\sigma,\tau_o) = e^{-\sigma\tau_z} + \frac{1}{2}\int_0^{\tau_o} \mathcal{E}_1(|\tau_z-\tau_z'|,\beta)\;J_\beta(\tau_z',\sigma,\tau_o)d\tau_z' \qquad (3.37)$$

where $\mathcal{E}_1$ is a generalized exponential integral function defined by

$$\mathcal{E}_1(\tau_z,\beta) = \int_1^\infty \frac{e^{-\tau_z\sqrt{t^2+\beta^2}}}{\sqrt{t^2+\beta^2}}\,dt \quad . \tag{3.38}$$

In arriving at equation (3.37), the following integral was used

$$\frac{1}{\pi}\int_{-\infty}^{\infty} e^{i\zeta\beta}K_o[t\sqrt{\zeta^2+\xi^2}]d\zeta = \frac{e^{-|\xi|\sqrt{t^2+\beta^2}}}{\sqrt{t^2+\beta^2}} \quad . \tag{3.39}$$

Smith [20] obtained a less general form of equation (3.37) by considering the radiation to be incident from the direction $\sigma=1$.

Equation (3.33) reveals that when $\beta=0$, the incident radiation on the boundary is uniform. Hence, each point on the boundary receives the same amount of external radiation and is indistinguishable from any other boundary point with respect to heat transfer properties. Energy transfer is therefore described by a single space coordinate normal to the boundary plane. Thus, $\beta=0$ corresponds to the one-dimensional model which has been analyzed extensively. However, other models which involve more complex boundary conditions such as the finite strip model can be expressed in terms of the cosine varying collimated boundary solution by applying the principle of superposition.

2. UNIFORM COLLIMATED FLUX STRIP

This section is concerned with a collimated flux of constant magnitude incident on a strip of finite width at the boundary $\tau_z=0$. The finite strip at the boundary $\tau_z=\tau_o$ receives no external radiation. Figure 3.4 exhibits the physical system. The finite strip solution enables an additional model to be investigated. When the strip width

becomes very large, the finite strip solution approaches the one-dimensional model. The Fourier integral representation of the boundary radiation $I_w^+(\tau_y)$ is given by

$$I_w^+(\tau_y) = \int_{-\infty}^{\infty} g(\beta) e^{i\beta\tau_y} d\beta \tag{3.40}$$

where

$$g(\beta) = \frac{1}{2\pi}\int_{-\infty}^{\infty} I_w^+(\tau_y) e^{-i\beta\tau_y} d\tau_y \quad . \tag{3.41}$$

The finite strip model boundary condition is obtained by allowing $I_w^+(\tau_y)$ to be constant and nonzero over a finite width of the boundary. Mathematically, the boundary condition is expressed as

$$I_w^+(\tau_y) = \begin{cases} 0 & \tau_y < -\tau_a \\ F_o & -\tau_a \leq \tau_y \leq \tau_a \\ 0 & \tau_y > \tau_a \end{cases} \tag{3.42}$$

where τ_a is an optical width related to the half strip width a by the usual integral

$$\tau_a = \int_o^a \kappa dx = \kappa a \quad . \tag{3.43}$$

Integrating equation (3.41) subject to the boundary conditions of equation (3.42) yields

$$g(\beta) = \frac{F_o}{\pi\beta} \sin(\beta\tau_a) \quad . \tag{3.44}$$

Substitution of equation (3.44) into equation (3.40) then gives an integral expression for the incident radiation in the form

$$I_w^+(\tau_y) = \frac{F_o}{\pi}\int_{-\infty}^{\infty} \frac{\sin(\beta\tau_a)}{\beta} e^{i\beta\tau_y} d\beta \quad . \tag{3.45}$$

The integral equation for the emissive power of the medium illuminated by a constant collimated flux can now be obtained from equation (3.30). Substituting equation (3.45) into equation (3.30) yields

$$4\,\bar{\sigma}\,T_B^4(\tau_y,\tau_z,\tau_o) = \frac{F_o}{\pi}\int_{-\infty}^{\infty}\frac{\sin(\beta\tau_a)}{\beta}\,e^{-\sigma\tau_z+i\beta\tau_y}\,d\beta$$

$$+\frac{2}{\pi}\int_1^{\infty}dt\int_{-\infty}^{\infty}d\tau_y'\int_0^{\tau_o}K_o[t\sqrt{(\tau_z-\tau_z')^2+(\tau_y-\tau_y')^2}]\;\bar{\sigma}\,T_B^4(\tau_y',\tau_z',\tau_o)d\tau_z' \qquad (3.46)$$

where T_B is the temperature of the medium. Multiplying equation (3.35) by $\sin(\beta\tau_a)d\beta/\pi\beta$ and integrating from $-\infty$ to ∞ reveals

$$\int_{-\infty}^{\infty}4\,\bar{\sigma}\,T_A^4(\tau_y,\tau_z,\tau_o)\,\frac{\sin(\beta\tau_a)d\beta}{\pi\beta} = \frac{F_o}{\pi}\int_{-\infty}^{\infty}\frac{\sin(\beta\tau_a)}{\beta}\,e^{i\beta\tau_y-\sigma\tau_z}\,d\beta$$

$$+\frac{2}{\pi}\int_1^{\infty}dt\int_{-\infty}^{\infty}d\tau_y'\int_0^{\tau_o}K_o[t\sqrt{(\tau_z-\tau_z')^2+(\tau_y-\tau_y')^2}]$$

$$\int_{-\infty}^{\infty}\bar{\sigma}\,T_A^4(\tau_y',\tau_z',\tau_o)\,\frac{\sin(\beta\tau_a)}{\pi\beta}\,d\beta d\tau_z' \quad . \qquad (3.47)$$

Comparing equations (3.46) and (3.47) results in an integral expression which relates the emissive power of the medium bounded by the constant collimated strip to that of the cosine varying collimated boundary

$$\bar{\sigma}\,T_B^4(\tau_y,\tau_z,\tau_o) = \frac{1}{\pi}\int_{-\infty}^{\infty}\frac{\sin(\beta\tau_a)}{\beta}\,\bar{\sigma}\,T_A^4(\tau_y,\tau_z,\tau_o)d\beta \quad . \qquad (3.48)$$

Substitution of equation (3.36) into equation (3.48) yields

$$\frac{4\bar{\sigma}}{F_o} T_B^4(\tau_y,\tau_z,\tau_o) = \frac{1}{\pi}\int_{-\infty}^{\infty} J_\beta(\tau_z,\sigma,\tau_o)\,\frac{\sin(\beta\tau_a)}{\beta}\,e^{i\beta\tau_y}\,d\beta \quad . \tag{3.49}$$

By making use of the real part of the exponential function and the evenness of the integrand equation (3.49) reduces to

$$J(\tau_y,\tau_z,\tau_o) = \frac{2}{\pi}\int_{0}^{\infty} J_\beta(\tau_z,\sigma,\tau_o)\,\frac{\sin(\beta\tau_a)\cos(\beta\tau_y)d\beta}{\beta} \tag{3.50}$$

where $J(\tau_y,\tau_z,\tau_o)$ is the dimensionless emissive power for the medium bounded by the constant collimated strip

$$J(\tau_y,\tau_z,\tau_o) = \frac{4\bar{\sigma}}{F_o} T_B^4(\tau_y,\tau_z,\tau_o) \quad . \tag{3.51}$$

3. COSINE VARYING DIFFUSE BOUNDARY CONDITION

The boundaries of the medium are black walls radiating in a nonuniform fashion due to prescribed temperatures. Since black body radiation is governed by the Stefan-Boltzmann law, the boundary conditions are given by

$$I_o^{+} = \frac{\bar{\sigma}}{\pi} T_2^4(\tau_y) \tag{3.52}$$

and

$$I_o^{-} = \frac{\bar{\sigma}}{\pi} T_1^4(\tau_y) \tag{3.53}$$

where T_1 denotes temperature of the lower wall at $\tau_z=\tau_o$ and T_2 temperature at $\tau_z=0$. Substituting equations (3.52) and (3.53) into equation (3.27) yields an integral equation for the emissive power

$$\bar{\sigma}\,T^4(\tau_y,\tau_z,\tau_o) = \frac{1}{4\pi}\int_0^{2\pi}\int_0^{\pi/2}\left[\bar{\sigma}\,T_2^4(\tau_y')e^{-\tau_z\sec\theta}\right.$$

$$\left. + \bar{\sigma}\,T_1^4(\tau_y')e^{-(\tau_o-\tau_z)\sec\theta}\right]\sin\theta\,d\theta\,d\phi$$

$$+ \frac{1}{2\pi} \int_1^\infty dt \int_{-\infty}^{\infty} d\tau_y' \int_0^{\tau_o} K_o[t\sqrt{(\tau_z-\tau_z')^2+(\tau_y-\tau_y')^2}] \;\; \bar{\sigma}\, T^4(\tau_y',\tau_z',\tau_o)d\tau_z' \; . \qquad (3.54)$$

The two inhomogeneous terms in equation (3.54) are transformed by equations (3.22) to (3.25) and the substitution $\eta=\tau_y-\tau_y'$ to yield

$$\bar{\sigma}\, T^4(\tau_y,\tau_z,\tau_o) = \frac{\tau_z}{2\pi} \int_{-\infty}^{\infty} \frac{\bar{\sigma}\, T_2^4(\tau_y-\eta)S_1(\sqrt{\tau_z^2+\eta^2})d\eta}{\tau_z^2+\eta^2}$$

$$+ \frac{(\tau_o-\tau_z)}{2\pi} \int_{-\infty}^{\infty} \frac{\bar{\sigma}\, T_1^4(\tau_y-\eta)S_1(\sqrt{(\tau_o-\tau_z)^2+\eta^2})d\eta}{(\tau_o-\tau_z)^2+\eta^2}$$

$$+ \frac{1}{2\pi} \int_1^\infty dt \int_{-\infty}^{\infty} d\tau_y' \int_0^{\tau_o} K_o[t\sqrt{(\tau_z-\tau_z')^2+(\tau_y-\tau_y')^2}] \; \bar{\sigma}\, T^4(\tau_y',\tau_z',\tau_o)d\tau_z' \qquad (3.55)$$

where

$$S_n(\xi) = \int_1^\infty \frac{e^{-\xi t}\, dt}{t^{n+1}\sqrt{t^2-1}} \qquad (3.56)$$

Note that the S_1-function can be expressed in terms of integrals of the modified Bessel function given by equation (3.26). A standard integral representation for the modified Bessel function is, from Luke [36,p.30],

$$K_\gamma(\xi) = \int_1^\infty e^{-\xi\cosh\mu} \cosh(\gamma\mu)d\mu \; . \qquad (3.57)$$

The substitution $t=\cosh\mu$ with $\gamma=0$ reduces equation (3.57) to

$$K_o(\xi) = \int_1^\infty \frac{e^{-\xi t}\, dt}{\sqrt{t^2-1}} = S_{-1}(\xi) \; . \qquad (3.58)$$

Integrating equation (3.58) twice with respect to ξ over the range (ξ,∞) results in

$$\int_{y=\xi}^{\infty}\int_{x=y}^{\infty} K_0(x)dxdy = \int_1^{\infty} \frac{e^{-\xi t}\,dt}{t^2\sqrt{t^2-1}} \quad . \tag{3.59}$$

The right-hand side of equation (3.59) is $S_1(\xi)$ from equation (3.56). Hence, $S_1(\xi)$ becomes

$$S_1(\xi) = \int_{y=\xi}^{\infty}\int_{x=y}^{\infty} K_0(x)dxdy \quad . \tag{3.60}$$

A series of simple substitutions changes the limits of integration of equation (3.60) so that a typical term is

$$\frac{S_1(\sqrt{\tau_z^2+\eta^2})}{\tau_z^2+\eta^2} = \int_1^{\infty}\int_1^{\infty} K_0(xy\sqrt{\tau_z^2+\eta^2})xdxdy \tag{3.61}$$

and equation (3.55) reduces to

$$\bar{\sigma}\,T^4(\tau_y,\tau_z,\tau_o) = \frac{\tau_z}{2\pi}\int_{-\infty}^{\infty} d\eta \int_1^{\infty} dx \int_1^{\infty} K_0(xy\sqrt{\tau_z^2+\eta^2})\;\bar{\sigma}\,T_2^4(\tau_y-\eta)xdy$$

$$+\frac{(\tau_o-\tau_z)}{2\pi}\int_{-\infty}^{\infty} d\eta \int_1^{\infty} dx \int_1^{\infty} K_0(xy\sqrt{(\tau_o-\tau_z)^2+\eta^2})\;\bar{\sigma}\,T_1^4(\tau_y-\eta)xdy$$

$$+\frac{1}{2\pi}\int_1^{\infty} dt \int_{-\infty}^{\infty} d\tau_y' \int_0^{\tau_o} K_0(t\sqrt{(\tau_z-\tau_z')^2+(\tau_y-\tau_y')^2})\;\bar{\sigma}\,T^4(\tau_y',\tau_z',\tau_o)d\tau_z' \quad . \tag{3.62}$$

Next, consider walls that radiate in a cosine fashion with the temperature of the medium denoted by T_c. Figure 3.3 shows the physical system. As before, the two-dimensional problem is reduced to that for the one-dimension by assuming

$$T_c^4(\tau_y,\tau_z,\tau_o) = T_o^4 f(\tau_z) e^{i\beta\tau_y} \tag{3.63}$$

$$T_1^4(\tau_y) = T_1^4 e^{i\beta\tau_y} \tag{3.64}$$

and

$$T_2^4(\tau_y) = T_2^4 e^{i\beta\tau_y} \tag{3.65}$$

which, along with equation (3.39), reduces equation (3.62) to

$$f(\tau_z) = \frac{1}{2}\,\theta_2^4\,\mathcal{E}_2(\tau_z,\beta) + \frac{1}{2}\,\theta_1^4\,\mathcal{E}_2(\tau_o-\tau_z,\beta) + \frac{1}{2}\int_0^{\tau_o} \mathcal{E}_1(|\tau_z-\tau_z'|,\beta) f(\tau_z')\,d\tau_z' \tag{3.66}$$

where

$$\theta_1 = T_1/T_o \tag{3.67}$$

$$\theta_2 = T_2/T_o \tag{3.68}$$

and $\mathcal{E}_2$ is a generalized exponential integral function

$$\mathcal{E}_2(\tau_z,\beta) = \int_1^\infty \frac{e^{-\tau_z\sqrt{t^2+\beta^2}}}{t^2}\,dt \quad . \tag{3.69}$$

A simplified form of equation (3.66) results from defining a dimensionless universal function ϕ_β as follows

$$\phi_\beta(\tau_z,\tau_o) = \frac{1}{2}\,\mathcal{E}_2(\tau_z,\beta) + \frac{1}{2}\int_0^{\tau_o} \phi_\beta(\tau_z',\tau_o)\,\mathcal{E}_1(|\tau_z-\tau_z'|,\beta)\,d\tau_z' \quad . \tag{3.70}$$

Replacement of τ_z by $\tau_o-\tau_z$ in equation (3.70) yields

$$\phi_\beta(\tau_o-\tau_z,\tau_o) = \frac{1}{2}\,\mathcal{E}_2(\tau_o-\tau_z,\beta)$$

$$+ \frac{1}{2}\int_0^{\tau_o} \phi_\beta(\tau_o-\tau_z',\tau_o)\,\mathcal{E}_1(|\tau_z-\tau_z'|,\beta)d\tau_z' \quad . \tag{3.71}$$

By multiplying equation (3.70) by θ_2^4 and equation (3.71) by θ_1^4 and adding, the following expression is obtained

$$\theta_2^4\phi_\beta(\tau_z,\tau_o) + \theta_1^4\phi_\beta(\tau_o-\tau_z,\tau_o) = \frac{1}{2}\,\theta_2^4\mathcal{E}_2(\tau_z,\beta) + \frac{1}{2}\,\theta_1^4\mathcal{E}_2(\tau_o-\tau_z,\beta)$$

$$+ \frac{1}{2}\int_0^{\tau_o} \mathcal{E}_1(|\tau_z-\tau_z'|,\beta)[\theta_2^4\phi_\beta(\tau_z',\tau_o) + \theta_1^4\phi_\beta(\tau_o-\tau_z',\tau_o)]d\tau_z' \quad . \tag{3.72}$$

A comparison of equations (3.66) and (3.72) then yields an expression for the dimensionless emissive power

$$f(\tau_z) = \theta_2^4\phi_\beta(\tau_z,\tau_o) + \theta_1^4\phi_\beta(\tau_o-\tau_z,\tau_o) \quad . \tag{3.73}$$

4. RELATIONSHIP BETWEEN DIFFUSE AND COLLIMATED CASES

An integral expression relating the emissive power for the cosine varying diffuse boundary condition to the emissive power for the cosine varying collimated boundary condition will now be developed. Physically, the diffuse problem should be associated in some manner with the collimated since the collimated selects a particular angle whereas the diffuse considers all possible directions. As in previous development, the technique is to construct an integral equation which has the same inhomogeneous term and kernel. Since the collimated problem has the simplest inhomogeneous term, it is advantageous to start with equation (3.37). Replacement of σ by $\sqrt{t^2+\beta^2}$ in equation

(3.37) results in

$$J_\beta(\tau_z,\sqrt{t^2+\beta^2},\tau_o) = e^{-\tau_z\sqrt{t^2+\beta^2}} + \frac{1}{2}\int_0^{\tau_o} \mathcal{E}_1(|\tau_z-\tau_z'|,\beta)J_\beta(\tau_z',\sqrt{t^2+\beta^2},\tau_o)d\tau_z' \quad . \tag{3.74}$$

Multiplying equation (3.74) by dt/t^2 and integrating from 1 to ∞ yields

$$\int_1^\infty J_\beta(\tau_z,\sqrt{t^2+\beta^2},\tau_o)\frac{dt}{t^2} = \mathcal{E}_2(\tau_z,\beta) + \frac{1}{2}\int_0^{\tau_o} \mathcal{E}_1(|\tau_z-\tau_z'|,\beta)\int_1^\infty J_\beta(\tau_z',\sqrt{t^2+\beta^2},\tau_o)\frac{dt}{t^2}\,d\tau_z' \quad . \tag{3.75}$$

Comparison of equation (3.70) with equation (3.75) results in the following relationship between the emissive power for the cosine varying collimated boundary and the emissive power for the cosine varying diffuse boundary

$$\phi_\beta(\tau_z,\tau_o) = \frac{1}{2}\int_1^\infty J_\beta(\tau_z,\sqrt{t^2+\beta^2},\tau_o)\frac{dt}{t^2} \quad . \tag{3.76}$$

The change of variable $\sigma=\sqrt{t^2+\beta^2}$ reduces equation (3.76) to the form

$$\phi_\beta(\tau_z,\tau_o) = \frac{1}{2}\int_{\sqrt{1+\beta^2}}^\infty \frac{J_\beta(\tau_z,\sigma,\tau_o)\sigma d\sigma}{(\sigma^2-\beta^2)^{3/2}} \quad . \tag{3.77}$$

A further reduction is accomplished by letting $x=\sqrt{1+\beta^2}/\sigma$ to arrive at

$$\phi_\beta(\tau_z,\tau_0) = \frac{1}{2}\int_0^1 \psi_1(x,\beta) J_\beta(\tau_z,\sqrt{1+\beta^2}/x,\tau_0)dx \tag{3.78}$$

where

$$\psi_1(x,\beta) = (1+\beta^2)/[1+\beta^2(1-x^2)]^{3/2} . \tag{3.79}$$

The ψ_1-function is presented in graphical form in Appendix C and contributes significantly to the mathematical complications involved in the numerical integrations of Chapters IV and V.

5. CONSTANT TEMPERATURE STRIP

The analysis of this section is concerned with obtaining the emissive power for the medium bounded by a pair of constant temperature strips shown in Figure 3.5. The formulation is similar to that for the case of the finite strip illuminated by a constant flux mentioned previously. The emissive power for the variable radiating black walls given by equation (3.62) can be rewritten in the following form

$$\begin{aligned}\bar{\sigma}\, T^4(\tau_y,\tau_z,\tau_0) = {} & \frac{\tau_z}{2\pi}\int_{-\infty}^{\infty} d\tau_y' \int_1^\infty dx \int_1^\infty K_0(xy\sqrt{\tau_z^2+(\tau_y-\tau_y')^2})\, \bar{\sigma}\, T_2^4(\tau_y')xdy \\ & + \frac{(\tau_0-\tau_z)}{2\pi}\int_{-\infty}^{\infty} d\tau_y' \int_1^\infty dx \int_1^\infty K_0(xy\sqrt{(\tau_0-\tau_z)^2+(\tau_y-\tau_y')^2})\, \bar{\sigma}\, T_1^4(\tau_y')xdy \\ & + \frac{1}{2\pi}\int_1^\infty dt \int_{-\infty}^{\infty} d\tau_y' \int_0^{\tau_0} K_0[t\sqrt{(\tau_z-\tau_z')^2+(\tau_y-\tau_y')^2}]\, \bar{\sigma}\, T^4(\tau_y',\tau_z',\tau_0)d\tau_z'. \end{aligned} \tag{3.80}$$

The boundary radiation $T_2^4(\tau_y')$ is expressed by Fourier integral theory as

$$T_2^4(\tau_y') = \int_{-\infty}^{\infty} g_1(\beta) e^{i\beta\tau_y'} d\beta \tag{3.81}$$

where

$$g_1(\beta) = \frac{1}{2\pi} \int_{-\infty}^{\infty} T_2^4(\tau_y') e^{-i\beta\tau_y'} \, d\tau_y' \quad . \tag{3.82}$$

The constant temperature finite strip theory is developed by allowing the lower and upper walls to radiate only over a finite portion of the boundaries. In particular, consider constant temperature strips of half width a with the boundary conditions given by

$$T_2^4(\tau_y') = \begin{cases} 0 & \tau_y < -\tau_a \\ T_2^4 & -\tau_a \leq \tau_y \leq \tau_a \\ 0 & \tau_y > \tau_a \end{cases} \tag{3.83}$$

and

$$T_1^4(\tau_y') = \begin{cases} 0 & \tau_y < -\tau_a \\ T_1^4 & -\tau_a \leq \tau_y \leq \tau_a \\ 0 & \tau_y > \tau_a \end{cases} \tag{3.84}$$

where τ_a is an optical width defined by equation (3.43).

Inserting equation (3.83) into equation (3.82) and integrating yields

$$g_1(\beta) = \frac{T_2^4}{\pi\beta} \sin(\beta\tau_a) \quad . \tag{3.85}$$

Next, substitution of equation (3.85) into equation (3.81) results in an integral expression for the boundary radiation

$$T_2^4(\tau_y') = \int_{-\infty}^{\infty} T_2^4 \frac{\sin(\beta\tau_a) e^{i\beta\tau_y'}}{\pi\beta} \, d\beta \quad . \tag{3.86}$$

In a similar fashion, the emissive power at τ_z=0 can be written as

$$T_1^4(\tau_y') = \int_{-\infty}^{\infty} T_1^4 \frac{\sin(\beta\tau_a)e^{i\beta\tau_y'}}{\pi\beta} d\beta \quad . \tag{3.87}$$

The integral equation for the emissive power of the medium bounded by the constant temperature strips then becomes

$$\bar{\sigma}\, T_D^4(\tau_y,\tau_z,\tau_o) =$$

$$\frac{\tau_z}{2\pi}\bar{\sigma}\, T_2^4 \int_{-\infty}^{\infty} d\tau_y' \int_{-\infty}^{\infty} \frac{\sin(\beta\tau_a)}{\pi\beta} e^{i\beta\tau_y'} d\beta \int_1^{\infty} dx \int_1^{\infty} K_o(xy\sqrt{\tau_z^2+(\tau_y-\tau_y')^2})xdy$$

$$+ \frac{(\tau_o-\tau_z)}{2\pi}\bar{\sigma}\, T_1^4 \int_{-\infty}^{\infty} d\tau_y' \int_{-\infty}^{\infty} \frac{\sin(\beta\tau_a)}{\pi\beta} e^{i\beta\tau_y'} d\beta \int_1^{\infty} dx \int_1^{\infty} K_o(xy\sqrt{(\tau_o-\tau_z)^2+(\tau_y-\tau_y')^2})xdy$$

$$+ \frac{1}{2\pi}\int_1^{\infty} dt \int_{-\infty}^{\infty} d\tau_y' \int_0^{\tau_o} K_o[t\sqrt{(\tau_z-\tau_z')^2+(\tau_y-\tau_y')^2}]\, \bar{\sigma}\, T_D^4(\tau_y',\tau_z',\tau_o)d\tau_z' \tag{3.88}$$

where T_D is the temperature of the medium.

Next, consideration is given to variable diffuse walls which radiate in a cosine fashion given by equations (3.64) and (3.65) with the temperature of the medium denoted by T_c. The integral equation for the emissive power of this medium follows from equation (3.80)

$$\bar{\sigma}\, T_c^4(\tau_y,\tau_z,\tau_o) = \frac{\tau_z}{2\pi}\bar{\sigma}\, T_2^4 \int_{-\infty}^{\infty} d\tau_y' \, e^{i\beta\tau_y'} \int_1^{\infty} dx \int_1^{\infty} K_o[xy\sqrt{\tau_z^2+(\tau_y-\tau_y')^2}]xdy$$

$$+ \frac{(\tau_o-\tau_z)}{2\pi}\bar{\sigma}\, T_1^4 \int_{-\infty}^{\infty} d\tau_y' \, e^{i\beta\tau_y'} \int_1^{\infty} dx \int_1^{\infty} K_o[xy\sqrt{(\tau_o-\tau_z)^2+(\tau_y-\tau_y')^2}]xdy$$

$$+ \frac{1}{2\pi}\int_1^{\infty} dt \int_{-\infty}^{\infty} d\tau_y' \int_0^{\tau_o} K_o[t\sqrt{(\tau_z-\tau_z')^2+(\tau_y-\tau_y')^2}]\, \bar{\sigma}\, T_c^4(\tau_y',\tau_z',\tau_o)d\tau_z' \quad . \tag{3.89}$$

When equation (3.89) is multiplied by $\sin(\beta\tau_a)d\beta/\pi\beta$ and integrated from $-\infty$ to ∞ and the resulting expression is compared with equation (3.88), the following integral relationship between the emissive powers of the medium bounded by the constant temperature strips and the cosine varying diffuse boundary is obtained

$$\bar{\sigma}\, T_D^4(\tau_y,\tau_z,\tau_o) = \frac{1}{\pi}\int_{-\infty}^{\infty} \bar{\sigma}\, T_c^4(\tau_y,\tau_z,\tau_o)\frac{\sin(\beta\tau_a)d\beta}{\beta} . \qquad (3.90)$$

Inserting equation (3.63) into equation (3.90) yields

$$\frac{T_D^4(\tau_y,\tau_z,\tau_o)}{T_o^4} = \frac{2}{\pi}\int_0^{\infty} f(\tau_z)\,\frac{\sin(\beta\tau_a)\cos(\beta\tau_y)}{\beta}\,d\beta . \qquad (3.91)$$

Equation (3.91) is expressed in terms of $\phi_\beta(\tau_z,\tau_o)$ by substituting equation (3.73) into equation (3.91) to yield

$$\frac{T_D^4(\tau_y,\tau_z,\tau_o)}{T_o^4} = \theta_2^4\phi(\tau_y,\tau_z,\tau_o) + \theta_1^4\phi(\tau_y,\tau_o-\tau_z,\tau_o) \qquad (3.92)$$

where

$$\phi(\tau_y,\tau_z,\tau_o) = \frac{2}{\pi}\int_0^{\infty} \phi_\beta(\tau_z,\tau_o)\sin(\beta\tau_a)\cos(\beta\tau_y)\,\frac{d\beta}{\beta} . \qquad (3.93)$$

Substitution of equation (3.78) into equation (3.93) yields an expression for the dimensionless emissive power of the constant temperature strip in terms of the dimensionless emissive power of the cosine varying collimated boundary condition as

$$\phi(\tau_y,\tau_z,\tau_o) =$$

$$\frac{1}{\pi}\int_0^{\infty}\left[\int_0^1 \psi_1(x,\beta)J_\beta(\tau_z,\sqrt{1+\beta^2}/x,\tau_o)dx\right]\sin(\beta\tau_a)\cos(\beta\tau_y)\,\frac{d\beta}{\beta} . \qquad (3.94)$$

C. DIFFERENTIAL EQUATION FOR EMISSIVE POWER

The differential equation that the emissive power satisfies for the cosine varying collimated boundary condition is needed for the development of the equations for both the finite and semi-finite media. The analysis will be concerned with only the finite medium since the semi-infinite medium is a limiting case. Differentiating equation (3.37) with respect to τ_z and applying Lebnitz's rule to the integral term yields

$$\frac{dJ_\beta(\tau_z,\sigma,\tau_o)}{d\tau_z} = -\sigma e^{-\sigma\tau_z} + \frac{1}{2} J_\beta(o,\sigma,\tau_o)\mathcal{E}_1(\tau_z,\beta)$$

$$- \frac{1}{2} J_\beta(\tau_o,\sigma,\tau_o)\mathcal{E}_1(\tau_o-\tau_z,\beta)$$

$$+ \frac{1}{2}\int_0^{\tau_o} \frac{d\, J_\beta(\tau_z',\sigma,\tau_o)}{d\tau_z'}\mathcal{E}_1(|\tau_z-\tau_z'|,\beta)d\tau_z' \quad . \tag{3.95}$$

Replacement of $\mathcal{E}_1$ by its integral form (3.38) yields

$$\frac{d\, J_\beta(\tau_z,\sigma,\tau_o)}{d\tau_z} = -\sigma\, e^{-\sigma\tau_z} + \frac{1}{2} J_\beta(o,\sigma,\tau_o)\int_1^\infty \frac{e^{-\tau_z\sqrt{t^2+\beta^2}}}{\sqrt{t^2+\beta^2}}\,dt$$

$$- \frac{1}{2} J_\beta(\tau_o,\sigma,\tau_o)\int_1^\infty \frac{e^{-(\tau_o-\tau_z)\sqrt{t^2+\beta^2}}}{\sqrt{t^2+\beta^2}}\,dt$$

$$+ \frac{1}{2}\int_0^{\tau_o} \frac{d\, J_\beta(\tau_z',\sigma,\tau_o)}{d\tau_z'}\mathcal{E}_1(|\tau_z-\tau_z'|,\beta)d\tau_z' \quad . \tag{3.96}$$

Since equation (3.96) is an integral equation for

$$\frac{d\, J_\beta(\tau_z,\sigma,\tau_o)}{d\tau_z}$$

the technique is to construct an integral equation which has the same kernel and inhomogeneous term and compare the result with equation (3.96). Letting $\sigma=\sqrt{t^2+\beta^2}$ in equation (3.37), multiplying the result by $\frac{1}{2} J_\beta(o,\sigma,\tau_o)dt/\sqrt{t^2+\beta^2}$ and integrating the equation from 1 to ∞ yields

$$\frac{1}{2} J_\beta(o,\sigma,\tau_o) \int_1^\infty J_\beta(\tau_z,\sqrt{t^2+\beta^2},\tau_o) \frac{dt}{\sqrt{t^2+\beta^2}}$$

$$= \frac{1}{2} J_\beta(o,\sigma,\tau_o) \int_1^\infty \frac{e^{-\tau_z\sqrt{t^2+\beta^2}}}{\sqrt{t^2+\beta^2}}\, dt$$

$$+ \frac{1}{2} \int_0^{\tau_o} \mathcal{E}_1(|\tau_z-\tau'_z|,\beta)\left[\frac{1}{2} J_\beta(o,\sigma,\tau_o)\right.$$

$$\left. \int_1^\infty J_\beta(\tau'_z,\sqrt{t^2+\beta^2},\tau_o) \frac{dt}{\sqrt{t^2+\beta^2}}\right] d\tau'_z \quad . \tag{3.97}$$

When τ_z is replaced by $\tau_o-\tau_z$ and τ'_z by $\tau_o-\tau'_z$, equation (3.37) reduces to

$$J_\beta(\tau_o-\tau_z,\sigma,\tau_o) = e^{-(\tau_o-\tau_z)\sigma}$$

$$+ \frac{1}{2} \int_0^{\tau_o} \mathcal{E}_1(|\tau_z-\tau'_z|,\beta) J_\beta(\tau_o-\tau'_z,\sigma,\tau_o) d\tau'_z \quad . \tag{3.98}$$

Next, by letting $\sigma=\sqrt{t^2+\beta^2}$ in equation (3.98), multiplying the result by

$-\frac{1}{2} J_\beta(\tau_o,\sigma,\tau_o)dt/\sqrt{t^2+\beta^2}$ and integrating from 1 to ∞, the following expression is obtained

$$-\frac{1}{2} J_\beta(\tau_o,\sigma,\tau_o) \int_1^\infty J_\beta(\tau_o-\tau_z,\sqrt{t^2+\beta^2},\tau_o) \frac{dt}{\sqrt{t^2+\beta^2}}$$

$$-\frac{1}{2} J_\beta(\tau_o,\sigma,\tau_o) \int_1^\infty \frac{e^{-(\tau_o-\tau_z)\sqrt{t^2+\beta^2}}}{\sqrt{t^2+\beta^2}} dt$$

$$+\frac{1}{2}\int_0^{\tau_o} \mathcal{E}_1(|\tau_z-\tau_z'|,\beta)$$

$$\left[-\frac{1}{2} J_\beta(\tau_o,\sigma,\tau_o)\int_1^\infty J_\beta(\tau_o-\tau_z',\sqrt{t^2+\beta^2},\tau_o) \frac{dt}{\sqrt{t^2+\beta^2}}\right] d\tau_z' \quad . \qquad (3.99)$$

Multiplying equation (3.37) by $-\sigma$ yields

$$-\sigma J_\beta(\tau_z,\sigma,\tau_o) = -\sigma\, e^{-\sigma\tau_z} + \frac{1}{2}\int_0^{\tau_o} \mathcal{E}_1(|\tau_z-\tau_z'|,\beta)[-\sigma J_\beta(\tau_z',\sigma,\tau_o)]d\tau_z'. \qquad (3.100)$$

Equations (3.97), (3.99), and (3.100) are then added to give

$$\frac{1}{2} J_\beta(o,\sigma,\tau_o) \int_1^\infty J_\beta(\tau_z,\sqrt{t^2+\beta^2},\tau_o) \frac{dt}{\sqrt{t^2+\beta^2}}$$

$$-\frac{1}{2} J_\beta(\tau_o,\sigma,\tau_o) \int_1^\infty J_\beta(\tau_o-\tau_z,\sqrt{t^2+\beta^2},\tau_o) \frac{dt}{\sqrt{t^2+\beta^2}} - \sigma J_\beta(\tau_z,\sigma,\tau_o)$$

$$= \frac{1}{2} J_\beta(o,\sigma,\tau_o) \int_1^\infty \frac{e^{-\tau_z\sqrt{t^2+\beta^2}}}{\sqrt{t^2+\beta^2}} dt$$

$$-\frac{1}{2} J_\beta(\tau_o,\sigma,\tau_o)\int_1^\infty \frac{e^{-(\tau_o-\tau_z)\sqrt{t^2+\beta^2}}}{\sqrt{t^2+\beta^2}} dt - \sigma\, e^{-\sigma\tau_z}$$

$$+ \frac{1}{2}\int_0^{\tau_o} \mathcal{E}_1(|\tau_z-\tau_z'|,\beta)\Big[\frac{1}{2} J_\beta(o,\sigma,\tau_o) \int_1^\infty J_\beta(\tau_z',\sqrt{t^2+\beta^2},\tau_o) \frac{dt}{\sqrt{t^2+\beta^2}}$$

$$- \frac{1}{2} J_\beta(\tau_o,\sigma,\tau_o) \int_1^\infty J_\beta(\tau_o-\tau_z',\sqrt{t^2+\beta^2},\tau_o) \frac{dt}{\sqrt{t^2+\beta^2}}$$

$$- \sigma J_\beta(\tau_z',\sigma,\tau_o)\Big] d\tau_z' \quad . \qquad (3.101)$$

A comparison of equation (3.101) with equation (3.96) yields the desired relationship

$$\frac{d\, J_\beta(\tau_z,\sigma,\tau_o)}{d\tau_z} + \sigma J_\beta(\tau_z,\sigma,\tau_o)$$

$$+ \frac{1}{2} J_\beta(\tau_o,\sigma,\tau_o) \int_1^\infty J_\beta(\tau_o-\tau_z,\sqrt{t^2+\beta^2},\tau_o) \frac{dt}{\sqrt{t^2+\beta^2}}$$

$$- \frac{1}{2} J_\beta(o,\sigma,\tau_o) \int_1^\infty J_\beta(\tau_z,\sqrt{t^2+\beta^2},\tau_o) \frac{dt}{\sqrt{t^2+\beta^2}} = 0 \quad . \qquad (3.102)$$

The one-dimensional analogue of equation (3.102) is obtained by Sobolev [5,p.73]. Letting τ_o become infinite in equation (3.102) yields an equation similar in form with that obtained by Smith [20] for a semi-infinite two-dimensional model.

D. BASIC EQUATIONS FOR RADIATIVE FLUX

The radiative heat flux in the x, y, and z-directions are given by the $\vec{i}$, $\vec{j}$, and $\vec{k}$-components of the radiative flux vector defined by equation (3.4). Since this investigation is concerned with two-dimensional radiative theory, the x-component of flux will be zero in accord with the coordinate system of Figure 3.1. The z-component of

flux is denoted by q_z and the y-component by q_y. Substituting the directional cosines $\cos\theta_z=\cos\theta$ and $\cos\theta_y=\sin\theta\sin\phi$ into equation (3.4) yields

$$q_z = \int_{4\pi} I \cos\theta d\omega \tag{3.103}$$

and

$$q_y = \int_{4\pi} I \sin\theta\sin\phi d\omega \quad . \tag{3.104}$$

After the intensity I is substituted into these equations in its positive and negative components given by equations (3.13) and (3.15) and the integration is performed over the solid angle, the components of the radiative flux are given by

$$q_z = \int_0^{2\pi}\int_0^{\pi/2}\Big[I_o^{+}(\tau_y')e^{-\tau_y\sec\theta} - I_o^{-}(\tau_y')e^{-(\tau_o-\tau_z)\sec\theta} + \frac{1}{\pi}\int_0^{\tau_z} \bar{\sigma}\, T^4(\tau_y',\tau_z',\tau_o)e^{-(\tau_z-\tau_z')\sec\theta}\sec\theta d\tau_z' - \frac{1}{\pi}\int_{\tau_z}^{\tau_o} \bar{\sigma}\, T^4(\tau_y',\tau_z',\tau_o)e^{-(\tau_z'-\tau_z)\sec\theta}\sec\theta d\tau_z'\Big]\cos\theta\sin\theta d\theta d\phi \tag{3.105}$$

and

$$q_y = \int_0^{2\pi}\int_0^{\pi/2}\Big[I_o^{+}(\tau_y')e^{-\tau_z\sec\theta} - I_o^{-}(\tau_y')e^{-(\tau_o-\tau_z)\sec\theta} + \frac{1}{\pi}\int_0^{\tau_z} \bar{\sigma}\, T^4(\tau_y',\tau_z',\tau_o)e^{-(\tau_z-\tau_z')\sec\theta}\sec\theta d\tau_z'$$

$$- \frac{1}{\pi} \int_{\tau_z}^{\tau_o} \bar{\sigma} T^4(\tau_y', \tau_z', \tau_o) e^{-(\tau_z' - \tau_z)\sec\theta} \sec\theta d\tau_z' \Big] \sin^2\theta \sin\phi d\theta d\phi \qquad (3.106)$$

where

$$\lambda = (\tau_y - \tau_y')/(\tau_z - \tau_z') = \tan\theta\sin\phi \quad . \qquad (3.107)$$

The last two integrals in equation (3.105) and (3.106) can be transformed in a manner similar to that mentioned in the previous sections. The presence of the additional trigonometric terms in the flux equations does not alter the integral form of either but does introduce constant multipliers in the z-flux and a variable multiplier in the y-flux. The components of flux reduce to

$$q_z = \int_0^{2\pi} \int_0^{\pi/2} \Big[I_o^+(\tau_y') e^{-\tau_z \sec\theta} - I_o^-(\tau_y') e^{-(\tau_o - \tau_z)\sec\theta} \Big] \cos\theta\sin\theta d\theta d\phi$$

$$+ \frac{2}{\pi} \int_{-\infty}^{\infty} d\eta \int_0^{\tau_z} d\tau_z' \, \bar{\sigma} T^4(\tau_y + \eta, \tau_z', \tau_o) \int_1^{\infty} dx \int_1^{\infty} K_o[xy\sqrt{(\tau_z - \tau_z')^2 + \eta^2}](\tau_z - \tau_z')xdy$$

$$- \frac{2}{\pi} \int_{-\infty}^{\infty} d\eta \int_{\tau_z}^{\tau_o} d\tau_z' \, \bar{\sigma} T^4(\tau_y + \eta, \tau_z', \tau_o)$$

$$\int_1^{\infty} dx \int_1^{\infty} K_o[xy\sqrt{(\tau_z - \tau_z')^2 + \eta^2}](\tau_z' - \tau_z)xdy \qquad (3.108)$$

and

$$q_y = \int_0^{2\pi} \int_0^{\pi/2} \Big[I_o^+(\tau_y') e^{-\tau_z \sec\theta} - I_o^-(\tau_y') e^{-(\tau_o - \tau_z)\sec\theta} \Big] \sin^2\theta \sin\phi d\theta d\phi$$

$$- \frac{2}{\pi} \int_{-\infty}^{\infty} d\eta \int_{0}^{\tau_o} d\tau_z' \int_{1}^{\infty} dx \int_{1}^{\infty} \eta \, \bar{\sigma} \, T^4(\tau_y+\eta, \tau_z', \tau_o) K_o[xy\sqrt{(\tau_z-\tau_z')^2+\eta^2}] x dy. \quad (3.109)$$

Equations (3.108) and (3.109) are the basic equations for components of flux which will be used in the following sections (1-5) to formulate expressions for flux due to various types of boundary radiation. Both components of flux involve the emissive power which has been determined in previous sections. The notation for flux and emissive power has been tabulated in Table 3.1.

1. COLLIMATED FLUX OF COSINE MAGNITUDE

A collimated flux of cosine magnitude is incident on the upper boundary as shown in Figure 3.2. Components of flux in the y- and z-directions are denoted by q_{yA} and q_{zA}, respectively. Boundary conditions for the cosine varying collimated model given by equations (3.28), (3.29), and (3.33) reduce equations (3.108) and (3.109) to the form

$$q_{zA}(\tau_z, \sigma, \tau_o) = \frac{F_o}{\sigma} e^{i\beta\tau_y - \sigma\tau_z}$$

$$+ \frac{2}{\pi} \int_{-\infty}^{\infty} d\eta \int_{0}^{\tau_z} d\tau_z' \int_{1}^{\infty} dx \int_{1}^{\infty} \bar{\sigma} \, T_A^4(\tau_y+\eta, \tau_z', \tau_o)[\tau_z-\tau_z'] K_o[xy\sqrt{(\tau_z-\tau_z')^2+\eta^2}] x dy$$

$$- \frac{2}{\pi} \int_{-\infty}^{\infty} d\eta \int_{\tau_z}^{\tau_o} d\tau_z' \int_{1}^{\infty} dx \int_{1}^{\infty} \bar{\sigma} \, T_A^4(\tau_y+\eta, \tau_z', \tau_o)[\tau_z'-\tau_z] K_o[xy\sqrt{(\tau_z-\tau_z')^2+\eta^2}] x dy \quad (3.110)$$

and

$$q_{yA}(\tau_z,\sigma,\tau_o) = -\frac{2}{\pi}\int_{-\infty}^{\infty} d\eta \int_{0}^{\tau_o} d\tau_z' \int_{1}^{\infty} dx$$

$$\int_{1}^{\infty} \eta\, \bar{\sigma}\, T_A^4(\tau_y+\eta,\tau_z',\tau_o) K_o[xy\sqrt{(\tau_z-\tau_z')^2+\eta^2}]\,x\,dy \qquad (3.111)$$

where T_A is the temperature of the medium. The application of the separation of variable technique with the use of equation (3.36) reduces equations (3.110) and (3.111) to

$$q_{zA}(\tau_z,\sigma,\tau_o) = F_o\cos(\beta\tau_y)\left[\frac{e^{-\sigma\tau_z}}{\sigma} + \frac{1}{2}\int_{0}^{\tau_z} \mathcal{E}_2(\tau_z-\tau_z',\beta) J_\beta(\tau_z',\sigma,\tau_o)\,d\tau_z'\right.$$

$$\left. - \frac{1}{2}\int_{\tau_z}^{\tau_o} \mathcal{E}_2(\tau_z'-\tau_z,\beta) J_\beta(\tau_z',\sigma,\tau_o)\,d\tau_z'\right] \qquad (3.112)$$

and

$$q_{yA}(\tau_z,\sigma,\tau_o) = -\frac{F_o}{2}\sin(\beta\tau_y)\int_{0}^{\tau_o} \frac{J_\beta(\tau_z',\sigma,\tau_o)}{|\tau_z-\tau_z'|}\frac{d}{d\beta}\,\mathcal{E}_2(|\tau_z-\tau_z'|,\beta)\,d\tau_z' \qquad (3.113)$$

where the derivative in equation (3.113) arises from an operational property of equation (3.39)

$$\frac{1}{\pi}\int_{-\infty}^{\infty} \eta\, e^{i\beta\eta}\, K_o(t\sqrt{\eta^2+\xi^2})\,d\eta = -\,i\,\frac{d}{d\beta}\left[\frac{e^{-|\xi|\sqrt{t^2+\beta^2}}}{\sqrt{t^2+\beta^2}}\right]. \qquad (3.114)$$

2. UNIFORM COLLIMATED FLUX STRIP

Reference to the expressions for radiative flux given by equations (3.105) and (3.106) indicates the dependence of the flux upon the

emissive power of the medium. Since the emissive power for the medium bounded by the finite strip has been expressed in terms of the emissive power for the medium subjected to the cosine varying boundary condition, the radiative flux for the finite strip should be related to the radiative flux of the cosine varying boundary. This section is concerned with the collimated flux boundary condition. The main interest is in the z-component of radiative flux.

The boundary conditions for the constant collimated flux incident on a strip of half width τ_a are given by equation (3.42). Figure 3.4 shows the physical model. When expressed in terms of the Fourier integral representation, the boundary term given by equation (3.42) results in the z-component of flux for the constant collimated strip of equation (3.108) to attain the form

$$q_{zB}(\tau_z,\sigma,\tau_o) = \frac{F_o}{\sigma\pi}\int_{-\infty}^{\infty}\frac{\sin(\beta\tau_a)}{\beta}\, e^{i\beta\tau_y-\sigma\tau_z}\, d\beta$$

$$+\frac{2}{\pi}\int_{-\infty}^{\infty}\int_{0}^{\tau_z}\int_{1}^{\infty}\int_{1}^{\infty}\overline{\sigma}\, T_B^4(\tau_y+\eta,\tau_z',\tau_o)K_o[xy\sqrt{(\tau_z-\tau_z')^2+\eta^2}]$$

$$(\tau_z-\tau_z')xdxdyd\tau_z d\eta$$

$$-\frac{2}{\pi}\int_{-\infty}^{\infty}\int_{\tau_z}^{\tau_o}\int_{1}^{\infty}\int_{1}^{\infty}\overline{\sigma}\, T_B^4(\tau_y+\eta,\tau_z',\tau_o)K_o[xy\sqrt{(\tau_z-\tau_z')^2+\eta^2}]$$

$$(\tau_z'-\tau_z)xdxdyd\tau_z d\eta \quad . \qquad (3.115)$$

When equation (3.110) is multiplied by $\sin(\beta\tau_a)d\beta/\pi\beta$ and integrated from $-\infty$ to ∞, the following expression involving the flux for the cosine varying collimated boundary is obtained

$$\int_{-\infty}^{\infty} \frac{\sin(\beta\tau_a)}{\pi\beta} q_{zA}(\tau_z,\sigma,\tau_o)d\beta = \frac{F_o}{\sigma\pi}\int_{-\infty}^{\infty} \frac{\sin(\beta\tau_a)}{\beta} e^{i\beta\tau_y-\sigma\tau_z}\, d\beta$$

$$+ \frac{2}{\pi}\int_{-\infty}^{\infty}\int_{0}^{\tau_z}\int_{1}^{\infty}\int_{1}^{\infty} K_o[xy\sqrt{(\tau_z-\tau_z')^2+\eta^2}]x(\tau_z-\tau_z')$$

$$\left[\int_{-\infty}^{\infty} \frac{\sin(\beta\tau_a)}{\pi\beta}\,\bar{\sigma}\, T_A^4(\tau_y+\eta,\tau_z',\tau_o)d\beta\right] dxdyd\tau_z'd\eta$$

$$- \frac{2}{\pi}\int_{-\infty}^{\infty}\int_{\tau_z}^{\tau_o}\int_{1}^{\infty}\int_{1}^{\infty} K_o[xy\sqrt{(\tau_z-\tau_z')^2+\eta^2}]x(\tau_z'-\tau_z)$$

$$\left[\int_{-\infty}^{\infty} \frac{\sin(\beta\tau_a)}{\pi\beta}\,\bar{\sigma}\, T_A^4(\tau_y+\eta,\tau_z',\tau_o)d\beta\right] dxdyd\tau_z'd\eta \qquad (3.116)$$

The relationship between the emissive power of the media for the cosine varying collimated boundary and the constant collimated strip boundary has previously been found. Rewrite equation (3.48) in the form

$$\bar{\sigma}\, T_B^4(\tau_y+\eta,\tau_z,\tau_o) = \frac{1}{\pi}\int_{-\infty}^{\infty} \frac{\sin(\beta\tau_a)}{\beta}\,\bar{\sigma}\, T_A^4(\tau_y+\eta,\tau_z,\tau_o)d\beta\ . \qquad (3.117)$$

Inserting equation (3.117) into equation (3.115) and comparing the result with equation (3.116) yields an integral expression for the z-component of flux for the collimated strip boundary in terms of the z-component of flux for the cosine varying collimated boundary

$$q_{zB}(\tau_z,\sigma,\tau_o) = \frac{1}{\pi}\int_{-\infty}^{\infty} \frac{\sin(\beta\tau_a)}{\beta}\, q_{zA}(\tau_z,\sigma,\tau_o)d\beta \ . \qquad (3.118)$$

3. COSINE VARYING DIFFUSE BOUNDARY CONDITION

Boundary conditions for the cosine varying black surfaces, given by equations (3.52) and (3.53) and shown schematically in Figure 3.3 provide nonhomogeneous terms in equations (3.108) and (3.109) which should also be written in terms of the position dependent Bessel functions if the previous transforms are to be utilized. The essential difference is the introduction of $S_2(\xi)$ instead of $S_1(\xi)$ defined by equation (3.56). As with $S_1(\xi)$, $S_2(\xi)$ can be written as an integral of the desired Bessel function. Integrating equation (3.59) with respect to ξ over the range (ξ,∞) results in

$$S_2(\xi) = \int_{z=\xi}^{\infty}\int_{y=z}^{\infty}\int_{x=y}^{\infty} K_o(x)dxdydz \ . \qquad (3.119)$$

Equations (3.108) and (3.109) then become

$$q_z(\tau_z,\tau_o) = \frac{2\tau_z^2}{\pi}\int_{-\infty}^{\infty}\int_{1}^{\infty}\int_{1}^{\infty}\int_{1}^{\infty} \overline{\sigma}\, T_2^4(\tau_y+\eta)K_o[xyz\sqrt{\tau_z^2+\eta^2}]y^2xdxdydzd\eta$$

$$- \frac{2(\tau_o-\tau_z)^2}{\pi}\int_{-\infty_1}^{\infty}\int_{1}^{\infty}\int_{1}^{\infty}\int_{1}^{\infty} \overline{\sigma}\, T_1^4(\tau_y+\eta)K_o[xyz\sqrt{(\tau_o-\tau_z)^2+\eta^2}]y^2xdxdydzd\eta$$

$$+ \frac{2}{\pi}\int_{-\infty}^{\infty}\int_{0}^{\tau_z}\int_{1}^{\infty}\int_{1}^{\infty} \overline{\sigma}\, T^4(\tau_y+\eta,\tau_z',\tau_o)K_o[xy\sqrt{(\tau_z-\tau_z')^2+\eta^2}](\tau_z-\tau_z')xdxdyd\tau_z'd\eta$$

$$- \frac{2}{\pi}\int_{-\infty}^{\infty}\int_{\tau_z}^{\tau_o}\int_{1}^{\infty}\int_{1}^{\infty} \overline{\sigma}\, T^4(\tau_y+\eta,\tau_z',\tau_o)K_o[xy\sqrt{(\tau_z-\tau_z')^2+\eta^2}](\tau_z'-\tau_z)xdxdyd\tau_z'd\eta \qquad (3.120)$$

and

$$q_y(\tau_z,\tau_o) = \frac{2\tau_z}{\pi}\int_{-\infty}^{\infty}\int_{1}^{\infty}\int_{1}^{\infty}\int_{1}^{\infty}\bar{\sigma}\,T_2^4(\tau_y+\eta)K_o[xyz\sqrt{\tau_z^2+\eta^2}]y^2x\eta dxdydzd\eta$$

$$-\frac{2(\tau_o-\tau_z)}{\pi}\int_{-\infty}^{\infty}\int_{1}^{\infty}\int_{1}^{\infty}\int_{1}^{\infty}\bar{\sigma}\,T_1^4(\tau_y+\eta)K_o[xy\sqrt{(\tau_o-\tau_z)^2+\eta^2}]y^2x\eta dxdydzd\eta$$

$$-\frac{2}{\pi}\int_{-\infty}^{\infty}\int_{0}^{\tau_o}\int_{1}^{\infty}\int_{1}^{\infty}\bar{\sigma}\,T^4(\tau_y+\eta,\tau_z',\tau_o)K_o[xy\sqrt{(\tau_z-\tau_z')^2+\eta^2}]\eta xdxdyd\tau_z'd\eta \quad (3.121)$$

The black surfaces radiate in a cosine fashion given by equations (3.64) and (3.65) with the temperature of the medium T_C expressed by equation (3.63). These boundary conditions reduce the two-dimensional flux equations to those for a single dimension

$$\bar{q}_{zC}(\tau_z,\tau_o) = 2\,\tau_z\,\theta_2^4\int_1^{\infty}\mathcal{E}_2(x\tau_z,\beta/x)dx - 2(\tau_o-\tau_z)\theta_1^4\int_1^{\infty}\mathcal{E}_2(x(\tau_o-\tau_z),\beta/x)dx$$

$$+2\int_0^{\tau_z}f(\tau_z')\mathcal{E}_2(\tau_z-\tau_z',\beta)d\tau_z' - 2\int_{\tau_z}^{\tau_o}f(\tau_z')\mathcal{E}_2(\tau_z'-\tau_z,\beta)d\tau_z' \quad (3.122)$$

and

$$\bar{q}_{yC}(\tau_z,\tau_o) = 2\,\theta_2^4\int_1^{\infty}\frac{d\mathcal{E}_2(x\tau_z,\beta/x)}{d\beta}dx + 2\,\theta_1^4\int_1^{\infty}\frac{d\,\mathcal{E}_2[x(\tau_o-\tau_z),\beta/x]}{d\beta}dx$$

$$+2\int_0^{\tau_o}f(\tau_z')\,\frac{d}{d\beta}\left[\frac{\mathcal{E}_2(|\tau_z-\tau_z'|,\beta)}{|\tau_z-\tau_z'|}\right]d\tau_z' \quad (3.123)$$

where

$$\bar{q}_{zC}(\tau_z,\tau_o) = q_{zC}(\tau_z,\tau_o)/\,\bar{\sigma}\,T_o^4\cos(\beta\tau_y) \quad (3.124)$$

and

$$\bar{q}_{yC}(\tau_z,\tau_o) = -q_{yC}(\tau_z,\tau_o)/\ \bar{\sigma}\ T_o^4 \sin(\beta\tau_y)\ . \qquad (3.125)$$

In view of the standard one-dimensional form for the radiative flux, it is desirable to introduce a function analogous to the $E_3(\tau_z)$-function. Define a generalized exponential integral function

$$\mathcal{E}_3(\tau_z,\beta) = \tau_z \int_1^\infty \mathcal{E}_2(\tau_z x,\beta/x)dx\ . \qquad (3.126)$$

Recall that $\mathcal{E}_2$ reduces to E_2 when $\beta=0$. Hence, $\mathcal{E}_3$ reduces to an integral of E_2 which is another form of E_3. Inserting the $\mathcal{E}_3$-function into the z-component of flux reduces it to a standard form analogous to the one-dimensional result obtained by Sparrow and Cess [7,p.224]

$$\bar{q}_{zC}(\tau_z,\tau_o) = 2\,\theta_2^4\,\mathcal{E}_3(\tau_z,\beta) - 2\,\theta_1^4\,\mathcal{E}_3(\tau_o-\tau_z,\beta)$$

$$+ 2\int_0^{\tau_z} f(\tau_z')\,\mathcal{E}_2(\tau_z-\tau_z',\beta)d\tau_z' - 2\int_{\tau_z}^{\tau_o} f(\tau_z')\,\mathcal{E}_2(\tau_z'-\tau_z,\beta)d\tau_z'\ . \qquad (3.127)$$

In a similar fashion, the y-component of flux is simplified by introducing the functions

$$G_2(\tau_z,\beta) = \frac{1}{\tau_z}\,\frac{d\mathcal{E}_2(\tau_z,\beta)}{d\beta} \qquad (3.128)$$

and

$$G_3(\tau_z,\beta) = \frac{d}{d\beta}\int_1^\infty \mathcal{E}_2(\tau_z x,\beta/x)dx = \frac{1}{\tau_z}\,\frac{d\mathcal{E}_3(\tau_z,\beta)}{d\beta}\ . \qquad (3.129)$$

This reduces the y-component of the flux to

$$\bar{q}_{yC}(\tau_z,\tau_o) = 2\,\theta_2^4\,G_3(\tau_z,\beta) + 2\,\theta_1^4\,G_3(\tau_o-\tau_z,\beta) + \int_0^{\tau_o} G_2(|\tau_z-\tau_z'|,\beta)f(\tau_z')d\tau_z' \quad . \tag{3.130}$$

The components of flux can be expressed in terms of ϕ_β by inserting equation (3.73) into equations (3.127) and (3.130) to obtain

$$\bar{q}_{zC}(\tau_z,\tau_o) = \theta_2^4\left[2\,\mathcal{E}_3(\tau_z,\beta) + 2\int_0^{\tau_z}\phi_\beta(\tau_z',\tau_o)\,\mathcal{E}_2(\tau_z-\tau_z',\beta)d\tau_z' - 2\int_{\tau_z}^{\tau_o}\phi_\beta(\tau_z',\tau_o)\,\mathcal{E}_2(\tau_z'-\tau_z,\beta)d\tau_z'\right]$$

$$-\theta_1^4\left[2\,\mathcal{E}_3(\tau_o-\tau_z,\beta) - 2\int_0^{\tau_z}\phi_\beta(\tau_o-\tau_z',\tau_o)\,\mathcal{E}_2(\tau_z-\tau_z',\beta)d\tau_z' + 2\int_{\tau_z}^{\tau_o}\phi_\beta\,(\tau_o-\tau_z',\tau_o)\,\mathcal{E}_2(\tau_z'-\tau_z,\beta)d\tau_z'\right] \tag{3.131}$$

and

$$\bar{q}_{yC}(\tau_z,\tau_o) = 2\,\theta_2^4\left[G_3(\tau_z,\beta) + \int_0^{\tau_o} G_2(|\tau_z-\tau_z'|,\beta)\phi_\beta(\tau_z',\tau_o)d\tau_z'\right]$$

$$+ 2\,\theta_1^4\left[G_3(\tau_o-\tau_z,\beta) + \int_0^{\tau_o} G_2(|\tau_z-\tau_z'|,\beta)\phi_\beta(\tau_o-\tau_z',\tau_o)d\tau_z'\right] . \tag{3.132}$$

A further simplification in form is obtained by defining functions

$$F_z(\tau_z,\tau_o) = 2\,\mathcal{E}_3(\tau_z,\beta) + 2\int_0^{\tau_z} \phi_\beta(\tau'_z,\tau_o)\,\mathcal{E}_2(\tau_z-\tau'_z,\beta)d\tau'_z$$

$$- 2\int_{\tau_z}^{\tau_o} \phi_\beta(\tau'_z,\tau_o)\,\mathcal{E}_2(\tau'_z-\tau_z,\beta)d\tau'_z \qquad (3.133)$$

and

$$F_y(\tau_z,\tau_o) = 2G_3(\tau_z,\beta) + 2\int_0^{\tau_o} G_2(|\tau_z-\tau'_z|,\beta)\phi_\beta(\tau'_z,\tau_o)d\tau'_z \quad . \qquad (3.134)$$

Replacing τ_z by $\tau_o-\tau_z$ in equations (3.133) and (3.134) yields

$$F_z(\tau_o-\tau_z,\tau_o) = 2\,\mathcal{E}_3(\tau_o-\tau_z,\beta) - 2\int_0^{\tau_z} \phi_\beta(\tau_o-\tau'_z,\tau_o)\,\mathcal{E}_2(\tau_z-\tau'_z,\beta)d\tau'_z$$

$$+ 2\int_{\tau_z}^{\tau_o} \phi_\beta(\tau_o-\tau'_z,\tau_o)\,\mathcal{E}_2(\tau'_z-\tau_z,\beta)d\tau'_z \qquad (3.135)$$

and

$$F_y(\tau_o-\tau_z,\tau_o) = 2G_3(\tau_o-\tau_z,\beta) + 2\int_0^{\tau_o} G_2(|\tau_z-\tau'_z|,\beta)\phi_\beta(\tau_o-\tau'_z,\tau_o)d\tau'_z \qquad (3.136)$$

Hence, equations (3.131) and (3.132) reduce to

$$\bar{q}_{zC}(\tau_z,\tau_o) = \theta_2^4 F_z(\tau_z,\tau_o) - \theta_1^4 F_z(\tau_o-\tau_z,\tau_o) \qquad (3.137)$$

and

$$\bar{q}_{yC}(\tau_z,\tau_o) = \theta_2^4 F_y(\tau_z,\tau_o) + \theta_1^4 F_y(\tau_o-\tau_z,\tau_o) \quad . \qquad (3.138)$$

Both components of flux are expressed in terms of the generalized $\mathcal{E}_2$-function. This fact uncovered a discrepancy in one of the functions defined by Olfe [14] in his analysis for a black wall radiating in a sinisodual fashion into a semi-infinite medium. Olfe reduced the two-dimensional equations to those for the one-dimension by directly utilizing the relationship between the local and fixed coordinate systems. A simple trigonometric identity and use of symmetry of the ϕ-wise integration, along with an integral property of Bessel functions led him directly from equations (3.20), (3.105), and (3.106) to the reduced forms. Olfe's reduced temperature and normal flux involve fundamental functions W_1, W_2, and W_3 defined by

$$W_n(\tau_z) = \int_0^{\pi/2} e^{-\tau_z \sec\theta} J_0(\beta\tau_z \tan\theta)(\cos\theta)^{n-2}\sin\theta d\theta \quad (3.139)$$

where J_0 is the zeroth order Bessel function. The functions W_1 and W_2 correspond to the functions $\mathcal{E}_1$ and $\mathcal{E}_2$ of the present analysis.

As already indicated, the present development expresses the y-component of flux in terms of the derivative of the $\mathcal{E}_2$-function. However, Olfe's component of flux parallel to the radiating wall involves functions U_2 and U_3 defined by

$$U_n(\tau_z) = \int_0^{\pi/2} e^{-\tau_z \sec\theta} J_1(\beta\tau_z \tan\theta)(\cos\theta)^{n-3} \sin^2\theta d\theta \quad (3.140)$$

where J_1 is the first order Bessel function.

Direct term by term comparisons for both developments indicate that since the derivative of the $\mathcal{E}_2$-function described the y-flux, a similar differential relationship should exist between the U_n- and

W_n-functions. In particular, the conclusion is that in order for Olfe's development to agree with the present analysis, the following relationship should be satisfied

$$\frac{dW_2}{d\beta} = \tau_z U_2 \tag{3.141}$$

Inspection of equations (3.139) and (3.140) reveals that equation (3.141) is valid. However, Olfe's initial definition of U_n did not satisfy equation (3.141) since the exponent of $\cos\theta$ was (n-2) instead of (n-3).

4. RELATIONSHIP BETWEEN DIFFUSE AND COLLIMATED CASES

An integral expression relating the z-component of flux for the cosine varying diffuse boundary to the z-component of flux for the cosine varying collimated boundary is obtained by writing equation (3.112) in the following form

$$\bar{q}_{zA}(\tau_z,\sigma,\tau_o) = \frac{1}{\sigma} e^{-\sigma\tau_z} + \frac{1}{2}\int_0^{\tau_o} J_\beta(\tau_z',\sigma,\tau_o)\,\mathrm{sign}(\tau_z-\tau_z')\,\mathcal{E}_2(|\tau_z-\tau_z'|,\beta)\,d\tau_z' \tag{3.142}$$

where $\bar{q}_{zA}(\tau_z,\sigma,\tau_o)$ is a dimensionless flux defined by

$$\bar{q}_{zA}(\tau_z,\sigma,\tau_o) = q_{zA}(\tau_z,\sigma,\tau_o)/F_o\cos(\beta\tau_y) \tag{3.143}$$

and

$$\mathrm{sign}(\tau_z-\tau_z') = \begin{cases} 1 & \tau_z' < \tau_z \\ 0 & \tau_z' = \tau_z \\ -1 & \tau_z' > \tau_z \end{cases} \tag{3.144}$$

Insertion of the sign-function into equation (3.133) reduces a portion of the z-component of flux for the radiating wall boundary condition to

$$F_z(\tau_z,\tau_o) = 2\mathcal{E}_3(\tau_z,\beta) + 2\int_0^{\tau_o} \phi_\beta(\tau'_z,\tau_o)\,\mathrm{sign}(\tau_z-\tau'_z)\,\mathcal{E}_2(|\tau_z-\tau'_z|,\beta)\,d\tau'_z . \quad (3.145)$$

But ϕ_β has already been related to J_β through equation (3.78). Hence, equation (3.145) becomes

$$F_z(\tau_z,\tau_o) = 2\mathcal{E}_3(\tau_z,\beta) + \int_1^{\infty} \frac{dt}{t^2}\left[\int_0^{\tau_o} J_\beta(\tau'_z,\sqrt{t^2+\beta^2},\tau_o)\,\mathrm{sign}(\tau_z-\tau'_z)\,\mathcal{E}_2(|\tau_z-\tau'_z|,\beta)\,d\tau'_z\right] . \quad (3.146)$$

Substituting $\sigma=\sqrt{t^2+\beta^2}$ in equation (3.142) and solving for the integral yields

$$\int_0^{\tau_o} J_\beta(\tau'_z,\sqrt{t^2+\beta^2},\tau_o)\,\mathrm{sign}(\tau_z-\tau'_z)\,\mathcal{E}_2(|\tau_z-\tau'_z|,\beta)\,d\tau'_z = 2\,\bar{q}_{zA}(\tau_z,\sqrt{t^2+\beta^2},\tau_o) - \frac{2\,e^{-\tau_z\sqrt{t^2+\beta^2}}}{\sqrt{t^2+\beta^2}} . \quad (3.147)$$

Substitution of equation (3.147) into equation (3.146) results in

$$F_z(\tau_z,\tau_o) = 2\mathcal{E}_3(\tau_z,\beta) + 2\int_1^{\infty} \bar{q}_{zA}(\tau_z,\sqrt{t^2+\beta^2},\tau_o)\,\frac{dt}{t^2} - 2\int_1^{\infty} \frac{e^{-\tau_z\sqrt{t^2+\beta^2}}}{t^2\sqrt{t^2+\beta^2}}\,dt . \quad (3.148)$$

Replacement of τ_z by $\tau_o-\tau_z$ in equation (3.148) yields

$$F_z(\tau_o-\tau_z,\tau_o) = 2\mathcal{E}_3(\tau_o-\tau_z,\beta) + 2\int_1^\infty \bar{q}_{zA}(\tau_o-\tau_z,\sqrt{t^2+\beta^2},\tau_o)\frac{dt}{t^2}$$

$$- 2\int_1^\infty \frac{e^{-(\tau_o-\tau_z)\sqrt{t^2+\beta^2}}}{t^2\sqrt{t^2+\beta^2}}\,dt \quad . \tag{3.149}$$

Substitution of equations (3.148) and (3.149) into equation (3.137) yields the desired relationship between the flux for the cosine varying diffuse boundary and the flux for the cosine varying collimated boundary in the form

$$\bar{q}_{zC}(\tau_z,\tau_o) = \theta_2^4\left[2\mathcal{E}_3(\tau_z,\beta) + 2\int_1^\infty \bar{q}_{zA}(\tau_z,\sqrt{t^2+\beta^2},\tau_o)\frac{dt}{t^2}\right.$$

$$\left. - 2\int_1^\infty \frac{e^{-\tau_z\sqrt{t^2+\beta^2}}}{t^2\sqrt{t^2+\beta^2}}\,dt\right]$$

$$- \theta_1^4\left[2\mathcal{E}_3(\tau_o-\tau_z,\beta) + 2\int_1^\infty \bar{q}_{zA}(\tau_o-\tau_z,\sqrt{t^2+\beta^2},\tau_o)\frac{dt}{t^2}\right.$$

$$\left. - 2\int_1^\infty \frac{e^{-(\tau_o-\tau_z)\sqrt{t^2+\beta^2}}}{t^2\sqrt{t^2+\beta^2}}\,dt\right] \quad . \tag{3.150}$$

5. CONSTANT TEMPERATURE STRIP

The analysis of this section is concerned with expressing the z-component of flux due to constant temperature strips in terms of the z-component of flux due to the cosine varying diffuse boundary.

Figures 3.3 and 3.5 exhibit these physical models. The z-component of flux for the cosine varying diffuse walls, equation (3.120), can be written in the following form

$$q_{zC}(\tau_z,\tau_o) = \frac{2}{\pi}\tau_z^2 \int_{-\infty}^{\infty}\int_1^{\infty}\int_1^{\infty}\int_1^{\infty} \bar{\sigma}\, T_2^4 e^{i\beta\tau'_y} K_o[xyz\sqrt{\tau_z^2+(\tau_y-\tau'_y)^2}]xy^2 dxdydzd\tau'_y$$

$$- \frac{2}{\pi}(\tau_o-\tau_z)^2 \int_{-\infty}^{\infty}\int_1^{\infty}\int_1^{\infty}\int_1^{\infty} \bar{\sigma}\, T_1^4 e^{i\beta\tau'_y} K_o[xyz\sqrt{(\tau_o-\tau_z)^2+(\tau_y-\tau'_y)^2}]xy^2 dxdydzd\tau'_y$$

$$+ \frac{2}{\pi}\int_{-\infty}^{\infty}\int_0^{\tau_z}\int_1^{\infty}\int_1^{\infty} \bar{\sigma}\, T_C^4(\tau_y+\eta,\tau'_z,\tau_o) K_o[xy\sqrt{(\tau_z-\tau'_z)^2+\eta^2}](\tau_z-\tau'_z)xdxdyd\tau'_z d\eta$$

$$- \frac{2}{\pi}\int_{-\infty}^{\infty}\int_{\tau_z}^{\tau_o}\int_1^{\infty}\int_1^{\infty} \bar{\sigma}\, T_C^4(\tau_y+\eta,\tau'_z,\tau_o)$$

$$K_o[xy\sqrt{(\tau_z-\tau'_z)^2+\eta^2}](\tau'_z-\tau_z)xdxdyd\tau'_z d\eta \ . \qquad (3.151)$$

By employing the Fourier integral representation of the constant temperature strip boundary conditions of equations (3.83) and (3.84) in equation (3.120), the z-component of flux for the constant temperature strip is obtained in the form

$$q_{zD}(\tau_z,\tau_o) = \frac{2}{\pi}\tau_z^2 \int_{-\infty}^{\infty}\int_1^{\infty}\int_1^{\infty}\int_1^{\infty}\left[\int_{-\infty}^{\infty} \bar{\sigma}\, T_2^4 \frac{\sin(\beta\tau_a)}{\pi\beta} e^{i\beta\tau'_y}\, d\beta\right]$$

$$K_o[xyz\sqrt{\tau_z^2+(\tau_y-\tau'_y)^2}]xy^2 dxdydzd\tau'_y$$

$$- \frac{2}{\pi} (\tau_o - \tau_z)^2 \int_{-\infty}^{\infty} \int_1^{\infty} \int_1^{\infty} \int_1^{\infty} \left[\int_{-\infty}^{\infty} \bar{\sigma} T_1^4 \frac{\sin(\beta\tau_a)}{\pi\beta} e^{i\beta\tau_y'} d\beta \right]$$

$$K_o[xyz\sqrt{(\tau_o-\tau_z)^2+(\tau_y-\tau_y')^2}]xy^2 dx dy dz d\tau_y'$$

$$+ \frac{2}{\pi} \int_{-\infty}^{\infty} \int_0^{\tau_z} \int_1^{\infty} \int_1^{\infty} \bar{\sigma} T_D^4(\tau_y+\eta, \tau_z', \tau_o)$$

$$K_o[xy\sqrt{(\tau_z-\tau_z')^2+\eta^2}](\tau_z-\tau_z')x dx dy d\tau_z' d\eta$$

$$- \frac{2}{\pi} \int_{-\infty}^{\infty} \int_{\tau_z}^{\tau_o} \int_1^{\infty} \int_1^{\infty} \bar{\sigma} T_D^4(\tau_y+\eta, \tau_z', \tau_o)$$

$$K_o[xy\sqrt{(\tau_z-\tau_z')^2+\eta^2}](\tau_z'-\tau_z)x dx dy d\tau_z' d\eta \ . \qquad (3.152)$$

The emissive power relationship between the constant temperature strip and the cosine varying diffuse boundary has previously been developed and is given by equation (3.90). Hence, multiplying equation (3.151) by $\sin(\beta\tau_a)d\beta/\pi\beta$, integrating it from $-\infty$ to ∞, and using equation (3.90) results in an expression which when compared with equation (3.152) yields

$$q_{zD}(\tau_z, \tau_o) = \frac{1}{\pi} \int_{-\infty}^{\infty} \frac{\sin(\beta\tau_a)}{\beta} q_{zC}(\tau_z, \tau_o) d\beta \ . \qquad (3.153)$$

Equation (3.153) relates the z-component of flux for the constant temperature strip to that of the cosine varying diffuse boundary in a fashion similar to that of equation (3.118) which connects the constant collimated strip with the cosine varying collimated boundary.

IV. SEMI-INFINITE MEDIUM

A. INTRODUCTION

This chapter is concerned with the radiative flux and emissive power at the boundary of a semi-infinite medium. The fundamental equations follow directly from Chapter III as a result of letting the optical thickness τ_0 become infinite. The radiative flux and emissive power at the boundary are expressed in terms of the generalized H-function which is analogous to the one-dimensional H-function of Chandrasekhar [1,p.105]. The generalized H-function is the emissive power at τ_z=0 due to a collimated flux of cosine magnitude incident on a semi-infinite medium. Since the generalized H-function is basic to the emissive power and flux at the boundary, a detailed study of its behavior is appropriate.

The method of successive approximations is used to obtain exact numerical data for the generalized H-function at discrete points. An interpolation technique is employed whereby intermediate values are obtained in terms of the exact values. This eliminates the repetitive and time consuming effort involved in calculating the generalized H-function by exact methods. The radiative flux and emissive power at the boundary for the finite strip models are tabulated for a wide range of the parameters.

B. EMISSIVE POWER FOR COSINE VARYING BOUNDARY CONDITIONS

The analysis of this section is concerned with the emissive power at the boundary of a semi-infinite medium for cosine varying boundary conditions. First consideration is given to the cosine varying collimated boundary since it generates the generalized H-function. The integral equation that the generalized H-function

satisfies is developed and solutions are obtained by exact and approximate techniques. The emissive power for the diffuse wall radiating in a cosine fashion is then expressed in terms of the generalized H-function and its moment. Reference will be made to Figures 3.2 to 3.5 which describe the various physical models for the finite medium. However, the models for the semi-infinite medium are obtained by letting the optical thickness τ_o become infinite.

1. COLLIMATED FLUX-FORMULATION OF THE GENERALIZED H-FUNCTION

Figure 3.2 shows the physical model for the cosine varying collimated boundary condition. When the optical thickness becomes infinite, the integral equation describing the emissive power follows from equation (3.37)

$$B_\beta(\tau_z,\sigma) = e^{-\sigma\tau_z} + \frac{1}{2}\int_0^\infty \mathcal{E}_1(|\tau_z-\tau_z'|,\beta)B_\beta(\tau_z',\sigma)d\tau_z' \tag{4.1}$$

where

$$B_\beta(\tau_z,\sigma) = \lim_{\tau_o\to\infty} J_\beta(\tau_z,\sigma,\tau_o) \ . \tag{4.2}$$

The integro-differential equation for $B_\beta(\tau_z,\sigma)$ is found by letting the optical thickness become infinite in equation (3.102)

$$\frac{dB_\beta(\tau_z,\sigma)}{d\tau_z} + \sigma B_\beta(\tau_z,\sigma) = B_\beta(o,\sigma)\Phi(\tau_z) \tag{4.3}$$

where

$$\Phi(\tau_z) = \frac{1}{2}\int_1^\infty \frac{B_\beta(\tau_z,\sqrt{t^2+\beta^2})dt}{\sqrt{t^2+\beta^2}} \tag{4.4}$$

and

$$B_\beta(o,\sigma) = 1 + \frac{1}{2}\int_0^\infty \mathcal{E}_1(\tau'_z,\beta)B_\beta(\tau'_z,\sigma)d\tau'_z \quad . \tag{4.5}$$

The emissive power can be found by solving either equation (4.1) or equation (4.3). However, equation (4.3) is the most suitable since the integro-differential equation can be reduced to a system of ordinary differential equations which are easily solved numerically. The initial condition $B_\beta(o,\sigma)$ is also an unknown function which must be determined before equation (4.3) can be solved. Since this investigation is concerned with the behavior at the boundary, the main objective of this section is to determine $B_\beta(o,\sigma)$. In particular, $B_\beta(o,\sigma)$ will be shown to be analogous to the one-dimensional H-function of Chandrasekhar. Therefore it is appropriate to recast equation (4.5) into an integral equation of the Chandrasekhar type.

When $\mathcal{E}_1(\tau'_z,\beta)$ is replaced in equation (4.5) by its integral form and the order of integration is interchanged, the following expression is obtained

$$B_\beta(o,\sigma) = 1 + \frac{1}{2}\int_1^\infty (t^2+\beta^2)^{-\frac{1}{2}} \int_0^\infty B_\beta(\tau'_z,\sigma)e^{-\tau'_z\sqrt{t^2+\beta^2}}\, d\tau'_z dt \quad . \tag{4.6}$$

An alternate form for $B_\beta(o,\sigma)$ results from defining a generalized reflection function

$$R_\beta(\sigma,\sqrt{t^2+\beta^2}) = \int_0^\infty B_\beta(\tau'_z,\sqrt{t^2+\beta^2})e^{-\sigma\tau'_z}\, d\tau'_z \tag{4.7}$$

which is analogous to the reflection function of Chandrasekhar. Inserting equation (4.7) into equation (4.6) yields

$$B_\beta(o,\sigma) = 1 + \frac{1}{2}\int_1^\infty \frac{R_\beta(\sqrt{t^2+\beta^2},\sigma)dt}{\sqrt{t^2+\beta^2}} \quad . \tag{4.8}$$

Equation (4.8) is further simplified by finding the relationship between the reflection function $R_\beta(\sqrt{t^2+\beta^2},\sigma)$ and the emissive power at the boundary. This relationship is obtained by letting $\sigma=\sqrt{t^2+\beta^2}$ in equation (4.3), multiplying it by $e^{-\sigma\tau_z}d\tau_z$ and integrating from 0 to ∞ to obtain

$$\int_0^\infty \frac{dB_\beta(\tau_z,\sqrt{t^2+\beta^2})}{d\tau_z} e^{-\sigma\tau_z}\, d\tau_z + \sqrt{t^2+\beta^2}\; R_\beta(\sigma,\sqrt{t^2+\beta^2})$$

$$- B_\beta(o,\sqrt{t^2+\beta^2}) \int_0^\infty \Phi(\tau_z)e^{-\sigma\tau_z}\, d\tau_z = 0 \quad . \tag{4.9}$$

Integrating the first term in equation (4.9) by parts and utilizing equation (4.7) yields

$$\int_0^\infty \frac{dB_\beta(\tau_z,\sqrt{t^2+\beta^2})}{d\tau_z} e^{-\sigma\tau_z}\, d\tau_z = \sigma R_\beta(\sigma,\sqrt{t^2+\beta^2}) - B_\beta(o,\sqrt{t^2+\beta^2}) \quad . \tag{4.10}$$

Substitution of equation (4.10) into equation (4.9) then results in

$$(\sigma+\sqrt{t^2+\beta^2})R_\beta(\sigma,\sqrt{t^2+\beta^2}) = B_\beta(o,\sqrt{t^2+\beta^2})\left[1 + \int_0^\infty \Phi(\tau_z)e^{-\sigma\tau_z}\, d\tau_z\right] . \tag{4.11}$$

An additional simplification is obtained by relating $\Phi(\tau_z)$ to the emissive power at the boundary. This simplification is accomplished

by multiplying equation (4.4) by $e^{-\sigma\tau_z}\,d\tau_z$ and integrating it from 0 to ∞ to obtain

$$\int_0^\infty \Phi(\tau_z)e^{-\sigma\tau_z}\,d\tau_z = \int_0^\infty \left[\frac{1}{2}\int_1^\infty \frac{B_\beta(\tau_z,\sqrt{t^2+\beta^2})dt}{\sqrt{t^2+\beta^2}}\right]e^{-\sigma\tau_z}\,d\tau_z \quad . \tag{4.12}$$

After interchanging the order of integration of equation (4.12), the following expression is obtained

$$\int_0^\infty \Phi(\tau_z)e^{-\sigma\tau_z}\,d\tau_z = \frac{1}{2}\int_1^\infty \frac{dt}{\sqrt{t^2+\beta^2}}\left[\int_0^\infty B_\beta(\tau_z,\sqrt{t^2+\beta^2})e^{-\sigma\tau_z}\,d\tau_z\right] . \tag{4.13}$$

Next, insertion of equation (4.7) into equation (4.13) gives

$$\int_0^\infty \Phi(\tau_z)e^{-\sigma\tau_z}\,d\tau_z = \frac{1}{2}\int_1^\infty \frac{R_\beta(\sigma,\sqrt{t^2+\beta^2})dt}{\sqrt{t^2+\beta^2}} \quad . \tag{4.14}$$

By utilizing the symmetry of the reflection function as shown in Appendix C, equations (4.8) and (4.14) can be combined to yield the relation

$$B_\beta(o,\sigma) = 1 + \int_0^\infty \Phi(\tau_z)e^{-\sigma\tau_z}\,d\tau_z \quad . \tag{4.15}$$

Substitution of equation (4.15) into equation (4.11) then gives the reflection function expressed in terms of the emissive power at the boundary as

$$R_\beta(\sigma,\sqrt{t^2+\beta^2}) = \frac{B_\beta(o,\sqrt{t^2+\beta^2})B_\beta(o,\sigma)}{\sigma + \sqrt{t^2+\beta^2}} \quad . \tag{4.16}$$

An integral equation for the emissive power at the boundary is obtained by inserting equation (4.16) into equation (4.8). This

yields

$$B_\beta(o,\sigma) = 1 + \frac{1}{2} B_\beta(o,\sigma) \int_1^\infty \frac{B_\beta(o,\sqrt{t^2+\beta^2})dt}{(\sigma+\sqrt{t^2+\beta^2})\sqrt{t^2+\beta^2}} \quad . \tag{4.17}$$

The change of variable $x = \sqrt{1+\beta^2}/\sqrt{t^2+\beta^2}$ reduces equation (4.17) to

$$B_\beta(o,\sigma) = 1 + \frac{1}{2} B_\beta(o,\sigma) \int_0^1 \frac{\sqrt{1+\beta^2}\ B_\beta(o,\sqrt{1+\beta^2}/x)dx}{\sqrt{1+\beta^2(1-x^2)}\ (x\sigma+\sqrt{1+\beta^2})} \quad . \tag{4.18}$$

A further transformation with $\mu=\sqrt{1+\beta^2}/\sigma$ reduces equation (4.18) to

$$H(\mu,\beta) = 1 + \mu H(\mu,\beta) \int_0^1 \frac{\psi(x,\beta)H(x,\beta)dx}{\mu+x} \tag{4.19}$$

where

$$\psi(x,\beta) = \frac{1}{2\sqrt{1+\beta^2(1-x^2)}} \tag{4.20}$$

and

$$H(\mu,\beta) = B_\beta(o,\sqrt{1+\beta^2}/\mu) \tag{4.21}$$

is the emissive power at the boundary.

Equation (4.19) is of the same form as the integral equation which the H-function of Chandrasekhar satisfies. When $\beta=0$, the two-dimensional function $H(\mu,\beta)$ reduces to the one-dimensional H-function. Therefore $H(\mu,\beta)$ will be referred to as the generalized H-function. Since the H-function plays a major role in the development of the one-dimensional analysis for a semi-infinite medium, the generalized H-function should also play a major role in the two-dimensional investigation. The generalized H-function will be shown to appear in the emissive power and radiative flux at the boundary for the cosine

varying diffuse and collimated models as well as for those of the finite strip. Hence, a detailed knowledge of the behavior of the generalized H-function is necessary.

2. CALCULATION OF THE GENERALIZED H-FUNCTION

Two methods of solution are considered in the present investigation. The first technique is the method of discrete ordinates, and the second involves direct iteration on the integral equation. Both of these methods have been used by Chandrasekhar [1] in his one-dimensional development of radiative transfer. Since the generalized H-function satisfies a nonlinear integral equation of the Chandrasekhar type, all of the theorems relating to the one-dimensional H-function should apply to the two-dimensional analysis with corresponding restrictions on the weight function $\psi(\mu,\beta)$.

a. METHOD OF DISCRETE ORDINATES

The method of discrete ordinates involves approximating the integral in equation (4.19) by a finite sum. This approach results in the generalized H-function satisfying the following equation

$$H(\mu,\beta) = 1 + \mu H(\mu,\beta) \sum_{j=1}^{n} \frac{a_j \psi(\mu_j,\beta) H(\mu_j,\beta)}{\mu+\mu_j} \tag{4.22}$$

where $a_{\pm j}(j=1,\ldots n,\ a_j=a_{-j})$ and $\mu_{\pm j}(j=1,\ldots n,\ \mu_{-j}=-\mu_j)$ are weights and divisions appropriate for a Gaussian quadrature in the interval $(-1,1)$. Chandrasekhar [1,p.114] shows that the unique solution of equation (4.42) can be represented by

$$H(\mu,\beta) = \frac{1}{\mu_1\mu_2\cdots\mu_n} \frac{\prod_{j=1}^{n} (\mu+\mu_j)}{\prod_{j=1}^{n} (1+\mu k_j(\beta))} \tag{4.23}$$

where the $k_j(\beta)$'s are the non-negative roots of the associated characteristic equation

$$1 = 2 \sum_{j=1}^{n} \frac{a_j \psi(\mu_j,\beta)}{1-\mu_j^2 k_j^2(\beta)} \quad . \tag{4.24}$$

Equation (4.22) and its solution (4.23) are valid for all values $\mu \geq 0$. Equation (4.22) requires $H(\mu,\beta)$ to be known at discrete ordinates $H(\mu_j,\beta)$ corresponding to each abscissa $\mu=\mu_j$ which are the divisions of the Gaussian quadrature. The solution to equation (4.22) does not explicitly contain $H(\mu_j,\beta)$ but does include the μ_j terms. If $H(\mu,\beta)$ is a smooth and continuous function, equation (4.23) should approach the exact value as n is increased. Increasing n has the effect of refining the divisions μ_j, thereby increasing the number of roots $k_j(\beta)$ which must be obtained from equation (4.24). Gaussian quadrature of even order was used to obtain the first four approximations to the generalized H-function. The first order approximation means that a Legendre polynomial of second degree was used. In general, the n-th order approximation uses a Legendre polynomial of degree 2n.

Tables D.1 and D.2 show the rate of convergence of the discrete ordinate method. The fourth order approximation indicates that two significant digits are obtained for small values of β. For larger β, three significant digits are common. The discrete ordinate method can then be used for a general analysis of the behavior of $H(\mu,\beta)$ when graphical data is required. Computational time involved for the approximate method is quite less than that by successive approximations.

The disadvantage in using the discrete ordinate method is that a high degree of accuracy requires a large order quadrature. Increasing the order of quadrature causes the characteristic roots of equation (4.24) to become closer and closer together. Hence, the roots are difficult to obtain accurately. For this reason, the discrete ordinate method was not applied to approximations greater than fourth order.

b. METHOD OF SUCCESSIVE APPROXIMATIONS

The method of successive approximations is a standard iterative technique to solve integral equations. The method consists of assuming an initial approximation to the unknown function, inserting it into the integrand, and performing the integration to yield a new approximation. If this technique is repeated with each new approximation, the result is a sequence of functions which converges to the exact solution. Denoting the n-th approximation to the generalized H-function by $H_n(\mu,\beta)$, the (n+1)-th approximation is obtained by solving

$$H_{n+1}(\mu,\beta) = 1 + \mu H_{n+1}(\mu,\beta) \int_0^1 \frac{\psi(\mu',\beta)H_n(\mu',\beta)d\mu'}{\mu+\mu'} , \qquad n=1,2,... \tag{4.25}$$

A standard initial approximation to start the iteration procedure with is the inhomogeneous term. However, the closer the initial approximation is to the true value, the fewer number of iterations will be required for convergence.

Iteration on the present form of equation (4.19) is not feasible due to the extremely slow rate of convergence. An initial approximation with an accuracy of two significant digits obtained from the

method of discrete ordinates and the use of an IBM 360 model 50 computer were not sufficient to warrant the computational time required to tabulate $H(\mu,\beta)$ to five significant digits. Chandrasekhar [1,p.107] has developed an alternate integral equation for the one-dimensional H-function which greatly increases the rate of convergence. When applied to the specific ψ defined by equation (4.20), the modified integral equation for the generalized H-function becomes

$$\frac{1}{H(\mu,\beta)} = \left[1 - \frac{1}{\beta}\arcsin\left(\frac{\beta}{\sqrt{1+\beta^2}}\right)\right]^{\frac{1}{2}} + \int_0^1 \frac{x\psi(x,\beta)H(x,\beta)dx}{x+\mu} . \quad (4.26)$$

When $\beta=0$, the square root term in equation (4.26) has the value zero which agrees with the one-dimensional result obtained by Chandrasekhar. Application of the method of successive approximations to equation (4.26) yields

$$\frac{1}{H_{n+1}(\mu,\beta)} = \left[1 - \frac{1}{\beta}\arcsin\left(\frac{\beta}{\sqrt{1+\beta^2}}\right)\right]^{\frac{1}{2}} + \int_0^1 \frac{x\psi(x,\beta)H_n(x,\beta)dx}{x+\mu} \quad (4.27)$$

$$n=1,2,\ldots$$

Solutions of equation (4.27) were obtained by using a sixteenth order Gaussian quadrature for the integral term and fifteen successive approximations. An initial approximation of unity was used to start the iterative process. The required number of quadrature points was obtained by trial and error. The test criterian was that the H-function did not change in the fifth decimal place. Iterations were performed using quadratures of order nine, sixteen, and twenty-five. A twenty-fifth order quadrature produced results which agreed to five

significant digits with those obtained from a sixteenth order quadrature. The ninth and sixteenth order results agreed to at least four significant digits except for very small μ. Hence, a sixteenth order Gaussian quadrature is the most applicable for the range of the parameters considered.

An alternate method of dividing the range of integration into two subintervals (0,.9) and (.9,1) was used to further check the previous results for the generalized H-function. This technique allows the quadrature points to be positioned in the region where they are most needed, i.e., in intervals where the function has a sharp peak or change of curvature. However, an eighth order quadrature in each subinterval produced essentially the same results as obtained from a sixteenth order quadrature in the whole interval. The results for a sixteenth order quadrature in each subinterval were in close agreement with the results from a twenty-fifth order quadrature in the entire interval. Thus, this alternate method of partitioning the interval was not utilized in tabulating the generalized H-functions.

Twenty iterations were then performed using the sixteenth order quadrature to determine the rate of convergence. The results from twenty iterations were compared with those obtained from fifteen and found to be in five decimal agreement. Functional evaluation was then performed for various values of μ using fifteen iterations and a sixteenth order Gaussian quadrature. Figure 4.1 shows the variation of $H(\mu,\beta)$ for selected values of μ and β. When $\beta=0$, the generalized H-function reduces to the one-dimensional H-function of Chandrasekhar. Figure 4.1 also reveals that the generalized H-function can be

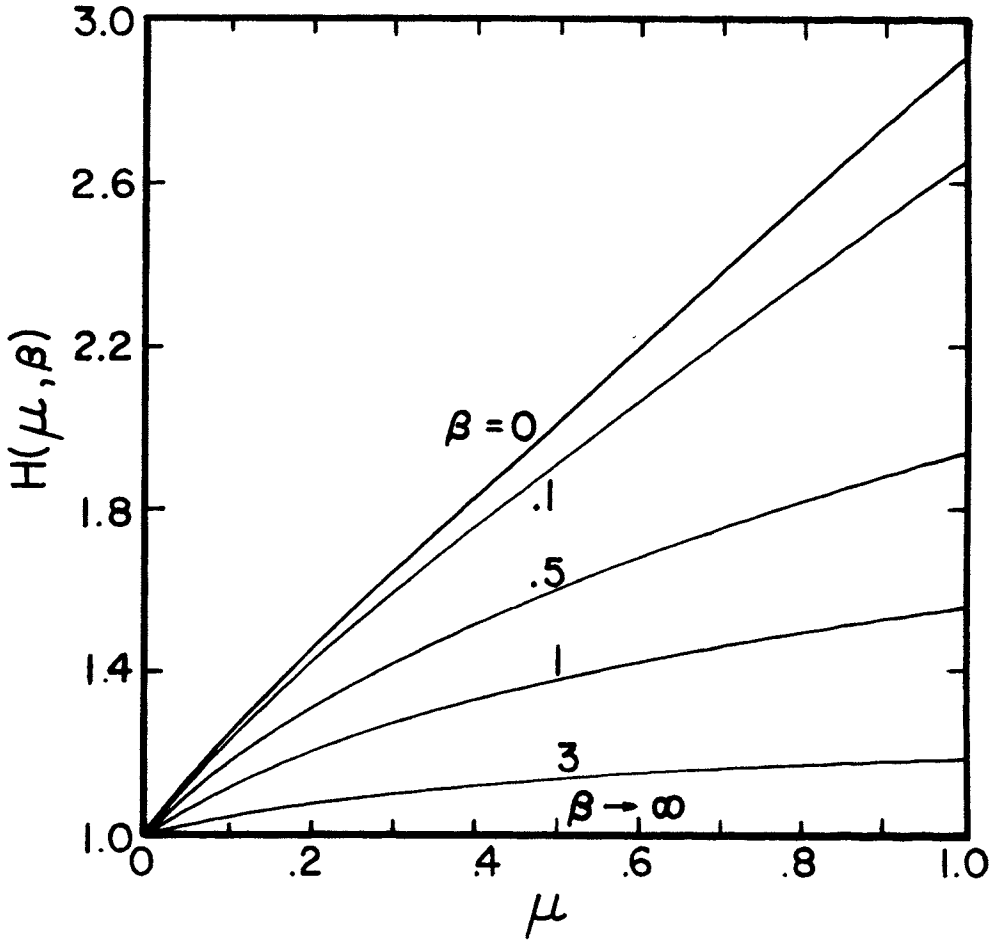

Figure 4.1 The generalized H-function versus μ for various values of β

approximated by the simpler one-dimensional H-function for small β. In particular, the generalized H-function of β=.10 differs from the one-dimensional H-function by .01196 at μ=.1, .02763 at μ=.5, and .26014 at μ=1. Hence, the error in the one-dimensional approximation is smallest at small β and μ values and increases with increasing μ.

Tables D.3 to D.6 exhibit the exact values of $H(\mu,\beta)$ and also the σ dependent form, $H(\sqrt{1+\beta^2}/\sigma,\beta)$. When β=0, $H(\mu,\beta)$ agrees to five significant digits with the one-dimensional H-function tabulated by Chandrasekhar [1,p.125]. Rybicki [19] uses the exponential kernel approximation and tabulates a function which is similar to the generalized H-function and agrees with $H(\sqrt{1+\beta^2}/\sigma,\beta)$ for five significant digits. Rybicki's function and $H(\sqrt{1+\beta^2}/\sigma,\beta)$ have reciprocal arguments with respect to the σ parameter. The limited range of β values which are available for comparison indicates five significant digits for β as large as β=20.

3. DIFFUSE BOUNDARY

Figure 3.3 shows the physical model for the cosine varying diffuse boundary condition. The emissive power for the corresponding semi-infinite medium follows from equation (3.78) by letting the optical thickness become infinite. This gives

$$\overline{\phi}_\beta(\tau_z) = \frac{1}{2}\int_0^1 \psi_1(x,\beta)B_\beta(\tau_z,\sqrt{1+\beta^2}/x)dx \qquad (4.28)$$

where

$$\overline{\phi}_\beta(\tau_z) = \lim_{\tau_o\to\infty} \phi_\beta(\tau_z,\tau_o) \quad . \qquad (4.29)$$

The emissive power at the wall $\tau_z=0$ is obtained by inserting equation (4.21) into equation (4.28). This yields an expression involving the generalized H-function

$$\overline{\phi}_\beta(o) = \frac{1}{2}\int_o^1 \psi_1(x,\beta)H(x,\beta)dx \quad . \tag{4.30}$$

A simplified form of the emissive power results from defining a moment of the generalized H-function as

$$h_n(\beta) = \int_o^1 x^n\psi_1(x,\beta)H(x,\beta)dx \quad . \tag{4.31}$$

When the emissive power is expressed in terms of $h_o(\beta)$, the following expression is obtained

$$\overline{\phi}_\beta(o) = \frac{1}{2}h_o(\beta) \quad . \tag{4.32}$$

Equation (4.32) is analogous to the one-dimensional zeroth moment of the H-function. In fact, when $\beta=0$, h_o reduces to the one-dimensional moment. The function $h_o(\beta)$ also appears in the constant temperature strip analysis of the next section. Thus, a tabulation of this function at selected values of β is useful.

The presence of $\psi_1(x,\beta)$ in the integrand of equation (4.31) complicates the numerical integration when β is large. Figure B.1 shows that $\psi_1(x,\beta)$ has a sharp peak at x=1 which becomes progressively steeper with increasing β. Therefore the integral (4.31) will require much more than a sixteenth order quadrature to obtain five significant digits for large β. The method outlined in Appendix B is used to smooth out the peak at x=1 by subtracting a function from the integrand

which causes the integrand to approach zero with increasing β. Since the peak occurs at x=1, $H(1,\beta)$ is a suitable function to subtract and later add in its integrated form. Figure B.2 shows how this technique redistributes the area under the β curves away from x=1.

Table D.7 lists values of $h_o(\beta)$ obtained from using a sixteenth order quadrature on the reduced form of equation (B.1). The data from a sixteenth order quadrature agree to five significant digits with that obtained by dividing the range of integration into subintervals (0,.9) and (.9,1) and using eighth order quadrature in each subinterval. Furthermore, the results from an eighth order quadrature in each subinterval agree to five significant digits with that obtained from a sixteenth order quadrature in each subinterval. Thus, the alternate method of dividing the integration into two separate regions was not used.

Figure 4.2 shows the variation of $\overline{\phi}_\beta(o)$ with β. The dimensionless emissive power $\overline{\phi}_\beta(o)$ has a maximum value of 1.0 at β=0 and decreases to 0.5 as β approaches infinity. The almost constant behavior of the emissive power at small β indicates that the two-dimensional emissive power can be approximated by the one-dimensional emissive power over this range. When β=.001, the one-dimensional emissive power and the two-dimensional emissive power differ by the value .0006. At β=.01, this difference increases to .0558. Hence, the error in the one-dimensional approximation increases with β. Therefore, except for small β values, the two-dimensional model must be employed.

C. EMISSIVE POWER FOR FINITE STRIP MODELS

The emissive power at the boundary for the constant temperature finite strip and the finite strip illuminated by a collimated flux of

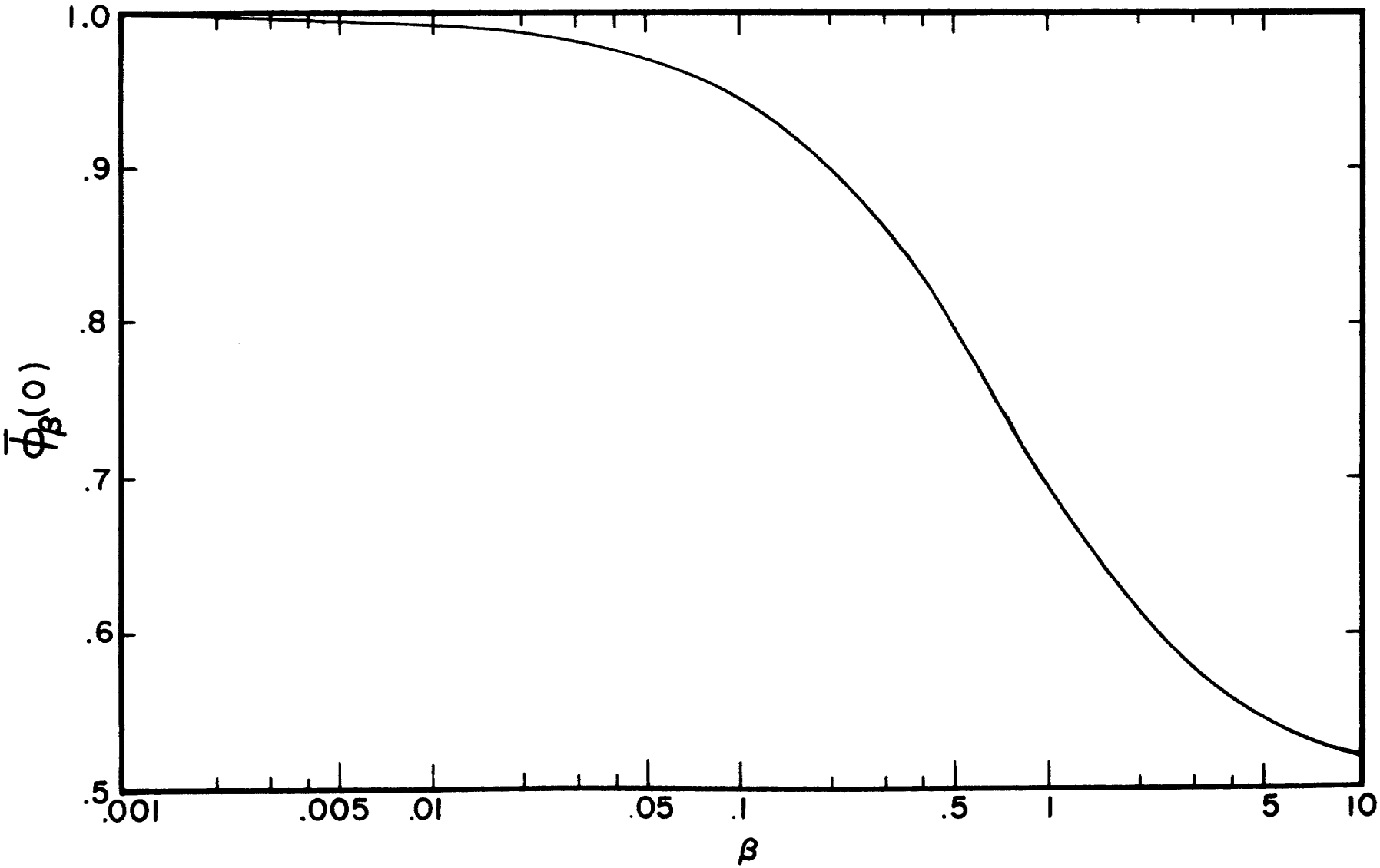

Figure 4.2 Variation in the emissive power at τ_z=0 with β for a diffuse wall radiating in a cosine fashion into a semi-infinite medium

constant magnitude have been shown to have the same mathematical form. The emissive power for each of the finite strip models involves complicated integrals of the product of an oscillating function and the generalized H-function or its moment $h_o(\beta)$. Transformations are performed on the equation for the emissive power of the constant collimated strip model which reduces it to a form favorable for numerical computation. The same transforms are then applied to the constant temperature strip since it has a similar form. Numerical techniques are discussed which reduce the computational time involved in integrating the generalized H-functions.

1. COLLIMATED FLUX-METHOD OF SOLUTION

The physical model for a finite strip subjected to a uniform collimated flux is shown in Figure 3.4. When the optical thickness becomes infinite, the emissive power for this medium is obtained from equation (3.50), that is,

$$B(\tau_y,\tau_z) = \frac{2}{\pi}\int_0^\infty B_\beta(\tau_z,\sigma)\sin(\beta\tau_a)\cos(\beta\tau_y)\,\frac{d\beta}{\beta} \tag{4.33}$$

where

$$B(\tau_y,\tau_z) = \lim_{\tau_o\to\infty} J(\tau_y,\tau_z,\tau_o) \quad . \tag{4.34}$$

The emissive power at the boundary $\tau_z=0$ is given by

$$B(\tau_y,o) = \frac{2}{\pi}\int_0^\infty B_\beta(o,\sigma)\sin(\beta\tau_a)\cos(\beta\tau_y)\,\frac{d\beta}{\beta} \quad . \tag{4.35}$$

The β dependence of the integrand in equation (4.35) is best exhibited by expressing $B_\beta(o,\sigma)$ in terms of the generalized H-function. Substituting $\mu=\sqrt{1+\beta^2}/\sigma$ into equation (4.21) yields $B_\beta(o,\sigma)=H(\sqrt{1+\beta^2}/\sigma,\beta)$.

Hence, the emissive power at the boundary for the collimated finite strip becomes

$$B(\tau_y,o) = \frac{2}{\pi}\int_o^\infty H(\sqrt{1+\beta^2}/\sigma,\beta)\sin(\beta\tau_a)\cos(\beta\tau_y)\,\frac{d\beta}{\beta} \quad . \tag{4.36}$$

Equation (4.36) can be put in a form which is more favorable for numerical computation by eliminating the cosine term in the integrand. Application of the double angle trigonometric formula for sine and cosine reduces equation (4.36) to

$$B(\tau_y,o) = \frac{1}{\pi}\int_o^\infty H(\sqrt{1+\beta^2}/\sigma,\beta)[\sin\beta(\tau_a+\tau_y) + \sin\beta(\tau_a-\tau_y)]\,\frac{d\beta}{\beta} \quad . \tag{4.37}$$

The solution of equation (4.37) involves integrals of the form $\int_o^\infty \phi(x)\sin(kx)dx/x$. The computation of integrals of this type by numerical quadrature presents great difficulty when the k parameter is large but finite. Increasing k causes the period of the trigonometric sine to decrease, thereby increasing the oscillation. Hence, the range of integration must be divided into such small increments that standard formulas such as Simpson's are impractical to use. Filon [37] developed a method for integrating trigonometric functions of the above form. However, this method proved to be useful only when ϕ diminishes rapidly. If ϕ is a slowly varying function, Filon's method requires such a large number of terms that it becomes impractical. Since the generalized H-function is a very slowly convergent function, other methods must be employed.

Since the generalized H-function approaches unity for large β and the trigonometric sine is bounded by ± 1, the integrand in equation (4.37) converges to zero in the manner of β^{-1}. Thus, the rate of convergence is quite slow at large values of β. If the infinite range of integration is to be divided into regions such that all contributions after an acceptable large β are to be considered negligible, the rate of convergence of the integrand to zero must be increased. One such way to accomplish this is to force the numerator portion of the integrand to approach zero for large β. Since the generalized H-function approaches unity for large β, the function

$$P(\sqrt{1+\beta^2}/\sigma,\beta) = H(\sqrt{1+\beta^2}/\sigma,\beta) - 1 \tag{4.38}$$

approaches zero. Hence, adding and subtracting unity from the integrand of equation (4.37) yields

$$B(\tau_y,o) = \frac{1}{\pi}\int_0^\infty [P(\sqrt{1+\beta^2}/\sigma,\beta)+1][\sin\beta(\tau_a+\tau_y)+\sin\beta(\tau_a-\tau_y)]\,\frac{d\beta}{\beta} \quad . \tag{4.39}$$

Application of the integral $\int_0^\infty \sin x\,dx/x=\pi/2$ reduces equation (4.39) to

$$B(\tau_y,o) = 1 + \frac{1}{\pi}\int_0^\infty P(\sqrt{1+\beta^2}/\sigma,\beta)[\sin\beta(\tau_a+\tau_y)+\sin\beta(\tau_a-\tau_y)]\,\frac{d\beta}{\beta} \quad . \tag{4.40}$$

A further simplification in form follows as a result of the substitution $x=\beta(\tau_a \pm \tau_y)$. The reduced emissive power is

$$B(\tau_y,o) = 1 + \frac{1}{\pi}\int_0^\infty \left[P\left(\sqrt{1+\left(\frac{x}{\tau_a+\tau_y}\right)^2}/\sigma,\ \frac{x}{\tau_a+\tau_y} \right) \right.$$

$$+ P\left[\sqrt{1+\left(\frac{x}{\tau_a-\tau_y}\right)^2}\,/\sigma,\ \frac{x}{\tau_a-\tau_y} \right] \frac{\sin x}{x}\,dx \quad . \qquad (4.41)$$

The infinite range of integration of equation (4.41) is divided into finite intervals of the type

$$\int_0^{\infty} P\left[\sqrt{1+\left(\frac{x}{\tau_a+\tau_y}\right)^2}\,/\sigma,\ \frac{x}{\tau_a+\tau_y} \right] \frac{\sin x}{x}\,dx$$

$$= \sum_{k=0}^{\infty} \int_{x=k\pi}^{(k+1)\pi} P\left[\sqrt{1+\left(\frac{x}{\tau_a+\tau_y}\right)^2}\,/\sigma,\ \frac{x}{\tau_a+\tau_y} \right] \frac{\sin x}{x}\,dx \quad . \qquad (4.42)$$

When the limits of integration of equation (4.42) are changed and the results are substituted into equation (4.41), the following series of integrals is obtained

$$B(\tau_y,o) = 1 + \frac{1}{\pi} \sum_{k=o}^{\infty} (-1)^k \int_0^{\pi} \left[P\left[\sqrt{1+\left(\frac{x+k\pi}{\tau_a+\tau_y}\right)^2}\,/\sigma,\ \frac{x+k\pi}{\tau_a+\tau_y} \right] \right.$$

$$\left. + P\left[\sqrt{1+\left(\frac{x+k\pi}{\tau_a-\tau_y}\right)^2}\,/\sigma,\ \frac{x+k\pi}{\tau_a-\tau_y} \right] \right] \frac{\sin x}{x+k\pi}\,dx \quad . \qquad (4.43)$$

The emissive power at locations beyond the strip width has a more simplified form. For $\tau_y > \tau_a$, equation (4.37) can be written as

$$B(\tau_y,o) = \frac{1}{\pi} \sum_{k=o}^{\infty} (-1)^k \int_0^{\pi} \left[P\left[\sqrt{1+\left(\frac{x+k\pi}{\tau_a+\tau_y}\right)^2}\,/\sigma,\ \frac{x+k\pi}{\tau_a+\tau_y} \right] \right.$$

$$- P\left[\sqrt{1+\left(\frac{x+k\pi}{\tau_y-\tau_a}\right)^2}\ /\sigma,\ \frac{x+k\pi}{\tau_y-\tau_a} \right] \frac{\sin x}{x+k\pi}\, dx \quad . \tag{4.44}$$

Equations (4.43) and (4.44) are selected for numerical evaluation for the following reasons: (a) the trigonometric function does not oscillate over the interval of integration, (b) the range of integration is finite, and (c) transformations are available for increasing the rate of convergence of slowly convergent alternating series. Table 4.1 shows the rate of convergence for the first ten terms of the series of equation (4.43) for $\sigma=1$ and $\tau_y=0$. For small half strip width τ_a the terms decrease quite rapidly in magnitude with the first term noticeably larger. However, at $\tau_a=100$, the convergence is very slow. Since the error involved in terminating an alternating series is at most equal to the absolute value of the first neglected term, ten terms insures three significant digits for $\tau_a=.01$. For $\tau_a=100.$, only one significant digit is apparent. Hence, a large number of terms is required to obtain $B(\tau_y,o)$ accurate to five significant digits. In order to make this series practical for numerical use, a transformation must be applied which reduces the number of terms required for convergence.

A technique which is suitable for speeding up the convergence of an alternating series is the Euler transform [38,p.100]. When applied to a series of the form

$$\sum_{n=o}^{\infty} (-1)^n v_n \ ,$$

the Euler transform yields

Table 4.1 Termwise evaluation of $B(\tau_y,o)$ for $\sigma=1$ and $\tau_y=0$

$$\int_0^{\pi}\left[P\left(\sqrt{1+\left(\frac{x+k\pi}{\tau_a+\tau_y}\right)^2}/\sigma,\frac{x+k\pi}{\tau_a+\tau_y}\right)+P\left(\sqrt{1+\left(\frac{x+k\pi}{\tau_a-\tau_y}\right)^2}/\sigma,\frac{x+k\pi}{\tau_a-\tau_y}\right)\right]\frac{\sin x}{x+k\pi}\,dx$$

k	τ_a=.01	τ_a=.10	τ_a=1.0	τ_a=10.0	τ_a=100.0
0	.099871	.638051	2.911267	6.081897	6.952027
1	-.001510	-.015089	-.147050	-.919206	-1.544883
2	.000519	.005208	.051400	.399125	.872624
3	-.000260	-.002628	-.026056	-.221572	-.593770
4	.000157	.001583	.015733	.140182	.441444
5	-.000105	-.001057	-.010520	-.096382	-.345882
6	.000075	.000755	.007528	.070213	.280651
7	-.000056	-.000567	-.005654	-.053373	-.233510
8	.000043	.000441	.004401	.041916	.198009
9	-.000035	-.000352	-.003523	-.033777	-.170427

$$\sum_{n=0}^{\infty} (-1)^n v_n = \frac{1}{2} v_0 - \frac{1}{4} (Dv_0) + \frac{1}{8} (D^2 v_0) + \ldots \frac{(-1)^P}{2^{P+1}} (D^P v_0) + \ldots \quad (4.45)$$

where $D^{P+1} v_n$ is a difference defined by $D^{P+1} v_n = D^P v_{n+1} - D^P v_n$. The Euler transform can be started at any finite term of the series. In fact, an error check involves starting the transform on the n-th term and comparing the results with that obtained by starting with the (n+1)-th term. In order to demonstrate the Euler transform technique, the data appearing in Table 4.1 for $\tau_a = 1$ is used. The series to be summed can be written as

$$S = 2.911267 - .147050 + .051400 - .026056$$
$$+ .015733 - .010520 + .007528 - .005654$$
$$+ .004401 - .003523 + \ldots$$

Starting the transform on the fifth term, $v_0 = .015733$ from which the following difference table is constructed

Table 4.2 Difference table for the Euler transform

	Dv_0	$D^2 v_0$	$D^3 v_0$	$D^4 v_0$	$D^5 v_0$
.015733					
	-.005213				
.010520		.002221			
	-.002992		-.001103		
.007528		.001118		.000606	
	-.001874		-.000497		.000355
.005654		.000621		.000251	
	-.001253		-.000246		
.004401		.000375			
	-.000878				
.003523					

Hence, applying equation (4.45) with $v_0 = .015733$ to the difference from Table 4.2 yields

$$S = 2.911267 - .147050 + .051400 - .026056$$
$$+ \frac{1}{2}(.015733) - \frac{1}{4}(-.005213) + \frac{1}{8}(.002221)$$
$$- \frac{1}{16}(-.001103) + \frac{1}{32}(.000606) - \frac{1}{64}(-.000355)$$
$$= 2.799101$$

Starting the transformation with v_o=.010520 yields

$$S = 2.911267 - .147050 + .051400 - .026056 + .015733$$
$$-\left[\frac{1}{2}(.010520) - \frac{1}{4}(-.002992) + \frac{1}{8}(.001118) - \frac{1}{16}(-.000497)\right.$$
$$\left. + \frac{1}{32}(.000251)\right] = 2.799108$$

The very good agreement between the fifth and sixth result of the transformed series indicates that ten terms in equation (4.43) are sufficient for five significant digits of accuracy. This approach is an improvement over the straight forward summation which yields no more than three significant digits as shown in Table 4.1. Ten terms of equation (4.43) along with the Euler transform are also sufficient for five digits for τ_a=100. This is an increase of three digits of accuracy as compared to only two digits obtained from direct summation of forty terms.

The computational time required to calculate the emissive power for the finite strip model is greatly reduced by the application of the Euler transformation to the series of equation (4.43). However, each term of equation (4.43) involves integrating the generalized H-functions which must also be calculated before the integration can be performed. Since a relatively large order quadrature is necessary to

integrate a function which has a sharp peak as does the P-function, a large amount of computational time is spent evaluating the integrand at each of the quadrature points. Thus, another method of determining the P-function in addition to direct iteration is desired.

In order to reduce the lengthy and repetitive computations required in integrating the $H(\sqrt{1+\beta^2}/\sigma,\beta)$ functions, an interpolation technique is utilized whereby it is sufficient to have exact values of $H(\sqrt{1+\beta^2}/\sigma,\beta)$ only at selected β values. The value of $H(\sqrt{1+\beta^2}/\sigma,\beta)$ at intermediate values of β is then approximated in terms of the exact values. The number and location of the β values is determined by trial and error with the test criterion that the approximation yields five significant digits of accuracy. This criterion is met by the sixty-four values of β given by Tables D.5 and D.6. These sixty-four values are distributed somewhat evenly over seven logarithmic cycles of the range $0 \leq \beta \leq 10{,}000$ with the exception of the cycle [1,10]. Any value of $H(\sqrt{1+\beta^2}/\sigma,\beta)$ for which $\beta>10{,}000$ is assumed to be unity. Inspection of Table D.6 shows that this is a good approximation. $H(\sqrt{1+\beta^2}/\sigma,\beta)$ is unity to five significant digits for $\beta=10{,}000$.

2. NUMERICAL AND GRAPHICAL RESULTS

The emissive power for the finite strip illuminated by a collimated flux of constant magnitude was computed for values of $\sigma=1$, 2, and 5. The sixty-four values of β listed in Tables D.5 and D.6 were used in the interpolation approximation of the generalized H-function and provided five significant digits for each of the σ values. Fewer than sixty-four data points are probably sufficient for increasing σ due to the smoothing effect of the P-curves as shown in Figure 4.3.

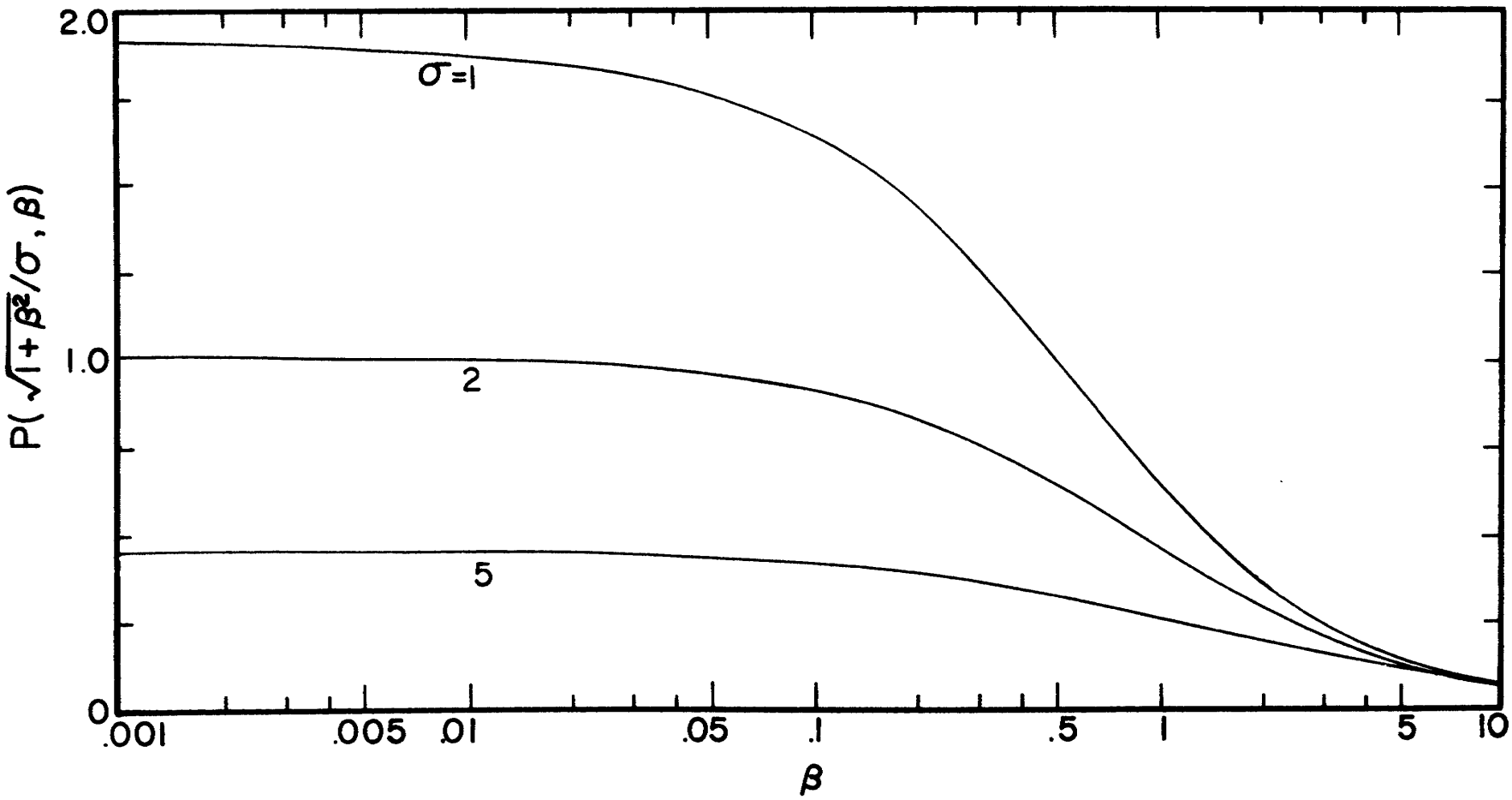

Figure 4.3 The P-function versus β for directions σ=1, 2, and 5

Tables D.8 to D.11 were obtained by using the Euler transformation and the interpolation method with forty-seventh order Gaussian quadrature for the integrations of each of the first ten terms in the series of equations (4.43) and (4.44). The relatively high order of quadrature is required for the integration of the first term which is more sensitive to the sharp peak of the P-function in the vicinity of $\beta=0$. Half strip width τ_a was also directly responsible for the magnitude of quadrature selected. A small half strip width of $\tau_a=.01$ required more quadrature points than did a larger half strip width of $\tau_a=100$.

Figure 4.4 shows the variation of the emissive power with half strip width τ_a for various values of σ. Since the incident radiation is uniform over the strip, the solution for large half strip width must approach the one-dimensional semi-infinite solution. The asymptotic behavior of the σ curves at large τ_a indicates that the finite strip solutions are approaching the one-dimensional solutions. In particular, when $\sigma=1$ and $\tau_a=100$, the finite strip solution differs from the one-dimensional result by .01851. At $\sigma=5$, this difference has reduced to .00185. Thus, a reasonably good approximation for half strip width greater than $\tau_a=100$ can be obtained by solving the much simpler one-dimensional model. The effect of decreasing the half strip width is shown in Figure 4.5 for direction $\sigma=1$. The emissive power across the strip decreases with decreasing half strip width and is essentially constant for $\tau_a=.01$. Results for half strip widths smaller than $\tau_a=.01$ were not obtained. However, the trend of the emissive power profile has been established for the limiting value of $\tau_a=0$.

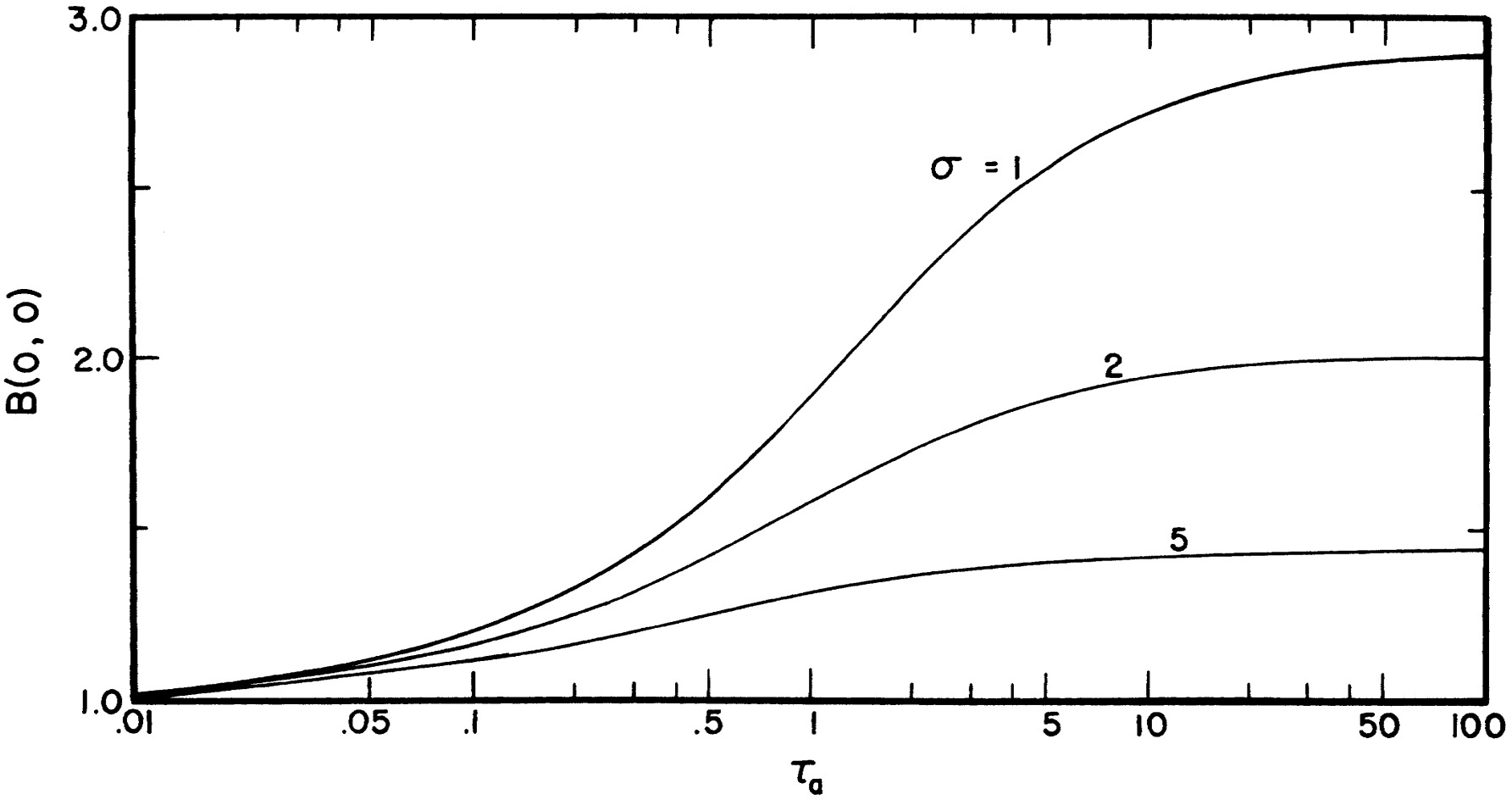

Figure 4.4 Variation in the emissive power at $\tau_z=0$ and $\tau_y=0$ for a semi-infinite medium bounded by a strip illuminated by a uniform collimated flux of magnitude F_o from directions $\sigma=1$, 2, and 5

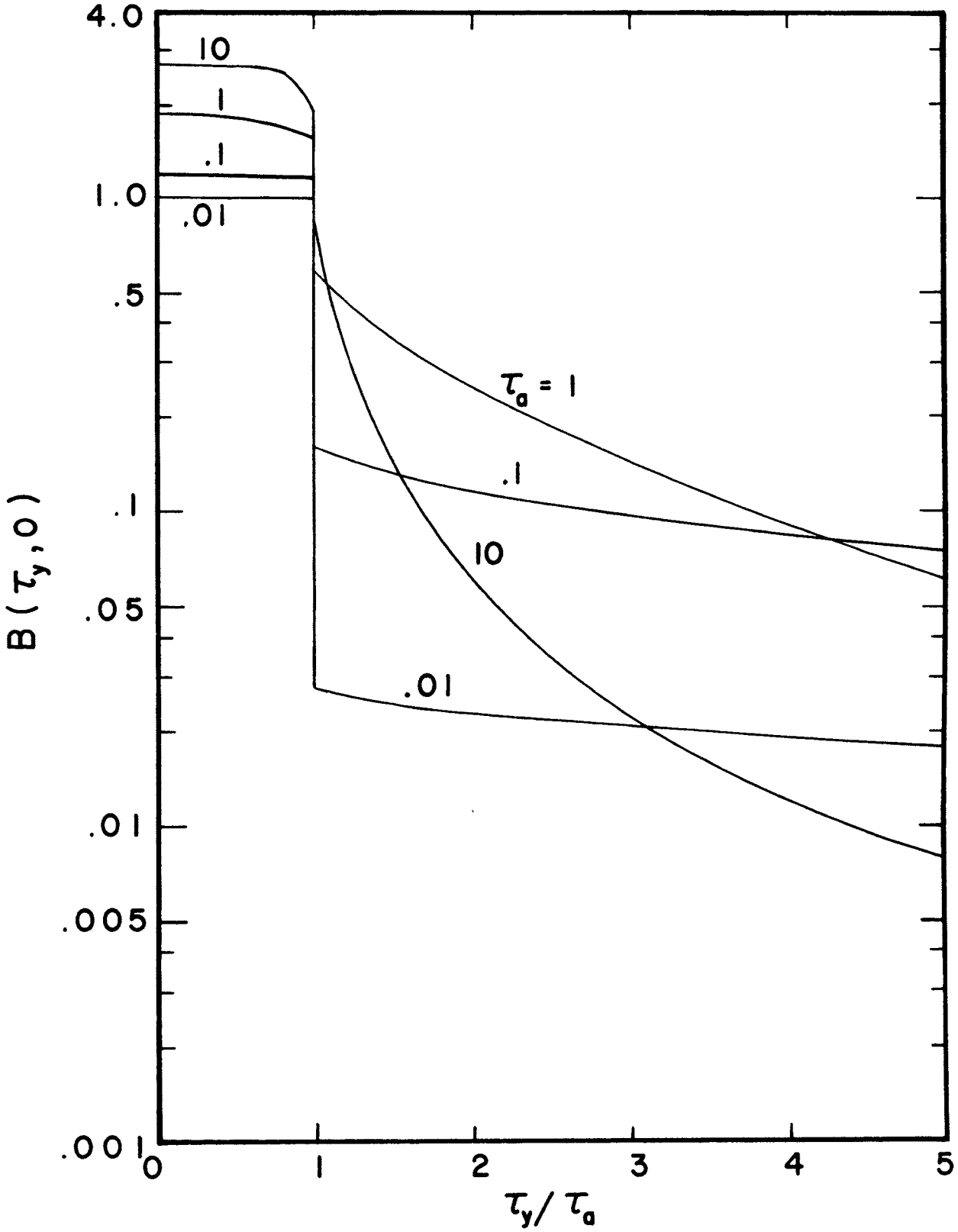

Figure 4.5 Variation in the emissive power at τ_z=0 with τ_y/τ_a for various values of τ_a for a semi-infinite medium bounded by a strip illuminated by a uniform collimated flux of magnitude F_o from direction σ=1

Figure 4.6 shows the effect of the change of direction of the incident radiation on the emissive power of the medium immediately adjacent to a strip of half width $\tau_a=1$. The emissive power is a maximum at the center and decreases across the strip with largest change occurring near the strip edge as shown by the enlarged scale in Figure 4.7. A discontinuity in the emissive power occurs at the strip edge due to the discontinuity of the incident flux at this location.

Temperature jumps are common phenomena in pure radiative transport theory where the conduction mode of energy transfer is not present to assure the continuity of temperature at the boundary. Thus, the temperature of the medium immediately adjacent to the boundary differs from the prescribed boundary value as shown in Figures 4.5 to 4.7. Physically, this type of temperature jump at the interface of the surface and bounding medium is explained by realizing that the temperature of the medium adjacent to the surface is directly affected by all other elements in the medium in addition to the surface.

Recall that $\sigma=\sec\theta_o$ where θ_o is the angle that the collimated flux makes with a normal to the plane of incidence. Figure 4.6 shows that the emissive power is a maximum for $\sigma=1$, i.e., when $\theta_o=0$, and approaches zero with increasing σ. When $\sigma\to\infty$, $\theta_o\to\pi/2$ and hence no energy enters the medium. Thus the temperature becomes constant since there is no driving force to produce a temperature difference between elements of the medium. Figure 4.6 also shows the effect of position away from the strip edge on the emissive power. The emissive power decreases with distance away from the strip edge.

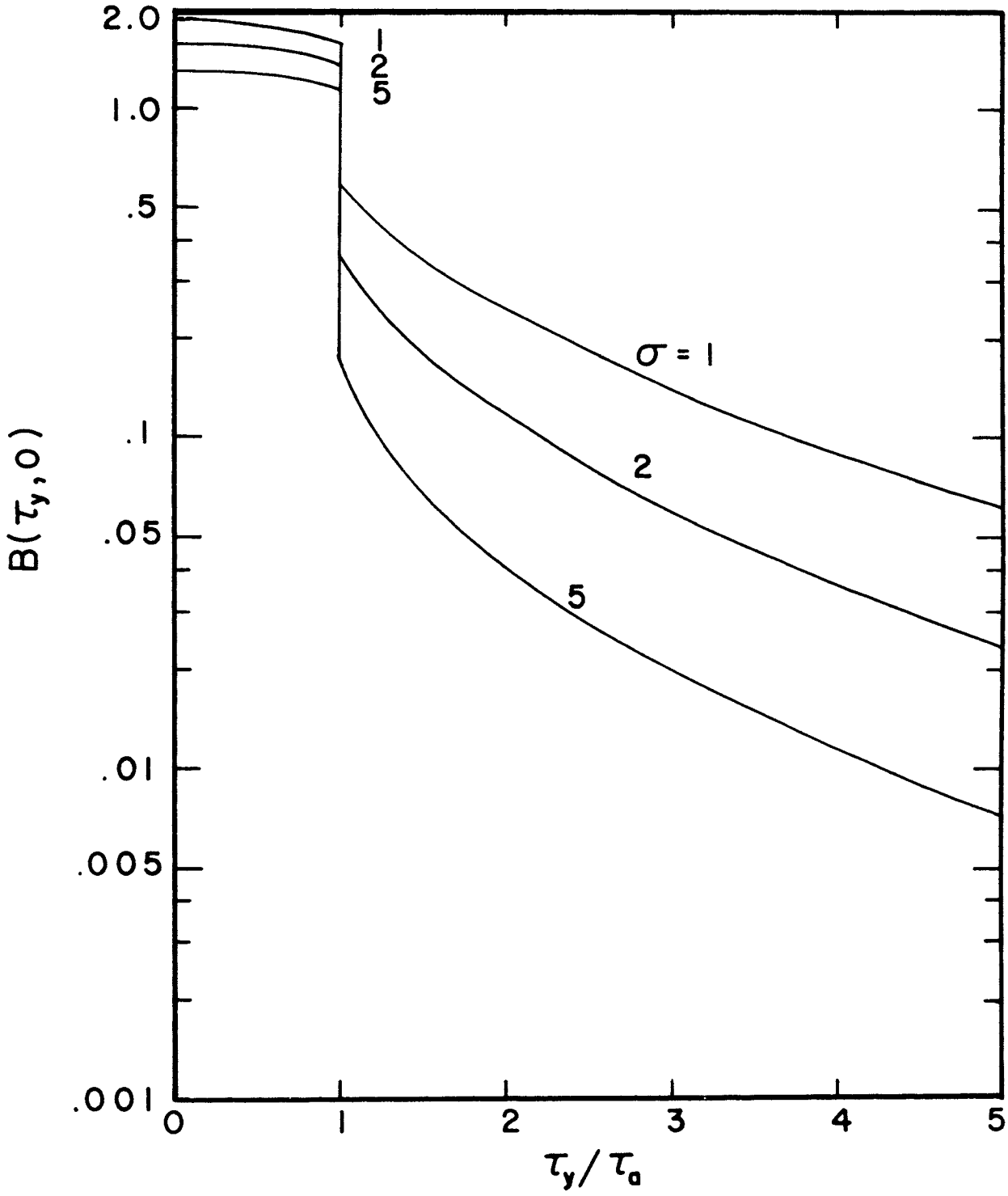

Figure 4.6 Variation in the emissive power at $\tau_z=0$ with τ_y/τ_a for $\tau_a=1$ for a semi-infinite medium bounded by a strip illuminated by a uniform collimated flux of magnitude F_o from directions $\sigma=1$, 2, and 5

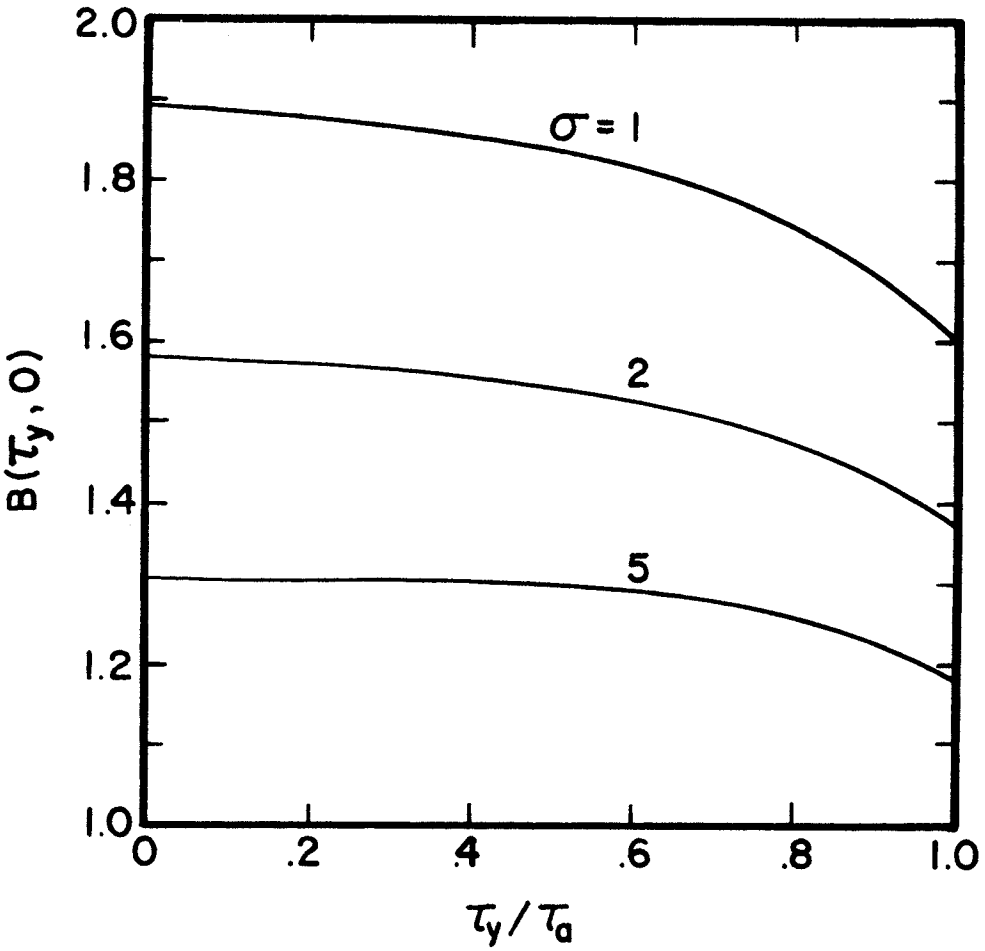

Figure 4.7 Variation in the emissive power at τ_z=0 with τ_y/τ_a for τ_a=1 for a semi-infinite medium bounded by a strip illuminated by a uniform collimated flux of magnitude F_o from directions σ=1, 2, and 5

3. DIFFUSE BOUNDARY

Figure 3.5 shows the physical model for the uniform temperature strip. The emissive power for the corresponding semi-infinite medium follows by letting the optical thickness become infinite in equation (3.94)

$$\bar{\phi}(\tau_y,\tau_z) = \frac{1}{\pi}\int_0^{\infty}\left[\int_0^1 \psi_1(x,\beta)B_\beta(\tau_z,\sqrt{1+\beta^2}/x)dx\right]\sin(\beta\tau_a)\cos(\beta\tau_y)\,\frac{d\beta}{\beta} \quad (4.46)$$

where

$$\bar{\phi}(\tau_y,\tau_z) = \lim_{\tau_o\to\infty}\phi(\tau_y,\tau_z,\tau_o) \quad . \quad (4.47)$$

By evaluating equation (4.46) at $\tau_z=0$ and utilizing equations (4.21) and (4.31), the emissive power at the boundary can be expressed in terms of the moment of the generalized H-function as

$$\bar{\phi}(\tau_y,0) = \frac{1}{\pi}\int_0^{\infty} h_0(\beta)\sin(\beta\tau_a)\cos(\beta\tau_y)\,\frac{d\beta}{\beta} \quad . \quad (4.48)$$

Equation (4.48) has the same form as the emissive power for the finite strip illuminated by a uniform collimated flux discussed in the previous section. Since $h_0(\beta)$ approaches unity as does $H(\mu,\beta)$ for large β values, a new function can be constructed for $h_0(\beta)$ that corresponds to the P-function. Thus, the method of solution used in the previous section is applicable to the constant temperature finite strip problem. The same computer program was utilized with the exception that the interpolation technique was performed from the data of Table D.7.

Table D.12 lists the variation in the emissive power of the medium immediately adjacent to the constant temperature strip as a

function of half strip width. At large half strip widths τ_a, the emissive power for the two-dimensional finite strip approaches the emissive power for the one-dimensional semi-infinite medium. This asympototic behavior occurs at relatively small τ_a values. When τ_a=20, the finite strip emissive power and the one-dimensional emissive power differ by .01835. For τ_a=50, this difference has decreased to .00747 and becomes .00368 when τ_a=100. Hence, for $\tau_a \geq 100$, the emissive power for the two-dimensional finite strip can be reasonably approximated by the simpler one-dimensional result.

For small τ_a values, the finite strip emissive power approaches the value of .50. When τ_a=.01, these two results differ by only .00979. Figure 4.8 and Table D.13 show the variation of the emissive power with τ_a. The behavior of the emissive power for the constant temperature strip is similar to that for the finite strip illuminated by a uniform flux. The emissive power is maximum at the center of the strip and decreases with distance across the strip as shown by the enlarged scale in Figure 4.9. A discontinuity in the emissive power occurs at the strip edge due to the discontinuity of the boundary condition at this location.

D. FLUX FOR COSINE VARYING BOUNDARY CONDITIONS

The analysis of this section is concerned with the z-component of the radiative flux at the boundary for a semi-infinite medium with cosine varying boundary conditions. The z-flux at the boundary due to the collimated cosine boundary is expressed in terms of the generalized H-function. This is accomplished by means of the generalized reflection function for the semi-infinite medium. The z-flux for the

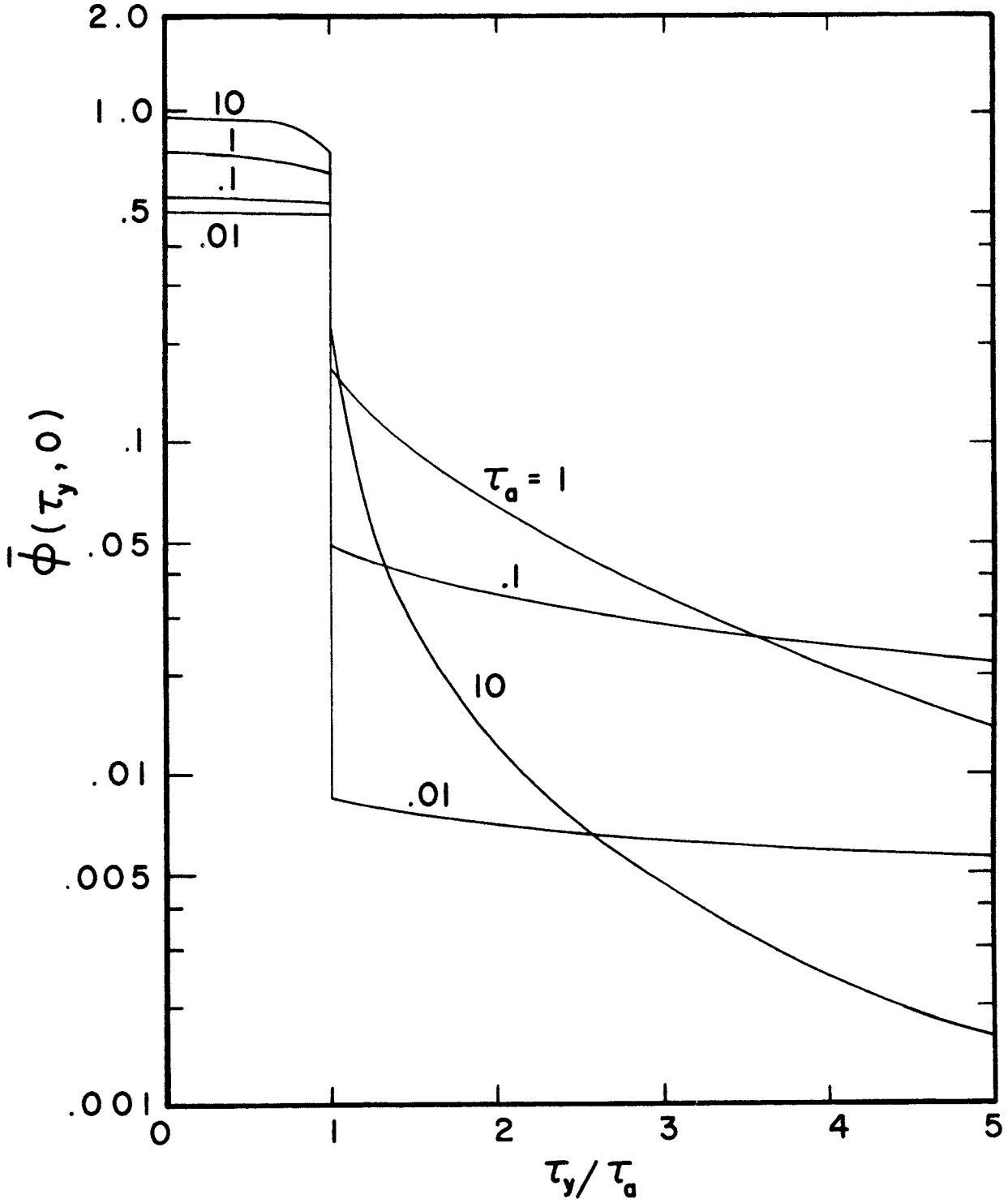

Figure 4.8 Variation in the emissive power at τ_z=0 with τ_y/τ_a for various values of τ_a for a semi-infinite medium bounded by a constant temperature strip

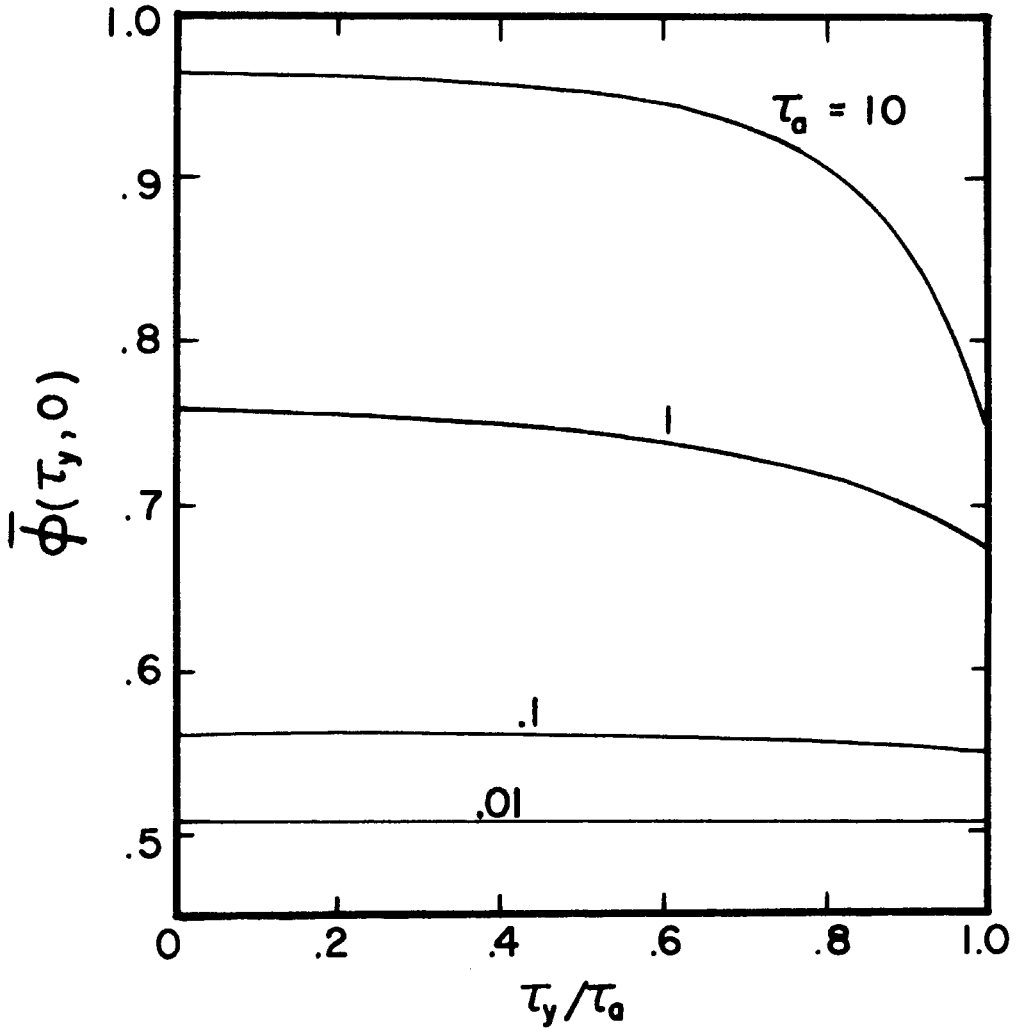

Figure 4.9 Variation in the emissive power at τ_z=0 with τ_y/τ_a for various values of τ_a for a semi-infinite medium bounded by a constant temperature strip

diffuse cosine varying boundary is then expressed in terms of the z-flux due to the collimated cosine boundary.

1. COLLIMATED FLUX

The physical model for the cosine varying collimated boundary condition is shown in Figure 3.2. The z-component of radiative flux for the corresponding semi-infinite medium follows from equation (3.112) by letting the optical thickness become infinite and utilizing equation (4.2). This gives

$$Q_\beta(\tau_z,\sigma) = \frac{1}{\sigma} e^{-\sigma\tau_z} + \frac{1}{2}\int_0^{\tau_z} B_\beta(\tau_z',\sigma)\,\mathcal{E}_2(\tau_z-\tau_z',\beta)d\tau_z'$$

$$- \frac{1}{2}\int_{\tau_z}^{\infty} B_\beta(\tau_z',\sigma)\,\mathcal{E}_2(\tau_z'-\tau_z,\beta)d\tau_z' \qquad (4.49)$$

where $Q_\beta(\tau_z,\sigma)$ is a dimensionless flux defined by

$$Q_\beta(\tau_z,\sigma) = \lim_{\tau_o\to\infty}\left[q_{zA}(\tau_z,\sigma,\tau_o)/F_o\cos(\beta\tau_y)\right] = \lim_{\tau_o\to\infty}\bar{q}_{zA}(\tau_z,\sigma,\tau_o). \qquad (4.50)$$

The boundary flux at τ_z=0 becomes

$$Q_\beta(o,\sigma) = \frac{1}{\sigma} - \frac{1}{2}\int_0^{\infty} B(\tau_z',\sigma)\,\mathcal{E}_2(\tau_z',\beta)d\tau_z' \quad . \qquad (4.51)$$

By substituting the definition of $\mathcal{E}_2(\tau_z,\beta)$ into equation (4.51), interchanging the order of integration, and utilizing equation (4.7), an expression for the flux at the boundary in terms of the generalized reflection function is obtained

$$Q_\beta(o,\sigma) = \frac{1}{\sigma} - \frac{1}{2}\int_1^{\infty} R_\beta(\sqrt{t^2+\beta^2},\sigma)\,\frac{dt}{t^2} \quad . \qquad (4.52)$$

Insertion of equation (4.16) into equation (4.52) gives a relationship between the dimensionless flux and the dimensionless emissive power at the boundary

$$Q_\beta(o,\sigma) = \frac{1}{\sigma} - \frac{1}{2}\int_1^\infty \frac{B_\beta(o,\sigma)B_\beta(o,\sqrt{t^2+\beta^2})}{t^2(\sigma^2+\sqrt{t^2+\beta^2})}\,dt \quad . \tag{4.53}$$

The change of variable $x=\sqrt{1+\beta^2}/\sqrt{t^2+\beta^2}$ introduces the generalized H-function into the expression for the flux at the boundary

$$Q_\beta(o,\sigma) = \frac{1}{\sigma} - \frac{B_\beta(o,\sigma)}{2}\int_0^1 \frac{x\psi_1(x,\beta)H(x,\beta)}{\sigma x+\sqrt{1+\beta^2}}\,dx \quad . \tag{4.54}$$

A further simplification in form is obtained by inserting $\sigma=\sqrt{1+\beta^2}/\mu$ in equation (4.54). Thus

$$\overline{Q}_\beta(o,\mu) = \frac{\mu}{\sqrt{1+\beta^2}}\left[1 - \frac{H(\mu,\beta)}{2}\int_0^1 \frac{x\psi_1(x,\beta)H(x,\beta)}{x+\mu}\,dx\right] \tag{4.55}$$

where

$$\overline{Q}_\beta(o,\mu) = Q_\beta(o,\sqrt{1+\beta^2}/\mu) \quad . \tag{4.56}$$

Equations (4.54) and (4.55) show that two forms are available for calculating the z-flux. The σ dependent form is tabulated since the angle of incidence of the collimated flux is usually specified. However, $\overline{Q}_\beta(o,\mu)$ is used to calculate the flux for the diffuse cosine boundary of the next section.

Tables D.14 to D.16 were obtained by dividing the range of integration into two intervals and using various order quadrature in each subinterval. The order of quadrature and the length of the

subinterval were obtained by trial and error. An eighth order Gaussian quadrature was sufficient for the first subinterval for each of the subdivisions considered. The second subinterval required special attention due to the sharp peak of $\psi_1(x,\beta)$ at x=1 for large β values. The quadrature and range of integration for the second interval are shown in Table 4.3.

Table 4.3 Order of quadrature and range of integration corresponding to values of β

Quadrature	Range of integration	Range of β
8	(.9,1)	$0 \leq \beta \leq 8$
16	(.9,1)	$8 \leq \beta \leq 17.5$
25	(.9,1)	$17.5 \leq \beta \leq 30$
37	(.95,1)	$30 \leq \beta \leq 60$
47	(.975,1)	$60 \leq \beta \leq 10{,}000$

The first range of $0 \leq \beta \leq 8$ yields at least five significant digits of accuracy for $Q_\beta(o,\sigma)$. The range $8 \leq \beta \leq 60$ results in at least four significant digits whereas $\beta > 60$ yields at least three significant digits for $Q_\beta(o,\sigma)$. Decreasing the length of the second interval increases the accuracy but still requires a relatively large number of quadrature points.

Figure 4.10 shows the behavior of $Q_\beta(o,\sigma)$ for the directions σ=1, 2, and 5. When β=0, the two-dimensional flux reduces to the one-dimensional result which is zero and independent of σ. $Q_\beta(o,\sigma)$ increases with increasing β and is asymptotic to $1/\sigma$ at large β values. This result is obtained by letting $\beta \to \infty$ in equation (4.54).

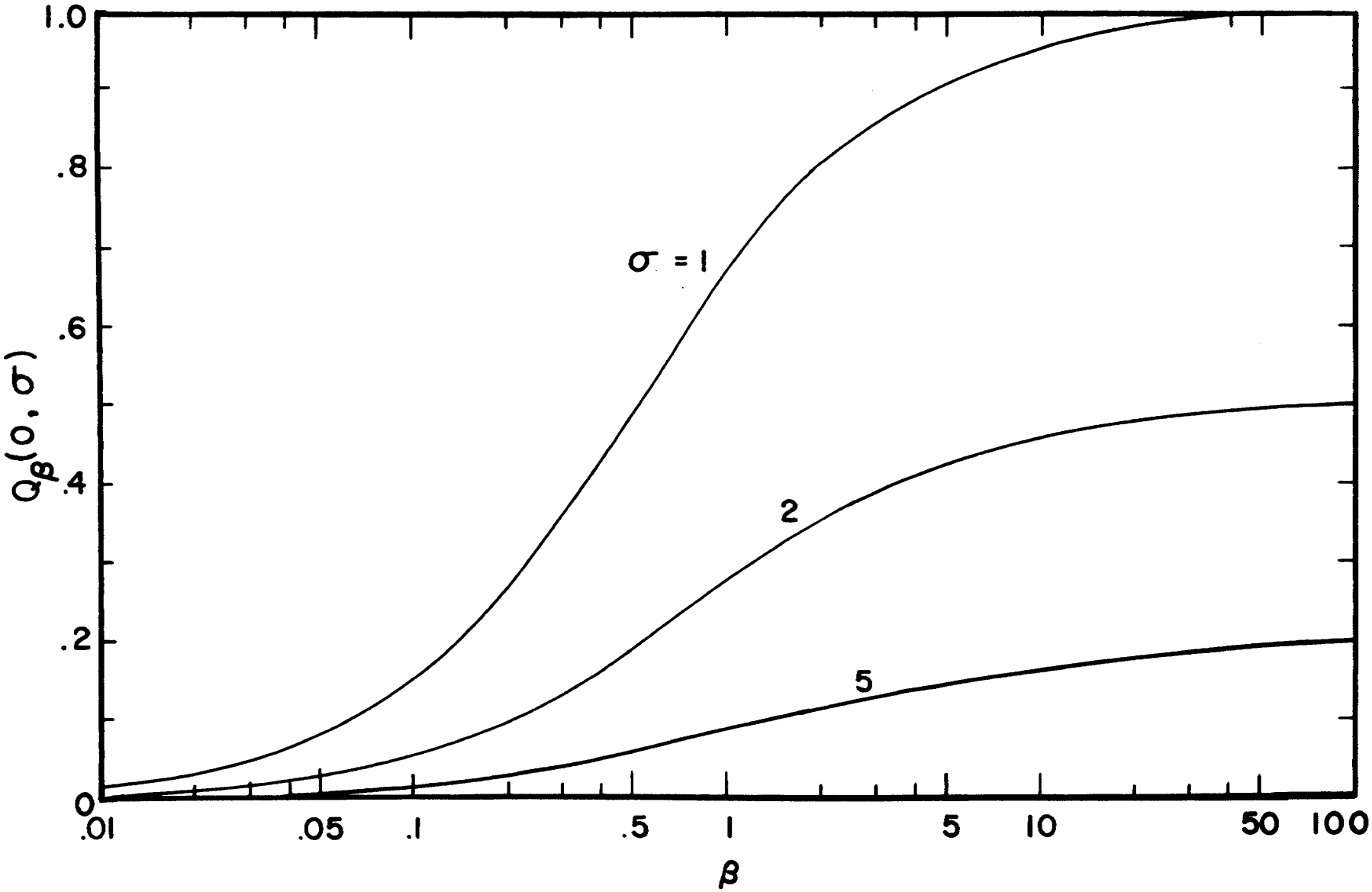

Figure 4.10 Variation in the normal flux at $\tau_z=0$ with β for a semi-infinite medium illuminated by a collimated flux of cosine magnitude from directions $\sigma=1$, 2, and 5

$Q_\beta(o,\sigma)$ is maximum at $\sigma=1$ which corresponds to the case when the incident radiation is normal to the medium and decreases to zero as σ approaches infinity. At small β values, $Q_\beta(o,\sigma)$ can be approximated by the simpler one-dimensional model. When $\beta=.001$ and $\sigma=1$, $Q_\beta(o,\sigma)$ and the one-dimensional result differ by .00167. At $\beta=.01$, this difference has increased to .01657.

2. DIFFUSE BOUNDARY

Figure 3.3 shows the physical model for the cosine varying diffuse boundary condition. The z-component of radiative flux for the corresponding semi-infinite model is obtained by letting the optical thickness become infinite in equation (3.150) and utilizing equation (4.50). This results in

$$F_\beta(\tau_z) = 2\,\mathcal{E}_3(\tau_z,\beta) + 2\int_1^\infty Q_\beta(\tau_z,\sqrt{t^2+\beta^2})\,\frac{dt}{t^2} - 2\int_1^\infty \frac{e^{-\tau_z\sqrt{t^2+\beta^2}}}{t^2\sqrt{t^2+\beta^2}}\,dt \quad (4.57)$$

where

$$F_\beta(\tau_z) = \lim_{\tau_o\to\infty}\,[\bar{q}_{zC}(\tau_z,\tau_o)/\theta_2^4] \quad . \quad (4.58)$$

The substitution $x=\sqrt{1+\beta^2}/\sqrt{t^2+\beta^2}$ reduces equation (4.57) to

$$F_\beta(\tau_z) = 2\,\mathcal{E}_3(\tau_z,\beta) + 2\int_0^1 \psi_1(x,\beta)Q_\beta(\tau_z,\sqrt{1+\beta^2}/x)dx$$

$$- 2\int_1^\infty \frac{e^{-\tau_z\sqrt{t^2+\beta^2}}}{t^2\sqrt{t^2+\beta^2}}\,dt \quad . \quad (4.59)$$

The z-flux at the boundary is obtained by inserting $\tau_z=0$ into equation (4.59) and using equation (4.56). This yields

$$F_\beta(o) = 1 + 2\int_0^1 \psi_1(x,\beta)\bar{Q}_\beta(o,x)dx + \frac{2}{\beta^2}\left(1-\sqrt{1+\beta^2}\right) . \quad (4.60)$$

The simplified form of equation (4.60) was made possible by observing that $\mathcal{E}_3(o,\beta)=.5$ and integrating the integral term. However, when $\tau_z\neq 0$, both of these terms present an added numerical difficulty.

Table D.17 lists values of the flux obtained by dividing the range of integration of equation (4.60) into two subintervals in accordance with Table 4.3. The numerical accuracy is essentially the same as the accuracy for the z-component of flux due to the cosine varying collimated boundary condition discussed in the previous section. When $\beta=0$, $F_\beta(o)$ reduces to the one-dimensional flux which is zero. The two-dimensional flux differs from the one-dimensional flux by .00133 when $\beta=.001$. At $\beta=.01$, this difference has increased to .01321. Hence, at small β values, $F_\beta(o)$ can be reasonably approximated by the simpler one-dimensional result. As β approaches infinity, $F_\beta(o)$ approaches unity as shown in Figure 4.11.

E. FLUX FOR FINITE STRIP

This section is concerned with the z-component of radiative flux at the boundary for the finite strip model. The fluxes for the uniform temperature strip and the uniform collimated strip are expressed in terms of the flux due to the cosine varying diffuse boundary condition and the cosine varying collimated boundary condition, respectively, and solved in a manner similar to the finite strip emissive power of the previous section.

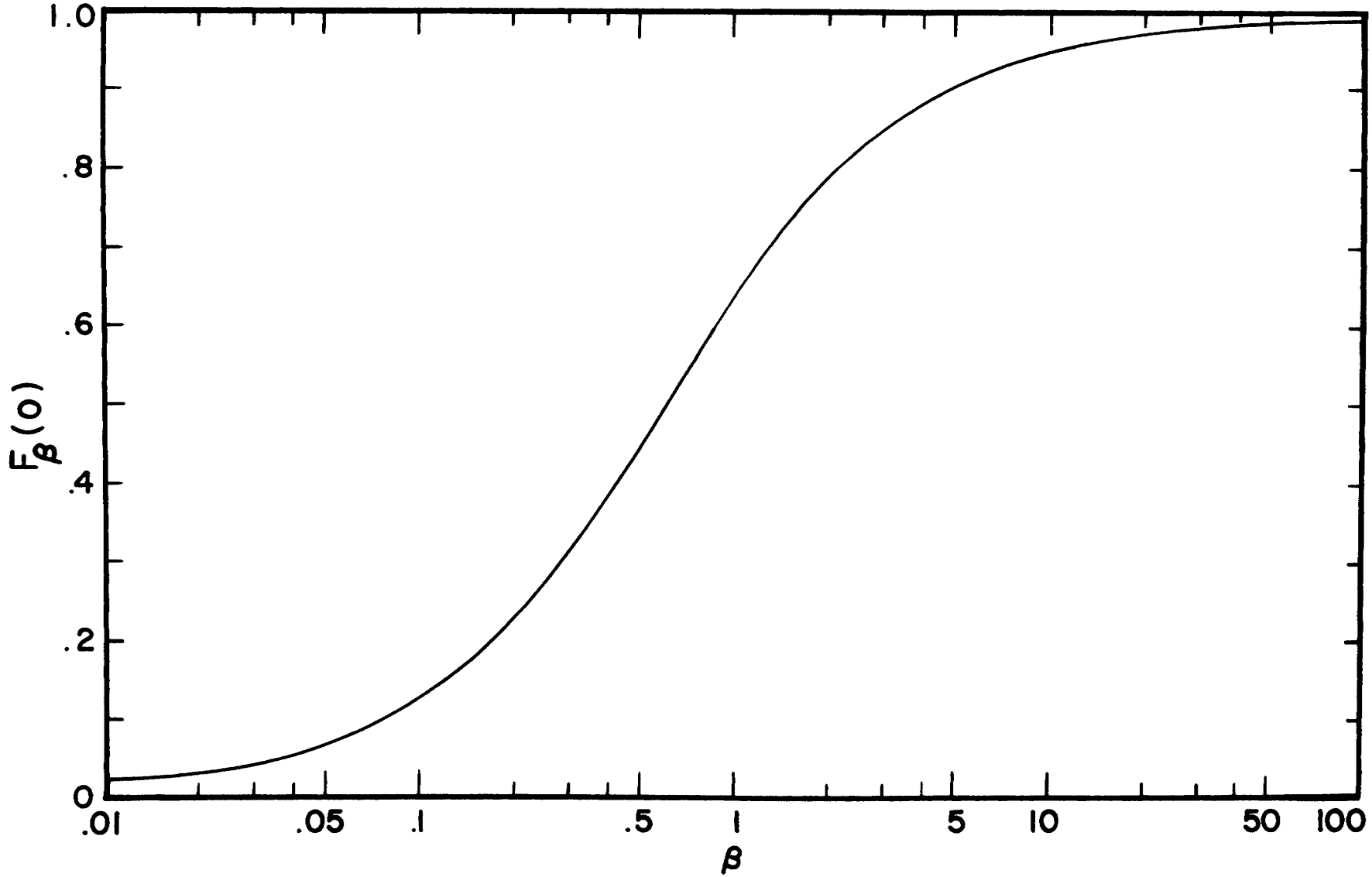

Figure 4.11 Variation in the normal flux at τ_z=0 with β for a diffuse wall radiating in a cosine fashion into a semi-infinite medium

1. COLLIMATED FLUX

The physical model for the finite strip constant collimated flux boundary condition is shown in Figure 3.4. When the optical thickness becomes infinite, the z-component of flux for this medium is obtained from equations (3.118) and (4.50) as

$$Q(\tau_y,\tau_z) = \frac{2}{\pi}\int_0^\infty Q_\beta(\tau_z,\sigma)\sin(\beta\tau_a)\cos(\beta\tau_y)\,\frac{d\beta}{\beta} \tag{4.61}$$

where $Q(\tau_y,\tau_z)$ is a dimensionless flux defined by

$$Q(\tau_y,\tau_z) = \lim_{\tau_o\to\infty}\,[q_{zB}(\tau_z,\sigma,\tau_o)/F_o] \quad . \tag{4.62}$$

The flux at the boundary τ_z=0 is

$$Q(\tau_y,o) = \frac{2}{\pi}\int_0^\infty Q_\beta(o,\sigma)\sin(\beta\tau_a)\cos(\beta\tau_y)\,\frac{d\beta}{\beta} \quad . \tag{4.63}$$

Integrals of the form of equation (4.63) are converted into a slowly converging alternating series by the method applied in calculating the emissive power of the finite strip of this chapter. The Euler transform is then applied to speed up the convergence of the resulting series. The success of the method depends on the nonoscillating part of the integrand approaching zero for sufficiently large β values. For this reason, functions of the type of the P-function of equation (4.38) are constructed. Inspection of Figure 4.10 shows that $Q_\beta(o,\sigma) \to \frac{1}{\sigma}$ as $\beta \to \infty$. Hence, the analogous P-functions to be used are σ dependent and defined as $P_\sigma = \frac{1}{\sigma} - Q_\beta(o,\sigma)$.

Tables D.18 to D.21 list the results of calculations by application of the Euler transform and the interpolation technique. The data for the interpolation approximation were obtained from Tables D.14 to D.16. Table D.18 shows the variation of Q(o,o) with half strip width τ_a at the center of the strip. Figure 4.12 depicts this variation. The finite strip flux approaches the one-dimensional value of zero as the half strip width becomes infinite. When τ_a=20 and σ=1, the two-dimensional flux and the one-dimensional flux differ by .05308. For τ_a=100, this difference has decreased to .01070. Hence, the two-dimensional flux can be approximated by the one-dimensional flux when $\tau_a \geq 100$. The flux is maximum when σ=1 which corresponds to the case when the incident radiation is normal to the strip and minimum when σ is very large. Increasing σ has the effect of allowing less energy to enter the medium.

Figure 4.13 shows the variation of the z-flux with position across and extending beyond a strip of half width τ_a=1 for constant collimated radiation from directions σ=1,2, and 5. The flux is directed into the medium over the entire strip width. This means that the amount of energy originating in the medium and passing through τ_z=0 in an outward direction as shown by the broken curves in Figure 4.13 is less than the energy which is incident on the boundary. However, a reversal in direction of flux takes place at the strip edge. A discontinuity in flux occurs at the strip edge due to the discontinuity of the incident radiation. The flux at locations beyond the strip edge is in an outward direction because no external radiation enters the medium at this location. Thus, any energy crossing

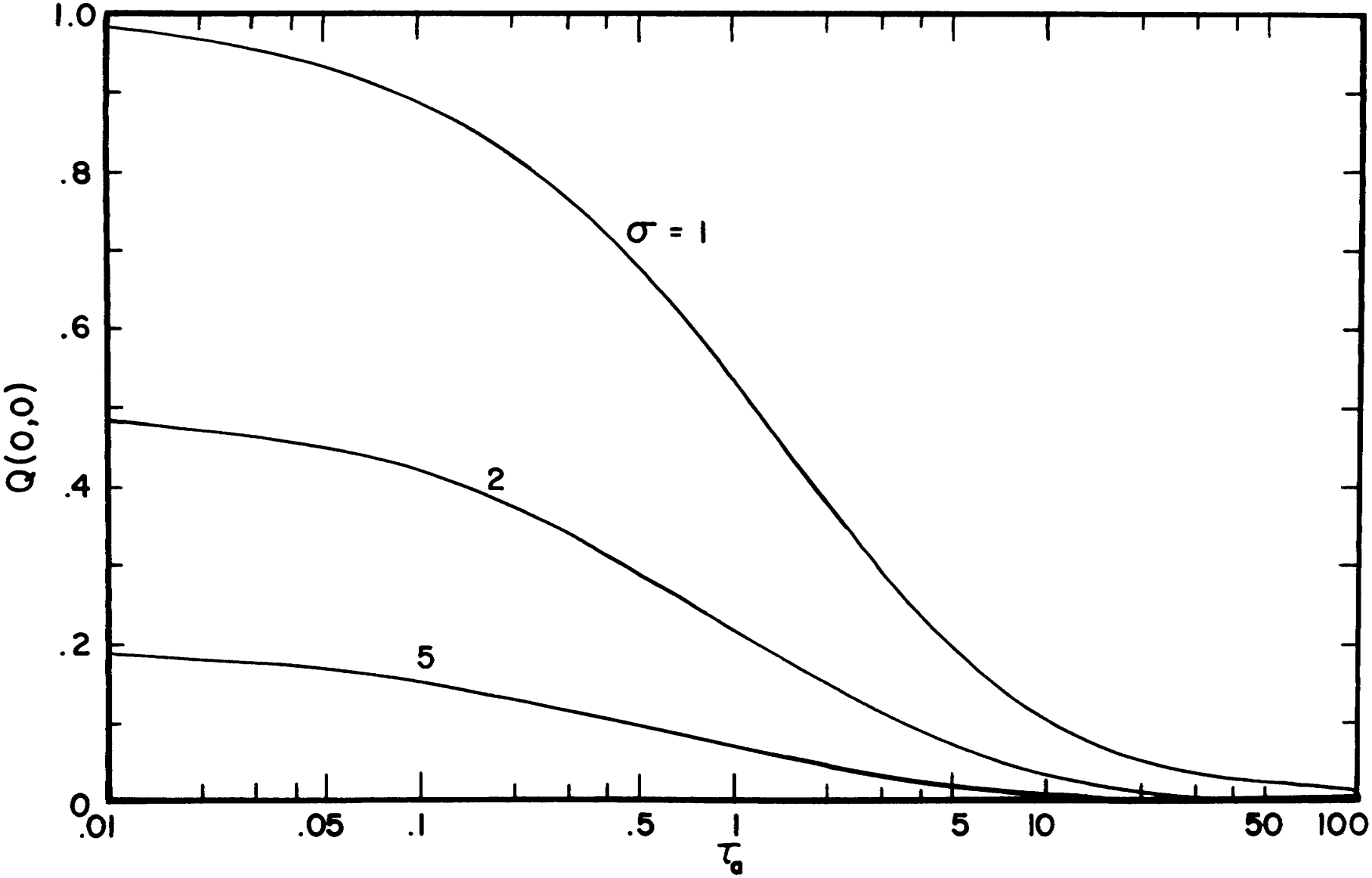

Figure 4.12 Variation in the normal flux at $\tau_z=0$ and $\tau_y=0$ with τ_a for a semi-infinite medium bounded by a strip illuminated by a uniform collimated flux of magnitude F_o from directions $\sigma=1$, 2, and 5

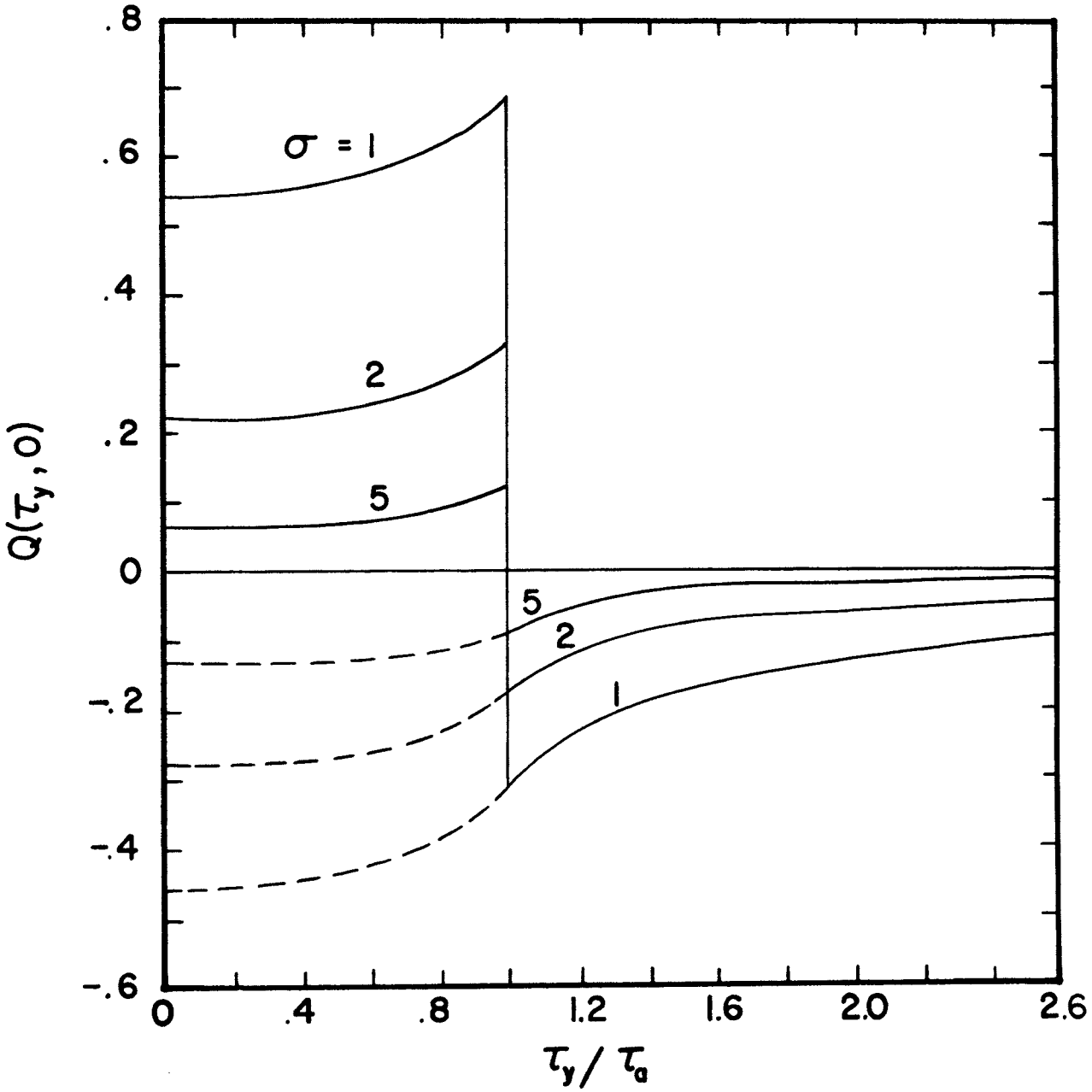

Figure 4.13 Variation in the normal flux at τ_z=0 with τ_y/τ_a for τ_a=1 for a semi-infinite medium bounded by a strip illuminated by a uniform collimated flux of magnitude F_o from directions σ=1, 2, and 5

the boundary must originate from interior of the medium. Since the medium is in radiative equilibrium, there can be no net transfer of energy. Hence, the area under the curve for the flux entering the medium must be the same as that under the curve for the flux leaving the medium. Inspection of Figure 4.13 shows that this trend appears to be satisfied.

Figure 4.13 reveals that for all σ values the flux entering the medium is a minimum at the center of the strip where the emissive power of the medium immediately adjacent to the boundary is maximum. Since the emissive power decreases with position across the strip, the flux increases to a maximum at the strip edge as shown. The flux is maximum at $\sigma=1$ and decreases inversely with σ since the area normal to the incident ratiation is directly proportional to the cosine of the angle of incidence and thus inversely proportional to σ. Figure 4.14 shows the variation in z-flux with change in half strip width for the direction $\sigma=1$. When $\tau_a \to 0$, the net flux entering the medium approaches the maximum value of unity. For $\tau_a=.01$, the net flux entering is almost unity. Hence, the emerging net flux corresponding to $\tau_a=.01$ at locations outside of the strip width must also have the same value as the net flux entering since the medium is in radiative equilibrium. This behavior indicates that the emerging flux curve must approach zero at a slow rate since the largest value the emerging flux attains is .0159 at the strip edge. When $\tau_a \to \infty$, the one-dimensional flux of zero is attained.

2. DIFFUSE BOUNDARY

Figure 3.5 shows the physical model for the constant temperature finite strip. The z-component of flux for the corresponding

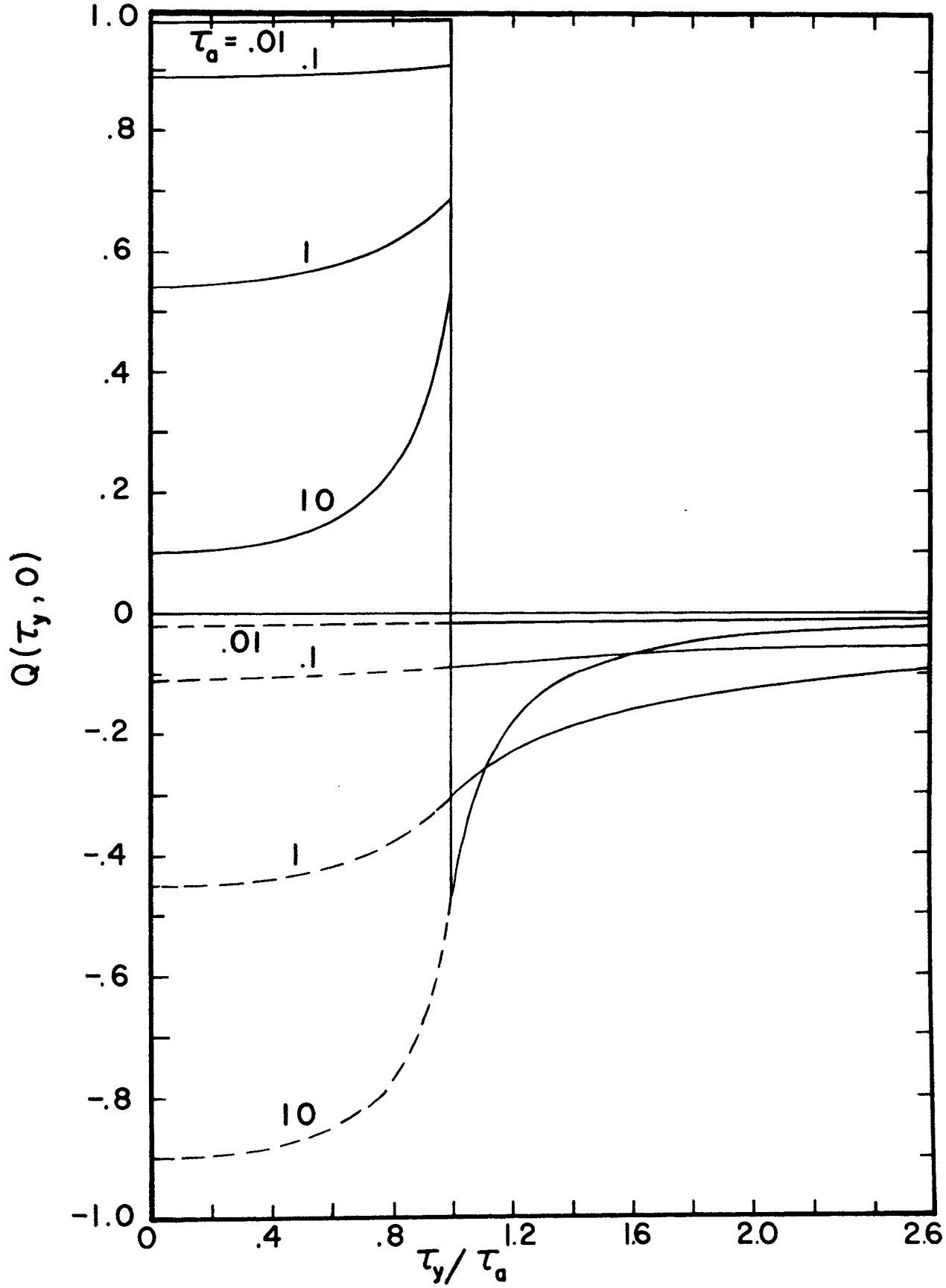

Figure 4.14 Variation in the normal flux at τ_z=0 with τ_y/τ_a for various values of τ_a for a semi-infinite medium bounded by a strip illuminated by a uniform collimated flux of magnitude F_o from direction σ=1

semi-infinite medium is obtained from equations (3.124), (3.153), and (4.58) by letting the optical thickness become infinite. This yields

$$F(\tau_y,\tau_z) = \frac{2}{\pi}\int_0^\infty F_\beta(\tau_z)\sin(\beta\tau_a)\cos(\beta\tau_y)\,\frac{d\beta}{\beta} \tag{4.64}$$

where $F(\tau_y,\tau_z)$ is a dimensionless flux defined by

$$F(\tau_y,\tau_z) = \lim_{\tau_o\to\infty}\left[q_{zD}(\tau_z,\tau_o)/\,\bar{\sigma}\,T_2^4\right] \quad . \tag{4.65}$$

The flux at the boundary τ_z=0 is

$$F(\tau_y,o) = \frac{2}{\pi}\int_0^\infty F_\beta(o)\sin(\beta\tau_a)\cos(\beta\tau_y)\,\frac{d\beta}{\beta} \quad . \tag{4.66}$$

Since $F_\beta(o)\to 1$ as $\beta\to\infty$, the function analogous to the P-function of equation (4.38) is defined as $P_\beta=1-F_\beta(o)$. Inserting P_β into equation (4.66) enables the Euler transformation and interpolation technique to be applied in calculating $F(\tau_y,o)$. Table D.22 lists the variation of the z-flux with half strip width. The finite strip solution approaches the constant temperature, one-dimensional solution of zero as the half strip width approaches infinity. Figure 4.15 shows this variation. Figure 4.16 and Table D.23 show the change of flux with position across and extending beyond strips of various half widths. The flux profiles are similar to those obtained for the constant collimated strip of the previous section. The broken curves indicate energy that is emerging from the medium through the strip.

F. CONCLUSION

The limited range of values of β and half strip width τ_a for which the two-dimensional models can be approximated by the simpler

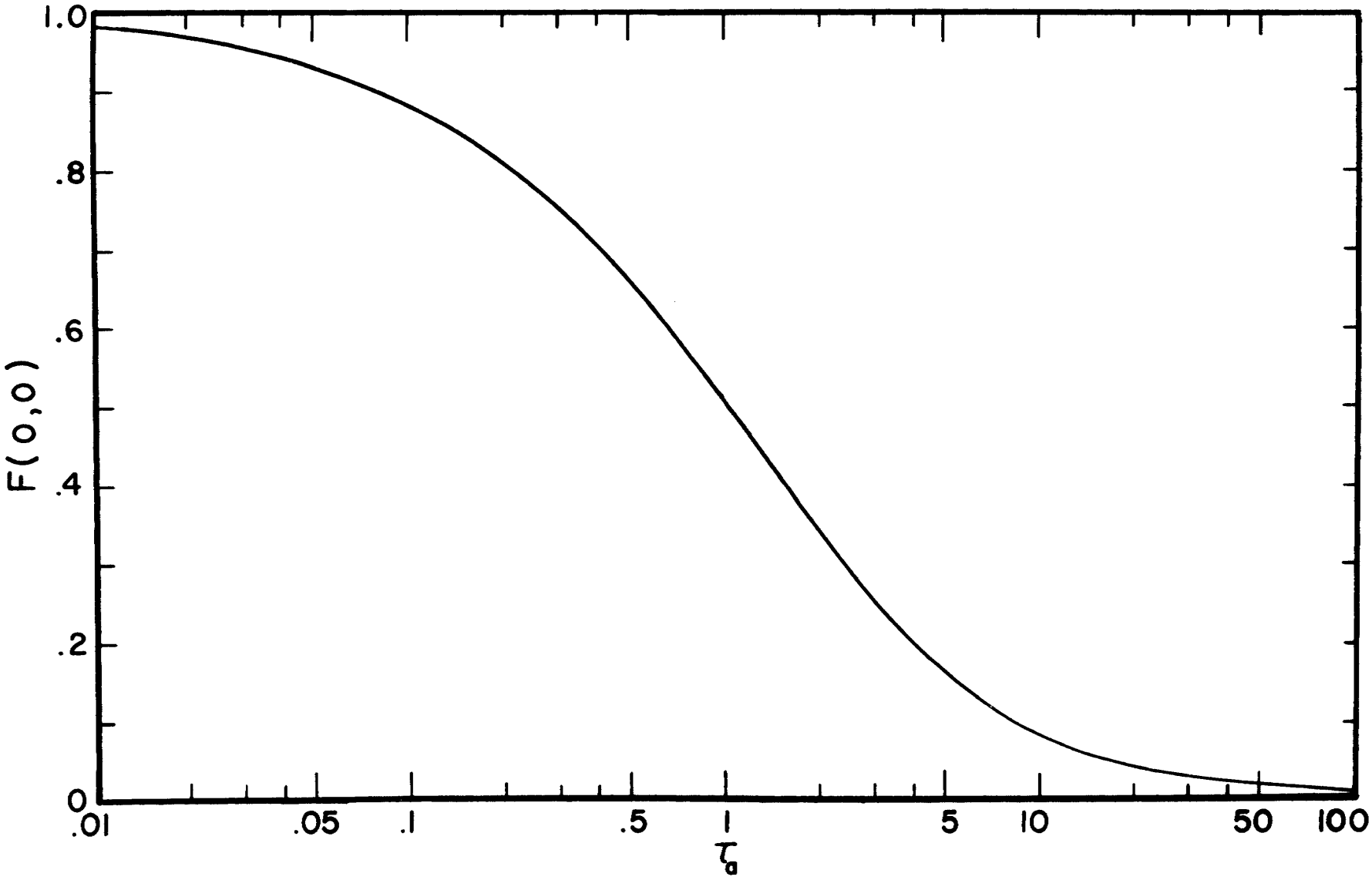

Figure 4.15 Variation in the normal flux at $\tau_z=0$ and $\tau_y=0$ with τ_a for a semi-infinite medium bounded by a constant temperature strip

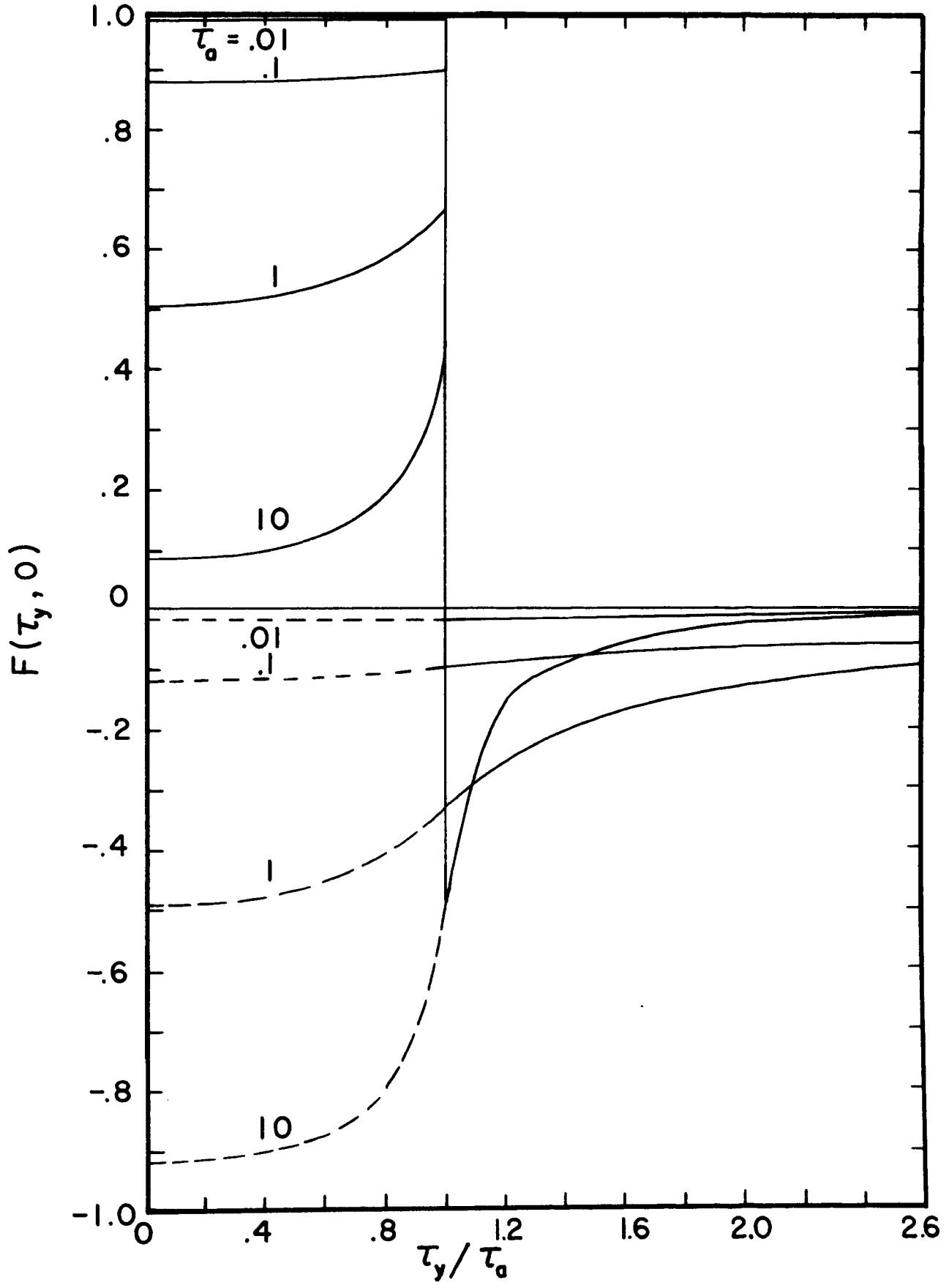

Figure 4.16 Variation in the normal flux at τ_z=0 with τ_y/τ_a for various values of τ_a for a semi-infinite medium bounded by a constant temperature strip

one-dimensional models indicates the necessity of the two-dimensional analysis. The two-dimensional cosine varying models can be approximated by the one-dimensional models when $\beta<0.1$, and the two-dimensional finite strip models can be approximated by the one-dimensional models when $\tau_a>100$. Thus, for other values of β or τ_a, the two-dimensional models must be considered.

V. FINITE MEDIUM

A. INTRODUCTION

The analysis of this chapter is concerned with the radiative flux and emissive power at the boundaries of a finite medium. The radiative flux and emissive power at the boundaries are expressed in terms of the generalized X- and Y-functions which are analogous to the X- and Y-functions of Chandrasekhar [1,p.183]. These generalized functions arise as a result of a collimated flux of cosine magnitude incident on a finite medium. The generalized X- and Y-functions are the dimensionless emissive power at the boundaries $\tau_z=0$ and $\tau_z=\tau_o$, respectively. The introduction of the generalized X- and Y-functions parallels the semi-infinite theory which generated a function analogous to the H-function of Chandrasekhar.

A detailed analysis of the generalized X- and Y-functions is presented and numerical methods of solution are discussed. Integral equations are developed which correspond to the integral equations for the one-dimensional X- and Y-functions of Chandrasekhar. The integro-differential equations that the generalized X- and Y-functions satisfy are developed. The integro-differential form is reduced to a system of ordinary differential equations and solved numerically for the generalized X- and Y-functions. The behavior of the emissive power and radiative flux at the boundaries of the finite medium as a function of β and optical thickness τ_o is investigated. Bounds on β and τ_o are obtained for which the finite model can be approximated by the simpler semi-infinite model. The one-dimensional approximation is also considered whereby the two-dimensional model can be replaced by the one-dimensional model.

B. EQUATIONS FOR THE GENERALIZED X- AND Y-FUNCTIONS

Since the generalized X- and Y-functions are basic to the development of the emissive power and flux at the boundaries, the study of their behavior is appropriate. In the first section the generalized X- and Y-functions are shown to satisfy a pair of coupled integral equations of the Chandrasekhar type. In the second section integro-differential equations, which are more suitable for numerical calculation, are developed for the generalized X- and Y-functions. The integro-differential equations for the generalized X- and Y-functions are then transformed into integro-differential equations for the moments of the generalized X- and Y-functions.

1. INTEGRAL EQUATION

The integral equations for the generalized X- and Y- functions which correspond to the one-dimensional X- and Y- functions will now be developed. These functions satisfy a pair of coupled, nonlinear, inhomogeneous integral equations which are difficult to solve and will not be utilized. However, this development is important because the generalized reflection and transmission functions are introduced. The generalized reflection and transmission functions will be used in later sections to find the radiative flux at the boundaries.

The equations describing the finite medium have previously been formulated in Chapter III. From equation (3.37), the dimensionless emissive power $J_\beta(\tau_z,\sigma,\tau_o)$ satisfies the following integral equation

$$J_\beta(\tau_z,\sigma,\tau_o) = e^{-\sigma\tau_z} + \frac{1}{2}\int_0^{\tau_o} \mathcal{E}_1(|\tau_z-\tau_z'|,\beta)J_\beta(\tau_z',\sigma,\tau_o)d\tau_z' \ . \qquad (5.1)$$

The integro-differential equation for $J_\beta(\tau_z,\sigma,\tau_o)$ is given by equation (3.102) and can be written as

$$\frac{dJ_\beta(\tau_z,\sigma,\tau_o)}{d\tau_z} + \sigma J_\beta(\tau_z,\sigma,\tau_o) - J_\beta(o,\sigma,\tau_o)\Phi(\tau_z,\tau_o) + J_\beta(\tau_o,\sigma,\tau_o)\Phi(\tau_o-\tau_z,\tau_o) = 0 \qquad (5.2)$$

where

$$\Phi(\tau_z,\tau_o) = \frac{1}{2}\int_1^\infty \frac{J_\beta(\tau_z,\sqrt{t^2+\beta^2},\tau_o)dt}{\sqrt{t^2+\beta^2}} \quad . \qquad (5.3)$$

Following the procedure outlined by Sobolev [5,p.74] for the one-dimensional theory, the generalized reflection function R_β is introduced through equation (5.2). Letting $\sigma=\sqrt{t^2+\beta^2}$ in equation (5.2), multiplying the latter by $e^{-\sigma\tau_z}\,d\tau_z$ and integrating it from 0 to τ_o yields

$$\int_0^{\tau_o} \frac{dJ_\beta(\tau_z,\sqrt{t^2+\beta^2},\tau_o)}{d\tau_z} e^{-\sigma\tau_z}\,d\tau_z + \sqrt{t^2+\beta^2}R_\beta(\sigma,\sqrt{t^2+\beta^2},\tau_o) = J_\beta(o,\sqrt{t^2+\beta^2},\tau_o)\int_0^{\tau_o}\Phi(\tau_z,\tau_o)e^{-\sigma\tau_z}\,d\tau_z - J_\beta(\tau_o,\sqrt{t^2+\beta^2},\tau_o)\int_0^{\tau_o}\Phi(\tau_o-\tau_z,\tau_o)e^{-\sigma\tau_z}\,d\tau_z \qquad (5.4)$$

where $R_\beta(\sigma,\sqrt{t^2+\beta^2},\tau_o)$ is analogous to the reflection function of Chandrasekhar and is defined as

$$R_\beta(\sigma,\sqrt{t^2+\beta^2},\tau_o) = \int_0^{\tau_o} J_\beta(x,\sqrt{t^2+\beta^2},\tau_o)e^{-\sigma x}\,dx \quad . \qquad (5.5)$$

The first term in equation (5.4) is expressed in terms of R_β by integrating once by parts to obtain

$$\int_0^{\tau_o} \frac{dJ_\beta(\tau_z,\sqrt{t^2+\beta^2},\tau_o)}{d\tau_z} e^{-\sigma\tau_z}\, d\tau_z = e^{-\sigma\tau_o} J_\beta(\tau_o,\sqrt{t^2+\beta^2},\tau_o)$$

$$- J_\beta(o,\sqrt{t^2+\beta^2},\tau_o) + \sigma R_\beta(\sigma,\sqrt{t^2+\beta^2},\tau_o) \quad . \tag{5.6}$$

Insertion of equation (5.6) into equation (5.4) yields

$$(\sigma+\sqrt{t^2+\beta^2})R_\beta(\sigma,\sqrt{t^2+\beta^2},\tau_o) = J_\beta(o,\sqrt{t^2+\beta^2},\tau_o)\left[1 + \int_0^{\tau_o} \Phi(\tau_z,\tau_o)e^{-\sigma\tau_z}\, d\tau_z\right]$$

$$- J_\beta(\tau_o,\sqrt{t^2+\beta^2},\tau_o)\left[e^{-\sigma\tau_o} + \int_0^{\tau_o} \Phi(\tau_o-\tau_z,\tau_o)e^{-\sigma\tau_z}\, d\tau_z\right] \quad . \tag{5.7}$$

A further simplification in equation (5.7) is obtained by relating the integral terms involving Φ and J_β at the boundaries. The first term containing Φ is related to $J_\beta(o,\sigma,\tau_o)$ by evaluating equation (5.1) at $\tau_z=0$. This gives

$$J_\beta(o,\sigma,\tau_o) = 1 + \frac{1}{2}\int_0^{\tau_o}\left[\int_1^\infty \frac{e^{-\tau_z'\sqrt{t^2+\beta^2}}}{\sqrt{t^2+\beta^2}}\, dt\right] J_\beta(\tau_z',\sigma,\tau_o)d\tau_z' \quad . \tag{5.8}$$

After interchanging the order of integration, equation (5.8) becomes

$$J_\beta(o,\sigma,\tau_o) = 1 + \frac{1}{2}\int_1^\infty \frac{dt}{\sqrt{t^2+\beta^2}}\left[\int_0^{\tau_o} J_\beta(\tau_z',\sigma,\tau_o)e^{-\tau_z'\sqrt{t^2+\beta^2}}\, d\tau_z'\right] . \tag{5.9}$$

The interior integral in equation (5.9) is another form of R_β obtained from equation (5.5) by interchanging $\sqrt{t^2+\beta^2}$ and σ. Therefore,

utilization of the expression

$$\int_0^{\tau_o} J_\beta(\tau_z',\sigma,\tau_o)e^{-\tau_z'\sqrt{t^2+\beta^2}}\,d\tau_z' = R_\beta(\sqrt{t^2+\beta^2},\sigma,\tau_o) \tag{5.10}$$

reduces equation (5.9) to

$$J_\beta(o,\sigma,\tau_o) = 1 + \frac{1}{2}\int_1^\infty \frac{R_\beta(\sqrt{t^2+\beta^2},\sigma,\tau_o)dt}{\sqrt{t^2+\beta^2}} \quad . \tag{5.11}$$

However, R_β can be related to Φ by multiplying equation (5.3) by $e^{-\sigma\tau_z}\,d\tau_z$ and integrating it from 0 to τ_o. This yields

$$\int_0^{\tau_o} \Phi(\tau_z,\tau_o)e^{-\sigma\tau_z}\,d\tau_z = \frac{1}{2}\int_0^{\tau_o}\left[\int_1^\infty J_\beta(\tau_z,\sqrt{t^2+\beta^2},\tau_o)\frac{dt}{\sqrt{t^2+\beta^2}}\right]e^{-\sigma\tau_z}\,d\tau_z. \tag{5.12}$$

By interchanging the order of integration in equation (5.12) and utilizing equation (5.5), the following expression is obtained

$$\int_0^{\tau_o} \Phi(\tau_z,\tau_o)e^{-\sigma\tau_z}\,d\tau_z = \frac{1}{2}\int_1^\infty R_\beta(\sigma,\sqrt{t^2+\beta^2},\tau_o)\,\frac{dt}{\sqrt{t^2+\beta^2}} \quad . \tag{5.13}$$

The symmetry of the reflection function R_β with respect to σ and $\sqrt{t^2+\beta^2}$ is shown in Appendix C. This symmetry enables equations (5.11) and (5.13) to be combined to produce the desired relation between Φ and $J_\beta(o,\sigma,\tau_o)$

$$J_\beta(o,\sigma,\tau_o) = 1 + \int_0^{\tau_o} \Phi(\tau_z,\tau_o)e^{-\sigma\tau_z}\,d\tau_z \quad . \tag{5.14}$$

Next, substitution of equation (5.14) into equation (5.7) yields

$$(\sigma+\sqrt{t^2+\beta^2})R_\beta(\sigma,\sqrt{t^2+\beta^2},\tau_o) = J_\beta(o,\sqrt{t^2+\beta^2},\tau_o)J_\beta(o,\sigma,\tau_o)$$

$$- J_\beta(\tau_o,\sqrt{t^2+\beta^2},\tau_o)\left[e^{-\sigma\tau_o} + \int_0^{\tau_o} \Phi(\tau_o-\tau_z,\tau_o)e^{-\sigma\tau_z}\, d\tau_z \right] . \qquad (5.15)$$

A similar reduction in the form of equation (5.15) is accomplished by expressing the term involving Φ as a function of $J_\beta(\tau_o,\sigma,\tau_o)$. This reduction is accomplished by evaluating equation (5.1) at $\tau_z=\tau_o$ to yield

$$J_\beta(\tau_o,\sigma,\tau_o) = e^{-\sigma\tau_o} + \frac{1}{2}\int_0^{\tau_o}\left[\int_1^\infty \frac{e^{-(\tau_o-\tau_z')\sqrt{t^2+\beta^2}}}{\sqrt{t^2+\beta^2}}\, dt\right] J_\beta(\tau_z',\sigma,\tau_o)d\tau_z' . \qquad (5.16)$$

An interchange of the order of integration in equation (5.16) yields

$$J_\beta(\tau_o,\sigma,\tau_o) = e^{-\sigma\tau_o} + \frac{1}{2}\int_1^\infty S_\beta(\sqrt{t^2+\beta^2},\sigma,\tau_o)\,\frac{dt}{\sqrt{t^2+\beta^2}} \qquad (5.17)$$

where $S_\beta(\sqrt{t^2+\beta^2},\sigma,\tau_o)$ is a symmetric function which is analogous to the transmission function of Chandrasekhar and is defined as

$$S_\beta(\sqrt{t^2+\beta^2},\sigma,\tau_o) = \int_0^{\tau_o} J_\beta(\tau_o-x,\sigma,\tau_o)e^{-x\sqrt{t^2+\beta^2}}\, dx \quad . \qquad (5.18)$$

The relationship between S_β and Φ is found by replacing τ_z by $\tau_o-\tau_z$ in equation (5.3), multiplying the latter by $e^{-\sigma\tau_z}\, d\tau_z$ and integrating it from 0 to τ_o to obtain

$$\int_0^{\tau_o} \Phi(\tau_o-\tau_z,\tau_o)e^{-\sigma\tau_z}\,d\tau_z$$

$$= \frac{1}{2}\int_0^{\tau_o}\left[\int_1^{\infty} J_\beta(\tau_o-\tau_z,\sqrt{t^2+\beta^2},\tau_o)\frac{dt}{\sqrt{t^2+\beta^2}}\right] e^{-\sigma\tau_z}\,d\tau_z \quad . \tag{5.19}$$

Next, reversing the order of integration of equation (5.19) and utilizing the symmetry of S_β results in the following expression

$$\int_0^{\tau_o} \Phi(\tau_o-\tau_z,\tau_o)e^{-\sigma\tau_z}\,d\tau_z = \frac{1}{2}\int_1^{\infty} S_\beta(\sqrt{t^2+\beta^2},\sigma,\tau_o)\,\frac{dt}{\sqrt{t^2+\beta^2}} \quad . \tag{5.20}$$

Finally, insertion of equation (5.20) into equation (5.17) results in the following integral relationship between $J_\beta(\tau_o,\sigma,\tau_o)$ and Φ

$$J_\beta(\tau_o,\sigma,\tau_o) = e^{-\sigma\tau_o} + \int_0^{\tau_o} \Phi(\tau_o-\tau_z,\tau_o)e^{-\sigma\tau_z}\,d\tau_z \quad . \tag{5.21}$$

Hence, the reflection function is expressed in terms of J_β at the boundaries as

$$R_\beta(\sigma,\sqrt{t^2+\beta^2},\tau_o)$$

$$= \frac{J_\beta(o,\sqrt{t^2+\beta^2},\tau_o)J_\beta(o,\sigma,\tau_o)-J_\beta(\tau_o,\sqrt{t^2+\beta^2},\tau_o)J_\beta(\tau_o,\sigma,\tau_o)}{\sigma+\sqrt{t^2+\beta^2}} \quad . \tag{5.22}$$

When equation (5.22) is substituted into equation (5.11), the following integral equation for $J_\beta(o,\sigma,\tau_o)$ is obtained

$$J_\beta(o,\sigma,\tau_o) = 1 + \frac{1}{2}\int_1^{\infty}\Bigg[$$

$$\frac{J_\beta(o,\sqrt{t^2+\beta^2},\tau_o)J_\beta(o,\sigma,\tau_o) - J_\beta(\tau_o,\sqrt{t^2+\beta^2},\tau_o)J_\beta(\tau_o,\sigma,\tau_o)}{\sqrt{t^2+\beta^2}(\sigma+\sqrt{t^2+\beta^2})}\Bigg]dt \quad . \tag{5.23}$$

Equation (5.23) is seen to have the same form as equation (4.17). Hence, the same transforms can be applied, and equation (5.23) then reduces to an integral equation for the generalized X-function

$$X(\mu,\tau_o,\beta) = 1+\mu \int_0^1 \frac{\psi(x,\beta)}{x+\mu} [X(\mu,\tau_o,\beta)X(x,\tau_o,\beta)-Y(\mu,\tau_o,\beta)Y(x,\tau_o,\beta)]dx \quad (5.24)$$

where the generalized X- and Y-functions are defined by

$$X(\mu,\tau_o,\beta) = J_\beta(o,\sqrt{1+\beta^2}/\mu,\tau_o) \quad (5.25)$$

and

$$Y(\mu,\tau_o,\beta) = J_\beta(\tau_o,\sqrt{1+\beta^2}/\mu,\tau_o) \ . \quad (5.26)$$

Equations (5.25) and (5.26) define the dimensionless emissive power at $\tau_z=0$ and at $\tau_z=\tau_o$ as the generalized X-function and the generalized Y-function, respectively. Equation (5.24) reveals that the emissive power at the boundary $\tau_z=0$ can be determined without a knowledge of the emissive power within the medium and is completely described by the emissive power at the boundaries. This equation is an improvement over the form of equation (5.8) which requires the emissive power within the medium to be known before the integration can be performed. In a similar fashion, the emissive power at the other boundary $\tau_z=\tau_o$ can be obtained from equation (5.16) if the emissive power within the medium is known. However, the success in expressing the emissive power at $\tau_z=0$ solely in terms of the emissive power at the boundaries by means of the integral equation for the generalized X-function indicates that the integral equation for the generalized Y-function should also depend only upon the emissive power at the boundaries.

Hence, in the next section the integral equation for the generalized Y-function will be developed.

The transmission function S_β can also be expressed in terms of J_β at the boundaries. Replacing τ_z by $\tau_o-\tau_z$ in equation (5.2) yields

$$\frac{dJ_\beta(\tau_o-\tau_z,\sigma,\tau_o)}{d\tau_z} - \sigma J_\beta(\tau_o-\tau_z,\sigma,\tau_o) + J_\beta(o,\sigma,\tau_o)\Phi(\tau_o-\tau_z,\tau_o)$$

$$- J_\beta(\tau_o,\sigma,\tau_o)\Phi(\tau_z,\tau_o) = 0 \quad . \tag{5.27}$$

By letting $\sigma=\sqrt{t^2+\beta^2}$ in equation (5.27), multiplying the latter by $e^{-\sigma\tau_z}\,d\tau_z$ and integrating it from 0 to τ_o, the following expression is obtained

$$\int_o^{\tau_o} \frac{dJ_\beta(\tau_o-\tau_z,\sqrt{t^2+\beta^2},\tau_o)}{d\tau_z} e^{-\sigma\tau_z}\,d\tau_z$$

$$- \sqrt{t^2+\beta^2} \int_o^{\tau_o} J_\beta(\tau_o-\tau_z,\sqrt{t^2+\beta^2},\tau_o)e^{-\sigma\tau_z}\,d\tau_z$$

$$+ J_\beta(o,\sqrt{t^2+\beta^2},\tau_o) \int_o^{\tau_o} \Phi(\tau_o-\tau_z,\tau_o)e^{-\sigma\tau_z}\,d\tau_z$$

$$- J_\beta(\tau_o,\sqrt{t^2+\beta^2},\tau_o) \int_o^{\tau_o} \Phi(\tau_z,\tau_o)e^{-\sigma\tau_z}\,d\tau_z = 0 \quad . \tag{5.28}$$

Next, integration of the first term in equation (5.28) by parts yields

$$(\sigma+\sqrt{t^2+\beta^2}) \int_0^{\tau_o} J_\beta(\tau_o-\tau_z,\sqrt{t^2+\beta^2},\tau_o)e^{-\sigma\tau_z}\, d\tau_z$$

$$= J_\beta(\tau_o,\sqrt{t^2+\beta^2},\tau_o)\left[1 + \int_0^{\tau_o} \Phi(\tau_z,\tau_o)e^{-\sigma\tau_z}\, d\tau_z\right]$$

$$- J_\beta(o,\sqrt{t^2+\beta^2},\tau_o)\left[e^{-\sigma\tau_o} + \int_0^{\tau_o} \Phi(\tau_o-\tau_z,\tau_o)e^{-\sigma\tau_z}\, d\tau_z\right] . \quad (5.29)$$

The first integral in equation (5.29) is S_β. The two integral terms involving Φ are related to J_β at the boundary by means of equations (5.14) and (5.21). Hence, equation (5.29) can be reduced to the following expression for S_β in terms of J_β at the boundaries

$$S_\beta(\sigma,\sqrt{t^2+\beta^2},\tau_o)$$

$$= \frac{J_\beta(o,\sqrt{t^2+\beta^2},\tau_o)J_\beta(\tau_o,\sigma,\tau_o) - J_\beta(\tau_o,\sqrt{t^2+\beta^2},\tau_o)J_\beta(o,\sigma,\tau_o)}{\sqrt{t^2+\beta^2} - \sigma} . \quad (5.30)$$

An integral equation for $J_\beta(\tau_o,\sigma,\tau_o)$ is obtained by inserting equation (5.30) into equation (5.20) and using equation (5.21) to arrive at

$$J_\beta(\tau_o,\sigma,\tau_o) = e^{-\sigma\tau_o}$$

$$+ \frac{1}{2}\int_1^\infty \frac{J_\beta(o,\sqrt{t^2+\beta^2},\tau_o)J_\beta(\tau_o,\sigma,\tau_o)-J_\beta(\tau_o,\sqrt{t^2+\beta^2},\tau_o)J_\beta(o,\sigma,\tau_o)}{\sqrt{t^2+\beta^2}(\sqrt{t^2+\beta^2} - \sigma)}\, dt . \quad (5.31)$$

Since equation (5.31) is of the same form as equation (5.23), the same transforms can be used to obtain the integral equation for the generalized Y-function. This results in

$$Y(\mu,\tau_0,\beta) = e^{-\tau_0\sqrt{1+\beta^2}/\mu}$$

$$+ \mu \int_0^1 \frac{\psi(x,\beta)}{\mu-x} [X(x,\tau_0,\beta)Y(\mu,\tau_0,\beta) - X(\mu,\tau_0,\beta)Y(x,\tau_0,\beta)]dx \quad . \quad (5.32)$$

Equations (5.24) and (5.32) are two coupled integral equations for the generalized X- and Y-functions. The integral equations for the generalized functions have the same form as the one-dimensional equations of Chandrasekhar. Since the solutions for the finite model must approach those of the semi-infinite model when the optical thickness of the medium becomes infinite, the generalized X-function approaches the generalized H-function and the generalized Y-function approaches zero in the limit. That is, $\lim_{\tau_0\to\infty} X(\mu,\tau_0,\beta)=H(\mu,\beta)$ and $\lim_{\tau_0\to\infty} Y(\mu,\tau_0,\beta)=0$. When the optical thickness approaches zero, the generalized X- and Y-functions are equal: $\lim_{\tau_0\to 0} X(\mu,\tau_0,\beta) = \lim_{\tau_0\to 0} Y(\mu,\tau_0,\beta)=1$.

Numerical evaluation of the generalized X- and Y-functions by direct iteration in the present form of equations (5.24) and (5.32) is not practical due to the extremely slow rate of convergence. This same problem was avoided in the semi-infinite theory by transforming the standard integral equation for the generalized H-function into a reduced form which was more suitable for iteration. However, such a form is not available for the generalized X- and Y-functions due to the complicated manner in which the two functions are related. Hence, an alternate method of calculating the generalized X- and Y-functions

is developed. This technique involves expressing the generalized X- and Y-functions by integro-differential form. The advantage of this form is that the integro-differential equations can be reduced to a system of ordinary differential equations which are more easily solved numerically.

2. INTEGRO-DIFFERENTIAL EQUATIONS

The integro-differential equations that the generalized X- and Y-functions satisfy are formulated in a manner similar to that of Sobolev [5,p.77]. This approach involves the integral equation for $J_\beta(\tau_o-\tau_z,\sigma,\tau_o)$. Replacing τ_z by $\tau_o-\tau_z$ and τ_z' by $\tau_o-\tau_z'$ in equation (5.1) yields

$$J_\beta(\tau_o-\tau_z,\sigma,\tau_o) = e^{-(\tau_o-\tau_z)\sigma} + \frac{1}{2}\int_0^{\tau_o} \mathcal{E}_1(|\tau_z-\tau_z'|,\beta)J_\beta(\tau_o-\tau_z',\sigma,\tau_o)d\tau_z' \quad . \tag{5.33}$$

In obtaining the differential form, the optical thickness is considered to be a variable.

Differentiating equations (5.1) and (5.33) with respect to τ_o yields

$$\frac{\partial J_\beta(\tau_z,\sigma,\tau_o)}{\partial\tau_o} = \frac{1}{2}J_\beta(\tau_z,\sigma,\tau_o)\int_1^\infty e^{-(\tau_o-\tau_z)\sqrt{t^2+\beta^2}}\frac{dt}{\sqrt{t^2+\beta^2}} + \frac{1}{2}\int_0^{\tau_o}\mathcal{E}_1(|\tau_z-\tau_z'|,\beta)\frac{\partial J_\beta(\tau_z',\sigma,\tau_o)}{\partial\tau_o}d\tau_z' \tag{5.34}$$

and

$$\frac{\partial J_\beta(\tau_o-\tau_z,\sigma,\tau_o)}{\partial\tau_o} = -\sigma\, e^{-(\tau_o-\tau_z)\sigma} + \frac{1}{2} J_\beta(o,\sigma,\tau_o)\,\mathcal{E}_1(\tau_o-\tau_z,\beta)$$

$$+ \frac{1}{2}\int_0^{\tau_o} \mathcal{E}_1(|\tau_z-\tau_z'|,\beta)\,\frac{\partial J_\beta(\tau_o-\tau_z',\sigma,\tau_o)}{\partial\tau_o}\,d\tau_z' \,. \qquad (5.35)$$

By letting $\sigma=\sqrt{t^2+\beta^2}$ in equation (5.33), multiplying the latter by $dt/\sqrt{t^2+\beta^2}$ and integrating it from 1 to ∞, the following expression is obtained

$$\int_1^\infty J_\beta(\tau_o-\tau_z,\sqrt{t^2+\beta^2},\tau_o)\,\frac{dt}{\sqrt{t^2+\beta^2}} = \int_1^\infty e^{-(\tau_o-\tau_z)\sqrt{t^2+\beta^2}}\,\frac{dt}{\sqrt{t^2+\beta^2}}$$

$$+ \frac{1}{2}\int_1^\infty \frac{dt}{\sqrt{t^2+\beta^2}}\int_0^{\tau_o} \mathcal{E}_1(|\tau_z-\tau_z'|,\beta)J_\beta(\tau_o-\tau_z',\sqrt{t^2+\beta^2},\tau_o)\,d\tau_z' \,. \qquad (5.36)$$

When equation (5.36) is multiplied by $J_\beta(\tau_o,\sigma,\tau_o)/2$ and the resulting expression is compared with equation (5.34), an integro-differential equation for $J_\beta(\tau_z,\sigma,\tau_o)$ results

$$\frac{\partial J_\beta(\tau_z,\sigma,\tau_o)}{\partial\tau_o} = \frac{1}{2} J_\beta(\tau_o,\sigma,\tau_o)\int_1^\infty J_\beta(\tau_o-\tau_z,\sqrt{t^2+\beta^2},\tau_o)\,\frac{dt}{\sqrt{t^2+\beta^2}} \,. \qquad (5.37)$$

Multiplying equation (5.33) by σ and adding the resulting expression to equation (5.35) yields

$$\frac{\partial J_\beta(\tau_o-\tau_z,\sigma,\tau_o)}{\partial\tau_o} + \sigma J_\beta(\tau_o-\tau_z,\sigma,\tau_o) = \frac{1}{2} J_\beta(o,\sigma,\tau_o)\,\mathcal{E}_1(\tau_o-\tau_z,\beta)$$

$$+ \frac{1}{2}\int_0^{\tau_o} \mathcal{E}_1(|\tau_z-\tau_z'|,\beta)\left[\frac{\partial J_\beta(\tau_o-\tau_z',\sigma,\tau_o)}{\partial\tau_o} + \sigma J_\beta(\tau_o-\tau_z',\sigma,\tau_o)\right] d\tau_z' \quad . \tag{5.38}$$

A comparison of equation (5.38) with the expression obtained by multiplying equation (5.36) by $J_\beta(o,\sigma,\tau_o)/2$ yields an integro-differential equation for $J_\beta(\tau_o-\tau_z,\sigma,\tau_o)$

$$\frac{\partial J_\beta(\tau_o-\tau_z,\sigma,\tau_o)}{\partial\tau_o} + \sigma J_\beta(\tau_o-\tau_z,\sigma,\tau_o)$$

$$= \frac{1}{2} J_\beta(o,\sigma,\tau_o)\int_1^\infty \frac{J_\beta(\tau_o-\tau_z,\sqrt{t^2+\beta^2},\tau_o)dt}{\sqrt{t^2+\beta^2}} \quad . \tag{5.39}$$

Equations (5.37) and (5.39) are two coupled integro-differential equations for the emissive power at optical depths τ_z and $\tau_o-\tau_z$. Before these equations can be solved, the emissive power at the boundaries $J_\beta(o,\sigma,\tau_o)$ and $J_\beta(\tau_o,\sigma,\tau_o)$ must be determined.

To do this, separate integro-differential equations for $J_\beta(o,\sigma,\tau_o)$ and $J_\beta(\tau_o,\sigma,\tau_o)$ are desirable. Insertion of $\tau_z=0$ in equations (5.37) and (5.39) yields

$$\frac{\partial J_\beta(o,\sigma,\tau_o)}{\partial\tau_o} = \frac{1}{2} J_\beta(\tau_o,\sigma,\tau_o)\int_1^\infty J_\beta(\tau_o,\sqrt{t^2+\beta^2},\tau_o)\frac{dt}{\sqrt{t^2+\beta^2}} \tag{5.40}$$

and

$$\frac{\partial J_\beta(\tau_o,\sigma,\tau_o)}{\partial\tau_o} + \sigma J_\beta(\tau_o,\sigma,\tau_o)$$

$$= \frac{1}{2} J_\beta(o,\sigma,\tau_o)\int_1^\infty J_\beta(\tau_o,\sqrt{t^2+\beta^2},\tau_o)\frac{dt}{\sqrt{t^2+\beta^2}} \quad . \tag{5.41}$$

Equations (5.40) and (5.41) reveal that the emissive power at the boundaries can be calculated without a knowledge of the emissive power interior to the medium. Since the primary interest is in the emissive power at the boundaries, equations (5.40) and (5.41) will be further reduced to a more favorable mathematical form.

The substitutions of $x=\sqrt{1+\beta^2}/\sqrt{t^2+\beta^2}$ and $\mu=\sqrt{1+\beta^2}/\sigma$ along with the use of equations (5.25) and (5.26) reduce equations (5.40) and (5.41) to integro-differential equations for the generalized X- and Y-functions in the form

$$\frac{\partial X(\mu,\tau_o,\beta)}{\partial \tau_o} = \frac{\sqrt{1+\beta^2}}{2} Y(\mu,\tau_o,\beta) \int_0^1 \frac{Y(x,\tau_o,\beta)dx}{x\sqrt{1+\beta^2(1-x^2)}} \tag{5.42}$$

and

$$\frac{\partial Y(\mu,\tau_o,\beta)}{\partial \tau_o} + \frac{\sqrt{1+\beta^2}}{\mu} Y(\mu,\tau_o,\beta)$$

$$= \frac{\sqrt{1+\beta^2}}{2} X(\mu,\tau_o,\beta) \int_0^1 \frac{Y(x,\tau_o,\beta)dx}{x\sqrt{1+\beta^2(1-x^2)}} \quad . \tag{5.43}$$

Equations (5.42) and (5.43) are the basic equations which can be reduced to a system of differential equations and solved numerically. These solutions can then be used to obtain the σ dependent form of the generalized X- and Y-functions from equations (5.40) and (5.41). Since $X(\mu,\tau_o,\beta)=J_\beta(o,\sqrt{1+\beta^2}/\mu,\tau_o)$, the substitution $\sigma=\sqrt{1+\beta^2}/\mu$ yields $X(\sqrt{1+\beta^2}/\sigma,\tau_o,\beta)=J_\beta(o,\sigma,\tau_o)$. In a similar fashion, $Y(\sqrt{1+\beta^2}/\sigma,\tau_o,\beta)$ $=J_\beta(\tau_o,\sigma,\tau_o)$. Thus, inserting $\mu=\sqrt{1+\beta^2}/\sigma$ into equations (5.42) and (5.43) yields

$$\frac{\partial J_\beta(0,\sigma,\tau_0)}{\partial \tau_0} = \frac{\sqrt{1+\beta^2}}{2} J_\beta(\tau_0,\sigma,\tau_0) \int_0^1 \frac{Y(x,\tau_0,\beta)dx}{x\sqrt{1+\beta^2(1-x^2)}} \tag{5.44}$$

and

$$\frac{\partial J_\beta(\tau_0,\sigma,\tau_0)}{\partial \tau_0} + \sigma J_\beta(\tau_0,\sigma,\tau_0) = \frac{\sqrt{1+\beta^2}}{2} J_\beta(0,\sigma,\tau_0) \int_0^1 \frac{Y(x,\tau_0,\beta)dx}{x\sqrt{1+\beta^2(1-x^2)}} . \tag{5.45}$$

Equations (5.44) and (5.45) can be reduced to a system of differential equations and solved in the same manner as the μ dependent form of equations (5.42) and (5.43).

3. MOMENTS OF GENERALIZED X- AND Y-FUNCTIONS

The emissive power at the boundaries for the cosine varying diffuse boundary condition involves moments of the generalized X- and Y-functions. The first class of weighted moments are defined as

$$\alpha_n(\beta,\tau_0) = \int_0^1 x^n \psi_0(x,\beta) X(x,\tau_0,\beta)dx \tag{5.46}$$

and

$$\beta_n(\beta,\tau_0) = \int_0^1 x^n \psi_0(x,\beta) Y(x,\tau_0,\beta)dx \tag{5.47}$$

where the weight function ψ_0 is defined as

$$\psi_0(x,\beta) = \frac{1}{\sqrt{1+\beta^2(1-x^2)}} . \tag{5.48}$$

A second class of useful moments are

$$x_n(\beta,\tau_0) = \int_0^1 x^n \psi_1(x,\beta) X(x,\tau_0,\beta)dx \tag{5.49}$$

and

$$y_n(\beta,\tau_0) = \int_0^1 x^n \psi_1(x,\beta) Y(x,\tau_0,\beta)dx \tag{5.50}$$

where ψ_1 has previously been defined by equation (3.79).

The moments α_0 and β_0 satisfy a simple identity which can be obtained from equation (5.24). By multiplying equation (5.24) by $\psi_0(\mu,\beta)d\mu$, integrating it from 0 to 1, and utilizing equations (5.46) and (5.47), the following expression is obtained

$$\alpha_0(\beta,\tau_0) = \int_0^1 \psi_0(\mu,\beta)d\mu + \frac{1}{2}\int_0^1\int_0^1 \frac{\mu\psi_0(x,\beta)\psi_0(\mu,\beta)}{x+\mu}$$

$$[X(\mu,\tau_0,\beta)X(x,\tau_0,\beta) - Y(\mu,\tau_0,\beta)Y(x,\tau_0,\beta)]dxd\mu \ . \tag{5.51}$$

Due to symmetry, μ and x are interchanged to obtain

$$\alpha_0(\beta,\tau_0) = \int_0^1 \psi_0(x,\beta)dx + \frac{1}{2}\int_0^1\int_0^1 \frac{x\psi_0(x,\beta)\psi_0(\mu,\beta)}{x+\mu}$$

$$[X(x,\tau_0,\beta)X(\mu,\tau_0,\beta) - Y(x,\tau_0,\beta)Y(\mu,\tau_0,\beta)]d\mu dx \ . \tag{5.52}$$

Adding equations (5.51) and (5.52) and integrating the initial term involving ψ_0 results in the desired relationship between α_0 and β_0

$$\alpha_0(\beta,\tau_0) = \frac{1}{\beta}\arcsin\left(\frac{\beta}{\sqrt{1+\beta^2}}\right) + \frac{1}{4}[\alpha_0^2(\beta,\tau_0) - \beta_0^2(\beta,\tau_0)] \ . \tag{5.53}$$

Equation (5.53) has the same form as the corresponding one-dimensional result obtained by Chandrasekhar [1,p.189]. When $\beta=0$, the two equations are identical.

Differential equations for the moments are obtained by multiplying equations (5.42) and (5.43) by $\psi_0(\mu,\beta)d\mu$ and integrating to yield

$$\frac{\partial \alpha_0(\beta,\tau_0)}{\partial \tau_0} = \frac{\sqrt{1+\beta^2}}{2}\,\beta_0(\beta,\tau_0)\beta_{-1}(\beta,\tau_0) \tag{5.54}$$

and

$$\frac{\partial \beta_0(\beta,\tau_0)}{\partial \tau_0} = \sqrt{1+\beta^2}\left[\frac{\alpha_0(\beta,\tau_0)}{2} - 1\right]\beta_{-1}(\beta,\tau_0) \quad . \tag{5.55}$$

A similar set of equations involving x_0 and y_0 follows as

$$\frac{\partial x_0(\beta,\tau_0)}{\partial \tau_0} = \frac{\sqrt{1+\beta^2}}{2}\,\beta_{-1}(\beta,\tau_0)y_0(\beta,\tau_0) \tag{5.56}$$

and

$$\frac{\partial y_0(\beta,\tau_0)}{\partial \tau_0} = \sqrt{1+\beta^2}\left[\frac{x_0(\beta,\tau_0)}{2}\,\beta_{-1}(\beta,\tau_0) - y_{-1}(\beta,\tau_0)\right] \quad . \tag{5.57}$$

Since the functions of the finite medium analysis approaches the corresponding ones in the semi-infinite theory, x_0 is bounded by h_0 and y_0 reduces to zero. That is, $h_0(\beta)=\lim_{\tau_0\to\infty} x_0(\beta,\tau_0)$ and $\lim_{\tau_0\to\infty} y_0(\beta,\tau_0)=0$ where h_0 has been defined by equation (4.31). When $\beta=0$, $x_0=\alpha_0$, $y_0=\beta_0$, $y_{-1}=\beta_{-1}$, and equations (5.56) and (5.57) are identical with equations (5.54) and (5.55). The one-dimensional form of equations (5.54) and (5.55) was developed by Heaslet and Warming [39].

C. EMISSIVE POWER FOR COSINE VARYING COLLIMATED BOUNDARY

The emissive power at the boundaries of a finite medium illuminated by a collimated flux of cosine magnitude has previously been

defined in terms of the generalized X- and Y-functions given by equations (5.27) and (5.28). The emissive power at the boundary $\tau_z=0$ is the generalized X-function and the emissive power at the other boundary is the generalized Y-function. Tables E.1 to E.14 list the numerical results for the σ dependent form of the generalized X- and Y-functions. These results are obtained from the computer program discussed at the end of this chapter. The μ dependent generalized X- and Y-functions are not tabulated but are used whenever integrations of generalized X- and Y-functions are required. The μ dependent form is more suitable for numerical integration than the σ dependent form. However, the σ dependent form is tabulated since physically the angle of the incident radiation and hence σ is usually specified.

The effect of σ on the generalized X-function is shown in Figure 5.1 for $\beta=1$ and in Figure 5.2 for $\beta=10$. The generalized X-function is maximum when the incident radiation is normal to the boundary, $\sigma=1$. Increasing σ allows less energy to enter the medium, thereby decreasing the emissive power. Figures 5.1 and 5.2 show the decrease of the generalized X-function to its limiting value of unity as σ approaches infinity. The generalized X-function levels off and approaches constant values at smaller optical thicknesses with increasing σ. This means that the generalized X-function is approaching the generalized H-function of semi-infinite theory. A knowledge of the values of σ, β, and τ_o for which the generalized X-function can be approximated by the generalized H-function is desirable.

Figure 5.1 reveals that for $\beta=1$ the generalized X-function levels off to the generalized H-function at $\tau_o=.8$ for $\sigma=5$. When $\sigma=10$, this

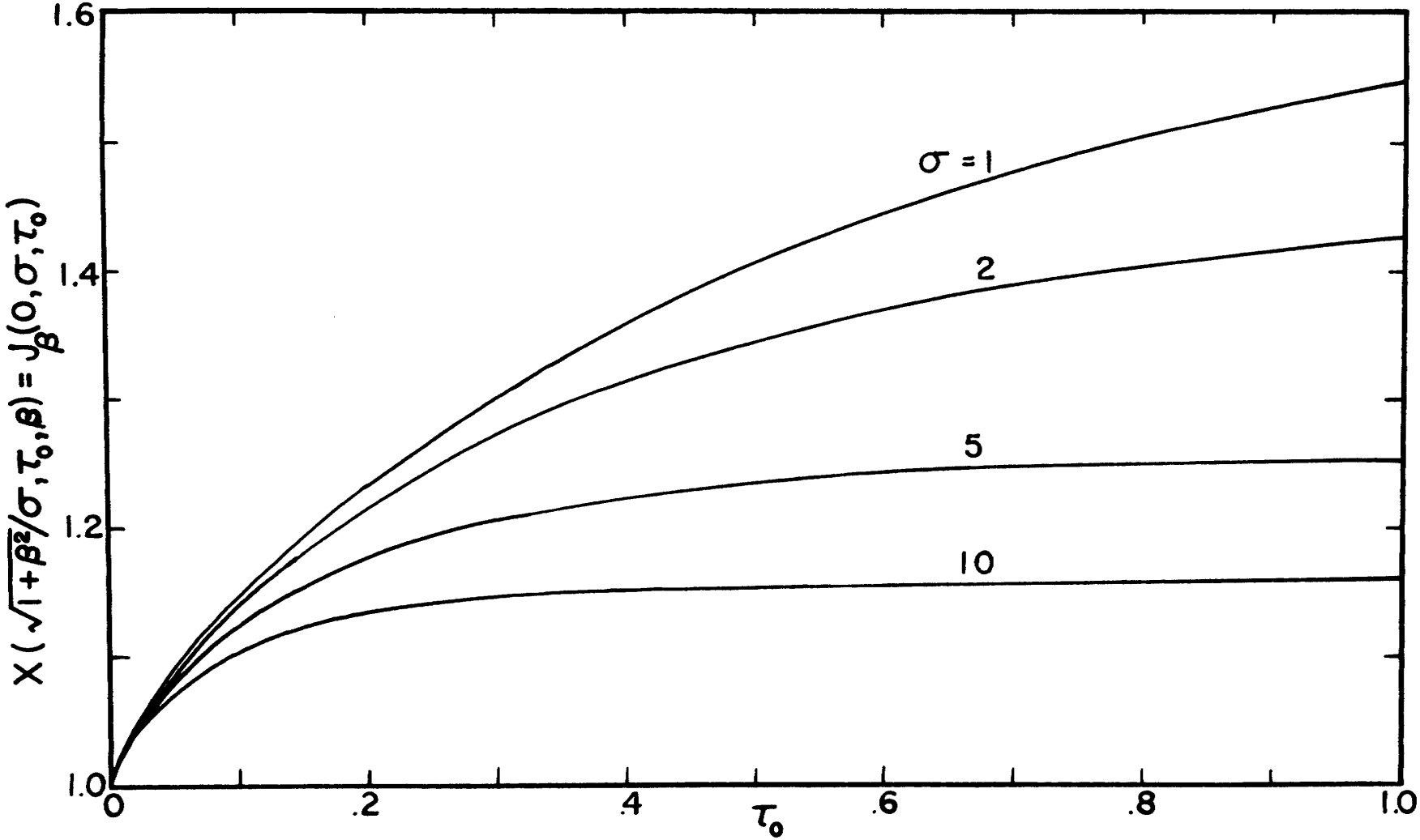

Figure 5.1 Variation of the generalized X-function with τ_0 for various values of σ for $\beta=1$

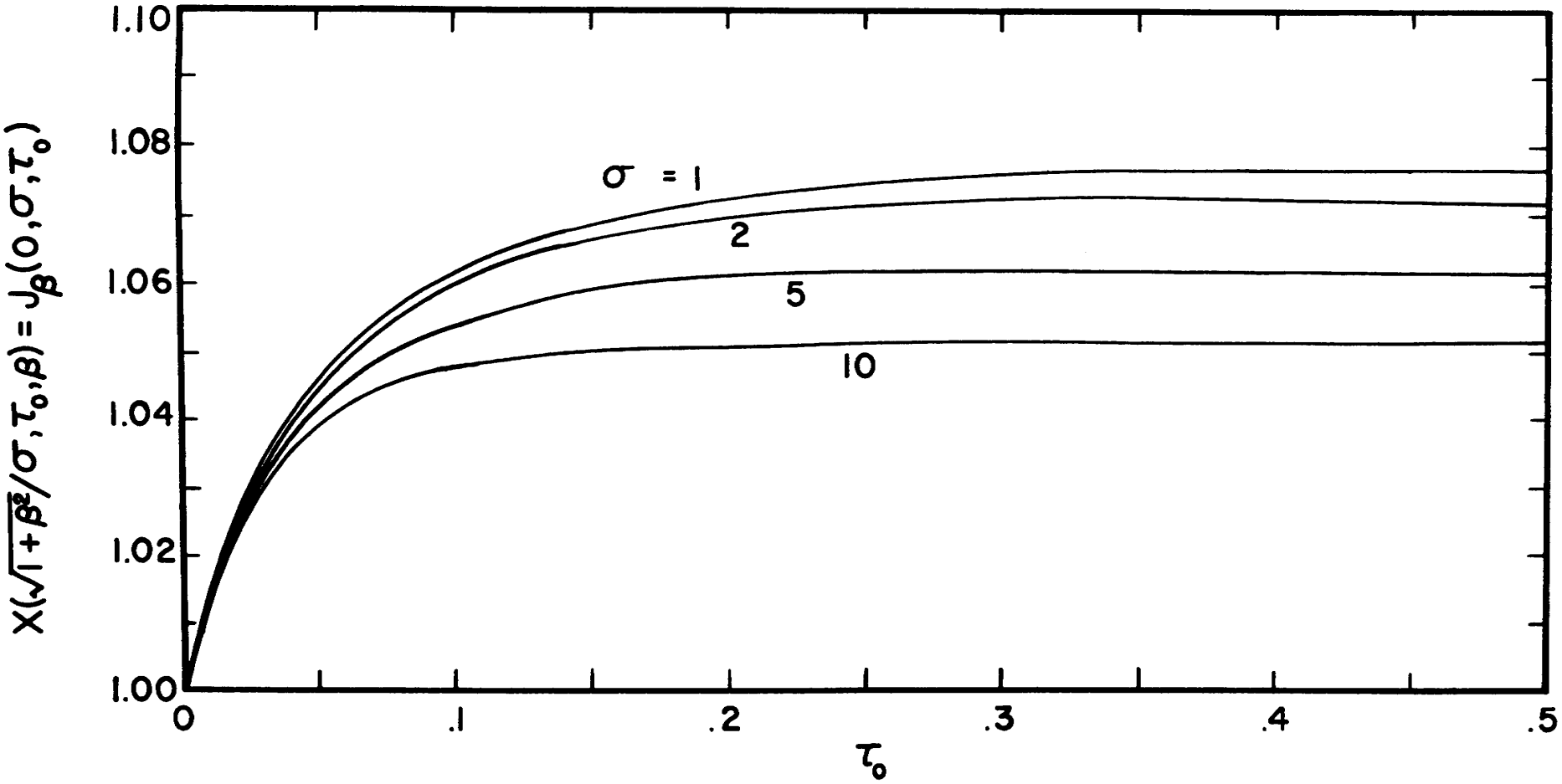

Figure 5.2 Variation of the generalized X-function with τ_0 for various values of σ for β=10

asymptotic behavior occurs for optical thicknesses as small as τ_0=.45. Figure 5.2 shows that for β=10 the magnitude of the generalized X-function is considerably smaller than the corresponding values in Figure 5.1 for β=1. In addition, the optical thicknesses at which the generalized X-function can be approximated by the generalized H-function are also decreased. In particular, the σ=5 curve now starts to level off to a constant value at τ_0=.25. The σ=10 curve exhibits asymptotic behavior at optical thickness of τ_0=.15 for β=10. Thus, increasing β causes a decrease in the value of the optical thickness necessary for approximating the generalized X-function by the generalized H-function.

The values of β and the optical thickness τ_0 for which the generalized X-function can be approximated by the generalized H-function are shown in Figure 5.3 for σ=1. The value of β at which the τ_0 curves merge into the semi-infinite H-function at $\tau_0=\infty$ yields the desired combination of β and τ_0. Figure 5.3 reveals that when τ_0=.1, a value of β=20 is the criterion for the approximation. For τ_0=3, this approximation can be used when $\beta \geq .8$. In particular, the generalized X-function can be approximated by the generalized H-function for any combination of $\beta \geq .8$ and $\tau_0 \geq 3$.

The effect of β and optical thickness τ_0 on the generalized X-function is shown in Figure 5.4 for σ=1. The generalized X-function is bounded by the one-dimensional X-function of Chandrasekhar at β=0 and unity when β approaches infinity. The generalized X-function levels off and approaches the generalized H-function at smaller optical thicknesses as β increases. Figure 5.4 and Tables E.1 to E.14

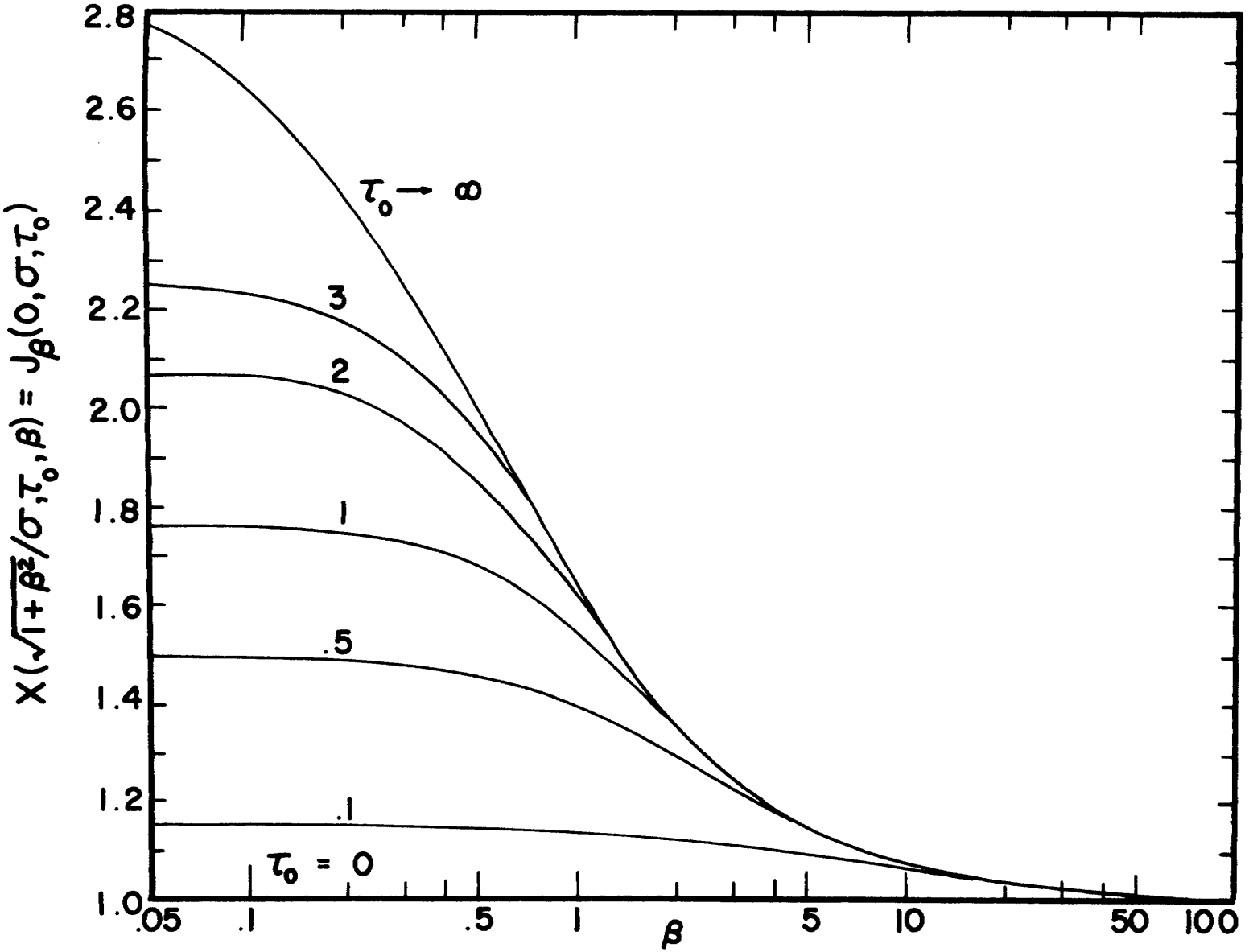

Figure 5.3 Variation of the generalized X-function with β for various values of τ_0 for σ=1

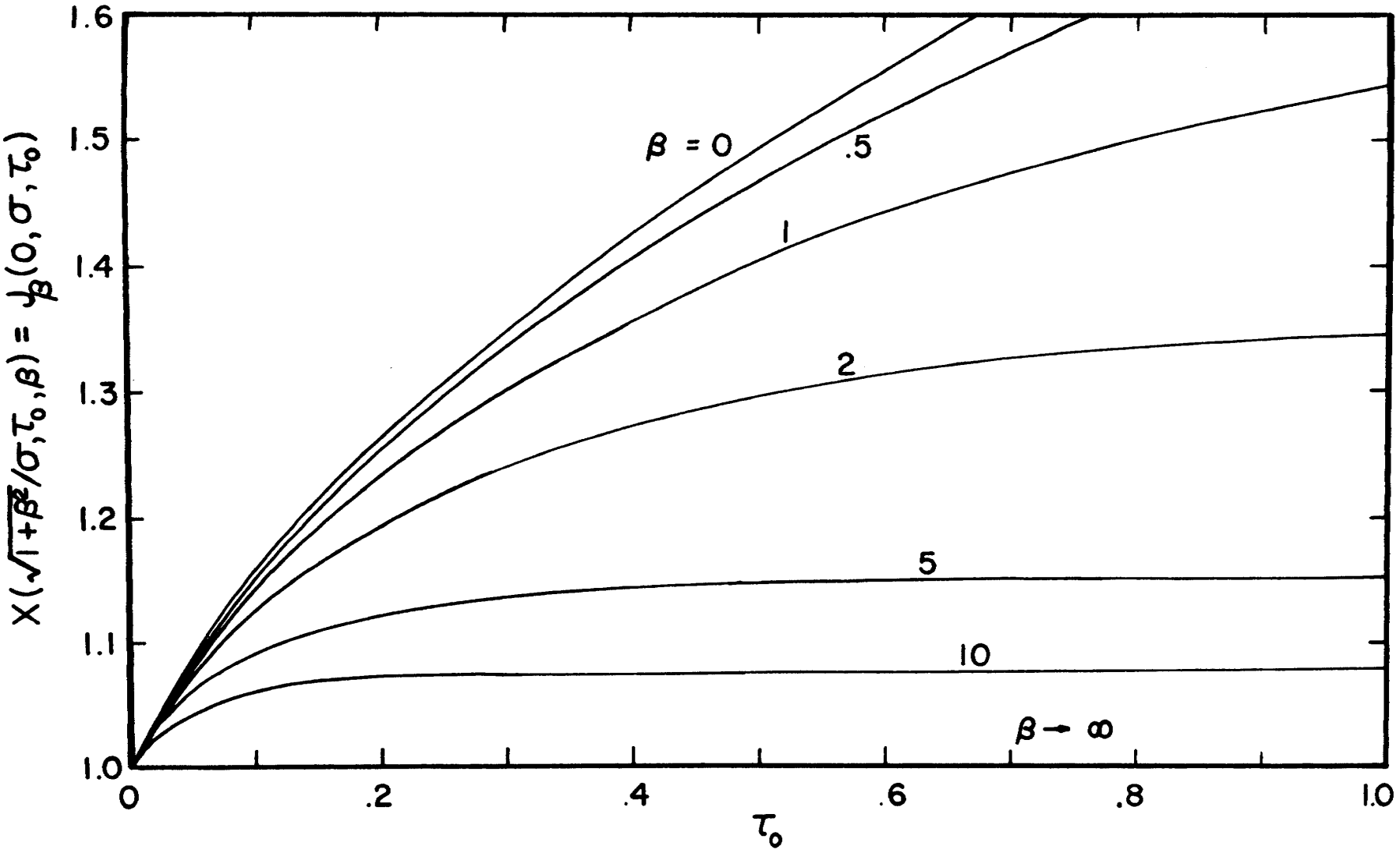

Figure 5.4 Variation of the generalized X-function with τ_0 for various values of β for σ=1

reveal that the generalized X-function can be approximated by the one-dimensional X-function at small β. When β=.5 and τ_0=1, the generalized X-function and the one-dimensional X-function differ by only .0746. At τ_0=3, this difference has increased to .2890 and attains a maximum of .8959 at the optical thick analysis. Hence, the error in the approximation increases with increasing optical thickness.

Figures 5.5 and 5.6 show the effect of σ on the generalized Y-function for β=1 and β=10, respectively. In both cases, the generalized Y-function is bounded by σ=1 and decreases to zero as σ approaches infinity. The generalized Y-function also approaches zero with increasing optical thickness. This behavior is a result of the energy being unable to penetrate to the infinite depth. Hence, the emissive power at $\tau_z=\tau_0$ and thus the generalized Y-function decrease with increasing optical thickness. Figures 5.5 and 5.6 reveal that the rate of decrease of the generalized Y-function to zero is slower than the rate of increase of the generalized X-function to the generalized H-function. In particular, when β=1 and σ=5, the generalized X-function differs from the optical thick generalized H-function by .0131 at τ_0=.8 whereas the generalized Y-function has the value .1134. At τ_0=3, this difference has decreased to .0001 for the generalized X- and H-functions with the generalized Y-function attaining the value .0088. Hence, the generalized Y-function requires a larger optical thickness to approximate the optical thick analysis than does the generalized X-function.

Figure 5.7 shows that there is an insufficient amount of data present to determine the combination of β and τ_0 for which the

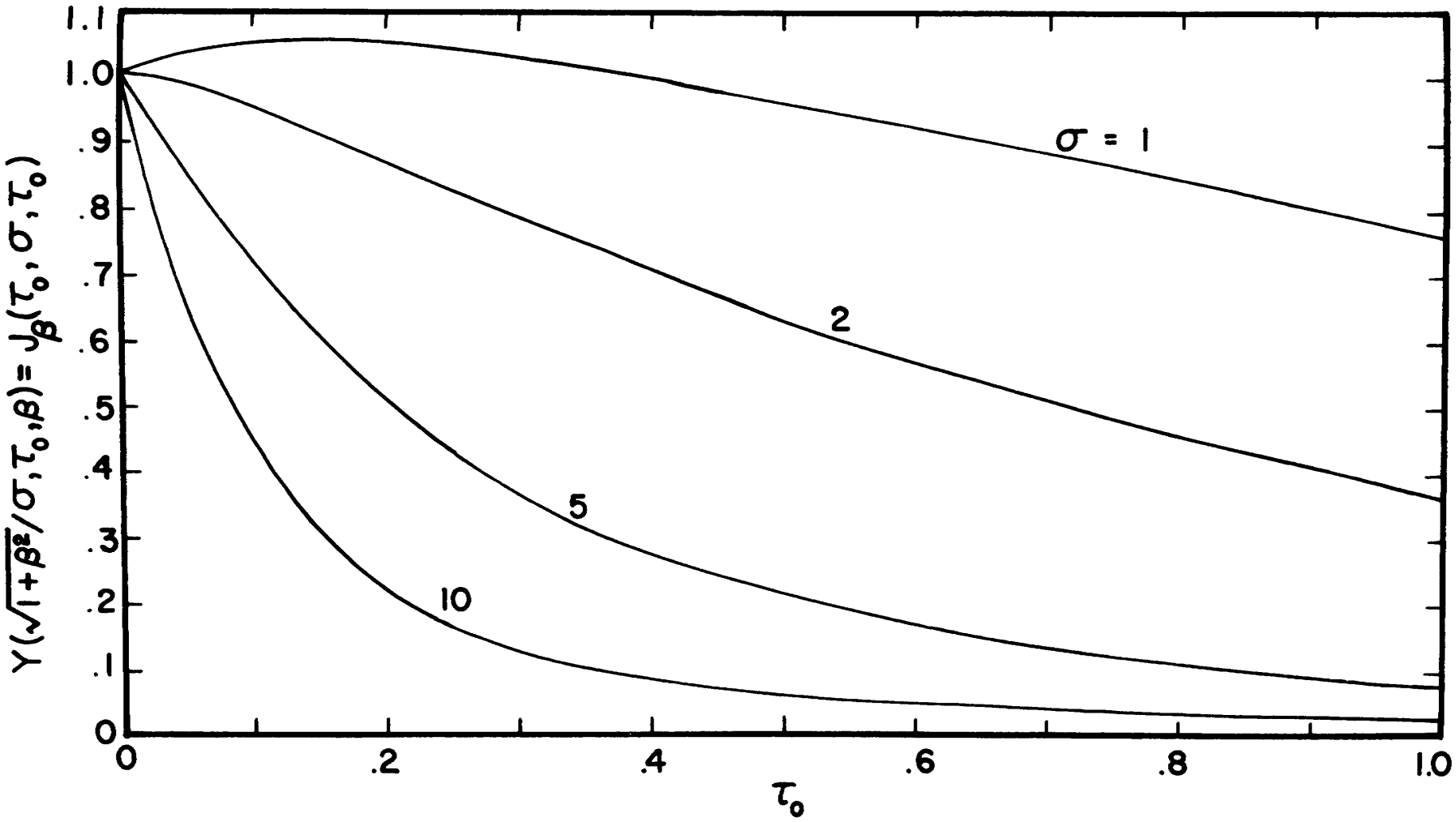

Figure 5.5 Variation of the generalized Y-function with τ_0 for various values of σ for β=1

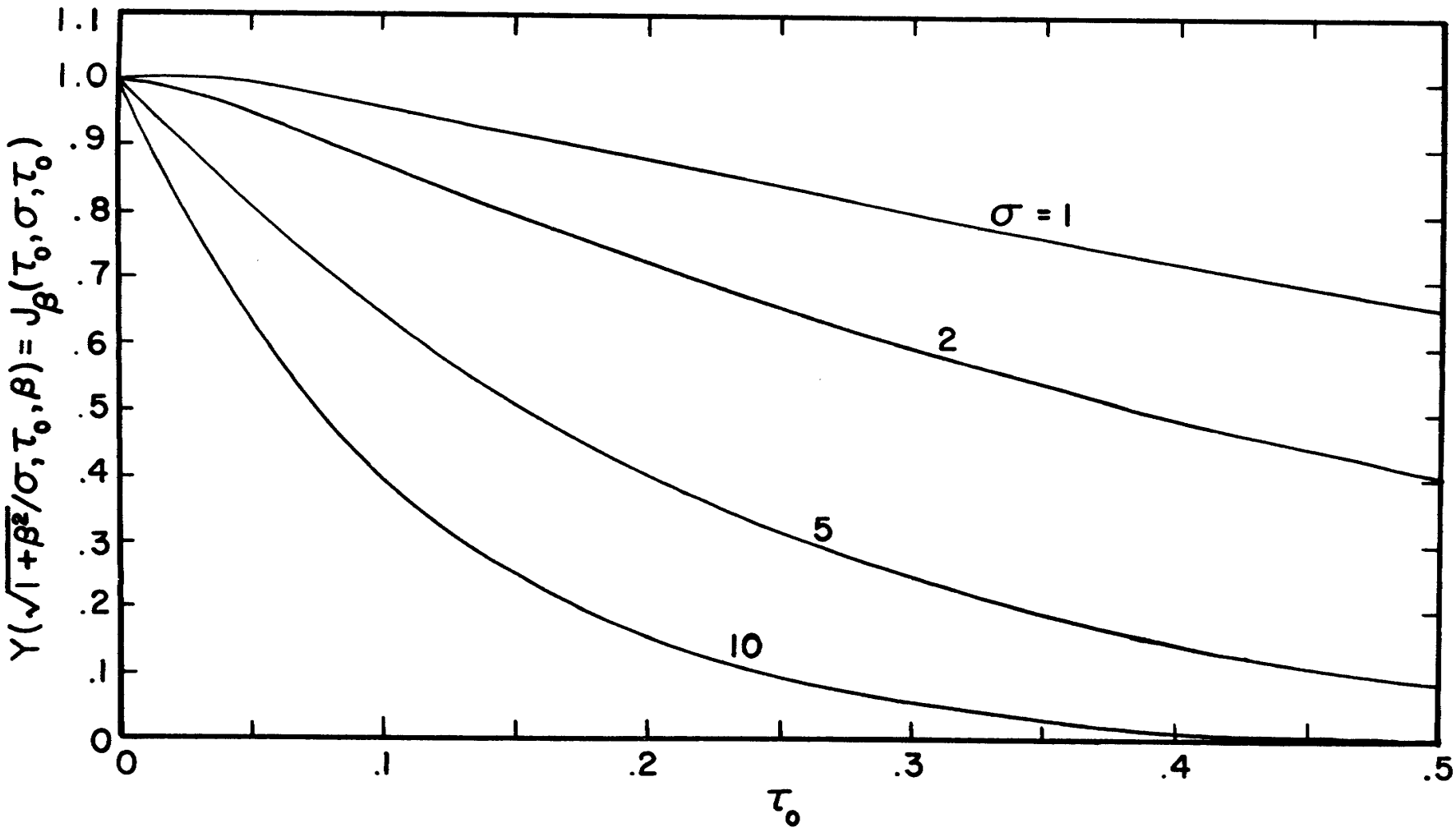

Figure 5.6 Variation of the generalized Y-function with τ_0 for various values of σ for β=10

generalized Y-function can be sufficiently approximated by the optical thick value of zero. A comparison of Figures 5.3 and 5.7 reveals that larger values of β are required for each constant τ_o curve to merge into the optical thick limit for the generalized Y-function than for the generalized X-function. Figure 5.7 also shows that the generalized Y-function, unlike the generalized X-function, is not bounded by unity and the optical thick value. At small values of β and τ_o, the generalized Y-function attains values which are greater than those corresponding to $\tau_o=0$. This same trend occurs for the one-dimensional Y-function of Chandrasekhar and hence is not a result which is characteristic of the two-dimensional analysis.

The effect of β and τ_o on the generalized Y-function is shown in Figure 5.8 for $\sigma=1$. At small β, the generalized Y-function increases to a maximum and then decreases to zero with increasing optical thickness. The maximum point shifts to smaller values of optical thickness as β increases. The generalized Y-function also decreases to zero when β approaches infinity. Figure 5.8 and Tables E.1 to E.14 show that for small β values the generalized Y-function can be approximated by the one-dimensional Y-function corresponding to $\beta=0$. When $\beta=.5$ and $\tau_o=1$, the generalized Y-function and the one-dimensional Y-function differ by .0717. However, at $\tau_o=3$, this difference has increased to .2322. The error in the approximation increases with increasing optical thickness.

D. EMISSIVE POWER FOR COSINE VARYING DIFFUSE BOUNDARY

The emissive power due to the cosine varying diffuse boundary condition can be expressed in terms of the moments of the generalized

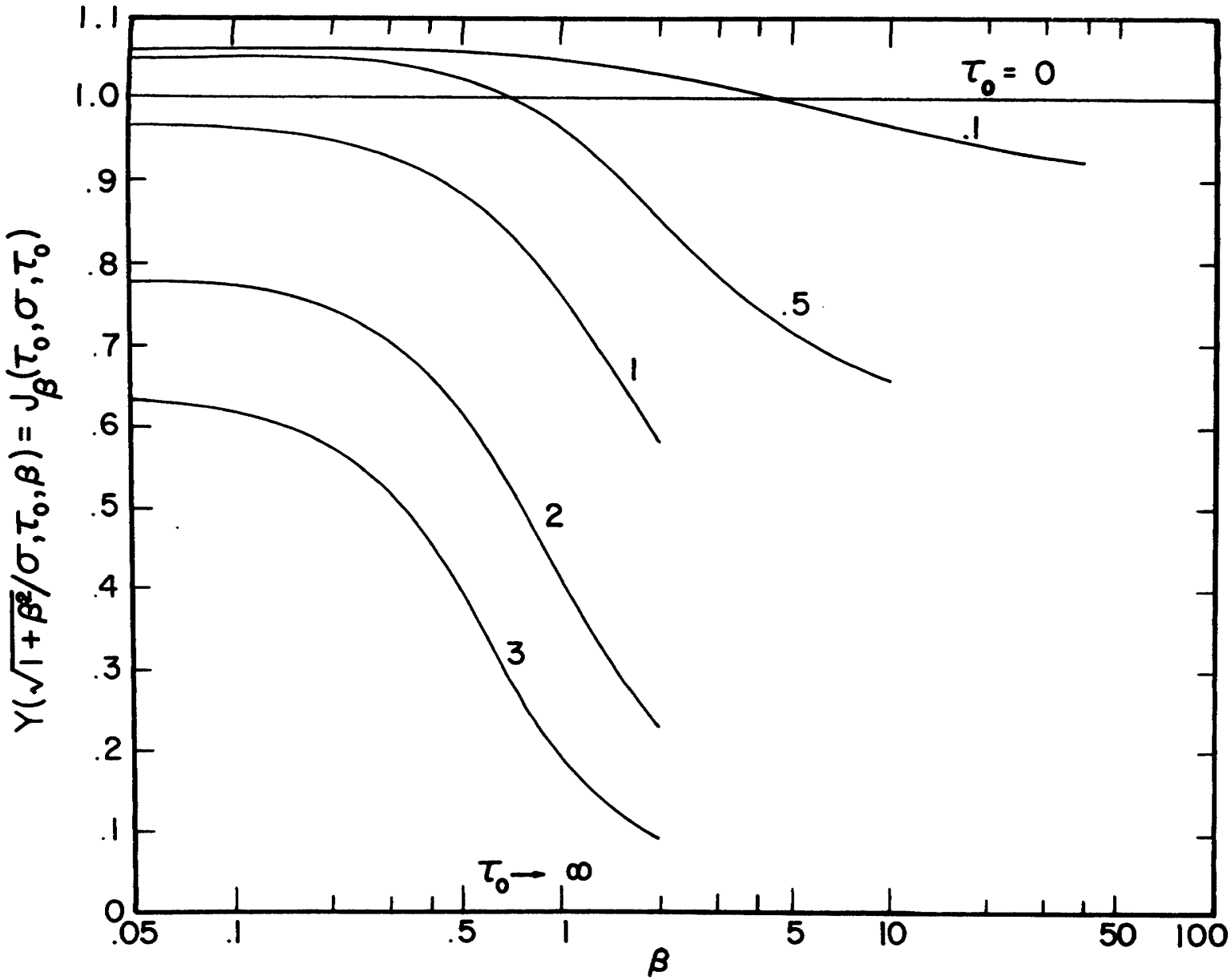

Figure 5.7 Variation of the generalized Y-function with β for various values of τ_0 for σ=1

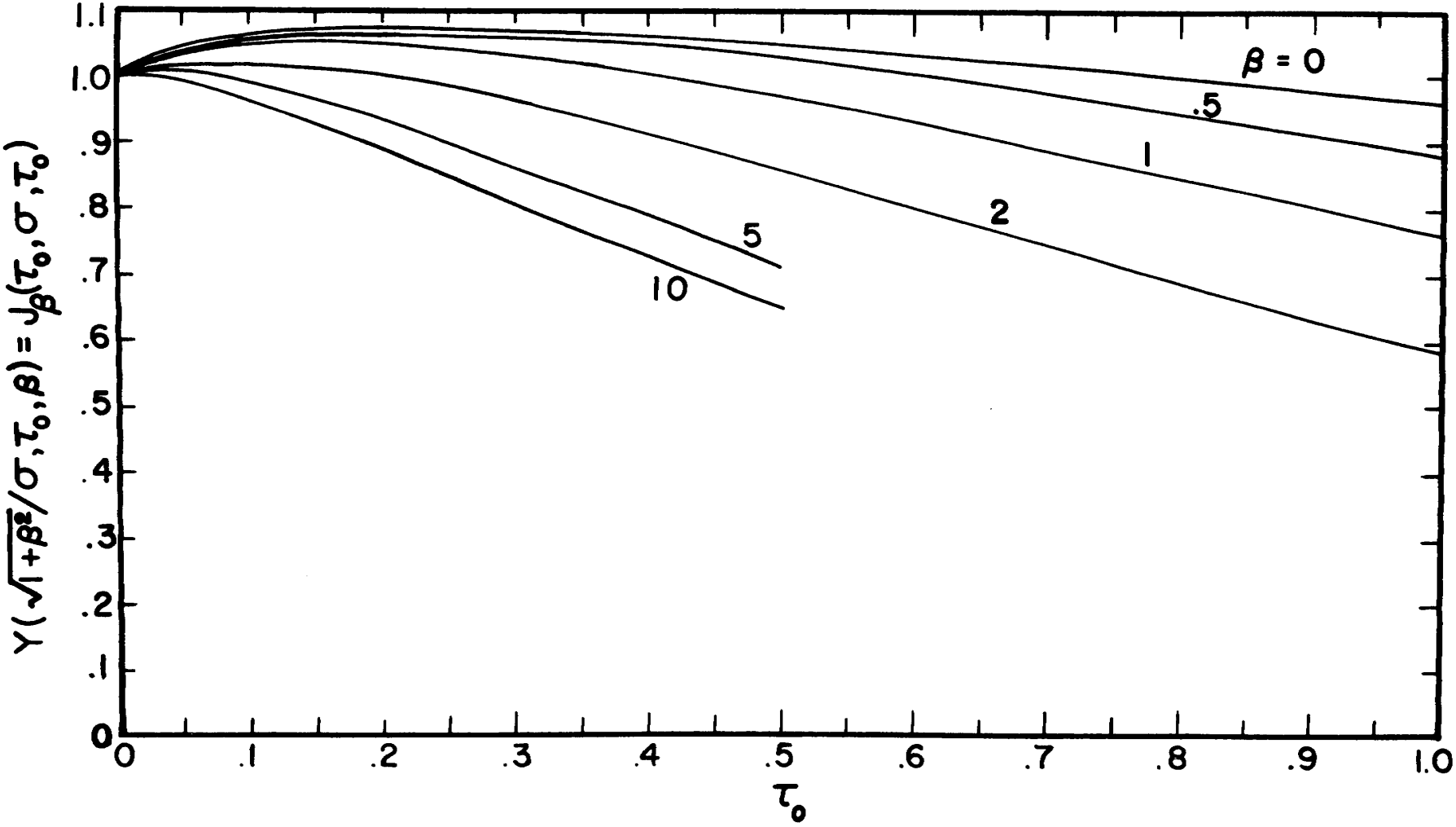

Figure 5.8 Variation of the generalized Y-function with τ_0 for various values of β for σ=1

X- and Y-functions. Evaluating equation (3.78) at $\tau_z=0$ and $\tau_z=\tau_o$ and utilizing equations (5.25) and (5.26) yields expressions for the emissive power for the diffuse wall

$$\phi_\beta(o,\tau_o) = \frac{1}{2}\int_o^1 \psi_1(x,\beta)X(x,\tau_o,\beta)dx \tag{5.58}$$

and

$$\phi_\beta(\tau_o,\tau_o) = \frac{1}{2}\int_o^1 \psi_1(x,\beta)Y(x,\tau_o,\beta)dx \quad . \tag{5.59}$$

Substitution of equations (5.49) and (5.50) with n=0 into equations (5.58) and (5.59) results in the simplified expressions for the emissive power at the boundaries in the form

$$\phi_\beta(o,\tau_o) = x_o(\beta,\tau_o)/2 \tag{5.60}$$

and

$$\phi_\beta(\tau_o,\tau_o) = y_o(\beta,\tau_o)/2 \quad . \tag{5.61}$$

The differential equations for $\phi_\beta(o,\tau_o)$ and $\phi_\beta(\tau_o,\tau_o)$ follow directly from equations (5.56) and (5.57) by utilizing equations (5.60) and (5.61) to arrive at

$$\frac{\partial\phi_\beta(o,\tau_o)}{\partial\tau_o} = \frac{\sqrt{1+\beta^2}}{2}\ \beta_{-1}(\beta,\tau_o)\phi_\beta(\tau_o,\tau_o) \tag{5.62}$$

and

$$2\frac{\partial\phi_\beta(\tau_o,\tau_o)}{\partial\tau_o} + \sqrt{1+\beta^2}\ y_{-1}(\beta,\tau_o) = \sqrt{1+\beta^2}\ \beta_{-1}(\beta,\tau_o)\phi_\beta(o,\tau_o) \quad . \tag{5.63}$$

Tables E.15 to E.18 list the emissive power at the boundaries for selected values of β and optical thickness τ_o. The results were calculated by the computer program discussed at the end of this chapter.

Figure 5.9 shows the emissive power at the boundary $\tau_z=0$ as a function of τ_o for various values of β. The emissive power is maximum at $\beta=0$ which corresponds to the one-dimensional model. Increasing β causes the emissive power to decrease and approach the minimum value of one-half as β becomes infinite. The emissive power levels off and approaches constant values at smaller optical thicknesses as β increases. This asymptotic behavior indicates that the emissive power for the finite medium is approaching the emissive power for the semi-infinite medium. In particular, when $\beta=10$, an optical thickness as small as $\tau_o=.1$ may be sufficient to approximate the finite analysis by the simpler semi-infinite model. Figure 5.9 and Tables E.15 to E.18 also reveal that approximating the two-dimensional model of $\beta\neq0$ by the one-dimensional model of $\beta=0$ yields satisfactory results for small β values. The error in the approximation increases with increasing optical thickness. In particular, when $\beta=.5$ the emissive power differs from the one-dimensional emissive power by .02759 at $\tau_o=1$, .08157 at $\tau_o=3$, and increases to a maximum of .20445 at the optical thick analysis.

Figure 5.10 and Tables E.15 to E.18 show the emissive power at $\tau_z=\tau_o$ as a function of τ_o for various values of β. The emissive power is maximum at $\beta=0$ and decreases to zero with increasing β or τ_o. The rate of decrease of the emissive power at $\tau_z=\tau_o$ to the semi-infinite value of zero is seen to be slower than the rate of increase of the emissive power at $\tau_z=0$ to the semi-infinite model. When $\beta=10$ and $\tau_o=.1$, the emissive power at $\tau_z=\tau_o$ has a value of .17942 whereas the emissive power at $\tau_z=0$ is already near to and approaching the

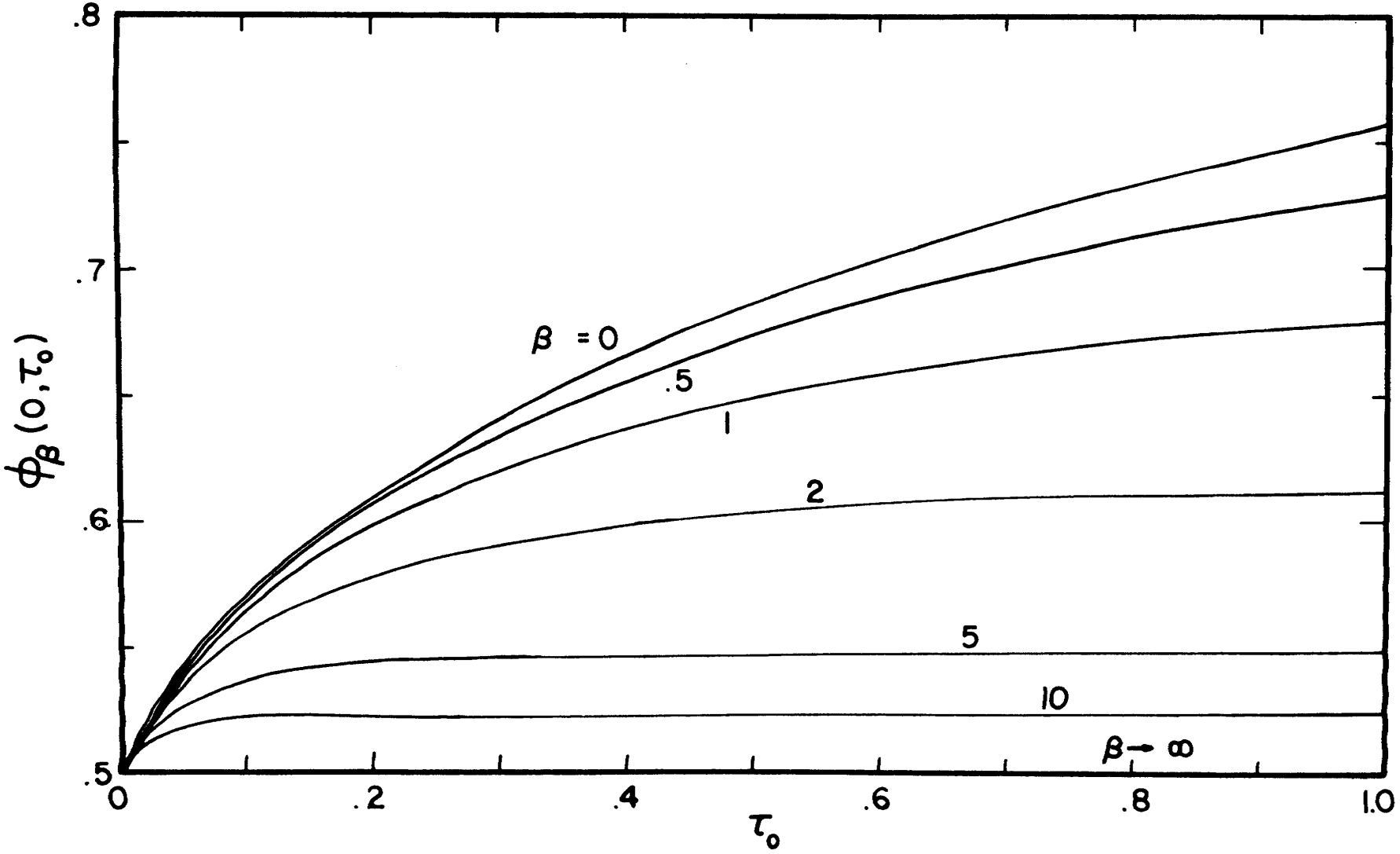

Figure 5.9 Variation in the emissive power at τ_z=0 with τ_0 for various values of β for a diffuse wall radiating in a cosine fashion into a finite medium

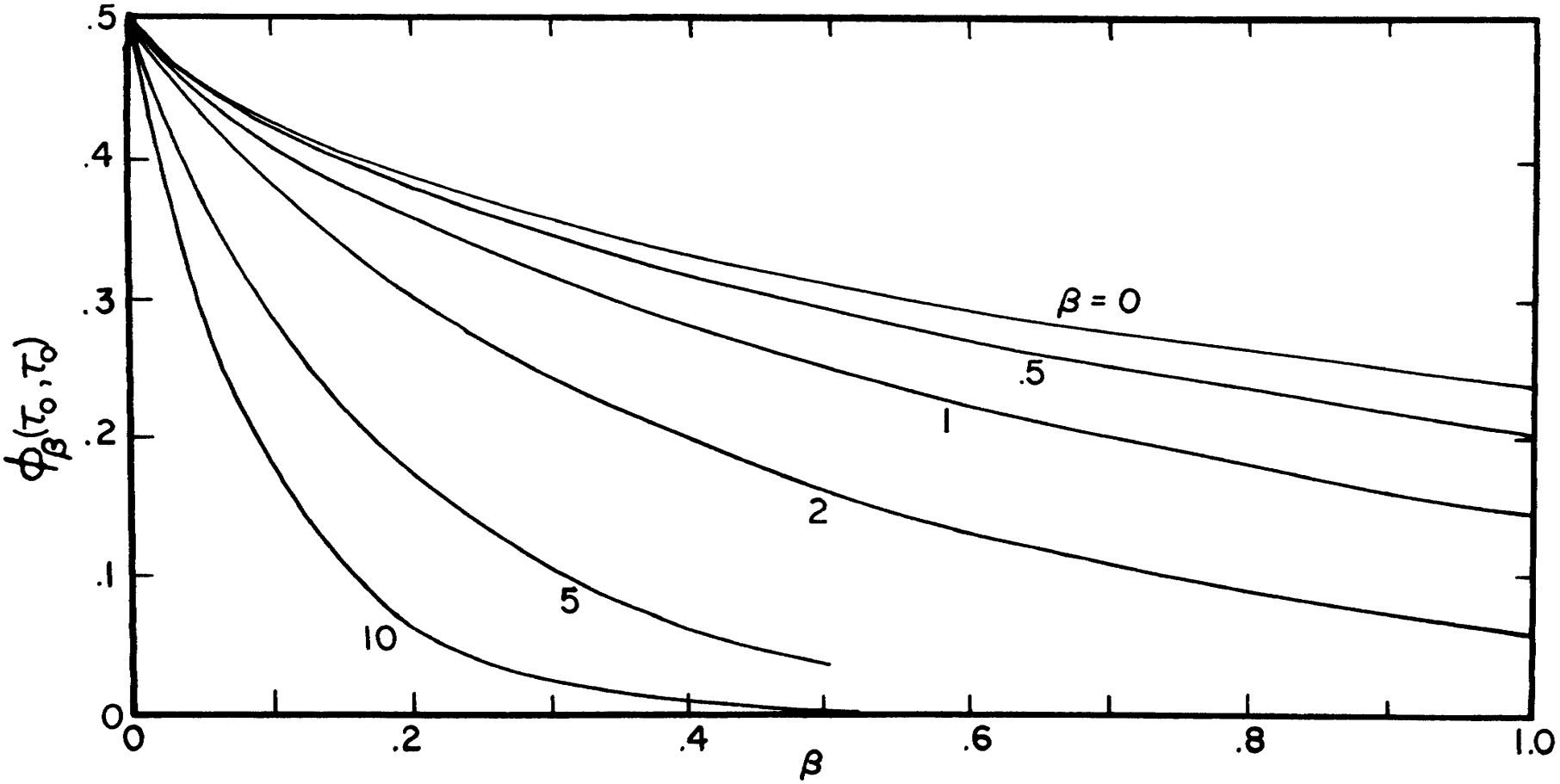

Figure 5.10 Variation in the emissive power at $\tau_z=\tau_o$ with τ_o for various values of β for a diffuse wall radiating in a cosine fashion into a finite medium.

semi-infinite model. Increasing τ_o to τ_o=.5 for β=10 causes the emissive power at $\tau_z=\tau_o$ to reduce to the value .00325. The error involved in approximating the emissive power at $\tau_z=\tau_o$ is of the same order of magnitude as the one-dimensional approximation for the emissive power at τ_z=0 for the range $\beta \leq .5$ and $\tau_o \leq 3$. When β=.5 and τ_o=1, the emissive power at $\tau_z=\tau_o$ differs from the one-dimensional emissive power at $\tau_z=\tau_o$ by .03354 and increases to .06122 at τ_o=3.

Figures 5.11 and 5.12 show the emissive power at the boundaries τ_z=0 and $\tau_z=\tau_o$ as a function of β for various values of τ_o. Both emissive powers are bounded by the value of 0.5 and that for the semi-infinite solution corresponding to $\tau_o=\infty$. Figure 5.12 reveals that the emissive power at infinity is zero. This follows since no energy has penetrated to the infinite depth. Figure 5.11 shows the combination of β and optical thickness τ_o which are sufficient to approximate the emissive power at τ_z=0 for the finite model by the emissive power at τ_z=0 for the semi-infinite analysis. The apparent value of β at which the constant optical thickness curves merge into the semi-infinite emissive power curve denoted by $\tau_o=\infty$ yields the desired values of β and τ_o. Figure 5.11 reveals that when τ_o=.1, a β value of 10 is the criterion for the approximation. For τ_o=3, this approximation can be used when $\beta \geq .6$. In particular, the finite model emissive power at τ_z=0 can be replaced by the simpler semi-infinite emissive power for any combination of $\tau_o \geq 3$ and $\beta \geq .6$.

Figure 5.12 shows the combination of β and optical thickness τ_o which are sufficient to approximate the emissive power at $\tau_z=\tau_o$ for the finite model by the zero emissive power for the semi-infinite

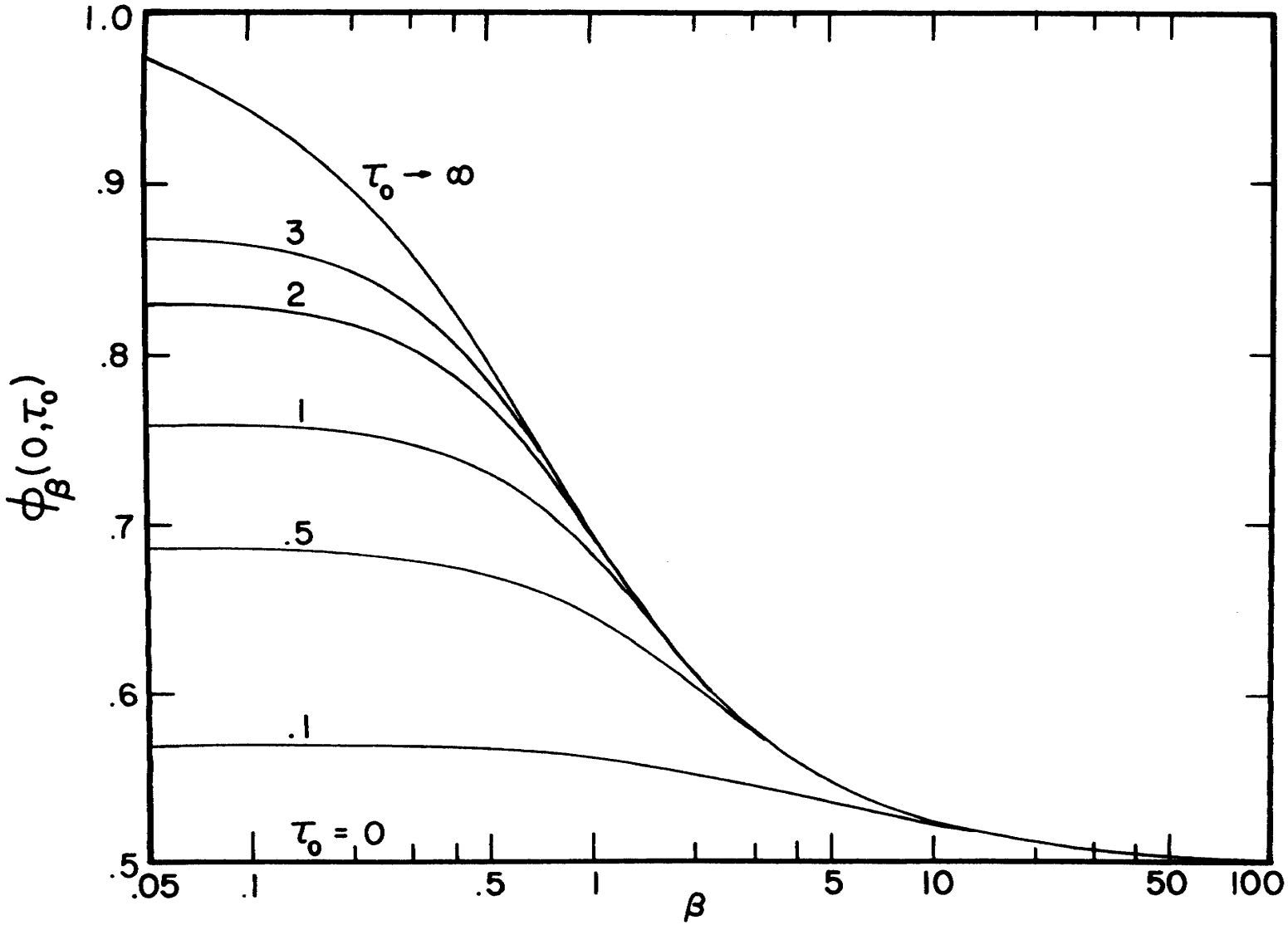

Figure 5.11 Variation in the emissive power at τ_z=0 with β for various values of τ_o for a diffuse wall radiating in a cosine fashion into a finite medium

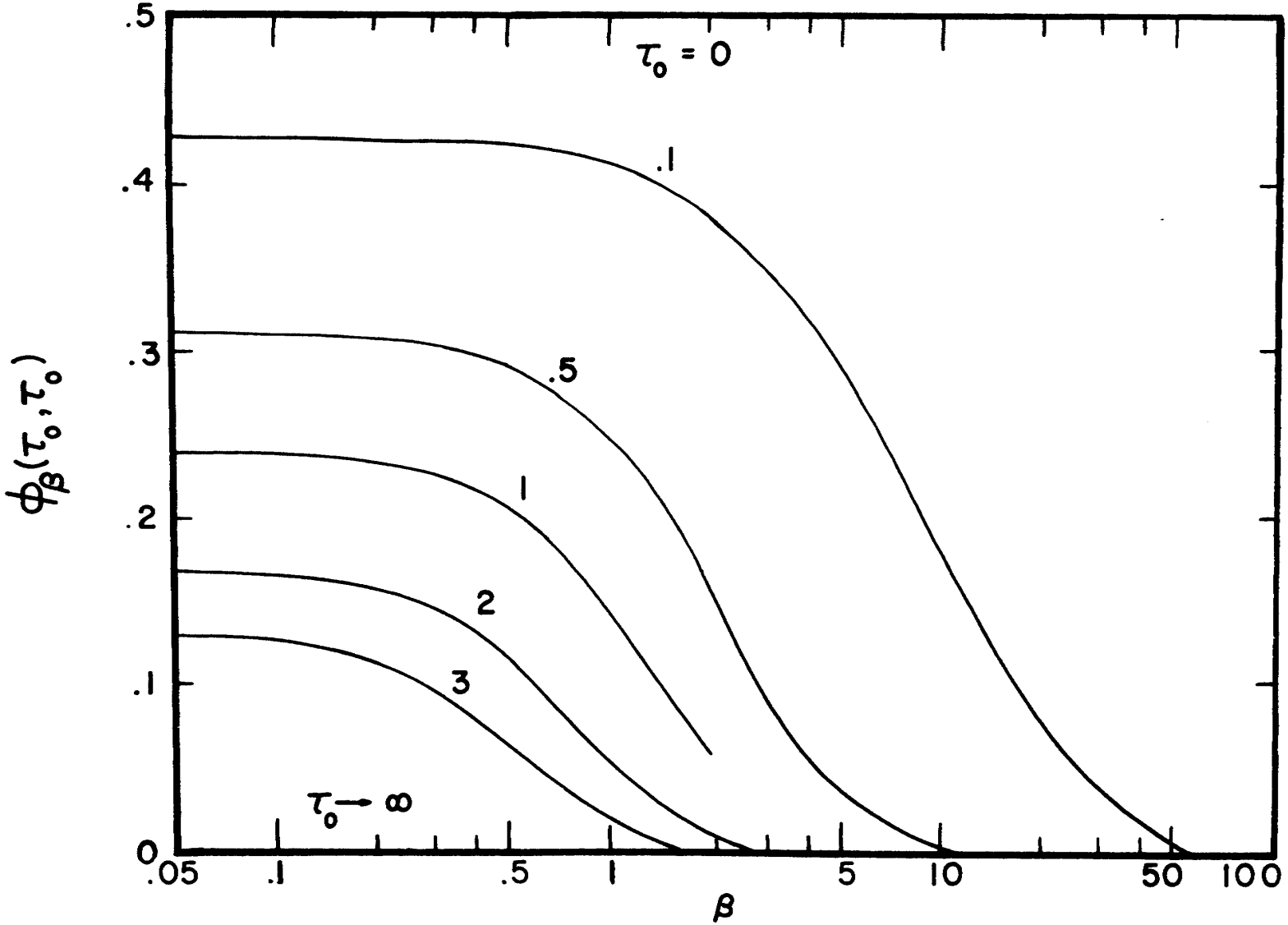

Figure 5.12 Variation in the emissive power at $\tau_z=\tau_o$ with β for various values of τ_o for a diffuse wall radiating in a cosine fashion into a finite medium

analysis. The same concept of selecting the value of β which causes the constant optical thickness curve to merge into the semi-infinite emissive power curve is applied. When $\tau_0=.1$, the value of β which allows the finite model to be approximated by the semi-infinite analysis is seen to be $\beta=55$. Increasing the optical thickness to $\tau_0=3$ causes the approximation to be valid for a smaller value of $\beta=2$. Thus, any combination of $\tau_0\geq 3$ and $\beta\geq 2$ permits the finite model emissive power at $\tau_z=\tau_0$ to be replaced by the semi-infinite value of zero.

The emissive power at the boundaries of the constant temperature finite strip could also be put in a form suitable for use in the computer program discussed in the finite strip theory of Chapter IV. Recall that this program integrates the product of an oscillating trigonometric function and a nonoscillating function. The nonoscillating function for the emissive power at $\tau_z=0$ is the moment of the generalized X-function $x_0(\beta,\tau_0)$. The nonoscillating function for the emissive power at $\tau_z=\tau_0$ is the moment of the generalized Y-function $y_0(\beta,\tau_0)$. The semi-infinite theory required the nonoscillating function, the generalized H-function, to be known at sixty-four values of β. Hence the finite theory functions $x_0(\beta,\tau_0)$ and $y_0(\beta,\tau_0)$ must be known for a large number of β values. The computer program at the end of this chapter must be run many times since each computer run assigns a specific value to β and calculates $x_0(\beta,\tau_0)$ and $y_0(\beta,\tau_0)$ for the range of optical thickness τ_0. Thus, the constant temperature finite strip analysis for the finite medium will not be solved due to the excessive amount of computational effort involved.

E. RADIATIVE FLUX FOR COSINE VARYING COLLIMATED BOUNDARY

The z-component of flux for the finite medium subjected to a collimated flux of cosine magnitude is given by equation (3.112) and can be written in the form

$$q_{zA}(\tau_z,\sigma,\tau_o)/F_o\cos\beta\tau_y = \frac{1}{\sigma}e^{-\sigma\tau_z} + \frac{1}{2}\int_0^{\tau_z} J_\beta(\tau_z',\sigma,\tau_o)\,\mathcal{E}_2(\tau_z-\tau_z',\beta)d\tau_z'$$

$$- \frac{1}{2}\int_{\tau_z}^{\tau_o} J_\beta(\tau_z',\sigma,\tau_o)\,\mathcal{E}_2(\tau_z'-\tau_z,\beta)d\tau_z' \quad . \tag{5.64}$$

The flux at the boundaries is obtained by evaluating equation (5.64) at $\tau_z=0$ and $\tau_z=\tau_o$

$$\mathcal{F}_A(o,\sigma,\tau_o) = \frac{1}{\sigma} - \frac{1}{2}\int_0^{\tau_o} J_\beta(\tau_z',\sigma,\tau_o)\,\mathcal{E}_2(\tau_z',\beta)d\tau_z' \tag{5.65}$$

and

$$\mathcal{F}_A(\tau_o,\sigma,\tau_o) = \frac{1}{\sigma}e^{-\sigma\tau_o} + \frac{1}{2}\int_0^{\tau_o} J_\beta(\tau_z',\sigma,\tau_o)\,\mathcal{E}_2(\tau_o-\tau_z',\beta)d\tau_z' \tag{5.66}$$

where the dimensionless flux $\mathcal{F}_A$ is defined as

$$\mathcal{F}_A(\tau_z,\sigma,\tau_o) = q_{zA}(\tau_z,\sigma,\tau_o)/F_o\cos\beta\tau_y = \bar{q}_{zA}(\tau_z,\sigma,\tau_o) \quad . \tag{5.67}$$

By inserting the definition of the $\mathcal{E}_2$-function from equation (3.69) into equations (5.65) and (5.66) and interchanging the order of integration, the flux at the boundary becomes

$$\mathcal{F}_A(o,\sigma,\tau_o) = \frac{1}{\sigma} - \frac{1}{2}\int_1^\infty \frac{dt}{t^2}\int_0^{\tau_o} J_\beta(\tau'_z,\sigma,\tau_o)e^{-\tau'_z\sqrt{t^2+\beta^2}}\,d\tau'_z \tag{5.68}$$

and

$$\mathcal{F}_A(\tau_o,\sigma,\tau_o) = \frac{1}{\sigma}e^{-\sigma\tau_o}$$

$$+ \frac{1}{2}\int_1^\infty \frac{dt}{t^2}\int_0^{\tau_o} J_\beta(\tau'_z,\sigma,\tau_o)e^{-(\tau_o-\tau'_z)\sqrt{t^2+\beta^2}}\,d\tau'_z \quad . \tag{5.69}$$

The interior integrals in equations (5.68) and (5.69) are the generalized reflection function $R_\beta(\sqrt{t^2+\beta^2},\sigma,\tau_o)$ and transmission function $S_\beta(\sqrt{t^2+\beta^2},\sigma,\tau_o)$, respectively. Insertion of these functions into equations (5.68) and (5.69) yields

$$\mathcal{F}_A(o,\sigma,\tau_o) = \frac{1}{\sigma} - \frac{1}{2}\int_1^\infty R_\beta(\sqrt{t^2+\beta^2},\sigma,\tau_o)\,\frac{dt}{t^2} \tag{5.70}$$

and

$$\mathcal{F}_A(\tau_o,\sigma,\tau_o) = \frac{1}{\sigma}e^{-\sigma\tau_o} + \frac{1}{2}\int_1^\infty S_\beta(\sqrt{t^2+\beta^2},\sigma,\tau_o)\,\frac{dt}{t^2} \quad . \tag{5.71}$$

The substitution $x=\sqrt{1+\beta^2}/\sqrt{t^2+\beta^2}$ further reduces equations (5.70) and (5.71) to

$$\mathcal{F}_A(o,\sigma,\tau_o) = \frac{1}{\sigma} - \frac{1}{2}\int_0^1 \psi_1(x,\beta)R_\beta(\sqrt{1+\beta^2}/x,\sigma,\tau_o)dx \tag{5.72}$$

and

$$\mathcal{F}_A(\tau_o,\sigma,\tau_o) = \frac{1}{\sigma}e^{-\sigma\tau_o} + \frac{1}{2}\int_0^1 \psi_1(x,\beta)S_\beta(\sqrt{1+\beta^2}/x,\sigma,\tau_o)dx \quad . \tag{5.73}$$

Next, the flux at the boundaries can be related to the emissive power at the boundaries by inserting equations (5.22) and (5.30) into equations (5.72) and (5.73). This yields

$$\mathcal{Z}_A(o,\sigma,\tau_o) = \frac{1}{\sigma} - \frac{1}{2}\int_0^1 \psi_1(x,\beta)$$

$$\left[\frac{J_\beta(o,\sqrt{1+\beta^2}/x,\tau_o)J_\beta(o,\sigma,\tau_o)-J_\beta(\tau_o,\sqrt{1+\beta^2}/x,\tau_o)J_\beta(\tau_o,\sigma,\tau_o)}{\sqrt{1+\beta^2}/x + \sigma}\right] dx \quad (5.74)$$

and

$$\mathcal{Z}_A(\tau_o,\sigma,\tau_o) = \frac{1}{\sigma} e^{-\sigma\tau_o} + \frac{1}{2}\int_0^1 \psi_1(x,\beta)$$

$$\left[\frac{J_\beta(o,\sqrt{1+\beta^2}/x,\tau_o)J_\beta(\tau_o,\sigma,\tau_o)-J_\beta(\tau_o,\sqrt{1+\beta^2}/x,\tau_o)J_\beta(o,\sigma,\tau_o)}{\sqrt{1+\beta^2}/x - \sigma}\right] dx \quad . \quad (5.75)$$

Finally, the substitution $\sigma=\sqrt{1+\beta^2}/\mu$ along with the use of equations (5.25) and (5.26) gives a relationship between the boundary flux and the generalized X- and Y-functions as

$$\bar{\mathcal{Z}}_A(o,\mu,\tau_o)$$

$$= \frac{\mu}{\sqrt{1+\beta^2}}\left[1 - \frac{1}{2}\int_0^1 \frac{x\psi_1(x,\beta)}{x+\mu}[X(x,\tau_o,\beta)X(\mu,\tau_o,\beta)-Y(x,\tau_o,\beta)Y(\mu,\tau_o,\beta)]dx\right] \quad (5.76)$$

and

$$\bar{\mathcal{Z}}_A(\tau_o,\mu,\tau_o) = \frac{\mu}{\sqrt{1+\beta^2}}\left[e^{-\tau_o\sqrt{1+\beta^2}/\mu}\right.$$

$$\left. + \frac{1}{2}\int_0^1 \frac{x\psi_1(x,\beta)}{\mu-x}[X(x,\tau_o,\beta)Y(\mu,\tau_o,\beta)-Y(x,\tau_o,\beta)X(\mu,\tau_o,\beta)]dx\right] \quad (5.77)$$

where $\bar{\mathcal{F}}_A$ is a dimensionless flux defined by

$$\bar{\mathcal{F}}_A(o,\mu,\tau_o) = \mathcal{F}_A(o,\sqrt{1+\beta^2}/\mu,\tau_o) \tag{5.78}$$

and

$$\bar{\mathcal{F}}_A(\tau_o,\mu,\tau_o) = \mathcal{F}_A(\tau_o,\sqrt{1+\beta^2}/\mu,\tau_o) \quad . \tag{5.79}$$

Tables E.19 to E.32 list the numerical behavior of the radiative flux at the boundaries for the cosine varying collimated boundary condition. The results were obtained from the computer program discussed at the end of this chapter. When $\beta=0$, the two-dimensional radiative flux reduces to the one-dimensional result. Within computational limits, the one-dimensional results at $\tau_z=0$ are seen to be identical to those at $\tau_z=\tau_o$.

The equality of the one-dimensional fluxes at $\tau_z=0$ and $\tau_z=\tau_o$ is a result of the assumption of radiative equilibrium which requires the divergence of the flux vector to be zero. For the one-dimensional analysis, this implies that a single derivative of the magnitude of the flux be equal to zero. Thus, the flux must be constant throughout the finite medium, depending only on the optical thickness τ_o. When the optical thickness approaches infinity, the finite model approaches the semi-infinite model. Hence, the flux is zero throughout the semi-infinite medium since no energy can penetrate into the infinite depth.

In the two-dimensional analysis of $\beta\neq0$, the radiative flux is a function of two position variables. Therefore the divergence equation has two independent derivatives and thus becomes a partial differential equation which does not have the simple form of the one-dimensional model. The result is that the normal component of flux is no

longer constant throughout the finite medium. The difference in the normal flux at $\tau_z=0$ and the normal flux at $\tau_z=\tau_o$ is attributed to the weakening of the normal flux by energy transfer into a horizontal direction due to the temperature variation in that direction. This horizontal transfer of energy is not present in the one-dimensional model since there is no horizontal temperature variation.

The effect of σ on the radiative flux at the boundaries due to the cosine varying collimated boundary condition is shown in Figure 5.13 for $\beta=1$ and in Figure 5.14 for $\beta=10$. The fluxes at $\tau_z=0$ and $\tau_z=\tau_o$ are presented on the same figure for ease of comparison. Both boundary fluxes are maximum at $\sigma=1$ and decrease to zero with increasing σ. The σ dependence of the boundary flux can be seen in equations (5.74) and (5.75). Figures 5.13 and 5.14 show the difference in the flux at $\tau_z=0$ and at $\tau_z=\tau_o$ with increasing σ and τ_o. The flux at $\tau_z=0$ levels off and approaches the optical thick result at smaller values of optical thickness with increasing σ, whereas the flux at $\tau_z=\tau_o$ decreases to the optical thick value of zero with increasing τ_o. The flux at $\tau_z=\tau_o$ decreases to zero with increasing optical thickness since no energy can penetrate into an infinitely large depth.

Figures 5.13 and 5.14 along with Tables E.19 to E.32 also reveal that the flux at $\tau_z=\tau_o$ decreases to the optical thick value of zero at a slower rate than the flux at $\tau_z=0$ decreases to the semi-infinite flux. When $\beta=1$ and $\sigma=2$, the flux at $\tau_z=0$ and the semi-infinite flux differ by .02537 at $\tau_o=1$, whereas the flux at $\tau_z=\tau_o$ has the value .19657. At $\tau_o=3$, this difference has decreased to .00040 with the flux at $\tau_z=\tau_o$ attaining the value .02810. A comparison of Figures

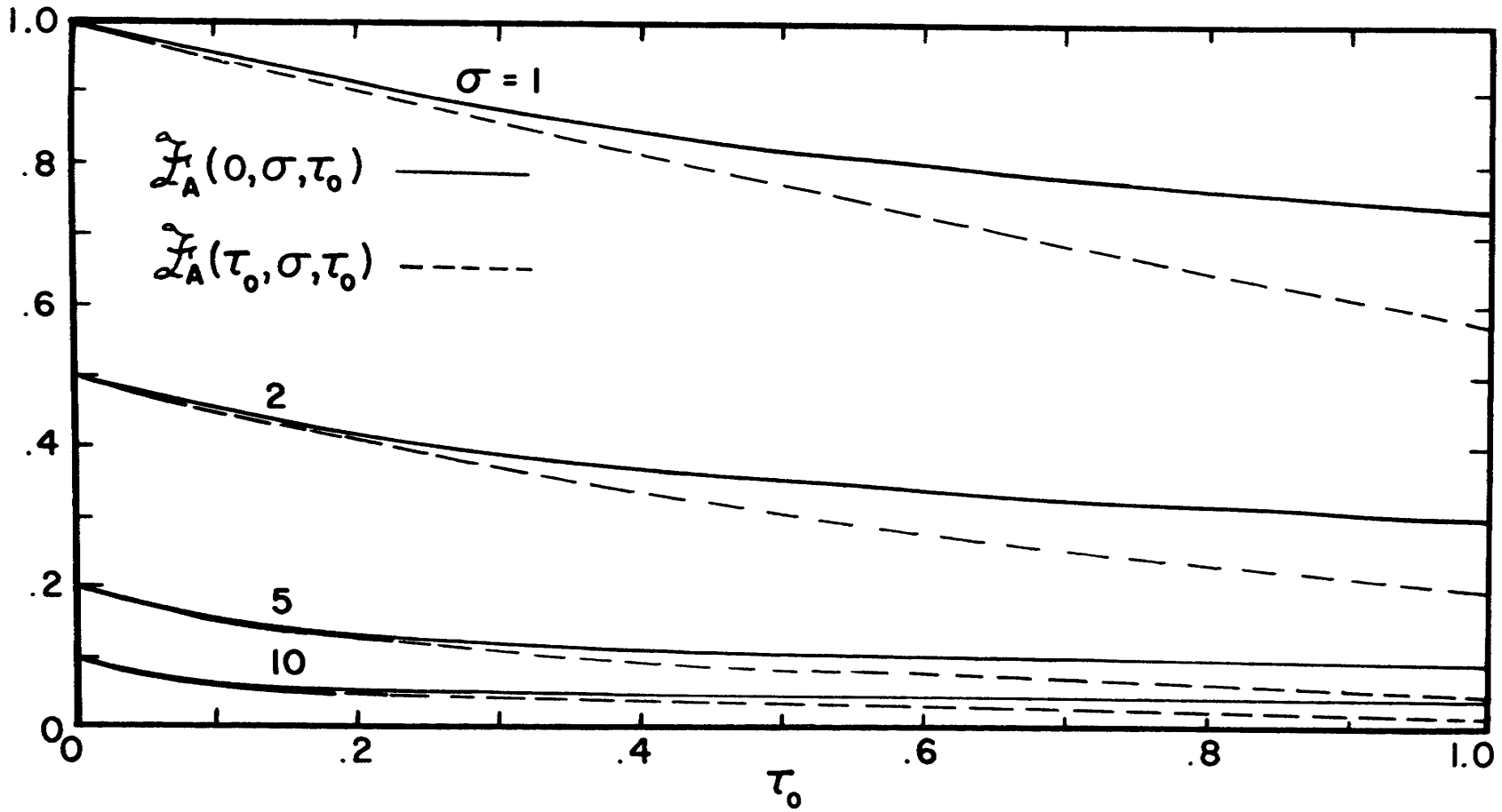

Figure 5.13 Variation in the normal flux at $\tau_z=0$ and $\tau_z=\tau_0$ with τ_0 for various values of σ for a finite medium illuminated by a collimated flux of cosine magnitude for $\beta=1$

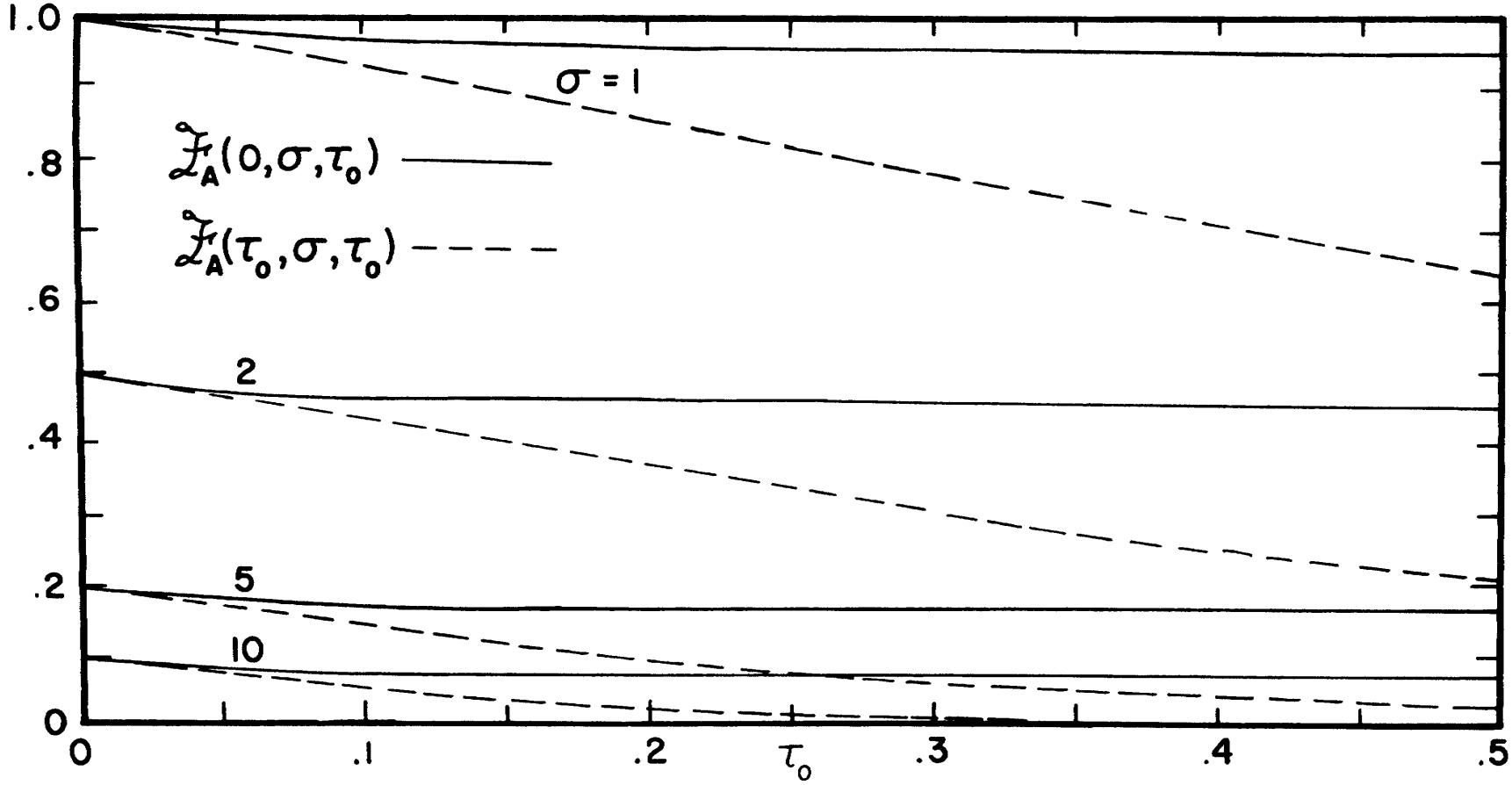

Figure 5.14 Variation in the normal flux at $\tau_z=0$ and $\tau_z=\tau_0$ with τ_0 for various values of σ for a finite medium illuminated by a collimated flux of cosine magnitude for $\beta=10$

5.13 and 5.14 shows that the magnitude of the flux at $\tau_z=0$ is considerably larger for $\beta=10$ than it is for $\beta=1$. Furthermore, the flux at $\tau_z=0$ levels off and approaches the optical thick solution at smaller values of τ_o. In particular, when $\beta=10$ and $\sigma=2$, the flux at $\tau_z=0$ and the optical thick limit differ by only .00027 at $\tau_o=.5$ as compared to .07395 for $\beta=1$.

Figure 5.15 shows that the flux at $\tau_z=0$ is bounded above by unity and below by the optical thick limit. The values of β at which the τ_o curves are asymptotic to the semi-infinite flux correspond to the values of β and τ_o for which the finite flux can be approximated by the semi-infinite flux for $\sigma=1$. When$\beta\geq 1$ and $\tau_o\geq 3$, the finite flux at $\tau_z=0$ can not differ by more than .00213 from the semi-infinite flux at $\tau_z=0$.

The flux at $\tau_z=\tau_o$ is bounded above by unity and below by the optical thick value of zero as shown in Figure 5.16 for $\sigma=1$. A comparison of Figures 5.15 and 5.16 reveals that the flux at $\tau_z=\tau_o$ requires larger values of β than the flux at $\tau_z=0$ to approximate the finite analysis by the semi-infinite theory. This requirement is apparent at small values of τ_o where the flux at $\tau_z=\tau_o$ is almost constant over the range $0\leq\beta\leq 40$. This constant behavior implies a small variation from the one-dimensional model ($\beta=0$). The flux starts to deviate from the almost horizontal one-dimensional constant value and decreases to zero at smaller values of β as τ_o is increased. Hence, increasing τ_o decreases the corresponding value of β necessary to approximate the finite flux at $\tau_z=\tau_o$ by the optical thick value of zero.

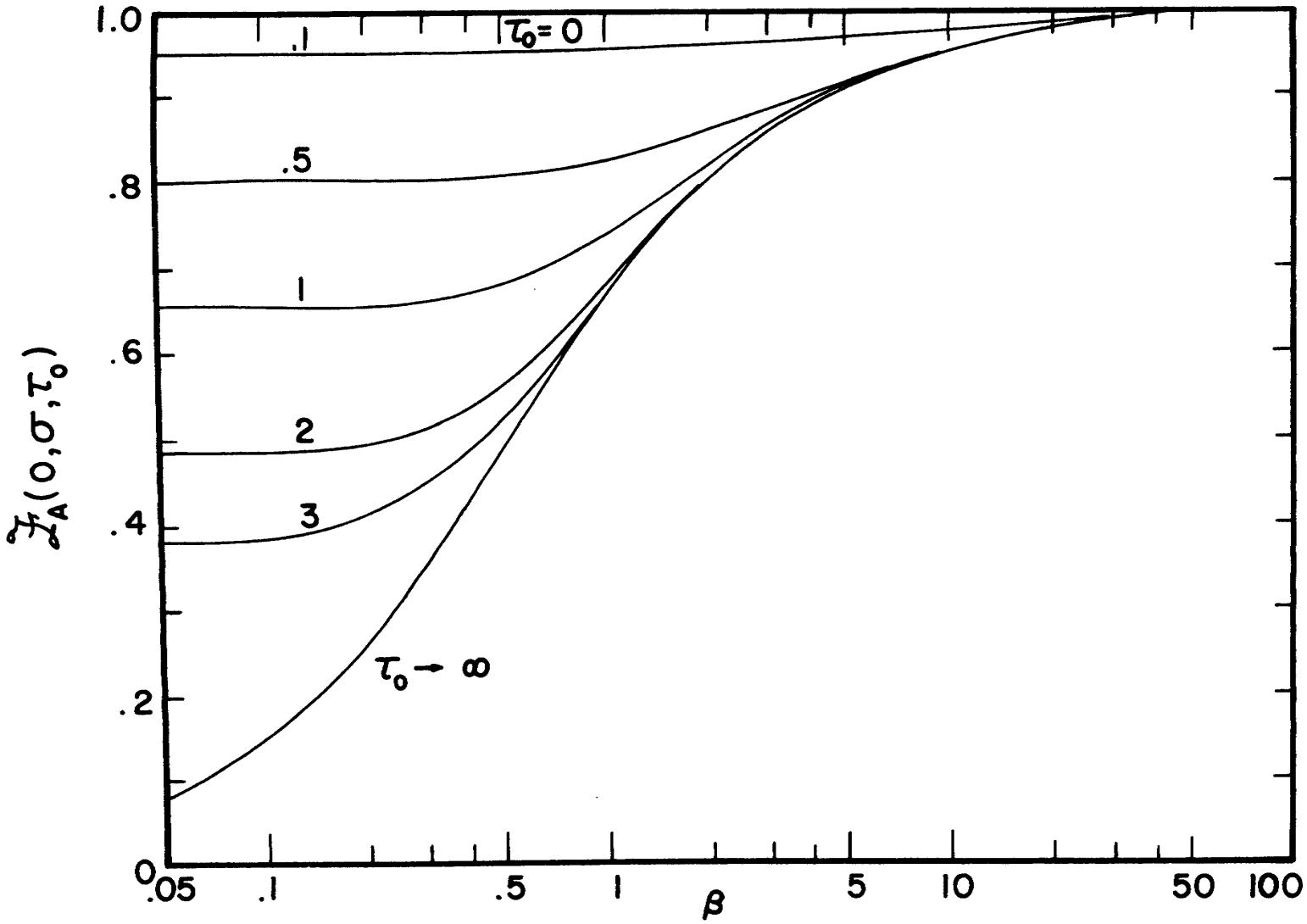

Figure 5.15 Variation in the normal flux at $\tau_z=0$ with β for various values of τ_0 for a finite medium illuminated by a collimated flux of cosine magnitude from direction $\sigma=1$

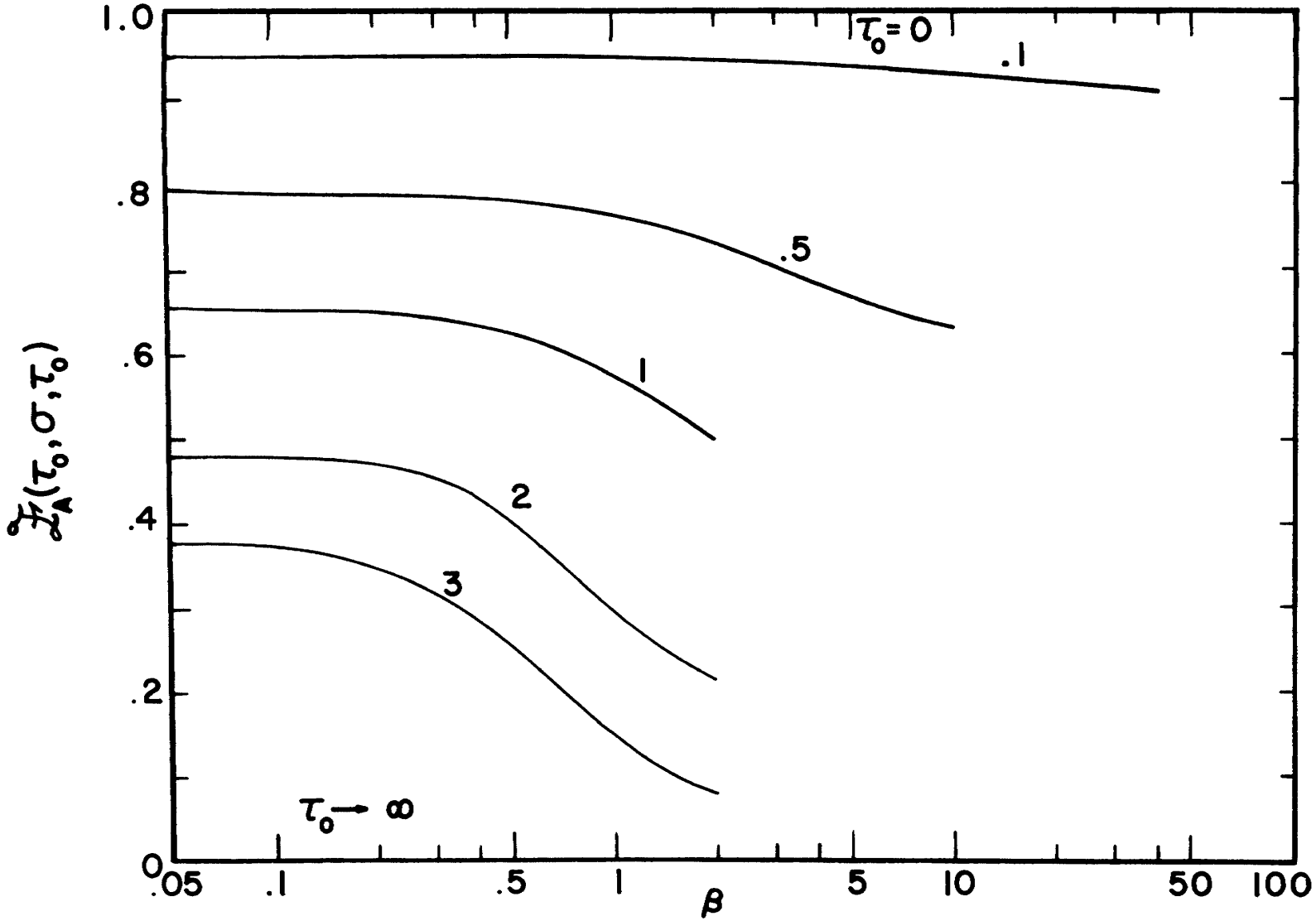

Figure 5.16 Variation in the normal flux at $\tau_z = \tau_0$ with β for various values of τ_0 for a finite medium illuminated by a collimated flux of cosine magnitude from direction $\sigma = 1$

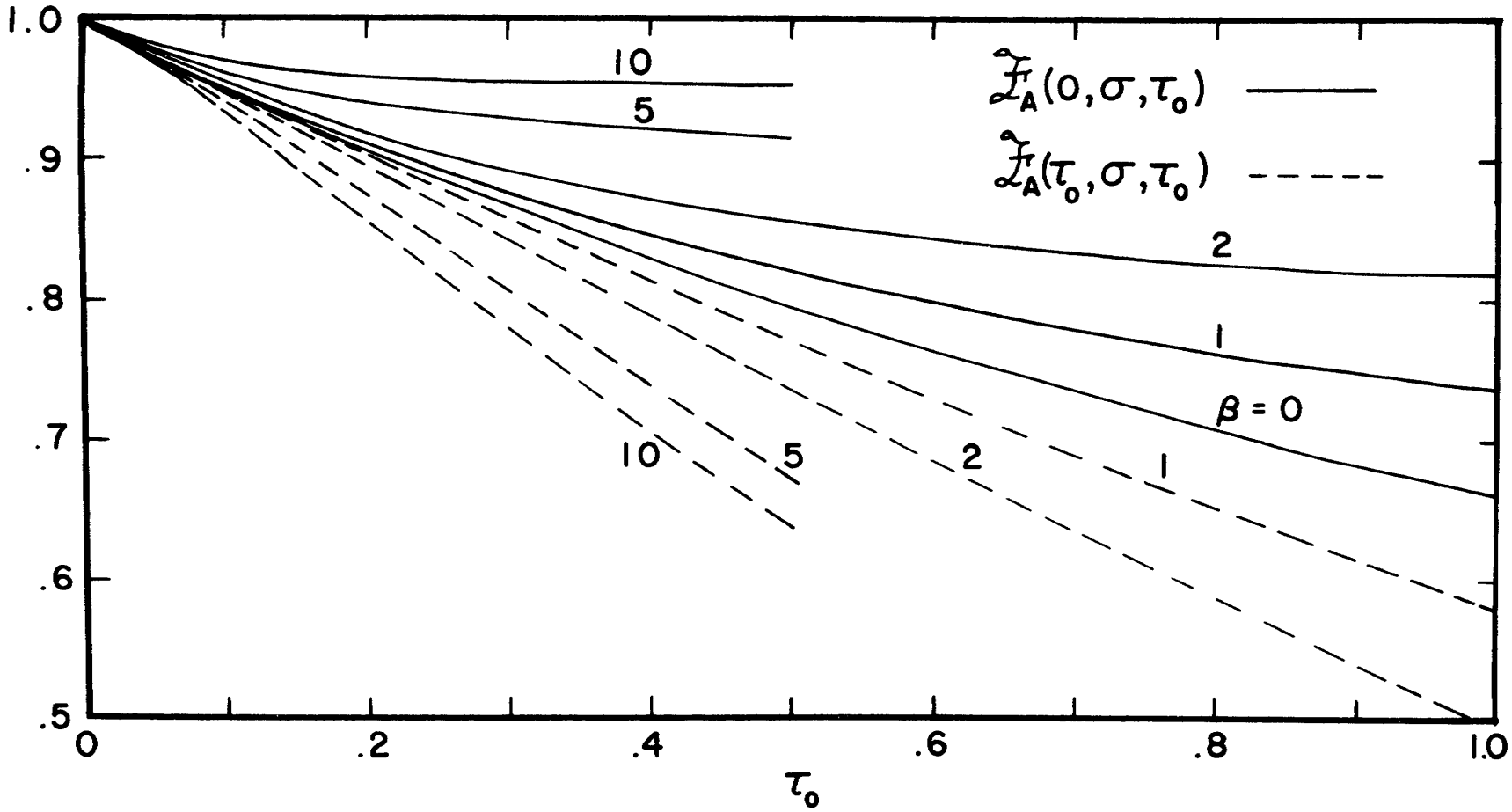

Figure 5.17 Variation in the normal flux at $\tau_z=0$ and $\tau_z=\tau_0$ with τ_0 for various values of β for a finite medium illuminated by a collimated flux of cosine magnitude from direction $\sigma=1$

The effect of β and τ_o on the flux at $\tau_z=0$ and the flux at $\tau_z=\tau_o$ is shown in Figure 5.17 for $\sigma=1$. The flux at $\tau_z=0$ is bounded above by unity and below by the one-dimensional flux. The flux at $\tau_z=\tau_o$ is bounded above by the one-dimensional flux and below by the value zero. The flux at $\tau_z=0$ levels off and approaches the optical thick limit at smaller values of τ_o for increasing values of β, whereas the flux at $\tau_z=\tau_o$ decreases to zero with increasing β and τ_o. Figure 5.17 reveals that the fluxes at $\tau_z=0$ and $\tau_z=\tau_o$ can be approximated by the one-dimensional flux for small β values. The deviation from the value of $\beta=0$ with increasing τ_o indicates that the error in the one-dimensional approximation increases with increasing τ_o.

F. RADIATIVE FLUX FOR COSINE VARYING DIFFUSE BOUNDARY

The z-component of flux for the cosine varying diffuse boundary condition is related to the z-component of flux for the cosine varying collimated boundary through equation (3.150) which reduces to

$$\mathcal{F}_C(\tau_z,\tau_o) = 2\,\mathcal{E}_3(\tau_z,\beta) + 2\int_1^\infty \bar{q}_{zA}(\tau_z,\sqrt{t^2+\beta^2},\tau_o)\,\frac{dt}{t^2}$$

$$- 2\int_1^\infty \frac{e^{-\tau_z\sqrt{t^2+\beta^2}}}{t^2\sqrt{t^2+\beta^2}}\,dt \qquad (5.80)$$

where the dimensionless diffuse flux $\mathcal{F}_C$ is defined by

$$\mathcal{F}_C(\tau_z,\tau_o) = \bar{q}_{zC}(\tau_z,\tau_o)/\theta_2^4 \quad . \qquad (5.81)$$

The change of variable $x=\sqrt{1+\beta^2}/\sqrt{t^2+\beta^2}$ along with equation (5.67) yields

$$\mathcal{F}_C(\tau_z,\tau_o) = 2\,\mathcal{E}_3(\tau_z,\beta) + 2\int_0^1 \psi_1(x,\beta)\,\overline{\mathcal{F}}_A(\tau_z,x,\tau_o)\,dx$$

$$- \frac{2}{\sqrt{1+\beta^2}}\int_0^1 x\psi_1(x,\beta)\,e^{-\tau_z\sqrt{1+\beta^2}/x}\,dx \quad . \qquad (5.82)$$

Evaluation of equation (5.82) at $\tau_z=0$ and $\tau_z=\tau_o$ yields the z-component of diffuse flux at the boundaries expressed in terms of the z-component of flux due to the collimated boundary in the form

$$\mathcal{F}_C(o,\tau_o) = 1 + 2\int_0^1 \psi_1(x,\beta)\,\overline{\mathcal{F}}_A(o,x,\tau_o)\,dx + \frac{2}{\beta^2}\,(1-\sqrt{1+\beta^2}) \qquad (5.83)$$

and

$$\mathcal{F}_C(\tau_o,\tau_o) = 2\,\mathcal{E}_3(\tau_o,\beta)$$

$$+ 2\int_0^1 \psi_1(x,\beta)\left[\,\overline{\mathcal{F}}_A(\tau_o,x,\tau_o) - \frac{x}{\sqrt{1+\beta^2}}\,e^{-\tau_o\sqrt{1+\beta^2}/x}\,\right]dx \quad . \qquad (5.84)$$

Tables E.33 to E.35 list the numerical behavior of the radiative flux at the boundaries for the cosine varying diffuse boundary condition. The results were obtained from the computer program discussed at the end of this chapter. When $\beta=0$, the two-dimensional flux reduces to the one-dimensional result. The one-dimensional fluxes at $\tau_z=0$ and $\tau_z=\tau_o$ are seen to be equal, whereas the two-dimensional fluxes of $\beta\neq0$ are different. The equality of the one-dimensional fluxes and the inequality of the two-dimensional fluxes at $\tau_z=0$ and $\tau_z=\tau_o$ follows from the same argument previously discussed in the section for the flux due to the cosine varying collimated boundary condition.

Figure 5.18 shows the flux at $\tau_z=0$ and at $\tau_z=\tau_o$ as a function of optical thickness for various values of β. A comparison of Figures 5.17 and 5.18 reveals that the flux for the diffuse case and the flux for the collimated case exhibit similar trends. The flux at $\tau_z=0$ for the diffuse case is bounded above by unity and below by the one-dimensional result. The flux at $\tau_z=\tau_o$ for the diffuse case is bounded above by the one-dimensional result and below by the optical thick value of zero. The flux at $\tau_z=0$ for the diffuse case levels off and approaches the optical thick limit at smaller values of τ_o with increasing β. The flux at $\tau_z=\tau_o$ for the diffuse case decreases to zero with increasing β at a more rapid rate than does the flux at $\tau_z=\tau_o$ for the collimated case at $\sigma=1$.

The variation in the flux at $\tau_z=0$ and at $\tau_z=\tau_o$ for the diffuse boundary as a function of β is shown for various values of τ_o in Figures 5.19 and 5.20, respectively. Except for numerical values, the flux at $\tau_z=0$ and at $\tau_z=\tau_o$ behave in a similar fashion for both the diffuse and collimated boundary conditions. This behavior is seen by comparing Figures 5.15 and 5.19 for the flux at $\tau_z=0$ and Figures 5.16 and 5.20 for the flux at $\tau_z=\tau_o$. The flux at $\tau_z=\tau_o$ for the diffuse boundary is seen to deviate from the nearly constant one-dimensional effect and decrease to zero at smaller values of β than does the flux at $\tau_z=\tau_o$ for the collimated boundary at $\sigma=1$.

G. NUMERICAL PROCEDURE

1. DESCRIPTION OF COMPUTER PROGRAM

The numerical results presented in this chapter are obtained from a single computer program. The main portion of the program

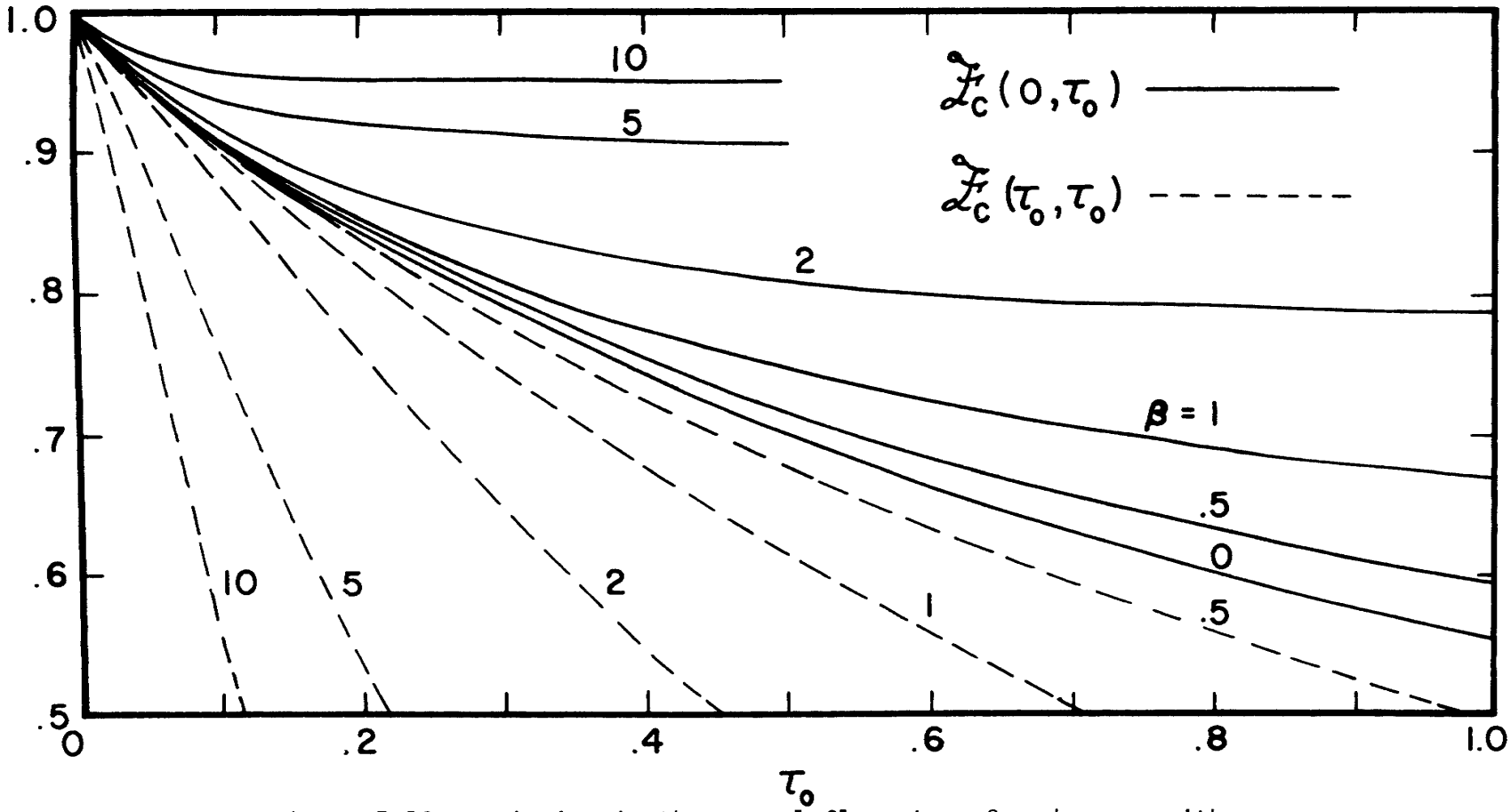

Figure 5.18 Variation in the normal flux at $\tau_z=0$ and $\tau_z=\tau_o$ with τ_o for various values of β for a diffuse wall radiating in a cosine fashion into a finite medium

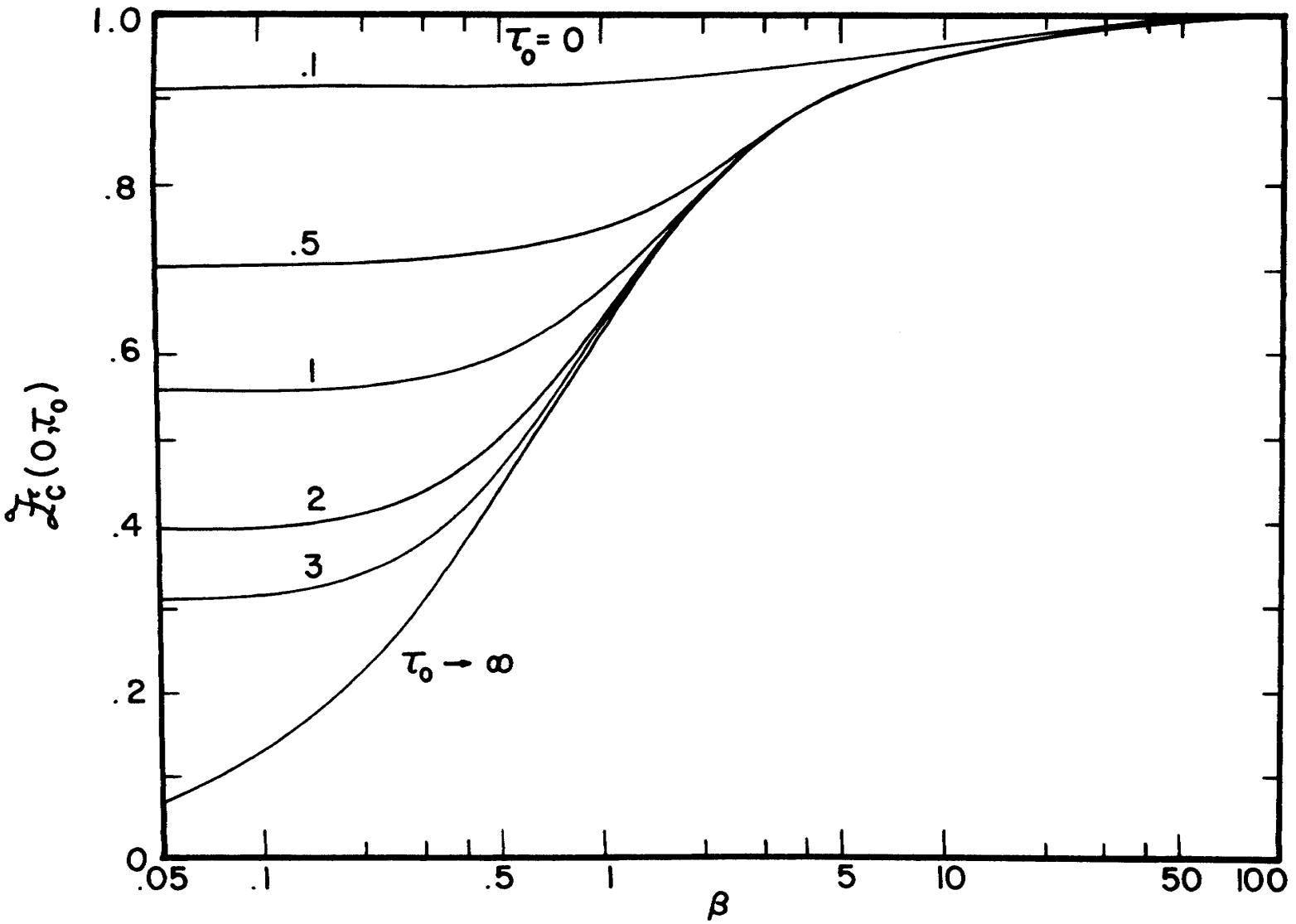

Figure 5.19 Variation in the normal flux at τ_z=0 with β for various values of τ_0 for a diffuse wall radiating in a cosine fashion into a finite medium

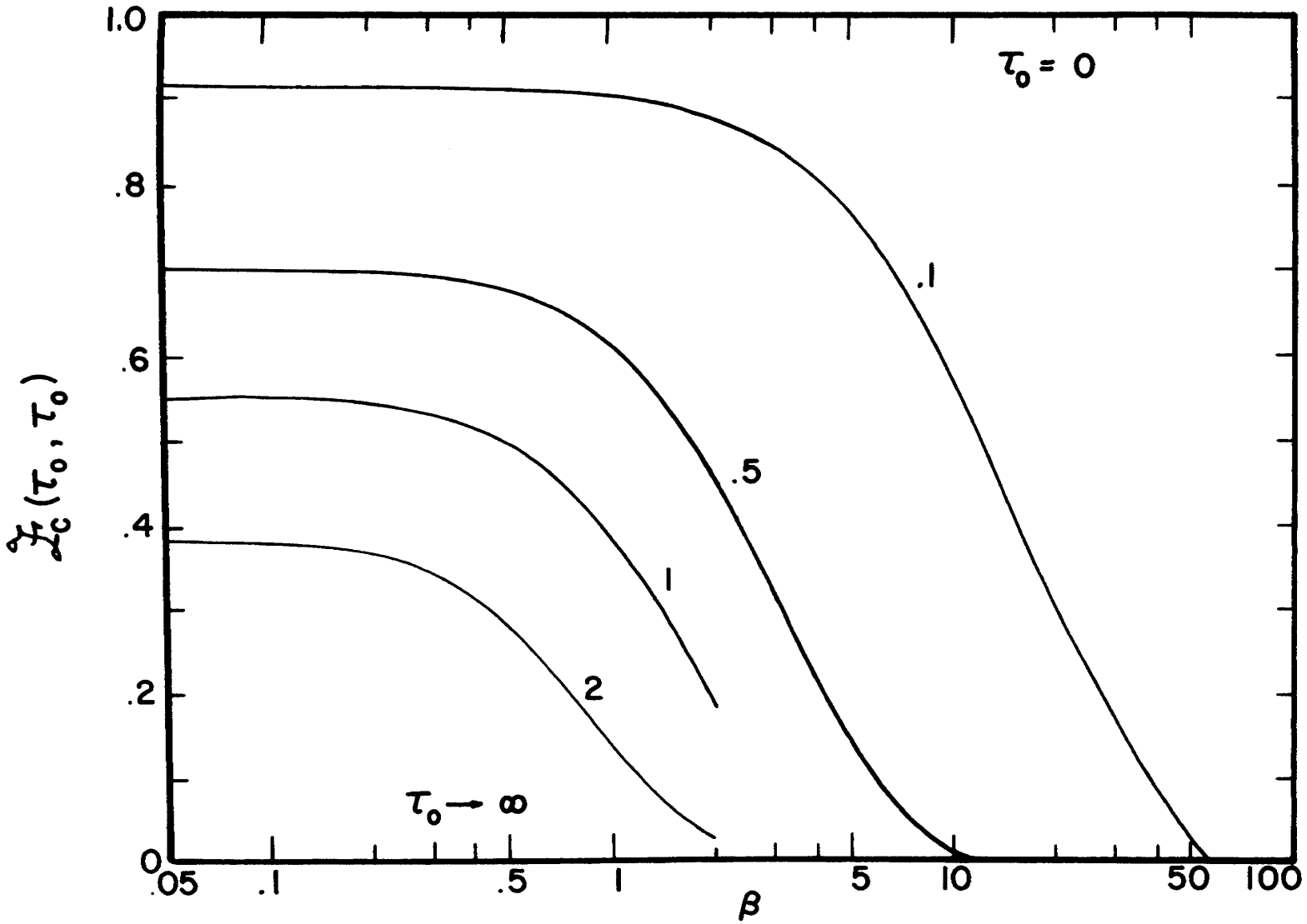

Figure 5.20 Variation in the normal flux at $\tau_z=\tau_o$ with β for various values of τ_o for a diffuse wall radiating in a cosine fashion into a finite medium

consists of solving a system of eighty differential equations by a fourth order Runge-Kutta routine. The step size depends upon the parameter β. A step size of .005 is used for β=0, .1, .5, 1, 2, and 5. Increasing β necessitates the use of a smaller step size. When β=10, a step size of .0025 is used which is decreased to .0005 for β=40. When β=100, the step size is .0001. Thus, for large β the small step size limits the magnitude of the optical thickness which is practical to attain because of the excessive computational time. However, the finite model solutions approach the semi-infinite solutions at very small optical thickness for large β.

The integral appearing in the integro-differential equations (5.42) and (5.43) is divided into two parts:

$$\int_0^1 \frac{\psi_0(x,\beta)}{x} Y(x,\tau_0,\beta)dx = \int_0^{\varepsilon_1} \frac{\psi_0(x,\beta)}{x} Y(x,\tau_0,\beta)dx + \int_{\varepsilon_1}^1 \frac{\psi_0(x,\beta)}{x} Y(x,\tau_0,\beta)dx \qquad (5.85)$$

where $0 \le \varepsilon_1 \le 1$. This division is necessary due to the singularity of the integrand and to the behavior of ψ_1 previously discussed in Chapter IV. Evaluating the first integral on the right-hand side of equation (5.85) by Gaussian quadrature of order n_1 with weights ω_{1k} and abscissas x_{1k} and the second integral by Gaussian quadrature of order n_2 with weights ω_{2k} and abscissas x_{2k} yields

$$\int_0^1 \frac{\psi_0(x,\beta)}{x} Y(x,\tau_0,\beta)dx = \sum_{k=1}^{n_1+n_2} \frac{\omega_k \psi_0(x_k,\beta)}{x_k} Y(x_k,\tau_0,\beta) \qquad (5.86)$$

where ω_k and x_k are weights and abscissas of the Gaussian quadrature defined in terms of the weights and abscissas of each interval as

$$x_k = \varepsilon_1 (x_{1k}+1)/2$$

$$\omega_k = \varepsilon_1 \omega_{1k}/2 \qquad k=1,2,\ldots n_1$$

$$x_k = \frac{1}{2}(1-\varepsilon_1)x_{2(k-n_1)} + (1+\varepsilon_1)/2$$

$$\omega_k = \frac{1}{2}(1-\varepsilon_1)\omega_{2(k-n_1)} \qquad k=n_1+1,n_1+2,\ldots n_1+n_2 \qquad (5.87)$$

An evaluation of the integro-differential equations (5.42) and (5.43) at discrete values corresponding to the abscissas of the quadrature and utilization of the reduced notation of equation (5.87) yield $2(n_1+n_2)$ ordinary differential equations

$$\frac{dX_i}{d\tau_o} = \frac{\sqrt{1+\beta^2}}{2} Y_i \sum_{k=1}^{n_1+n_2} \frac{\omega_k \psi_{ok} Y_k}{x_k}$$

$$\frac{dY_i}{d\tau_o} = -\frac{\sqrt{1+\beta^2}}{x_i} Y_i + \frac{\sqrt{1+\beta^2}}{2} X_i \sum_{k=1}^{n_1+n_2} \frac{\omega_k \psi_{ok} Y_k}{x_k} \qquad i=1,2,\ldots n_1+n_2 \qquad (5.88)$$

where

$$X_i = X(x_i,\tau_o,\beta)$$

$$Y_i = Y(x_i,\tau_o,\beta)$$

$$\psi_{oi} = \psi_o(x_i,\beta) \qquad i=1,2,\ldots n_1+n_2 \qquad (5.89)$$

with initial conditions $X(x_i,o,\beta) = Y(x_i,o,\beta) = 1$.

The $2(n_1+n_2)$ values of the generalized X- and Y-functions obtained from solving the system of differential equations (5.88) are

sufficient for all of the integrations performed in this chapter with the exception of the z-component of flux at $\tau_z=\tau_o$ for the cosine varying collimated boundary. This exception is due to a singularity at $\mu=x$ as seen in equation (5.77). The singularity in the flux can be avoided by performing the integration with quadrature of order n_3 in the first interval $(0,\varepsilon_2)$ and quadrature of order n_4 in the second interval $(\varepsilon_2,1)$ where $0\leq\varepsilon_2\leq 1$. In order to avoid the singularity, n_1 can not be equal to n_3 nor can n_1 and n_3 both be of odd order if $\varepsilon_1=\varepsilon_2$. If $\varepsilon_1\neq\varepsilon_2$, any combination of n_1 and n_3 is permissible. The same discussion is also true for the quadrature of order n_2 and n_4. Evaluation of equations (5.42) and (5.43) at the discrete abscissas corresponding to the quadratures of order n_3 and n_4 yields an additional $2(n_3+n_4)$ ordinary differential equations

$$\frac{dX_{n_1+n_2+j}}{d\tau_o} = \frac{\sqrt{1+\beta^2}}{2} Y_{n_1+n_2+j} \sum_{k=1}^{n_1+n_2} \frac{\omega_k \psi_{ok} Y_k}{x_k}$$

$$\frac{dY_{n_1+n_2+j}}{d\tau_o} = -\frac{\sqrt{1+\beta^2}}{\bar{x}_j} Y_{n_1+n_2+j} + \frac{\sqrt{1+\beta^2}}{2} X_{n_1+n_2+j} \sum_{k=1}^{n_1+n_2} \frac{\omega_k \psi_{ok} Y_k}{x_k} \qquad (5.90)$$

$$j=1,2,\ldots n_3+n_4$$

where the weights $\bar{\omega}_j$ and abscissas $\bar{x}_j$ are defined in terms of the weights ω_{3j} and abscissas x_{3j} of the interval $(0,\varepsilon_2)$ and the weights ω_{4j} and abscissas x_{4j} of the interval $(\varepsilon_2,1)$ as

$$\bar{x}_j = \frac{1}{2}\varepsilon_2(x_{3j}+1)$$

$$\bar{\omega}_j = \frac{1}{2}\varepsilon_2\omega_{3j} \qquad j=1,2,\ldots n_3$$

$$\bar{x}_j = \frac{1}{2}(1-\varepsilon_2)x_{4(j-n_3)} + \frac{1}{2}(1+\varepsilon_2)$$

$$\bar{\omega}_j = \frac{1}{2}(1-\varepsilon_2)\omega_{4(j-n_3)} \qquad j=n_3+1,n_3+2,\ldots n_3+n_4 \qquad (5.91)$$

and

$$X_{n_1+n_2+j} = X(\bar{x}_j,\tau_o,\beta)$$

$$Y_{n_1+n_2+j} = Y(\bar{x}_j,\tau_o,\beta) \qquad j=1,2,\ldots n_3+n_4 \qquad (5.92)$$

with initial conditions $X(\bar{x}_j,o,\beta)=Y(\bar{x}_j,o,\beta)=1$.

An additional eight differential equations are necessary to evaluate the σ dependent form of the generalized X- and Y- functions corresponding to σ=1,2,5, and 10. These equations are

$$\frac{dJ_\beta(o,\sigma_m,\tau_o)}{d\tau_o} = \frac{\sqrt{1+\beta^2}}{2} J_\beta(\tau_o,\sigma_m,\tau_o) \sum_{k=1}^{n_1+n_2} \frac{\omega_k \psi_{ok} Y_k}{x_k}$$

$$\frac{dJ_\beta(\tau_o,\sigma_m,\tau_o)}{d\tau_o} = -\sigma_m J_\beta(\tau_o,\sigma_m,\tau_o)$$

$$+ \frac{\sqrt{1+\beta^2}}{2} J_\beta(o,\sigma_m,\tau_o) \sum_{k=1}^{n_1+n_2} \frac{\omega_k \psi_{ok} Y_k}{x_k} \qquad m=1,2,3,4 \quad (5.93)$$

where σ_1=1, σ_2=2, σ_3=5, and σ_4=10 with initial conditions expressed in terms of the generalized X- and Y-functions as $X(\sqrt{1+\beta^2}/\sigma,o,\beta) = Y(\sqrt{1+\beta^2}/\sigma,o,\beta) = 1$.

The two functions $X(1,\tau_o,\beta)$ and $Y(1,\tau_o,\beta)$ used in integrating the emissive power expressions $\phi_\beta(o,\tau_o)$ and $\phi_\beta(\tau_o,\tau_o)$ also contribute two differential equations of the form

$$\frac{dX(1,\tau_o,\beta)}{d\tau_o} = \frac{\sqrt{1+\beta^2}}{2} Y(1,\tau_o,\beta) \sum_{k=1}^{n_1+n_2} \frac{\omega_k \psi_{ok} Y_k}{x_k}$$

$$\frac{dY(1,\tau_o,\beta)}{d\tau_o} = -\sqrt{1+\beta^2}\, Y(1,\tau_o,\beta) + \frac{\sqrt{1+\beta^2}}{2} X(1,\tau_o,\beta) \sum_{k=1}^{n_1+n_2} \frac{\omega_k \psi_{ok} Y_k}{x_k} \quad (5.94)$$

with initial conditions $X(1,o,\beta) = Y(1,o,\beta) = 1$.

Two more differential equations are required for the moments α_o and β_o. These equations are

$$\frac{d\alpha_o(\beta,\tau_o)}{d\tau_o} = \frac{\sqrt{1+\beta^2}}{2} \beta_o(\beta,\tau_o) \sum_{k=1}^{n_1+n_2} \frac{\omega_k \psi_{ok} Y_k}{x_k}$$

$$\frac{d\beta_o(\beta,\tau_o)}{d\tau_o} = \sqrt{1+\beta^2}\left[\frac{\alpha_o(\beta,\tau_o)}{2} - 1\right] \sum_{k=1}^{n_1+n_2} \frac{\omega_k \psi_{ok} Y_k}{x_k} \quad (5.95)$$

with initial conditions $\alpha_o(\beta,o) = \beta_o(\beta,o) = 1$.

Equations (5.88), (5.90), and (5.93) to (5.95) were solved with $\varepsilon_1 = \varepsilon_2 = .9$, $n_1 = n_2 = 8$, and $n_3 = n_4 = 9$. This assumption constitutes a system of eighty ordinary differential equations. These values were obtained by trial and error. The division of the interval used in calculating the generalized X- and Y-functions into two parts determined by $\varepsilon_1 = .9$ was selected as the most efficient after comparing the results from $\varepsilon_1 = .9$ with the values obtained by varying ε_1 over a wide range of values. Eighth order Gaussian quadrature was used in each interval and the results compared with the results of sixteenth order quadrature in each interval. The test criterion was that the generalized X- and Y-functions did not change in the fifth decimal. Values of

$n_1=n_2=8$ and $\varepsilon_1=.9$ generally satisfies the test criterion with the generalized Y-function more difficult to obtain accurately at large values of β and τ_o.

The division of the interval used in calculating the radiative flux into two parts determined by $\varepsilon_2=.9$ was also obtained by trial and error. Various orders of quadratures were utilized and the results compared. Quadrature of order $n_3=n_4=9$ was found to usually yield five significant digits of accuracy for the flux. Ninth order quadrature, in addition to providing the specified accuracy, also fulfilled the requirement of $n_1\neq n_3$ and $n_2\neq n_4$ when $\varepsilon_1=\varepsilon_2$. Hence, the singularity in the flux due to the diffuse boundary was avoided. At the same time, $n_3=n_4=9$ differing from $n_1=n_2=8$ by unity, helped to keep the total number of differential equations to a minimum.

The results listed in Tables E.1 to E.14 for the σ dependent generalized X- and Y-functions follow directly as the solution of equation (5.93). The emissive power at $\tau_z=0$ and $\tau_z=\tau_o$ for the cosine varying diffuse boundary condition is calculated by reducing equations (5.58) and (5.59) to the form

$$\phi_\beta(o,\tau_o) = \frac{1}{2}\sum_{k=1}^{n_1+n_2} \omega_k\psi_1(x_k,\beta)[X_k-X(1,\tau_o,\beta)] + \frac{1}{2}X(1,\tau_o,\beta) \qquad (5.96)$$

$$\phi_\beta(\tau_o,\tau_o) = \frac{1}{2}\sum_{k=1}^{n_1+n_2} \omega_k\psi_1(x_k,\beta)[Y_k-Y(1,\tau_o,\beta)] + \frac{1}{2}Y(1,\tau_o,\beta) \quad . \qquad (5.97)$$

Tables E.15 to E.18 list $\phi_\beta(o,\tau_o)$ and $\phi_\beta(\tau_o,\tau_o)$ obtained from equations (5.96) and (5.97). The radiative flux at $\tau_z=0$ and $\tau_z=\tau_o$ for the cosine varying collimated boundary condition are calculated from the reduced forms of equations (5.74) and (5.75) with quadrature

given by equation (5.91)

$$\mathcal{Z}_A(o,\sigma_m,\tau_o) = \frac{1}{\sigma_m}$$

$$- \frac{1}{2} \sum_{k=1}^{n_3+n_4} \bar{\omega}_k \psi_1(\bar{x}_k,\beta) \frac{J_\beta(o,\sigma_m,\tau_o)X_{n_1+n_2+k} - J_\beta(\tau_o,\sigma_m,\tau_o)Y_{n_1+n_2+k}}{\sqrt{1+\beta^2}/\bar{x}_k + \sigma_m} \quad (5.98)$$

and

$$\mathcal{Z}_A(\tau_o,\sigma_m,\tau_o) = \frac{1}{\sigma_m} e^{-\sigma_m\tau_o}$$

$$+ \frac{1}{2} \sum_{k=1}^{n_3+n_4} \bar{\omega}_k \psi_1(\bar{x}_k,\beta) \frac{J_\beta(\tau_o,\sigma_m,\tau_o)X_{n_1+n_2+k} - J_\beta(o,\sigma_m,\tau_o)Y_{n_1+n_2+k}}{\sqrt{1+\beta^2}/\bar{x}_k - \sigma_m} \quad (5.99)$$

Tables E.19 to E.32 list the numerical results obtained from equations (5.98) and (5.99). The μ dependent form of $\mathcal{Z}_A$ is needed for the integration of the cosine varying diffuse flux of equations (5.83) and (5.84). Evaluating equations (5.76) and (5.77) at the abscissas of the quadrature of equation (5.91) yields

$$\bar{\mathcal{Z}}_A(o,\bar{x}_i,\tau_o)$$

$$= \frac{\bar{x}_i}{\sqrt{1+\beta^2}} \left[1 - \frac{1}{2} \sum_{k=1}^{n_1+n_2} \omega_k x_k \psi_1(x_k,\beta) \frac{X_k X_{n_1+n_2+i} - Y_k Y_{n_1+n_2+i}}{\bar{x}_i + x_k} \right] \quad (5.100)$$

and

$$\bar{\mathcal{Z}}_A(\tau_o,\bar{x}_i,\tau_o) - \frac{\bar{x}_i e^{-\tau_o\sqrt{1+\beta^2}/\bar{x}_i}}{\sqrt{1+\beta^2}}$$

$$= \frac{\bar{x}_i}{2\sqrt{1+\beta^2}} \sum_{k=1}^{n_1+n_2} \omega_k x_k \psi_1(x_k,\beta) \frac{X_k Y_{n_1+n_2+i} - Y_k X_{n_1+n_2+i}}{\bar{x}_i - x_k} \quad (5.101)$$

The cosine varying diffuse flux is calculated by utilizing equations (5.100) and (5.101) and expressing equations (5.83) and (5.84) as

$$\mathcal{Z}_C(o,\tau_o) = 1 + \frac{2}{\beta^2}(1-\sqrt{1+\beta^2}) + 2\sum_{k=1}^{n_3+n_4} \bar{\omega}_k \psi_1(\bar{x}_k,\beta)\bar{\mathcal{Z}}_A(o,\bar{x}_k,\tau_o) \quad (5.102)$$

and

$$\mathcal{Z}_C(\tau_o,\tau_o) = 2\mathcal{E}_3(\tau_o,\beta) + 2\sum_{k=1}^{n_3+n_4} \bar{\omega}_k \psi_1(\bar{x}_k,\beta)\left[\bar{\mathcal{Z}}_A(\tau_o,\bar{x}_k,\tau_o) - \frac{\bar{x}_k e^{-\tau_o\sqrt{1+\beta^2}/\bar{x}_k}}{\sqrt{1+\beta^2}}\right] . \quad (5.103)$$

Tables E.33 to E.35 list the numerical results obtained from equations (5.102) and (5.103). The $\mathcal{E}_3$-function appearing in equation (5.103) is calculated by the method discussed in Appendix A.

2. COMPARISON OF THE GENERALIZED X- AND Y-FUNCTIONS

Since the generalized X- and Y-functions reduce to the X- and Y-functions of Chandrasekhar when $\beta=0$, it is appropriate to compare the solutions tabulated in Tables E.1 and E.2 with results that appear in the literature. This comparison will furnish a method of checking the numerical technique and provide a degree of confidence in the results for $\beta\neq 0$ for which no known results are available. Recall that the generalized X- and Y-functions have arguments that depend upon both β and σ with connecting relationship given by $\mu=\sqrt{1+\beta^2}/\sigma$. Thus, to compare Chandrasekhar's $X(\mu,\tau_o)$ function with the generalized X-function, the argument of the generalized X-function must be evaluated at $\mu=1/\sigma$. Hence, to compare $X(.5,1)$ with the generalized X-function means that $\beta=0$, $\sigma=2$, and $\tau_o=1$. This value would correspond to the result in Table E.1. Similar results hold for the generalized Y-function.

Table 5.1 Comparison of Chandrasekhar's X- and Y-functions with the generalized X- and Y-functions for $\beta=0$

	$X(.5,\tau_o)$				$Y(.5,\tau_o)$			
τ_o	REF.(40)	REF.(41)	REF.(43)	PRESENT METHOD	REF.(40)	REF.(41)	REF.(43)	PRESENT METHOD
.10		1.15277	1.15232	1.1522		.966939	.966513	.9663
.20	1.24480	1.24456	1.24479	1.2447	.898582	.898214	.898584	.8984
.40	1.37252	1.37252	1.37252	1.3725	.766758	.766827	.766763	.7668
.60	1.46000	1.46003	1.46000	1.4600	.657032	.657095	.657038	.6570
.80	1.52442	1.52443	1.52442	1.5244	.569437	.569436	.569443	.5694
1.0	1.57404	1.57403	1.57403	1.5740	.500045	.500032	.500051	.5000
2.0	1.71531	1.71535	1.71535	1.7153	.310552	.310557	.310555	.3105

In Table 5.1 the $X(.5,\tau_o)$ and $Y(.5,\tau_o)$ results are compared with those of the generalized X- and Y-functions at $\beta=0$. Reference is made to the works of Carlstedt and Mullikin [40], Bellman, et al. [41], Sobouti [42], and Crosbie and Viskanta [43]. The results which appear in Table 5.1 have previously been compiled by Crosbie and Viskanta [43]. It is apparent from the very limited range of the parameters that appear in Table 5.1 that the maximum discrepancy occurs at small τ_o and improves rapidly with increasing τ_o. However, the Y-function, and hence the generalized Y-function, is more sensitive to change in τ_o at very small and also very large values of τ_o.

H. CONCLUSION

The behavior of the radiative flux and the emissive power with β and the optical thickness τ_o for the finite medium indicates that there exists values of β and τ_o for which the finite analysis can be approximated by the simpler semi-infinite development. In general, this approximation can occur either at large τ_o and small β or at large β and small τ_o. Any combination of $\beta\geq 1$ and $\tau_o\geq 3$ enables the finite theory functions at $\tau_z=0$ to be replaced by the semi-infinite solution at $\tau_z=0$. However, the finite theory functions at $\tau_z=\tau_o$ do not approach the optical thick limit as rapidly with β and τ_o as do the finite theory functions at $\tau_z=0$. Hence, the effect at the boundary $\tau_z=\tau_o$ is usually significantly different from the optical thick solution even though the functions at $\tau_z=0$ can be replaced by those from the semi-infinite analysis.

The one-dimensional approximation has limited usefulness since it is only valid for small values of β. The error in the one-dimensional approximation is smallest at small τ_o and increases with

increasing τ_o. Except for small values of β, the two-dimensional model must be considered.

VI. CONCLUSION AND RECOMMENDATIONS

The present investigation treats radiative transfer in a two-dimensional absorbing and emitting gray medium in radiative equilibrium. The exact formulations of the equations for the radiative flux and emissive power are presented for the finite optical thick media subjected to the following types of boundary conditions: (1) cosine varying diffuse, (2) cosine varying collimated, (3) constant temperature strip, and (4) the strip illuminated by a uniform collimated flux. The solutions for the cosine varying diffuse and cosine varying collimated models are used to construct solutions for the constant temperature strip and the strip illuminated by a uniform collimated flux, respectively. The two-dimensional equations are reduced to one-dimensional equations by the technique of separation of variables. The corresponding equations for a semi-infinite medium are obtained from the finite optical thick equations by letting the optical thickness become infinite. The reduced one-dimensional equations for both the finite and the semi-infinite models are solved exactly for values of radiative flux and emissive power at the boundaries. A wide range of exact numerical data is presented.

Error bounds are determined whereby the one-dimensional model can be utilized to approximate the more complex two-dimensional analysis. These error bounds are obtained for the radiative flux and emissive power at the boundaries for both the finite and semi-infinite models. Error bounds are also determined whereby the two-dimensional finite model can be approximated by the simpler two-dimensional semi-infinite analysis. In general, the approximations are of limited use.

Chapter's IV and V indicate that the two-dimensional cosine varying models can be satisfactorily approximated by the one-dimensional model for $\beta<.1$ and the finite strip models can be approximated by the one-dimensional model for half strip width $\tau_a>100$. Chapter V reveals that any combination of $\beta\geq 1$ and $\tau_o\geq 3$ enables the two-dimensional finite model results at the boundary $\tau_z=0$ to be approximated by the two-dimensional semi-infinite results at $\tau_z=0$. The two-dimensional finite model results at the boundary $\tau_z=\tau_o$ can be approximated by the optical thick value of zero but requires larger values of β and τ_o than do the functions at $\tau_z=0$.

The following are recommended for future studies. First, the present investigation can be extended to include the exact numerical solutions of the rigorously formulated equations for the y-components of flux presented in Chapter III. In fact, both components of the radiative flux as well as the emissive power can be evaluated at interior points of the medium and not restricted to the behavior at the boundaries as in the present analysis. Future consideration can also be given to the radiative flux and emissive power for the two-dimensional finite medium bounded by the finite strips. This analysis involves obtaining a large number of β solutions to the system of differential equations described in the section on numerical procedure of Chapter V.

The cosine varying solutions obtained in this investigation can be extended to construct solutions to problems involving more complex kinds of boundary conditions in a fashion similar to the finite strip models. Two useful semi-infinite models which involve uniform

collimated radiation over a portion of the boundary and are acceptable for use of the superposition principle are

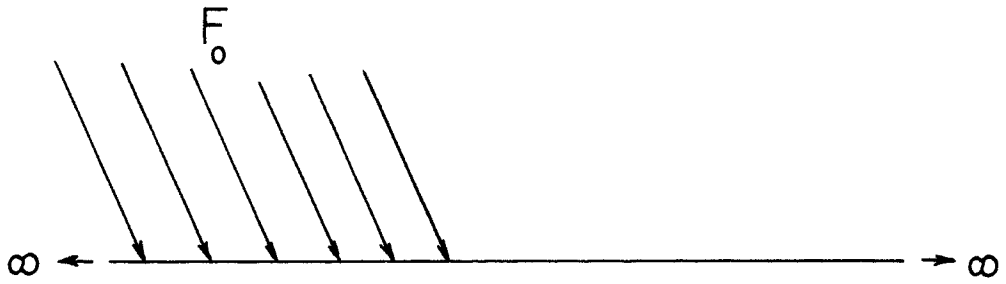

and

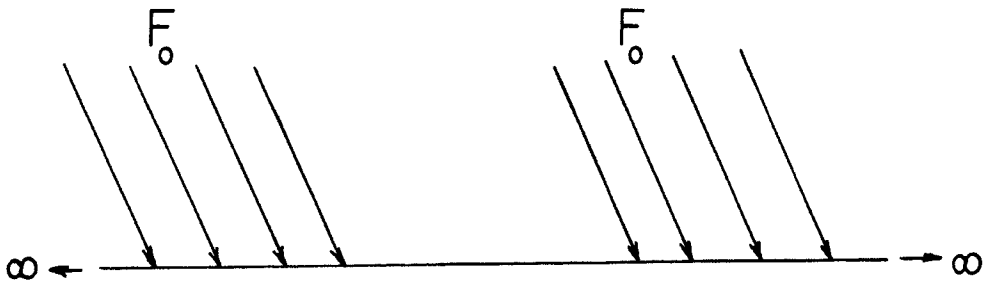

These two models could be used to simulate solar energy striking a cloud cover in a planetary atmosphere.

The two-dimensional gray medium assumption can be relaxed to account for the more realistic nongray analysis and the effect of line or band shape on the radiative transfer studied. This assumption involves a frequency dependent absorption coefficient which can be approximated by various existing models, such as, rectangular, triangular, and exponential. Other more complex two-dimensional configurations can be examined for both gray and nongray media. Additional models include the rectangular and triangular boxes and the triangular wedge as shown. Both collimated and diffuse boundary conditions can be considered.

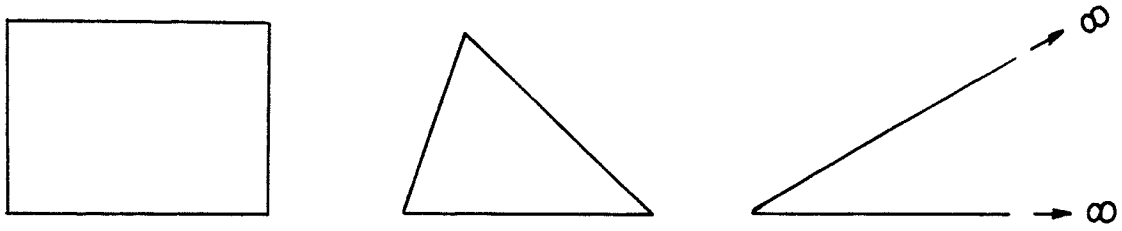

Spherical and cylindrical geometries can also be investigated for both gray and nongray two-dimensional media.

The concept of separation of variables need be investigated for the three-dimensional plane parallel model to determine if the three-dimensional equations can be reduced to one-dimensional equations. In particular, this reduction need be considered for a two-dimensional cosine varying collimated boundary condition in order to determine if the analogous three-dimensional generalized H-, X- and Y-functions can be generated.

BIBLIOGRAPHY

1. Chandrasekhar, S. Radiative Transfer, Dover Publications Inc., New York, 1960.

2. Eddington, A. The Internal Constitution of the Stars, Dover Publications Inc., New York, 1959.

3. Rosseland, S. Theoretical Astrophysics, Oxford University Press, London, 1936.

4. Kourganoff, V. Basic Methods in Transfer Problems, Dover Publications Inc., New York, 1963.

5. Sobolev, V.V. A Treatise on Radiative Transfer, Van Nostrand Company Inc., Princeton, New Jersey, 1963.

6. Love, T.J. Radiative Heat Transfer, Merrill Publishing Company, Columbus, Ohio, 1968.

7. Sparrow, E.M., and Cess, R.D. Radiation Heat Transfer, Brooks Cole Publishing Co., Belmont, California, 1966.

8. Cheng, P. "Two-Dimensional Radiating Gas Flow by a Moment Method," AIAA Journal 2, 1662 (1964).

9. Cheng, P. "Dynamics of a Radiating Gas With Applications to Flow Over a Wavy Wall," AIAA Journal 4, 238 (1966).

10. Khosla, P.K. "Two-Dimensional High Speed Flow of a Radiating Gas," J. Quant. Spectrosc. Radiat. Transfer 8, 145 (1968).

11. Glicksman, L.R. "An Approximate Method for Multidimensional Problems of Radiative Energy Transfer in an Absorbing Emitting Media," Journal of Heat Transfer C91, 502 (1969).

12. Taitel, Y. "Formulation of Two-Dimensional Radiant Heat Flux for Absorbing-Emitting Plane Layer With Nonisothermal Bounding Walls," AIAA Journal 7, 1832 (1969).

13. Lunardini, V.J., and Chang, Y.P. "On the Nonlinearity of Two-Dimensional Heat Transfer in a Conducting and Radiating Medium," Int. J. Heat Mass Transfer 13, 1240 (1970).

14. Olfe, D.B. "Radiative Equilibrium of a Gray Medium Bounded by Nonisothermal Walls," AIAA 4th Thermophysics Conference, Paper No. 69-633 (1969).

15. Cheng, P. "Exact Solutions for Multidimensional Radiative Transfer in Cartesian Coordinate Configurations," AIAA 10th Aerospace Sciences Meeting, Paper No. 72-21 (1972).

16. Chandrasekhar, S. "On the Diffuse Reflection of a Pencil of Radiation by a Plane Parallel Atmosphere," Proc. Nat. Acad. Sci. 44, 933 (1958).

17. Bellman, R., Kalaba, R., and Ueno, S. "On the Diffuse Reflection of Parallel Rays by an Inhomogeneous Flat Layer as a Limiting Process," J. Math. Anal. and Appl. 7, 91 (1963).

18. Bellman, R., Kalaba, R., and Ueno, S. "Invariant Imbedding and Time Dependent Diffuse Reflection of a Pencil of Radiation by a Finite Inhomogeneous Flat Layer - I.," J. Math. Anal. and Appl. 7, 310 (1963).

19. Rybicki, G. B. "The Searchlight Problem With Isotropic Scattering," J. Quant. Spectrosc. Radiat. Transfer 12, 827 (1971).

20. Smith, M.G. "The Transport Equation With Plane Symmetry and Isotropic Scattering," Proc. Camb. Phil. Soc. 60, 909 (1964).

21. Smith, M.G., and Hunt, G.E. "The Isotropic Scattering of Radiation in a Finite Homogeneous Two-Dimensional Atmosphere," Proc. Camb. Phil. Soc. 63, 209 (1967).

22. Hunt, G.E. "The Transport Equation of Radiative Transfer With Axial Symmetry," SIAM. J. Appl. Math. 16, 229 (1968).

23. Hunt, G.E. "The Transport Equation of Radiative Transfer With Isotropic Scattering," Proc. Camb. Phil. Soc. 65, 199 (1969).

24. Hunt, G.E. "The Transport Equation of Radiative Transfer in a Three-Dimensional Space With Anisotropic Scattering," J. Inst. Math. Appl. 3, 181 (1967).

25. Bobco, R.P. "Directional Emissivities From a Two-Dimensional Absorbing-Scattering Medium: The Semi-infinite Slab," Journal of Heat Transfer C89, 313 (1967).

26. Love, T.J., and Turner, W.D. "Directional Emittance From Emitting, Absorbing, and Scattering Media," AIAA Fourth Thermophysics Conference, Paper No. 69-625 (1969).

27. Elliott, J.P. "Milne's Problem With a Point Source," Proc. Roy. Soc. A228, 424 (1955).

28. Erdmann, R.C. "Neutron Transport From a Point Source in Two Adjacent, Dissimilar, Semi-infinite Media," J. Math. Phys. 8, 1040 (1967).

29. Williams, M.M.R. "Approximate Solutions of the Neutron Transport Equation in Two and Three Dimensional Systems," Nukleonik 9, 305 (1967).

30. Williams, M.M.R. "Diffusion Length and Criticality Problems in Two and Three Dimensional, One Speed Neutron Transport Theory. I. Rectangular Coordinates," J. Math. Phys. 9, 1873 (1968).

31. Williams, M.M.R. "Diffusion Length and Criticality Problems in Two and Three Dimensional, One Speed Neutron Transport Theory. II. Circular Cylindrical Coordinates," J. Math. Phys. 9, 1885 (1968).

32. Kaper, H.G. "Elementary Solutions of the Reduced Three-Dimensional Transport Equation," J. Math. Phys. 10, 286 (1969).

33. Sotoodehia, A., and Erdmann, R.C. "Two-Dimensional Transport in a Slab," SIAM J. Appl. Math. 18, 160 (1970).

34. Garrettson, G., and Leonard, A. "Green's Function for Multi-dimensional Neutron Transport in a Slab," J. Math. Phys. 11, 725 (1970).

35. Goody, R.M. Atmospheric Radiation I. Theoretical Basis, Oxford University Press, New York, 1964.

36. Luke, Y.L. Integrals of Bessel Functions, McGraw-Hill Book Co., Inc., New York, 1962.

37. Filon, L.N.G. "On a Quadrature Formula for Trigonometric Integrals," Proc. Roy. Soc. Edinburgh 49, 38 (1928).

38. Davis, P.J., and Rabinowitz, P. Numerical Integration, Blaisdell Publishing Company, London, 1967.

39. Heaslet, M.A., and Warming, R.F. "Theoretical Predictions of Spectral Line Formation by Noncoherent Scattering," J. Quant. Spectrosc. Radiat. Transfer 8, 1101 (1968).

40. Carlstedt, J.L., and Mullikin, T.W. "Chandrasekhar's X- and Y-Functions," Astrophys. J. Suppl. 12, 449 (1966).

41. Bellman, R., Kagiwada, H., Kalaba, R., and Ueno, S. "Numerical Results for Chandrasekhar's X and Y Functions of Radiative Transfer," J. Quant. Spectrosc. Radiat. Transfer 6, 479 (1966).

42. Sobouti, Y. "Chandrasekhar's X-, Y-, and Related Functions," Astrophys. J. Suppl. 7, 411 (1963).

43. Crosbie, A.L., and Viskanta, R. "Nongray Radiative Transfer in a Planar Medium Exposed to a Collimated Flux," J. Quant. Spectrosc. Radiat. Transfer 10, 465 (1970).

VITA

William Francis Breig was born on February 6, 1940, in St. Marys, Missouri. He received his primary and secondary education in St. Marys, Missouri. He received his college education from Southeast Missouri State College, in Cape Girardeau, Missouri; the University of Missouri-Rolla, in Rolla, Missouri; and the University of Missouri-Columbia, in Columbia, Missouri. He received a Bachelor of Science degree in Applied Mathematics in August 1962, a Master of Science degree in Applied Mathematics in August 1966, and a Master of Science degree in Engineering Mechanics in June 1968 all from the University of Missouri-Rolla, in Rolla, Missouri.

He was employed by the Missouri Pacific Railroad as a systems analyst for the period from September 1962 to August 1963. In September 1963 he enrolled in the Graduate School of the University of Missouri-Columbia and held a Graduate Assistantship in Mathematics for the period from September 1964 to June 1965. He has been enrolled in the Graduate School of the University of Missouri-Rolla since September 1965 and has held a Graduate Assistantship in Mathematics for the period from September 1966 to June 1967; a Graduate Assistantship in Engineering Mechanics from June 1967 to June 1970; and a Graduate Assistantship in Mechanical and Aerospace Engineering from September 1970 to June 1971.

APPENDIX A

THE $\mathcal{E}_n$-FUNCTION

The $\mathcal{E}_1$, $\mathcal{E}_2$, and $\mathcal{E}_3$-functions are two-dimensional analogs of the exponential integral functions E_1, E_2, and E_3. Since the two functions are identical when $\beta=0$, the $\mathcal{E}_n$-function may be considered a generalized exponential integral. As with the one-dimensional exponential integrals, series expansions and recursive formulas are required for the evaluation of the $\mathcal{E}_n$-function.

The functions $\mathcal{E}_1$, $\mathcal{E}_2$, and $\mathcal{E}_3$ have previously been defined as

$$\mathcal{E}_1(\tau,\beta) = \int_1^\infty e^{-\tau\sqrt{t^2+\beta^2}} \frac{dt}{\sqrt{t^2+\beta^2}} \tag{A.1}$$

$$\mathcal{E}_2(\tau,\beta) = \int_1^\infty e^{-\tau\sqrt{t^2+\beta^2}} \frac{dt}{t^2} \tag{A.2}$$

and

$$\mathcal{E}_3(\tau,\beta) = \tau \int_1^\infty \mathcal{E}_2(\tau t,\beta/t)dt \quad . \tag{A.3}$$

A simple integration by parts of the $\mathcal{E}_1$-function yields

$$\mathcal{E}_2(\tau,\beta) = e^{-\tau\sqrt{1+\beta^2}} - \tau\,\mathcal{E}_1(\tau,\beta) \tag{A.4}$$

where $\mathcal{E}_2(o,\beta)=1$. Equation (A.4) is the recursion formula which is analogous to the one-dimensional case

$$E_2(\tau) = e^{-\tau} - \tau E_1(\tau) \tag{A.5}$$

where $E_n(\tau)$ are the exponential integrals defined by

$$E_n(\tau) = \int_1^\infty e^{-\tau x} \frac{dx}{x^n} . \qquad (A.6)$$

Since $\mathcal{E}_1(\tau,0)=E_1(\tau)$ and $\mathcal{E}_2(\tau,0)=E_2(\tau)$, equation (A.4) reduces to equation (A.5) when $\beta=0$. The $\mathcal{E}_3$-function can be expressed in terms of $\mathcal{E}_2$ by the insertion of equation (A.4) into equation (A.3)

$$\mathcal{E}_3(\tau,\beta) = \tau \int_1^\infty e^{-\tau\sqrt{t^2+\beta^2}}\, dt - \tau^2 \int_1^\infty\int_1^\infty x^2 e^{-\tau\sqrt{t^2x^2+\beta^2}} \frac{dxdt}{\sqrt{t^2x^2+\beta^2}} . \qquad (A.7)$$

The second integral in equation (A.7) can be integrated once by parts to yield

$$\mathcal{E}_3(\tau,\beta) = \tau \int_1^\infty e^{-\tau\sqrt{t^2+\beta^2}}\, dt - \tau\mathcal{E}_2(\tau,\beta)$$

$$-\tau \int_1^\infty \int_1^\infty e^{-\tau\sqrt{t^2x^2+\beta^2}} \frac{dxdt}{t^2} . \qquad (A.8)$$

Since the double integral in equation (A.8) is another form of $\mathcal{E}_3$, equation (A.8) can be rewritten as

$$2\,\mathcal{E}_3(\tau,\beta) = \tau \int_1^\infty e^{-\tau\sqrt{t^2+\beta^2}}\, dt - \tau\,\mathcal{E}_2(\tau,\beta) . \qquad (A.9)$$

When $\beta=0$, equation (A.9) reduces to the standard one-dimensional form

$$2E_3(\tau) = e^{-\tau} - \tau E_2(\tau) . \qquad (A.10)$$

An expression for $\mathcal{E}_3$ which depends only upon $\mathcal{E}_1$ and $\mathcal{E}_2$ can be obtained by eliminating the integral term in equation (A.9). The derivative of $\mathcal{E}_1$ is

$$\mathcal{E}_0(\tau,\beta) = -\frac{d\,\mathcal{E}_1(\tau,\beta)}{d\tau} = \int_1^\infty e^{-\tau\sqrt{t^2+\beta^2}}\,dt \quad . \qquad (A.11)$$

Insertion of equation (A.11) into equation (A.9) yields

$$2\,\mathcal{E}_3(\tau,\beta) = -\tau\frac{d\,\mathcal{E}_1(\tau,\beta)}{d\tau} - \tau\,\mathcal{E}_2(\tau,\beta) \qquad (A.12)$$

which, along with equation (A.4), enables $\mathcal{E}_3$ to be expressed as a function of either $\mathcal{E}_1$ or $\mathcal{E}_2$.

Since neither $\mathcal{E}_1$ nor $\mathcal{E}_2$ can be integrated in closed form, a series representation is necessary. A series expansion for $\mathcal{E}_2$ about zero is appropriate for small β, whereas $\mathcal{E}_1$ is more suitable for expansion whenever β is large. A Taylor series expansion of $\mathcal{E}_2$ about $\beta=0$ yields

$$\mathcal{E}_2(\tau,\beta) = E_2(\tau) - \frac{\tau}{2}\beta^2E_3(\tau) + \frac{\tau}{8}[\tau E_4(\tau) + E_5(\tau)]\beta^4$$

$$- \frac{\tau}{48}[\tau^2E_5(\tau) + 3\tau E_6(\tau) + 3E_7(\tau)]\beta^6$$

$$+ \frac{\tau}{384}[\tau^3E_6(\tau) + 6\tau^2E_7(\tau) + 15\tau E_8(\tau) + 15E_9(\tau)]\beta^8 + \ldots . \qquad (A.13)$$

A series representation of $\mathcal{E}_2$ for small β can also be obtained by Laplace transform techniques. Consideration of the first two nonzero terms of a binomial series expansion of the square root exponent in the $\mathcal{E}_2$-function results in

$$\mathcal{E}_2(\tau,\beta) \simeq \int_1^\infty e^{-\tau t}\,e^{-\beta^2\tau/2t}\,\frac{dt}{t^2} \quad . \qquad (A.14)$$

But

$$\frac{e^{-\beta^2\tau/2t}}{t^2} = \sum_{n=0}^{\infty} \frac{(-1)^n}{n!} \left(\frac{\tau\beta^2}{2}\right)^n \frac{1}{t^{n+2}} \quad . \tag{A.15}$$

Hence, upon interchanging summation and integration operations, the following expression is obtained

$$\mathcal{E}_2(\tau,\beta) \simeq \sum_{n=0}^{\infty} \frac{(-1)^n}{n!} \left(\frac{\tau\beta^2}{2}\right)^n e^{-\tau} \int_0^{\infty} \frac{e^{-\tau t}\, dt}{(t+1)^{n+2}} \quad . \tag{A.16}$$

The integral in equation (A.16) is recognized as a Laplace transform given by

$$L\left[\frac{1}{(t+1)^{n+2}}\right] = e^{\tau} E_{n+2}(\tau) \quad . \tag{A.17}$$

A second representation for $\mathcal{E}_2$ then becomes

$$\mathcal{E}_2(\tau,\beta) \simeq \sum_{n=0}^{\infty} \frac{(-1)^n}{n!} \left(\frac{\tau\beta^2}{2}\right)^n E_{n+2}(\tau) \quad . \tag{A.18}$$

The first two nonzero terms in equations (A.13) and (A.18) agree exactly. A more involved series was obtained by considering the first three nonzero terms in the above binomial expansion. The third order approximation resulted in a series which also had the same form as equation (A.13) but differed by constant coefficients.

A series representation for large values of β is best obtained from the $\mathcal{E}_1$-function. A substitution $t=\beta\sinh\xi$ reduces the $\mathcal{E}_1$-function to a recognizable form so that an integral tabulated in Luke [36,p.30] can be used. This integral, given by

$$K_0(\tau\beta) = \int_0^{\infty} e^{-\tau\beta\cosh\xi}\, d\xi \tag{A.19}$$

reduces the $\mathcal{E}_1$-function to the form

$$\mathcal{E}_1(\tau,\beta) = K_0(\tau\beta) - \int_0^c e^{-\tau\beta\cosh\xi}\, d\xi \qquad (A.20)$$

where $c=\sinh^{-1}(1/\beta)$. The integrand in equation (A.20) can now be expanded in a series around $\xi=0$ and integrated to yield

$$\mathcal{E}_1(\tau,\beta) = K_0(x) - c\, e^{-x}\left[1 - \frac{x\,c^2}{3!} + \frac{x(3x-1)c^4}{5!}\right.$$

$$- \frac{x(15x^2-15x+1)c^6}{7!} + \frac{x(105x^3-210x^2+63x-1)c^8}{9!}$$

$$\left. - \frac{x(945x^4-3150x^3+2205x^2-255x+1)c^{10}}{11!} + \ldots\right] \qquad (A.21)$$

where $x=\tau\beta$.

Tables A.1 to A.6 and Figures A.1 to A.3 show the numerical and graphical behavior of the $\mathcal{E}_1$, $\mathcal{E}_2$, and $\mathcal{E}_3$-functions. Series expansions given by equations (A.13) and (A.21) were used to obtain the tabulated data. The binomial representation of $\mathcal{E}_2$ was not utilized since it is the result of an approximation and does not give exact results. However, it was found to be in excellent agreement with the exponential series for very small values of β and τ. This behavior is expected since both have the same form with the first two nonzero terms being exactly equal.

Five terms of equation (A.13) were used to compute $\mathcal{E}_2$ for $0\leq\beta\leq.5$ from which $\mathcal{E}_1$ was obtained using the recursion equation. The results for $.5\leq\beta\leq10$ were obtained from equation (A.21) with six terms in the series representation of $\mathcal{E}_1$. The two series representations

have excellent agreement in a region of overlap $.1 \leq \beta \leq .5$ with best results for small τ. An agreement of five significant digits was not uncommon in this region and in the range $0 \leq \tau \leq 1$. At large τ, the product $\tau\beta$ is the dominant term in equation (A.21). Hence, equation (A.21) requires additional terms for large τ. Once the appropriate series is selected for the range of β values, the calculation of the $\mathcal{E}_3$-function follows from equation (A.12).

The relatively small range of β for which the series representation of equation (A.21) is valid is due to the presence of the factorial terms. However, for sufficiently small β, the term $c=\sinh^{-1}(1/\beta)$ becomes dominant. Therefore, additional terms are needed for small β values. However, as β grows large, the term $c=\sinh^{-1}(1/\beta)$ approaches zero quite rapidly, thereby requiring fewer terms. The exponential series does not have large factorial terms and hence has slower convergence. The presence of the exponential integral functions aids in the convergence since they become quite small with increasing argument.

The results which are reported in this investigation for the $\mathcal{E}_1$-function have been spot-checked with results that appear in reference [44] and found to have a favorable agreement. The verification of the validity of $\mathcal{E}_1$ is handicapped by the form that reference [44] reports the numerical data. Results are tabulated for a function $E(\beta,x)$ defined by

$$E(\beta,x) = \int_0^x \frac{(1 - e^{-\sqrt{\beta^2+t^2}})dt}{\sqrt{t^2+\beta^2}} \quad . \tag{A.22}$$

It can be shown that $E(\beta,x)$ is related to $\mathcal{E}_1$ by the following equation

$$\mathcal{E}_1(\tau,\beta) = K_0(\tau\beta) - \sinh^{-1}(1/\beta) + E(\tau\beta,\tau) \quad . \tag{A.23}$$

Table A.1 The function $\mathcal{E}_1(\tau,\beta)$ for various values of τ and β

τ	β=0	β=.05	β=.10	β=.20	β=.50
.000	∞	∞	∞	∞	∞
.001	.63315D+1	.63309D+1	.63290D+1	.63216D+1	.62742D+1
.002	.56393D+1	.56387D+1	.56369D+1	.56295D+1	.55820D+1
.003	.52349D+1	.52343D+1	.52324D+1	.52250D+1	.51775D+1
.004	.49482D+1	.49476D+1	.49457D+1	.49383D+1	.48909D+1
.005	.47261D+1	.47254D+1	.47236D+1	.47162D+1	.46687D+1
.010	.40379D+1	.40373D+1	.40354D+1	.40280D+1	.39806D+1
.015	.36374D+1	.36368D+1	.36349D+1	.36275D+1	.35801D+1
.020	.33547D+1	.33540D+1	.33522D+1	.33448D+1	.32974D+1
.025	.31365D+1	.31358D+1	.31340D+1	.31266D+1	.30793D+1
.030	.29591D+1	.29584D+1	.29566D+1	.29492D+1	.29019D+1
.035	.28098D+1	.28092D+1	.28074D+1	.28000D+1	.27528D+1
.040	.26812D+1	.26806D+1	.26787D+1	.26714D+1	.26242D+1
.045	.25683D+1	.25677D+1	.25659D+1	.25585D+1	.25114D+1
.050	.24679D+1	.24672D+1	.24654D+1	.24581D+1	.24110D+1
.060	.22953D+1	.22946D+1	.22928D+1	.22855D+1	.22385D+1
.070	.21508D+1	.21502D+1	.21483D+1	.21411D+1	.20942D+1
.080	.20269D+1	.20263D+1	.20244D+1	.20172D+1	.19705D+1
.090	.19187D+1	.19181D+1	.19163D+1	.19090D+1	.18626D+1
.100	.18229D+1	.18223D+1	.18204D+1	.18133D+1	.17670D+1
.200	.12226D+1	.12220D+1	.12203D+1	.12134D+1	.11693D+1
.300	.90567D+0	.90512D+0	.90348D+0	.89700D+0	.85558D+0
.400	.70238D+0	.70186D+0	.70032D+0	.69425D+0	.65564D+0
.500	.55977D+0	.55929D+0	.55785D+0	.55221D+0	.51642D+0
.600	.45438D+0	.45393D+0	.45260D+0	.44736D+0	.41433D+0
.700	.37376D+0	.37335D+0	.37212D+0	.36728D+0	.33690D+0
.800	.31059D+0	.31021D+0	.30907D+0	.30462D+0	.27675D+0
.900	.26018D+0	.25983D+0	.25878D+0	.25468D+0	.22917D+0
1.000	.21938D+0	.21906D+0	.21810D+0	.21433D+0	.19103D+0
1.250	.14641D+0	.14615D+0	.14538D+0	.14235D+0	.12388D+0
1.500	.10002D+0	.99812D-1	.99193D-1	.96779D-1	.82226D-1
1.750	.69488D-1	.69323D-1	.68830D-1	.66913D-1	.55503D-1
2.000	.48900D-1	.48769D-1	.48378D-1	.46861D-1	.37945D-1
3.000	.13048D-1	.12997D-1	.12846D-1	.12264D-1	.90040D-2
4.000	.37793D-2	.37599D-2	.37025D-2	.34835D-2	.23459D-2
5.000	.11483D-2	.11410D-2	.11194D-2	.10379D-2	.74519D-3

Table A.2 The function $\mathcal{E}_1(\tau,\beta)$ for various values of τ and β

τ	β=1.0	β=2.0	β=3.0	β=5.0	β=10.0
.000	∞	∞	∞	∞	∞
.001	.61433D+1	.58503D+1	.55986D+1	.52166D+1	.46224D+1
.002	.54511D+1	.51582D+1	.49065D+1	.45245D+1	.39306D+1
.003	.50467D+1	.47537D+1	.45021D+1	.41202D+1	.35266D+1
.004	.47600D+1	.44671D+1	.42155D+1	.38337D+1	.32406D+1
.005	.45379D+1	.42450D+1	.39934D+1	.36118D+1	.30192D+1
.010	.38498D+1	.35571D+1	.33059D+1	.29253D+1	.23367D+1
.015	.34494D+1	.31570D+1	.29063D+1	.25271D+1	.19441D+1
.020	.31668D+1	.28749D+1	.26248D+1	.22474D+1	.16709D+1
.025	.29488D+1	.26573D+1	.24080D+1	.20326D+1	.14637D+1
.030	.27716D+1	.24807D+1	.22322D+1	.18591D+1	.12985D+1
.035	.26226D+1	.23323D+1	.20847D+1	.17142D+1	.11624D+1
.040	.24942D+1	.22046D+1	.19580D+1	.15902D+1	.10476D+1
.045	.23816D+1	.20927D+1	.18472D+1	.14822D+1	.94930D+0
.050	.22814D+1	.19933D+1	.17489D+1	.13870D+1	.86391D+0
.060	.21094D+1	.18230D+1	.15810D+1	.12255D+1	.72278D+0
.070	.19657D+1	.16811D+1	.14417D+1	.10930D+1	.61100D+0
.080	.18425D+1	.15599D+1	.13233D+1	.98169D+0	.52054D+0
.090	.17351D+1	.14545D+1	.12209D+1	.88659D+0	.44620D+0
.100	.16401D+1	.13617D+1	.11311D+1	.80430D+0	.38435D+0
.200	.10500D+1	.79692D+0	.59973D+0	.34840D+0	.10042D+0
.300	.74494D+0	.51948D+0	.35572D+0	.16990D+0	.29793D-1
.400	.55402D+0	.35569D+0	.22196D+0	.87354D-1	.93432D-2
.500	.42370D+0	.25067D+0	.14266D+0	.46303D-1	.30239D-2
.600	.33015D+0	.18008D+0	.93504D-1	.25039D-1	.99897D-3
.700	.26076D+0	.13116D+0	.62148D-1	.13734D-1	.33480D-3
.800	.20807D+0	.96541D-1	.41744D-1	.76142D-2	.11342D-3
.900	.16739D+0	.71640D-1	.28271D-1	.42563D-2	.38742D-4
1.000	.13554D+0	.53514D-1	.19274D-1	.23951D-2	.13321D-4
1.250	.81761D-1	.26385D-1	.75621D-2	.58161D-3	.94394D-6
1.500	.50486D-1	.13313D-1	.30360D-2	.14448D-3	.68400D-7
1.750	.31698D-1	.68302D-2	.12390D-2	.36476D-4	.50351D-8
2.000	.20156D-1	.35480D-2	.51193D-3	.93205D-5	.37499D-9
3.000	.35811D-2	.28017D-3	.16153D-4	.42926D-7	.1242D-13
4.000	.68942D-3	.23915D-4	.54987D-6	.21274D-9	.4417D-18
5.000	.13832D-3	.21349D-5	.19552D-7	.1099D-11	.1633D-22

Table A.3 The function $\mathcal{E}_2(\tau,\beta)$ for various values of τ and β

τ	β=0	β=.05	β=.10	β=.20	β=.50
.000	.10000D+1	.10000D+1	.10000D+1	.10000D+1	.10000D+1
.001	.99266D+0	.99266D+0	.99266D+0	.99266D+0	.99260D+0
.002	.98672D+0	.98672D+0	.98671D+0	.98670D+0	.98660D+0
.003	.98130D+0	.98129D+0	.98129D+0	.98127D+0	.98111D+0
.004	.97621D+0	.97621D+0	.97620D+0	.97617D+0	.97597D+0
.005	.97138D+0	.97137D+0	.97137D+0	.97133D+0	.97108D+0
.010	.94967D+0	.94966D+0	.94964D+0	.94957D+0	.94907D+0
.015	.93055D+0	.93054D+0	.93051D+0	.93040D+0	.92966D+0
.020	.91310D+0	.91309D+0	.91305D+0	.91291D+0	.91193D+0
.025	.89689D+0	.89688D+0	.89683D+0	.89666D+0	.89545D+0
.030	.88167D+0	.88165D+0	.88160D+0	.88139D+0	.87995D+0
.035	.86725D+0	.86723D+0	.86717D+0	.86693D+0	.86527D+0
.040	.85353D+0	.85351D+0	.85344D+0	.85317D+0	.85129D+0
.045	.84042D+0	.84039D+0	.84031D+0	.84001D+0	.83791D+0
.050	.82783D+0	.82780D+0	.82772D+0	.82738D+0	.82508D+0
.060	.80404D+0	.80401D+0	.80391D+0	.80351D+0	.80080D+0
.070	.78183D+0	.78179D+0	.78168D+0	.78122D+0	.77812D+0
.080	.76096D+0	.76091D+0	.76078D+0	.76027D+0	.75679D+0
.090	.74124D+0	.74119D+0	.74105D+0	.74048D+0	.73664D+0
.100	.72254D+0	.72249D+0	.72233D+0	.72171D+0	.71752D+0
.200	.57420D+0	.57411D+0	.57385D+0	.57280D+0	.56575D+0
.300	.46911D+0	.46900D+0	.46866D+0	.46732D+0	.45837D+0
.400	.38936D+0	.38924D+0	.38885D+0	.38732D+0	.37714D+0
.500	.32664D+0	.32650D+0	.32609D+0	.32444D+0	.31356D+0
.600	.27618D+0	.27604D+0	.27561D+0	.27390D+0	.26268D+0
.700	.23494D+0	.23480D+0	.23436D+0	.23264D+0	.22137D+0
.800	.20085D+0	.20070D+0	.20027D+0	.19857D+0	.18743D+0
.900	.17240D+0	.17226D+0	.17184D+0	.17017D+0	.15933D+0
1.000	.14849D+0	.14835D+0	.14794D+0	.14633D+0	.13589D+0
1.250	.10348D+0	.10336D+0	.10299D+0	.10155D+0	.92354D-1
1.500	.73100D-1	.72994D-1	.72677D-1	.71430D-1	.63584D-1
1.750	.52168D-1	.52078D-1	.51809D-1	.50755D-1	.44212D-1
2.000	.37534D-1	.37458D-1	.37234D-1	.36356D-1	.30988D-1
3.000	.10641D-1	.10608D-1	.10509D-1	.10123D-1	.78844D-2
4.000	.31982D-2	.31844D-2	.31435D-2	.29864D-2	.21224D-2
5.000	.99646D-3	.99099D-3	.97480D-3	.91312D-3	.59209D-3

Table A.4 The function $\mathcal{E}_2(\tau,\beta)$ for various values of τ and β

τ	β=1.0	β=2.0	β=3.0	β=5.0	β=10.0
.000	.10000D+1	.10000D+1	.10000D+1	.10000D+1	.10000D+1
.001	.99244D+0	.99191D+0	.99124D+0	.98969D+0	.98537D+0
.002	.98627D+0	.98522D+0	.98388D+0	.98080D+0	.97224D+0
.003	.98062D+0	.97905D+0	.97705D+0	.97245D+0	.95972D+0
.004	.97531D+0	.97322D+0	.97056D+0	.96447D+0	.94763D+0
.005	.97026D+0	.96765D+0	.96434D+0	.95676D+0	.93589D+0
.010	.94745D+0	.94231D+0	.93581D+0	.92103D+0	.88101D+0
.015	.92726D+0	.91965D+0	.91007D+0	.88845D+0	.83090D+0
.020	.90877D+0	.89876D+0	.88621D+0	.85809D+0	.78449D+0
.025	.89154D+0	.87919D+0	.86378D+0	.82949D+0	.74123D+0
.030	.87531D+0	.86069D+0	.84252D+0	.80237D+0	.70075D+0
.035	.85991D+0	.84308D+0	.82225D+0	.77655D+0	.66277D+0
.040	.84523D+0	.82625D+0	.80286D+0	.75188D+0	.62707D+0
.045	.83116D+0	.81009D+0	.78423D+0	.72826D+0	.59348D+0
.050	.81765D+0	.79455D+0	.76630D+0	.70560D+0	.56182D+0
.060	.79207D+0	.76506D+0	.73231D+0	.66289D+0	.50380D+0
.070	.76814D+0	.73743D+0	.70050D+0	.62331D+0	.45208D+0
.080	.74562D+0	.71140D+0	.67061D+0	.58649D+0	.40589D+0
.090	.72432D+0	.68679D+0	.64242D+0	.55217D+0	.36459D+0
.100	.70410D+0	.66345D+0	.61577D+0	.52012D+0	.32761D+0
.200	.54362D+0	.48002D+0	.41133D+0	.29098D+0	.11390D+0
.300	.43076D+0	.35544D+0	.28053D+0	.16562D+0	.40109D-1
.400	.34636D+0	.26656D+0	.19347D+0	.95137D-1	.14216D-1
.500	.28121D+0	.20158D+0	.13440D+0	.54968D-1	.50600D-2
.600	.22995D+0	.15336D+0	.93860D-1	.31891D-1	.18062D-2
.700	.18906D+0	.11721D+0	.65803D-1	.18561D-1	.64623D-3
.800	.15612D+0	.89918D-1	.46277D-1	.10829D-1	.23160D-3
.900	.12939D+0	.69183D-1	.32629D-1	.63310D-2	.83124D-4
1.000	.10757D+0	.53363D-1	.23054D-1	.37075D-2	.29869D-4
1.250	.68504D-1	.28128D-1	.97472D-2	.97869D-3	.23214D-5
1.500	.44144D-1	.14969D-1	.41547D-2	.26001D-3	.18125D-6
1.750	.28701D-1	.80250D-2	.17818D-2	.69415D-4	.14199D-7
2.000	.18792D-1	.43267D-2	.76789D-3	.18602D-4	.11154D-8
3.000	.36260D-2	.38032D-3	.27385D-4	.98506D-7	.4328D-13
4.000	.73581D-3	.34820D-4	.10109D-5	.53607D-9	.1712D-17
5.000	.15768D-3	.32711D-5	.38134D-7	.2968D-11	.6863D-22

Table A.5 The function $\mathcal{E}_3(\tau,\beta)$ for various values of τ and β

τ	β=0	β=.05	β=.10	β=.20	β=.50
.000	.50000D+0	.50000D+0	.50000D+0	.50000D+0	.50000D+0
.001	.49900D+0	.49900D+0	.49900D+0	.49900D+0	.49900D+0
.002	.49801D+0	.49801D+0	.49801D+0	.49801D+0	.49801D+0
.003	.49703D+0	.49703D+0	.49703D+0	.49703D+0	.49702D+0
.004	.49605D+0	.49605D+0	.49605D+0	.49605D+0	.49604D+0
.005	.49507D+0	.49507D+0	.49507D+0	.49507D+0	.49507D+0
.010	.49027D+0	.49027D+0	.49027D+0	.49027D+0	.49025D+0
.015	.48557D+0	.48557D+0	.48557D+0	.48557D+0	.48553D+0
.020	.48096D+0	.48096D+0	.48096D+0	.48095D+0	.48089D+0
.025	.47644D+0	.47644D+0	.47644D+0	.47642D+0	.47634D+0
.030	.47199D+0	.47199D+0	.47199D+0	.47197D+0	.47185D+0
.035	.46762D+0	.46762D+0	.46761D+0	.46759D+0	.46744D+0
.040	.46332D+0	.46332D+0	.46331D+0	.46328D+0	.46310D+0
.045	.45908D+0	.45908D+0	.45907D+0	.45904D+0	.45882D+0
.050	.45491D+0	.45491D+0	.45490D+0	.45486D+0	.45460D+0
.060	.44676D+0	.44675D+0	.44674D+0	.44669D+0	.44634D+0
.070	.43883D+0	.43882D+0	.43881D+0	.43874D+0	.43831D+0
.080	.43112D+0	.43111D+0	.43109D+0	.43101D+0	.43048D+0
.090	.42361D+0	.42360D+0	.42357D+0	.42348D+0	.42286D+0
.100	.41629D+0	.41628D+0	.41625D+0	.41615D+0	.41542D+0
.200	.35194D+0	.35192D+0	.35185D+0	.35159D+0	.34980D+0
.300	.30004D+0	.30000D+0	.29990D+0	.29949D+0	.29670D+0
.400	.25728D+0	.25724D+0	.25710D+0	.25657D+0	.25294D+0
.500	.22160D+0	.22155D+0	.22139D+0	.22076D+0	.21647D+0
.600	.19155D+0	.19149D+0	.19131D+0	.19061D+0	.18584D+0
.700	.16606D+0	.16599D+0	.16580D+0	.16505D+0	.15995D+0
.800	.14432D+0	.14425D+0	.14405D+0	.14326D+0	.13796D+0
.900	.12570D+0	.12563D+0	.12543D+0	.12462D+0	.11922D+0
1.000	.10969D+0	.10962D+0	.10941D+0	.10860D+0	.10320D+0
1.250	.78572D-1	.78506D-1	.78308D-1	.77524D-1	.72385D-1
1.500	.56739D-1	.56678D-1	.56497D-1	.55778D-1	.51131D-1
1.750	.41239D-1	.41185D-1	.41024D-1	.40387D-1	.36323D-1
2.000	.30133D-1	.30086D-1	.29946D-1	.29396D-1	.25921D-1
3.000	.89307D-2	.89075D-2	.88386D-2	.85699D-2	.69503D-2
4.000	.27613D-2	.27512D-2	.27210D-2	.26042D-2	.19317D-2
5.000	.87780D-3	.87359D-3	.86109D-3	.81317D-3	.54778D-3

Table A.6 The function $\mathcal{E}_3(\tau,\beta)$ for various values of τ and β

τ	β=1.0	β=2.0	β=3.0	β=5.0	β=10.0
.000	.50000D+0	.50000D+0	.50000D+0	.50000D+0	.50000D+0
.001	.49900D+0	.49899D+0	.49899D+0	.49897D+0	.49888D+0
.002	.49800D+0	.49799D+0	.49797D+0	.49789D+0	.49759D+0
.003	.49701D+0	.49698D+0	.49694D+0	.49679D+0	.49617D+0
.004	.49603D+0	.49598D+0	.49590D+0	.49565D+0	.49464D+0
.005	.49505D+0	.49497D+0	.49485D+0	.49449D+0	.49302D+0
.010	.49018D+0	.48993D+0	.48954D+0	.48838D+0	.48376D+0
.015	.48540D+0	.48490D+0	.48412D+0	.48186D+0	.47312D+0
.020	.48068D+0	.47988D+0	.47864D+0	.47506D+0	.46156D+0
.025	.47603D+0	.47488D+0	.47310D+0	.46805D+0	.44938D+0
.030	.47145D+0	.46990D+0	.46754D+0	.46087D+0	.43678D+0
.035	.46692D+0	.46496D+0	.46196D+0	.45358D+0	.42392D+0
.040	.46245D+0	.46004D+0	.45637D+0	.44620D+0	.41093D+0
.045	.45804D+0	.45515D+0	.45077D+0	.43877D+0	.39790D+0
.050	.45369D+0	.45029D+0	.44519D+0	.43130D+0	.38491D+0
.060	.44514D+0	.44069D+0	.43407D+0	.41633D+0	.35928D+0
.070	.43680D+0	.43124D+0	.42304D+0	.40142D+0	.33441D+0
.080	.42865D+0	.42194D+0	.41213D+0	.38666D+0	.31052D+0
.090	.42068D+0	.41279D+0	.40137D+0	.37213D+0	.28776D+0
.100	.41290D+0	.40381D+0	.39077D+0	.35787D+0	.26621D+0
.200	.34372D+0	.32290D+0	.29542D+0	.23531D+0	.11498D+0
.300	.28740D+0	.25715D+0	.22036D+0	.15005D+0	.46787D-1
.400	.24107D+0	.20434D+0	.16311D+0	.94125D-1	.18484D-1
.500	.20269D+0	.16215D+0	.12014D+0	.58435D-1	.71759D-2
.600	.17076D+0	.12856D+0	.88193D-1	.36022D-1	.27536D-2
.700	.14410D+0	.10187D+0	.64578D-1	.22093D-1	.10479D-2
.800	.12177D+0	.80695D-1	.47198D-1	.13498D-1	.39641D-3
.900	.10302D+0	.63900D-1	.34445D-1	.82228D-2	.14924D-3
1.000	.87263D-1	.50592D-1	.25110D-1	.49971D-2	.55981D-4
1.250	.57846D-1	.28209D-1	.11351D-1	.14277D-2	.47660D-5
1.500	.38527D-1	.15728D-1	.51137D-2	.40476D-3	.40086D-6
1.750	.25759D-1	.87717D-2	.22984D-2	.11416D-3	.33440D-7
2.000	.17277D-1	.48940D-2	.10315D-2	.32079D-4	.27731D-8
3.000	.35827D-2	.47673D-3	.41550D-4	.19583D-6	.1265D-12
4.000	.76390D-3	.46827D-4	.16677D-5	.11757D-8	.5605D-17
5.000	.15880D-3	.46299D-5	.66975D-7	.7008D-11	.2445D-22

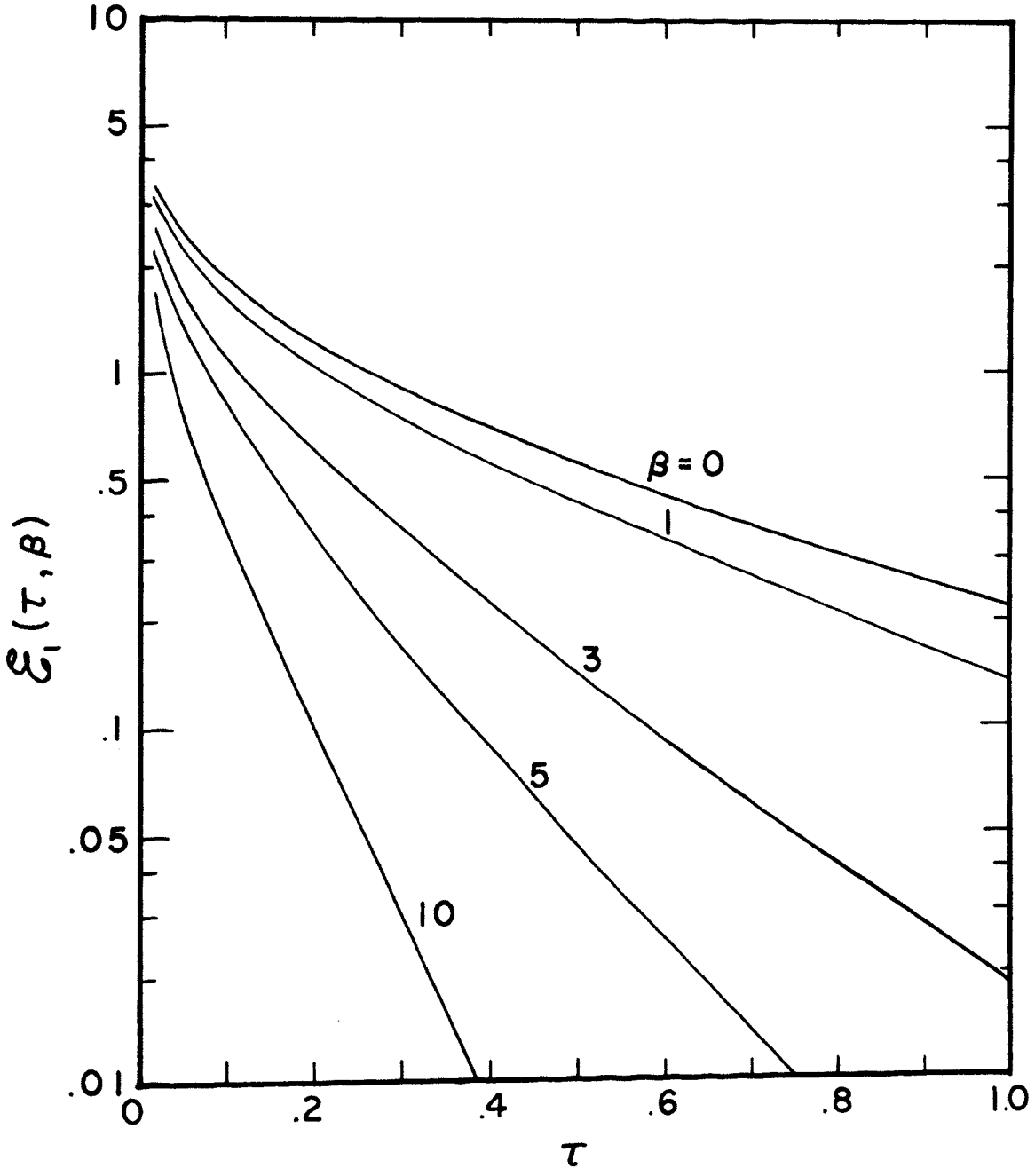

Figure A.1 Variation in the generalized $\mathcal{E}_1(\tau,\beta)$-function with τ for various values of β

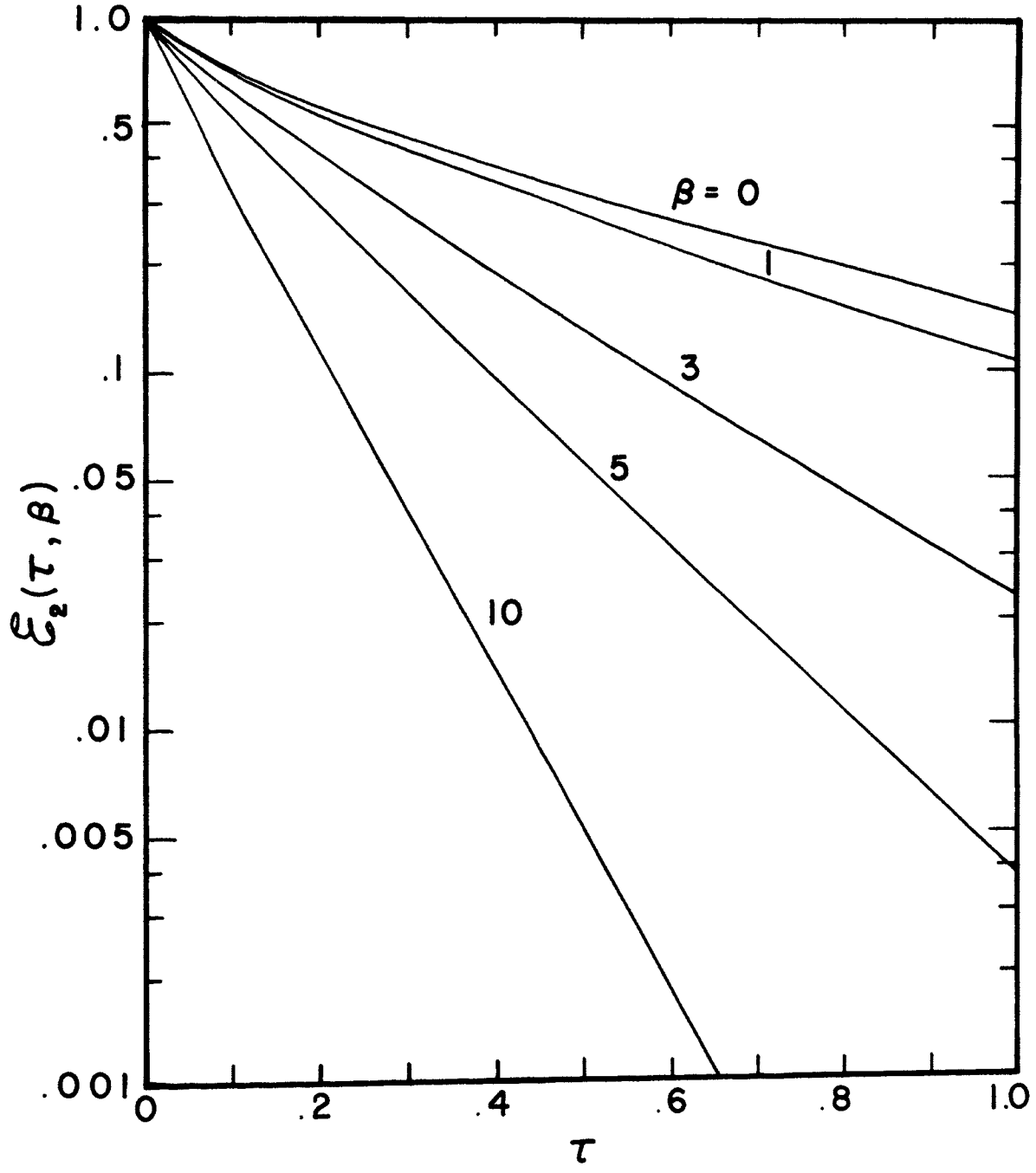

Figure A.2 Variation in the generalized $\mathcal{E}_2(\tau,\beta)$-function with τ for various values of β

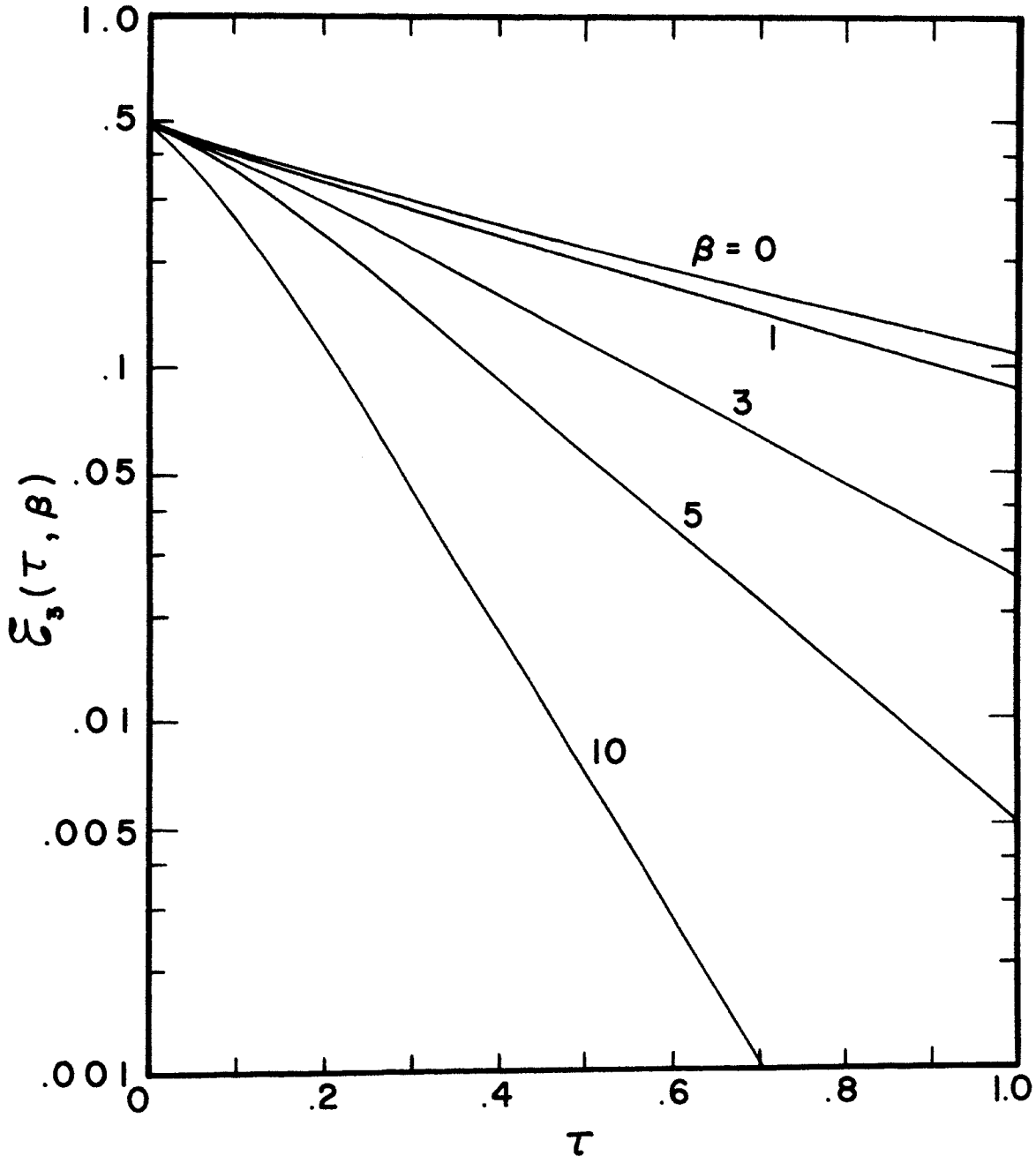

Figure A.3 Variation in the generalized $\mathcal{E}_3(\tau,\beta)$-function with τ for various values of β

APPENDIX B

NUMERICAL PROCEDURE FOR SELECTED INTEGRALS

The occurrence of the function $\psi_1(x,\beta)$ defined by equation (3.79) in the integrand complicates the numerical integration when β is large. An analytical integration of $\psi_1(x,\beta)$ over the range $0 \leq x \leq 1$ yields unity. However, when the integral is evaluated numerically by a ninth order Gaussian quadrature, the resulting sum diverges rapidly from unity for values of $\beta \geq 3$. Increasing the order of the quadrature does not appreciably increase the range of β for which accurate results can be obtained. A thirty-seventh order quadrature yields four significant digits for $\beta \leq 5$.

Inspection of Figure B.1 shows why merely increasing the order of quadrature is not practical when β is large. The area under each β curve is unity. For large β, $\psi_1(o,\beta) \to o$ and $\psi_1(1,\beta) \to \infty$. Hence, the main contribution to the area comes from the small region in the immediate neighborhood of the sharp spike at x=1. Therefore, additional quadrature points are needed in this interval. However, since the Gaussian quadrature is distributed over the range $-1<x<1$, only a small portion of the quadrature points will appear in the critical interval. Additional quadrature points can be forced into the critical region by subdividing the total interval into two parts, i.e., (0,.9) and (.9,1).

An alternate method is employed whereby the area is redistributed over a larger portion of the initial interval. This approach is accomplished by subtracting various functions from the integrands and later adding the equivalent integrated function. In particular,

the emissive power for the cosine varying diffuse boundary from the semi-infinite theory is written as

$$\bar{\phi}_{\beta}(o) = \frac{1}{2}\int_{o}^{1} \psi_{1}(x,\beta)[H(x,\beta)-H(1,\beta)]dx + \frac{1}{2} H(1,\beta) \quad . \tag{B.1}$$

The integrand in equation (B.1) is shown in Figure B.2 which exhibits the redistribution of the area away from the end point. $H(1,\beta)$ is selected since the spike occurs at $x=1$ and also because $H(x,\beta)-H(1,\beta)$ approaches zero for large β values. In a similar fashion, the corresponding emissive power for the finite medium is written as

$$\phi_{\beta}(o,\tau_{o}) = \frac{1}{2}\int_{o}^{1} \psi_{1}(x,\beta)[X(x,\tau_{o},\beta)-X(1,\tau_{o},\beta)]dx + \frac{1}{2} X(1,\tau_{o},\beta) \tag{B.2}$$

and

$$\phi_{\beta}(\tau_{o},\tau_{o}) = \frac{1}{2}\int_{o}^{1} \psi_{1}(x,\beta)[Y(x,\tau_{o},\beta)-Y(1,\tau_{o},\beta)]dx + \frac{1}{2} Y(1,\tau_{o},\beta) \quad . \tag{B.3}$$

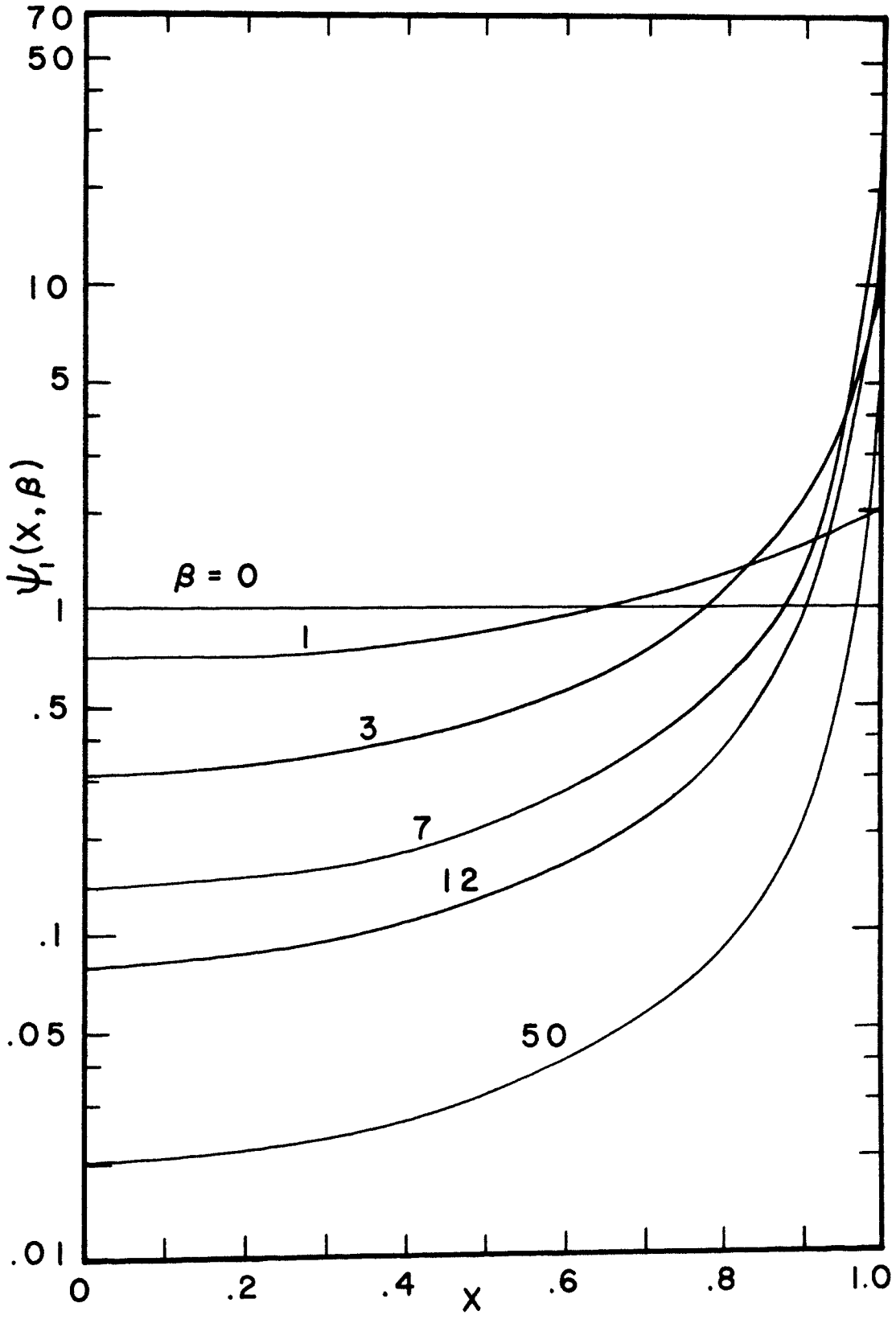

Figure B.1 Variation of $\psi_1(x,\beta)$ with x for various values of β

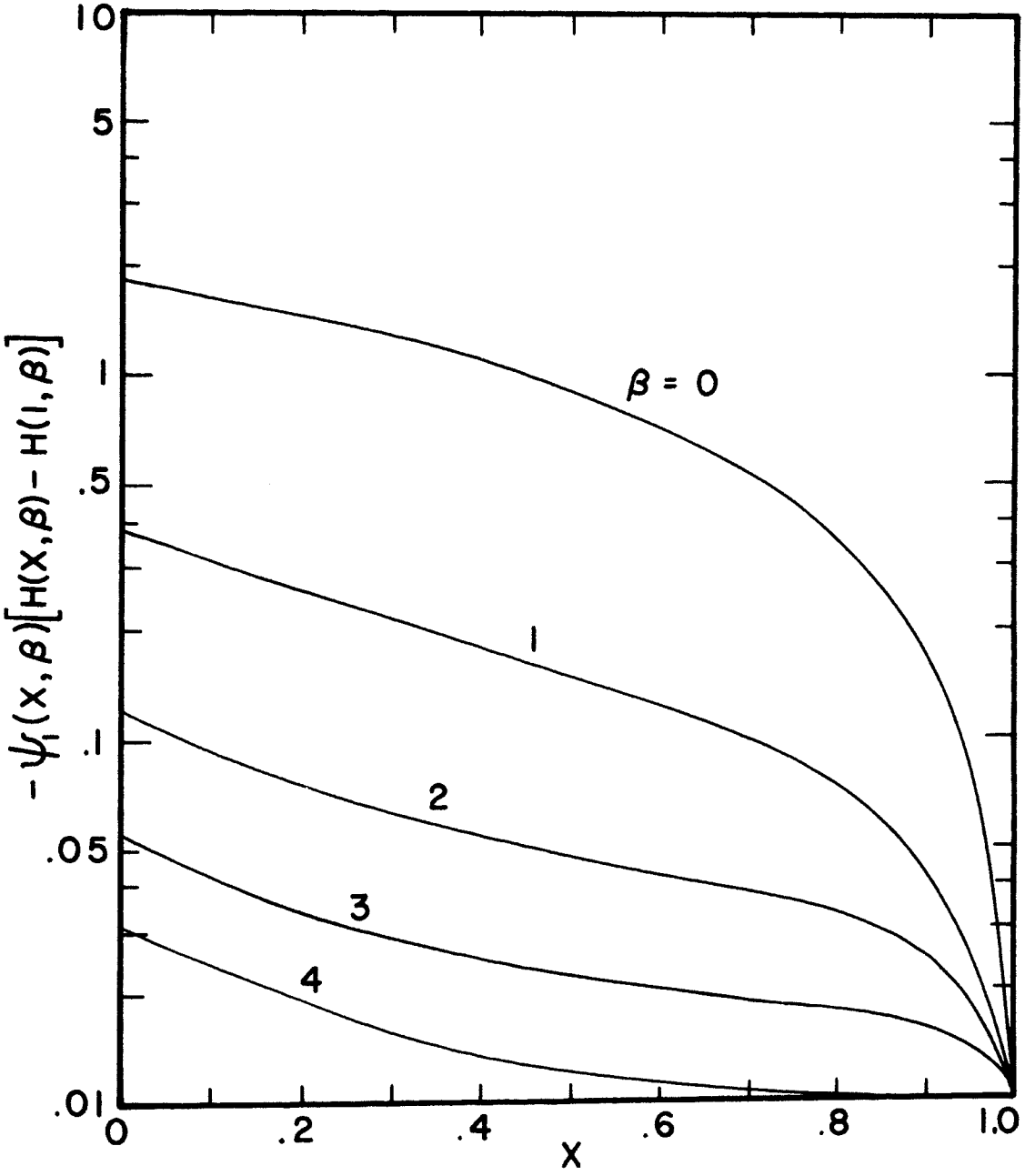

Figure B.2 Variation of $-\psi_1(x,\beta)[H(x,\beta)-H(1,\beta)]$ with x for various values of β

APPENDIX C

SYMMETRY OF THE GENERALIZED REFLECTION AND TRANSMISSION FUNCTIONS

When a collimated flux of cosine magnitude is incident upon a plane parallel medium of finite optical thickness τ_0 from a direction $\sigma=\sec\theta_0$, a pair of functions arise which are analogous to the reflection and transmission functions of Chandrasekhar. Since Chandrasekhar's functions are symmetric, the generalized functions should also be equal when $\beta=0$. The desired symmetry is shown in a manner similar to that of Kourganoff [4,p.167] who considered the one-dimensional semi-infinite analysis and hence had only to demonstrate the symmetry of the reflection function since the transmission function is zero. However, the same type of symmetry argument is easily extended to include the transmission function.

Since the semi-infinite theory is the limiting case of the finite, it is necessary to exhibit only the symmetry of the generalized reflection and transmission functions for the finite medium. The generalized reflection function $R_\beta(\sigma,s,\tau_0)$ and the generalized transmission function $S_\beta(\sigma,s,\tau_0)$ are defined as

$$R_\beta(\sigma,s,\tau_0) = \int_0^{\tau_0} J_\beta(x,s,\tau_0)e^{-x\sigma}dx \tag{C.1}$$

and

$$S_\beta(\sigma,s,\tau_0) = \int_0^{\tau_0} J_\beta(\tau_0-x,s,\tau_0)e^{-x\sigma}dx \tag{C.2}$$

where the dimensionless emissive power $J_\beta(\tau_z,\sigma,\tau_0)$ satisfies the following integral equation

$$J_\beta(\tau_z,\sigma,\tau_o) = e^{-\sigma\tau_z} + \frac{1}{2}\int_0^{\tau_o} \mathcal{E}_1(|\tau_z-\tau_z'|,\beta)J_\beta(\tau_z',\sigma,\tau_o)d\tau_z' \quad . \quad (C.3)$$

The kernel appearing in equation (C.3) is the generalized exponential integral function $\mathcal{E}_1$ which is described in detail in Appendix A.

First, consideration will be given to demonstrate the symmetry of $R_\beta(\sigma,s,\tau_o)$ in σ and s. Replacing σ by s in equation (C.3) yields an integral equation for $J_\beta(\tau_z,s,\tau_o)$ given by

$$J_\beta(\tau_z, s,\tau_o) = e^{-s\tau_z} + \frac{1}{2}\int_0^{\tau_o} \mathcal{E}_1(|\tau_z-\tau_z'|,\beta)J_\beta(\tau_z',s,\tau_o)d\tau_z' \quad . \quad (C.4)$$

When equation (C.3) is multiplied by $J_\beta(\tau_z,s,\tau_o)d\tau_z$ and integrated from o to τ_o, the following expression is obtained

$$\int_0^{\tau_o} J_\beta(\tau_z,\sigma,\tau_o)J_\beta(\tau_z,s,\tau_o)d\tau_z = \int_0^{\tau_o} J_\beta(\tau_z, s,\tau_o)e^{-\sigma\tau_z}\, d\tau_z$$

$$+ \int_0^{\tau_o} J_\beta(\tau_z,s,\tau_o)\left[\frac{1}{2}\int_0^{\tau_o} \mathcal{E}_1(|\tau_z-\tau_z'|,\beta)J_\beta(\tau_z',\sigma,\tau_o)d\tau_z'\right] d\tau_z \quad . \quad (C.5)$$

Similarly, equation (C.4) is multiplied by $J_\beta(\tau_z,\sigma,\tau_o)d\tau_z$ and integrated from o to τ_o to yield

$$\int_0^{\tau_o} J_\beta(\tau_z,\sigma,\tau_o)J_\beta(\tau_z,s,\tau_o)d\tau_z = \int_0^{\tau_o} J_\beta(\tau_z,\sigma,\tau_o)e^{-s\tau_z}\, d\tau_z$$

$$+ \int_0^{\tau_o} J_\beta(\tau_z,\sigma,\tau_o)\left[\frac{1}{2}\int_0^{\tau_o} \mathcal{E}_1(|\tau_z-\tau_z'|,\beta)J_\beta(\tau_z',s,\tau_o)d\tau_z'\right] d\tau_z \quad . \quad (C.6)$$

Since the left-hand sides of equations (C.5) and (C.6) are equal, the right-hand sides are equated to obtain

$$\int_0^{\tau_0} J_\beta(\tau_z,s,\tau_0)e^{-\sigma\tau_z}\,d\tau_z$$

$$+\int_0^{\tau_0} J_\beta(\tau_z,s,\tau_0)\left[\frac{1}{2}\int_0^{\tau_0} \mathcal{E}_1(|\tau_z-\tau_z'|,\beta)J_\beta(\tau_z',\sigma,\tau_0)d\tau_z'\right]d\tau_z$$

$$=\int_0^{\tau_0} J_\beta(\tau_z,\sigma,\tau_0)e^{-s\tau_z}\,d\tau_z$$

$$+\int_0^{\tau_0} J_\beta(\tau_z,\sigma,\tau_0)\left[\frac{1}{2}\int_0^{\tau_0} \mathcal{E}_1(|\tau_z-\tau_z'|,\beta)J_\beta(\tau_z',s,\tau_0)d\tau_z'\right]d\tau_z \quad . \tag{C.7}$$

The multiple integral terms appearing in equation (C.7) are equal since $\mathcal{E}_1(|\tau_z-\tau_z'|,\beta)$ is symmetric in τ_z and τ_z', thereby permitting τ_z and τ_z' to be interchanged. Hence, equation (C.7) reduces to

$$\int_0^{\tau_0} J_\beta(\tau_z,s,\tau_0)e^{-\sigma\tau_z}\,d\tau_z = \int_0^{\tau_0} J_\beta(\tau_z,\sigma,\tau_0)e^{-s\tau_z}\,d\tau_z. \tag{C.8}$$

Finally, utilization of equation (C.1) in equation (C.8) yields

$$R_\beta(\sigma,s,\tau_0) = R_\beta(s,\sigma,\tau_0) \tag{C.9}$$

which is the desired symmetry relation.

The symmetry of the transmission function can be obtained in a similar fashion. Replacement of τ_z by $\tau_0-\tau_z$ and τ_z' by $\tau_0-\tau_z'$ in equations (C.3) and (C.4) yields

$$J_\beta(\tau_o-\tau_z,\sigma,\tau_o) = e^{-\sigma(\tau_o-\tau_z)}$$

$$+ \frac{1}{2}\int_0^{\tau_o} \mathcal{E}_1(|\tau_z'-\tau_z|,\beta)J_\beta(\tau_o-\tau_z',\sigma,\tau_o)d\tau_z' \qquad (C.10)$$

and

$$J_\beta(\tau_o-\tau_z,s,\tau_o) = e^{-s(\tau_o-\tau_z)}$$

$$+ \frac{1}{2}\int_0^{\tau_o} \mathcal{E}_1(|\tau_z'-\tau_z|,\beta)J_\beta(\tau_o-\tau_z',s,\tau_o)d\tau_z' \quad . \qquad (C.11)$$

Multiplication of equation (C.10) by $J_\beta(\tau_z,s,\tau_o)d\tau_z$ and integration from o to τ_o yields

$$\int_0^{\tau_o} J_\beta(\tau_z,s,\tau_o)J_\beta(\tau_o-\tau_z,\sigma,\tau_o)d\tau_z$$

$$= \int_0^{\tau_o} J_\beta(\tau_z,s,\tau_o)e^{-\sigma(\tau_o-\tau_z)}d\tau_z$$

$$+ \int_0^{\tau_o} J_\beta(\tau_z,s,\tau_o)\left[\frac{1}{2}\int_0^{\tau_o} \mathcal{E}_1(|\tau_z-\tau_z'|,\beta)J_\beta(\tau_o-\tau_z',\sigma,\tau_o)d\tau_z'\right]d\tau_z \quad . \qquad (C.12)$$

Similarly, multiplication of equation (C.11) by $J_\beta(\tau_z,\sigma,\tau_o)d\tau_z$ and integration from o to τ_o yields

$$\int_0^{\tau_o} J_\beta(\tau_z,\sigma,\tau_o)J_\beta(\tau_o-\tau_z,s,\tau_o)d\tau_z = \int_0^{\tau_o} J_\beta(\tau_z,\sigma,\tau_o)e^{-s(\tau_o-\tau_z)}\,d\tau_z$$

$$+\int_0^{\tau_o} J_\beta(\tau_z,\sigma,\tau_o)\left[\frac{1}{2}\int_0^{\tau_o} \mathcal{E}_1(|\tau_z-\tau_z'|,\beta)J_\beta(\tau_o-\tau_z',s,\tau_o)d\tau_z'\right] d\tau_z \quad . \quad (C.13)$$

The substitution $\tau_z=\tau_o-x$ makes the integral on the left-hand side of equation (C.12) equal to the integral on the left-hand side of equation (C.13). This operation results in

$$\int_0^{\tau_o} J_\beta(\tau_z,s,\tau_o)e^{-\sigma(\tau_o-\tau_z)}d\tau_z$$

$$+\int_0^{\tau_o} J_\beta(\tau_z,s,\tau_o)\left[\frac{1}{2}\int_0^{\tau_o} \mathcal{E}_1(|\tau_z'-\tau_z|,\beta)J_\beta(\tau_o-\tau_z',\sigma,\tau_o)d\tau_z'\right] d\tau_z$$

$$=\int_0^{\tau_o} J_\beta(\tau_z,\sigma,\tau_o)e^{-s(\tau_o-\tau_z)}\,d\tau_z$$

$$+\int_0^{\tau_o} J_\beta(\tau_z,\sigma,\tau_o)\left[\frac{1}{2}\int_0^{\tau_o} \mathcal{E}_1(|\tau_z'-\tau_z|,\beta)J_\beta(\tau_o-\tau_z',s,\tau_o)d\tau_z'\right] d\tau_z \quad . \quad (C.14)$$

Replacement of τ_z by $\tau_o-\tau_z$ and τ_z' by $\tau_o-\tau_z'$ in the second term on the left-hand side of equation (C.14) and utilization of the symmetry of $\mathcal{E}_1(|\tau_z'-\tau_z|,\beta)$ in τ_z and τ_z' yields

$$\int_0^{\tau_o} J_\beta(\tau_z,s,\tau_o)e^{-\sigma(\tau_o-\tau_z)}\,d\tau_z = \int_0^{\tau_o} J_\beta(\tau_z,\sigma,\tau_o)e^{-s(\tau_o-\tau_z)}d\tau_z \quad . \quad (C.15)$$

Equation (C.15) can be put in a form similar to equation (C.2) by the substitution $x=\tau_o-\tau_z$. This change of variable yields

$$\int_0^{\tau_o} J_\beta(\tau_o - x, s, \tau_o) e^{-\sigma x}\, dx = \int_0^{\tau_o} J_\beta(\tau_o - x, \sigma, \tau_o) e^{-sx}\, dx \quad . \quad (C.16)$$

Utilization of equation (C.2) in equation (C.16) yields finally

$$S_\beta(\sigma, s, \tau_o) = S_\beta(s, \sigma, \tau_o) \quad (C.17)$$

which is the desired symmetry.

APPENDIX D

TABLES OF RESULTS FOR THE SEMI-INFINITE MEDIUM

Table D.1 Approximate values of the function $H(.5,\beta)$

β	FIRST ORDER	SECOND ORDER	THIRD ORDER	FOURTH ORDER	EXACT
.00	1.8660	1.9657	1.9902	1.9995	2.0127
.10	1.7773	1.8713	1.8942	1.9030	1.9151
.20	1.6979	1.7838	1.8051	1.8133	1.8246
.30	1.6272	1.7047	1.7243	1.7319	1.7424
.40	1.5647	1.6344	1.6522	1.6592	1.6689
.50	1.5098	1.5725	1.5886	1.5950	1.6039
.60	1.5311	1.5183	1.5329	1.5387	1.5469
.70	1.4196	1.4711	1.4843	1.4896	1.4971
.80	1.3828	1.4300	1.4420	1.4468	1.4537
.90	1.3506	1.3942	1.4051	1.4096	1.4159
1.00	1.3223	1.3629	1.3729	1.3770	1.3828
2.00	1.1672	1.1920	1.1979	1.2001	1.2031
3.00	1.1087	1.1263	1.1310	1.1327	1.1348
4.00	1.0796	1.0931	1.0970	1.0985	1.1002
5.00	1.0626	1.0733	1.0767	1.0780	1.0796
6.00	1.0515	1.0604	1.0632	1.0645	1.0659
7.00	1.0437	1.0512	1.0538	1.0548	1.0562
8.00	1.0379	1.0445	1.0467	1.0477	1.0490
9.00	1.0335	1.0393	1.0413	1.0422	1.0434
10.00	1.0300	1.0351	1.0369	1.0378	1.0390

Table D.2 Approximate values of the function $H(1,\beta)$

β	FIRST ORDER	SECOND ORDER	THIRD ORDER	FOURTH ORDER	EXACT
.00	2.7320	2.8644	2.8886	2.8966	2.9078
.10	2.4842	2.6033	2.6246	2.6319	2.6408
.20	2.2804	2.3838	2.4028	2.4093	2.4173
.30	2.1121	2.2013	2.2180	2.2238	2.2311
.40	1.9725	2.0498	2.0646	2.0697	2.0762
.50	1.8563	1.9240	1.9370	1.9416	1.9474
.60	1.7591	1.8192	1.8307	1.8348	1.8400
.70	1.6773	1.7316	1.7419	1.7455	1.7502
.80	1.6082	1.6580	1.6671	1.6704	1.6746
.90	1.5494	1.5956	1.6039	1.6068	1.6107
1.00	1.4992	1.5425	1.5500	1.5527	1.5562
2.00	1.2434	1.2718	1.2769	1.2783	1.2801
3.00	1.1546	1.1753	1.1799	1.1813	1.1826
4.00	1.1121	1.1278	1.1320	1.1334	1.1347
5.00	1.0875	1.1001	1.1038	1.1052	1.1064
6.00	1.0717	1.0821	1.0853	1.0866	1.0879
7.00	1.0606	1.0695	1.0723	1.0735	1.0748
8.00	1.0525	1.0602	1.0627	1.0638	1.0651
9.00	1.0463	1.0530	1.0553	1.0563	1.0576
10.00	1.0414	1.0474	1.0495	1.0504	1.0517

Table D.3 The function $H(\mu,\beta)$ for various values of μ and β

	$H(\mu,\beta)$					
μ	β=0	β=.50	β=1.0	β=2.0	β=5.0	β=10.0
.00	1.0000	1.0000	1.0000	1.0000	1.0000	1.0000
.01	1.0342	1.0272	1.0203	1.0123	1.0052	1.0026
.02	1.0622	1.0487	1.0360	1.0216	1.0091	1.0046
.03	1.0882	1.0682	1.0499	1.0298	1.0126	1.0063
.04	1.1128	1.0863	1.0628	1.0372	1.0157	1.0078
.05	1.1365	1.1034	1.0749	1.0441	1.0185	1.0092
.06	1.1596	1.1199	1.0863	1.0507	1.0212	1.0106
.07	1.1821	1.1357	1.0972	1.0568	1.0237	1.0118
.08	1.2042	1.1510	1.1076	1.0627	1.0260	1.0130
.09	1.2259	1.1658	1.1177	1.0682	1.0283	1.0141
.10	1.2473	1.1802	1.1274	1.0736	1.0304	1.0152
.11	1.2684	1.1943	1.1367	1.0788	1.0325	1.0162
.12	1.2893	1.2081	1.1458	1.0837	1.0345	1.0171
.13	1.3100	1.2215	1.1547	1.0885	1.0364	1.0181
.14	1.3305	1.2347	1.1633	1.0932	1.0382	1.0190
.15	1.3508	1.2476	1.1717	1.0976	1.0400	1.0198
.16	1.3709	1.2603	1.1798	1.1020	1.0417	1.0207
.17	1.3910	1.2728	1.1878	1.1062	1.0433	1.0215
.18	1.4109	1.2850	1.1956	1.1103	1.0449	1.0222
.19	1.4306	1.2971	1.2032	1.1143	1.0464	1.0230
.20	1.4503	1.3089	1.2107	1.1182	1.0479	1.0237
.25	1.5473	1.3657	1.2457	1.1363	1.0548	1.0271
.30	1.6425	1.4188	1.2776	1.1523	1.0609	1.0300
.35	1.7364	1.4688	1.3069	1.1668	1.0663	1.0326
.40	1.8292	1.5161	1.3341	1.1800	1.0712	1.0350
.45	1.9213	1.5611	1.3593	1.1921	1.0755	1.0371
.50	2.0127	1.6039	1.3828	1.2031	1.0795	1.0390
.55	2.1036	1.6448	1.4049	1.2134	1.0832	1.0407
.60	2.1941	1.6840	1.4256	1.2229	1.0866	1.0423
.65	2.2842	1.7215	1.4452	1.2317	1.0897	1.0438
.70	2.3739	1.7576	1.4636	1.2400	1.0926	1.0452
.75	2.4634	1.7922	1.4811	1.2477	1.0953	1.0465

Table D.4 The function $H(\mu,\beta)$ for various values of μ and β

	$H(\mu,\beta)$					
μ	β=0	β=.50	β=1.0	β=2.0	β=5.0	β=10.0
.80	2.5527	1.8255	1.4976	1.2550	1.0978	1.0476
.85	2.6417	1.8576	1.5134	1.2618	1.1002	1.0488
.90	2.7305	1.8886	1.5284	1.2683	1.1024	1.0498
.95	2.8192	1.9185	1.5426	1.2743	1.1045	1.0508
1.00	2.9078	1.9474	1.5562	1.2801	1.1064	1.0517
1.50	3.7876	2.1907	1.6646	1.3244	1.1212	1.0586
2.00	4.6619	2.3738	1.7395	1.3535	1.1306	1.0629
2.50	5.5333	2.5171	1.7945	1.3742	1.1372	1.0660
3.00	6.4033	2.6324	1.8367	1.3896	1.1420	1.0682
3.50	7.2722	2.7272	1.8701	1.4015	1.1457	1.0699
4.00	8.1405	2.8066	1.8972	1.4110	1.1486	1.0712
4.50	9.0083	2.8741	1.9196	1.4188	1.1510	1.0723
5.00	9.8758	2.9322	1.9385	1.4253	1.1530	1.0732
5.50	10.743	2.9827	1.9546	1.4308	1.1547	1.0740
6.00	11.610	3.0271	1.9685	1.4355	1.1561	1.0746
6.50	12.477	3.0663	1.9806	1.4396	1.1573	1.0752
7.00	13.343	3.1012	1.9913	1.4432	1.1584	1.0757
7.50	14.210	3.1326	2.0008	1.4463	1.1593	1.0761
8.00	15.077	3.1608	2.0092	1.4491	1.1602	1.0765
8.50	15.943	3.1864	2.0168	1.4516	1.1609	1.0768
9.00	16.810	3.2098	2.0237	1.4539	1.1616	1.0771
9.50	17.676	3.2311	2.0299	1.4559	1.1622	1.0774
10.00	18.543	3.2507	2.0356	1.4578	1.1628	1.0776
15.00	27.205	3.3838	2.0732	1.4699	1.1663	1.0793
20.00	35.867	3.4570	2.0932	1.4763	1.1682	1.0801
25.00	44.528	3.5032	2.1056	1.4802	1.1694	1.0806
30.00	53.189	3.5351	2.1141	1.4828	1.1701	1.0810
40.00	70.510	3.5762	2.1248	1.4862	1.1711	1.0814
50.00	87.831	3.6016	2.1314	1.4882	1.1717	1.0817
60.00	105.15	3.6188	2.1358	1.4896	1.1721	1.0819
80.00	139.79	3.6407	2.1414	1.4913	1.1726	1.0821
100.00	174.43	3.6540	2.1448	1.4924	1.1729	1.0822

Table D.5 The function $H(\sqrt{1+\beta^2}/\sigma,\beta)$ for various values of σ and β

	$H(\sqrt{1+\beta^2}/\sigma,\beta)=B_\beta(0,\sigma)$					
β	σ=1.0	σ=2.0	σ=3.0	σ=4.0	σ=5.0	σ=10.0
.000	2.9078	2.0127	1.7052	1.5473	1.4503	1.2473
.001	2.9049	2.0117	1.7046	1.5469	1.4500	1.2472
.002	2.9020	2.0107	1.7040	1.5465	1.4497	1.2471
.004	2.8962	2.0087	1.7029	1.5457	1.4491	1.2468
.008	2.8847	2.0047	1.7007	1.5442	1.4480	1.2463
.010	2.8790	2.0027	1.6995	1.5434	1.4474	1.2461
.020	2.8509	1.9929	1.6939	1.5396	1.4446	1.2448
.030	2.8235	1.9832	1.6884	1.5359	1.4417	1.2436
.040	2.7966	1.9736	1.6830	1.5321	1.4389	1.2424
.050	2.7704	1.9642	1.6776	1.5284	1.4361	1.2412
.060	2.7447	1.9549	1.6722	1.5248	1.4334	1.2400
.080	2.6951	1.9367	1.6618	1.5176	1.4280	1.2376
.100	2.6476	1.9190	1.6515	1.5106	1.4227	1.2353
.200	2.4384	1.8377	1.6039	1.4775	1.3976	1.2244
.300	2.2682	1.7671	1.5616	1.4479	1.3750	1.2143
.400	2.1282	1.7056	1.5240	1.4213	1.3546	1.2052
.500	2.0119	1.6520	1.4906	1.3974	1.3362	1.1968
.600	1.9144	1.6051	1.4608	1.3759	1.3196	1.1892
.800	1.7616	1.5273	1.4103	1.3392	1.2908	1.1758
1.000	1.6489	1.4662	1.3696	1.3089	1.2670	1.1645
1.250	1.5451	1.4064	1.3286	1.2782	1.2425	1.1526
1.500	1.4685	1.3599	1.2959	1.2532	1.2224	1.1427
1.750	1.4100	1.3228	1.2692	1.2325	1.2056	1.1343
2.000	1.3641	1.2926	1.2470	1.2151	1.1914	1.1270
2.500	1.2969	1.2464	1.2122	1.1875	1.1685	1.1150
3.000	1.2504	1.2127	1.1862	1.1663	1.1508	1.1054
3.500	1.2163	1.1872	1.1660	1.1497	1.1367	1.0975
4.000	1.1903	1.1672	1.1498	1.1361	1.1251	1.0909
4.500	1.1699	1.1510	1.1365	1.1249	1.1154	1.0852
5.000	1.1534	1.1377	1.1254	1.1154	1.1072	1.0803
6.000	1.1284	1.1171	1.1079	1.1003	1.0938	1.0721
7.000	1.1104	1.1018	1.0947	1.0887	1.0836	1.0656

Table D.6 The function $H(\sqrt{1+\beta^2}/\sigma,\beta)$ for various values of σ and β

	$H(\sqrt{1+\beta^2}/\sigma,\beta)=B_\beta(0,\sigma)$					
β	σ=1.0	σ=2.0	σ=3.0	σ=4.0	σ=5.0	σ=10.0
8.0	1.0968	1.0901	1.0845	1.0796	1.0753	1.0602
9.0	1.0862	1.0808	1.0762	1.0722	1.0686	1.0556
10.0	1.0777	1.0733	1.0694	1.0660	1.0630	1.0518
12.5	1.0623	1.0594	1.0568	1.0545	1.0524	1.0442
15.0	1.0520	1.0499	1.0481	1.0464	1.0448	1.0386
17.5	1.0446	1.0431	1.0417	1.0404	1.0392	1.0343
20.0	1.0390	1.0379	1.0368	1.0357	1.0348	1.0308
25.0	1.0312	1.0305	1.0298	1.0291	1.0285	1.0257
30	1.0260	1.0255	1.0250	1.0245	1.0241	1.0220
35	1.0223	1.0219	1.0216	1.0212	1.0209	1.0193
40	1.0195	1.0192	1.0189	1.0187	1.0184	1.0172
60	1.0130	1.0129	1.0128	1.0126	1.0125	1.0119
80	1.0098	1.0097	1.0096	1.0095	1.0095	1.0091
100	1.0078	1.0077	1.0077	1.0077	1.0076	1.0074
125	1.0062	1.0062	1.0062	1.0061	1.0061	1.0060
150	1.0052	1.0052	1.0051	1.0051	1.0051	1.0050
175	1.0044	1.0044	1.0044	1.0044	1.0044	1.0043
200	1.0039	1.0039	1.0039	1.0038	1.0038	1.0038
250	1.0031	1.0031	1.0031	1.0031	1.0031	1.0030
300	1.0026	1.0026	1.0026	1.0026	1.0025	1.0025
400	1.0019	1.0019	1.0019	1.0019	1.0019	1.0019
500	1.0015	1.0015	1.0015	1.0015	1.0015	1.0015
600	1.0013	1.0013	1.0013	1.0013	1.0013	1.0013
800	1.0009	1.0009	1.0009	1.0009	1.0009	1.0009
1000	1.0007	1.0007	1.0007	1.0007	1.0007	1.0007
1500	1.0005	1.0005	1.0005	1.0005	1.0005	1.0005
2000	1.0003	1.0003	1.0003	1.0003	1.0003	1.0003
3000	1.0002	1.0002	1.0002	1.0002	1.0002	1.0002
4000	1.0001	1.0001	1.0001	1.0001	1.0001	1.0001
5000	1.0001	1.0001	1.0001	1.0001	1.0001	1.0001
8000	1.0000	1.0000	1.0000	1.0000	1.0000	1.0000
10000	1.0000	1.0000	1.0000	1.0000	1.0000	1.0000

Table D.7 Moment of the function $H(\mu,\beta)$

β	$h_0(\beta)$	β	$h_0(\beta)$
.000	2.0000	8.0	1.0613
.001	1.9988	9.0	1.0546
.002	1.9976	10.0	1.0492
.004	1.9953	12.5	1.0395
.008	1.9908	15.0	1.0330
.010	1.9885	17.5	1.0283
.020	1.9772	20.0	1.0248
.030	1.9660	25.0	1.0198
.040	1.9551	30	1.0165
.050	1.9442	35	1.0142
.060	1.9336	40	1.0124
.080	1.9127	60	1.0083
.100	1.8924	80	1.0062
.200	1.7995	100	1.0050
.300	1.7194	125	1.0040
.400	1.6504	150	1.0033
.500	1.5911	175	1.0028
.600	1.5398	200	1.0025
.800	1.4568	250	1.0020
1.000	1.3935	300	1.0016
1.250	1.3337	400	1.0012
1.500	1.2887	500	1.0010
1.750	1.2539	600	1.0008
2.000	1.2263	800	1.0006
2.500	1.1855	1000	1.0005
3.000	1.1570	1500	1.0003
3.500	1.1359	2000	1.0002
4.000	1.1198	3000	1.0001
4.500	1.1071	4000	1.0001
5.000	1.0968	5000	1.0001
6.000	1.0811	8000	1.0000
7.000	1.0698	10000	1.0000

Table D.8 Emissive power at $\tau_z=0$ and $\tau_z=\tau_o$ for a semi-infinite medium bounded by a strip illuminated by a uniform collimated flux of magnitude F_o from directions σ = 1, 2, and 5

	B(0,0)		
τ_a	σ = 1.0	σ = 2.0	σ = 5.0
.00	1.00000	1.00000	1.00000
.01	1.03142	1.02688	1.02152
.02	1.05592	1.04688	1.03629
.05	1.11694	1.09467	1.06909
.10	1.19941	1.15593	1.10736
.20	1.33038	1.24727	1.15861
.50	1.60451	1.42049	1.24227
1.00	1.89099	1.58084	1.30843
2.00	2.20948	1.73794	1.36539
5.00	2.56350	1.88818	1.41376
10.00	2.72660	1.94916	1.43192
20.00	2.81582	1.98082	1.44113
50.00	2.87072	1.99993	1.44665
100.00	2.88930	2.00636	1.44850
∞	2.90781	2.01278	1.45035

Table D.9 Emissive power at $\tau_z=0$ for a semi-infinite medium bounded by a strip illuminated by a uniform collimated flux of magnitude F_0 from direction $\sigma=1$

	$B(\tau_y,0)$				
τ_y/τ_a	$\tau_a=.01$	$\tau_a=.10$	$\tau_a=1.0$	$\tau_a=10.0$	$\tau_a=100.0$
0.00	1.03142	1.19942	1.89098	2.72658	2.88930
.20	1.03132	1.19843	1.88339	2.71977	2.88853
.40	1.03100	1.19537	1.85971	2.69617	2.88578
.60	1.03042	1.18994	1.81672	2.64203	2.87892
.80	1.02947	1.18129	1.74598	2.50757	2.85664
1.00	1.02796	1.16519	1.60473	1.90788	1.94929
1.02	.02778	.16251	.57901	.74313	.34458
1.04	.02760	.16033	.56018	.64572	.20389
1.06	.02744	.15847	.54393	.57220	.14177
1.08	.02727	.15678	.52934	.51329	.10760
1.10	.02711	.15523	.51596	.46455	.08620
1.12	.02696	.15376	.50356	.42340	.07160
1.14	.02681	.15238	.49195	.38814	.06104
1.16	.02666	.15107	.48101	.35758	.05306
1.18	.02652	.14981	.47066	.33085	.04682
1.20	.02639	.14861	.46081	.30728	.04181
1.40	.02529	.13851	.38198	.17001	.01924
1.60	.02446	.13062	.32513	.11078	.01185
1.80	.02378	.12405	.28124	.07909	.00825
2.00	.02319	.11838	.24608	.05983	.00616
3.00	.02104	.09785	.14074	.02291	.00231
4.00	.01956	.08415	.09017	.01228	.00123
5.00	.01843	.07395	.06216	.00768	.00077

Table D.10 Emissive power at $\tau_z=0$ for a semi-infinite medium bounded by a strip illuminated by a uniform collimated flux of magnitude F_o from direction $\sigma=2$

	$B(\tau_y,0)$				
τ_y/τ_a	$\tau_a=.01$	$\tau_a=.10$	$\tau_a=1.0$	$\tau_a=10.0$	$\tau_a=100.0$
0.00	1.02687	1.15593	1.58083	1.94915	2.00636
.20	1.02677	1.15502	1.57592	1.94660	2.00609
.40	1.02647	1.15219	1.56041	1.93761	2.00514
.60	1.02592	1.14714	1.53148	1.91614	2.00276
.80	1.02502	1.13903	1.48146	1.85759	1.99500
1.00	1.02343	1.12363	1.36897	1.49039	1.50480
1.02	.02322	.12096	.34655	.36691	.13583
1.04	.02302	.11890	.33096	.30415	.07509
1.06	.02284	.11713	.31787	.26027	.05080
1.08	.02267	.11553	.30637	.22703	.03806
1.10	.02251	.11405	.29601	.20074	.03028
1.12	.02235	.11267	.28657	.17935	.02505
1.14	.02221	.11136	.27785	.16160	.02130
1.16	.02206	.11012	.26974	.14665	.01848
1.18	.02193	.10894	.26216	.13388	.01628
1.20	.02181	.10781	.25504	.12287	.01453
1.40	.02076	.09845	.20063	.06332	.00666
1.60	.01996	.09127	.16413	.04005	.00410
1.80	.01929	.08539	.13744	.02817	.00285
2.00	.01871	.08039	.11699	.02113	.00213
3.00	.01661	.06292	.06075	.00798	.00080
4.00	.01518	.05188	.03668	.00426	.00043
5.00	.01409	.04403	.02429	.00266	.00027

Table D.11 Emissive power at $\tau_z=0$ for a semi-infinite medium bounded by a strip illuminated by a uniform collimated flux of magnitude F_o from direction $\sigma=5$

	$B(\tau_y,0)$				
τ_y/τ_a	$\tau_a=.01$	$\tau_a=.10$	$\tau_a=1.0$	$\tau_a=10.0$	$\tau_a=100.0$
0.00	1.02152	1.10736	1.30842	1.43191	1.44850
.20	1.02142	1.10661	1.30617	1.43115	1.44841
.40	1.02112	1.10429	1.29890	1.42845	1.44814
.60	1.02059	1.10007	1.28475	1.42186	1.44745
.80	1.01973	1.09315	1.25817	1.40273	1.44521
1.00	1.01814	1.07930	1.18269	1.22056	1.22473
1.02	.01790	.07677	.16489	.14130	.04202
1.04	.01769	.07491	.15368	.11023	.02225
1.06	.01751	.07332	.14476	.09072	.01485
1.08	.01734	.07189	.13724	.07693	.01106
1.10	.01718	.07057	.13071	.06656	.00878
1.12	.01703	.06936	.12492	.05845	.00725
1.14	.01689	.06822	.11971	.05192	.00616
1.16	.01676	.06714	.11498	.04655	.00534
1.18	.01664	.06612	.11066	.04207	.00470
1.20	.01652	.06515	.10667	.03828	.00419
1.40	.01551	.05734	.07840	.01886	.00192
1.60	.01474	.05159	.06133	.01174	.00118
1.80	.01410	.04704	.04968	.00820	.00082
2.00	.01354	.04330	.04120	.00613	.00061
3.00	.01155	.03110	.01977	.00230	.00023
4.00	.01023	.02414	.01146	.00123	.00012
5.00	.00925	.01955	.00741	.00077	.00007

Table D.12 Emissive power at $\tau_z=0$ and $\tau_y=0$ for a semi-infinite medium bounded by a constant temperature strip

τ_a	$\overline{\phi}(0,0)$	τ_a	$\overline{\phi}(0,0)$	τ_a	$\overline{\phi}(0,0)$
.00	.50000	.20	.59946	10.0	.96343
.01	.50979	.50	.67883	20.0	.98165
.02	.51732	1.00	.75875	50.0	.99263
.05	.53588	2.00	.84293	100.0	.99632
.10	.56065	5.00	.92821	∞	1.00000

Table D.13 Emissive power at $\tau_z=0$ for a semi-infinite medium bounded by a constant temperature strip

	$\overline{\phi}(\tau_y,0)$				
τ_y/τ_a	τ_a=.01	τ_a=.10	τ_a=1.0	τ_a=10.0	τ_a=100.0
0.00	.50979	.56065	.75874	.96342	.99632
.20	.50976	.56034	.75647	.96194	.99616
.40	.50966	.55937	.74939	.95674	.99562
.60	.50947	.55765	.73647	.94435	.99425
.80	.50917	.55490	.71505	.91126	.98979
1.00	.50866	.54973	.67146	.74081	.74908
1.02	.00860	.04885	.16337	.19117	.07762
1.04	.00854	.04815	.15752	.16279	.04327
1.06	.00848	.04756	.15250	.14182	.02925
1.08	.00843	.04702	.14801	.12531	.02189
1.10	.00837	.04652	.14392	.11188	.01740
1.12	.00832	.04605	.14012	.10071	.01439
1.14	.00827	.04561	.13658	.09128	.01223
1.16	.00822	.04519	.13325	.08321	.01061
1.18	.00818	.04479	.13011	.07625	.00935
1.20	.00814	.04441	.12712	.07018	.00834
1.40	.00778	.04120	.10343	.03652	.00382
1.60	.00751	.03871	.08660	.02308	.00235
1.80	.00729	.03664	.07379	.01622	.00164
2.00	.00710	.03487	.06368	.01215	.00122
3.00	.00641	.02846	.03435	.00458	.00046
4.00	.00593	.02421	.02104	.00244	.00024
5.00	.00557	.02106	.01403	.00153	.00015

Table D.14 Normal flux at $\tau_z=0$ for a semi-infinite medium illuminated by a collimated flux of cosine magnitude from direction $\sigma=1$

β	$Q_\beta(0,\sigma)$	β	$Q_\beta(0,\sigma)$
.000	.00000000	8.0	.94233
.001	.00167663	9.0	.94832
.002	.00334890	10.0	.95317
.004	.00668037	12.5	.96208
.008	.0132915	15.0	.96815
.010	.0165713	17.5	.97253
.020	.0327180	20.0	.97585
.030	.0484535	25.0	.98055
.040	.0637906	30	.98371
.050	.0787419	35	.98600
.060	.0933192	40	.98774
.080	.121398	60	.99177
.100	.148113	80	.99381
.200	.263895	100	.99504
.300	.355676	125	.99605
.400	.429387	150	.99674
.500	.489332	175	.99726
.600	.538674	200	.99766
.800	.614364	250	.99825
1.000	.669109	300	.99865
1.250	.718955	400	.99914
1.500	.755571	500	.99942
1.750	.783568	600	.99958
2.000	.805671	800	.99975
2.500	.838381	1000	.99984
3.000	.861479	1500	.99992
3.500	.878699	2000	.99995
4.000	.892051	3000	.99998
4.500	.902721	4000	.99999
5.000	.911450	5000	.99999
6.000	.924889	8000	.99999
7.000	.934764	10000	.99999

Table D.15 Normal flux at $\tau_z=0$ for a semi-infinite medium illuminated by a collimated flux of cosine magnitude from direction $\sigma=2$

β	$Q_\beta(0,\sigma)$	β	$Q_\beta(0,\sigma)$
.000	.000000000	8.0	.44805
.001	.000580502	9.0	.45298
.002	.00115993	10.0	.45705
.004	.00231557	12.5	.46468
.008	.00461408	15.0	.47001
.010	.00575697	17.5	.47393
.020	.0114085	20.0	.47694
.030	.0169566	25.0	.48127
.040	.0224034	30	.48422
.050	.0277509	35	.48637
.060	.0330010	40	.48803
.080	.0432167	60	.49191
.100	.0530657	80	.49388
.200	.0972966	100	.49509
.300	.134316	125	.49608
.400	.165466	150	.49676
.500	.191843	175	.49727
.600	.214340	200	.49767
.800	.250425	250	.49826
1.000	.277912	300	.49866
1.250	.304170	400	.49915
1.500	.324361	500	.49942
1.750	.340416	600	.49958
2.000	.353532	800	.49975
2.500	.373790	1000	.49984
3.000	.388818	1500	.49992
3.500	.400482	2000	.49995
4.000	.409837	3000	.49998
4.500	.417527	4000	.49999
5.000	.423973	5000	.49999
6.000	.434195	8000	.49999
7.000	.441955	10000	.49999

Table D.16 Normal flux at $\tau_z=0$ for a semi-infinite medium illuminated by a collimated flux of cosine magnitude from direction $\sigma=5$

β	$Q_\beta(0,\sigma)$	β	$Q_\beta(0,\sigma)$
.000	.000000000	8.0	.15996
.001	.000167345	9.0	.16300
.002	.000334437	10.0	.16559
.004	.000667861	12.5	.17070
.008	.00133168	15.0	.17449
.010	.00166208	17.5	.17739
.020	.00329912	20.0	.17970
.030	.00491145	25.0	.18313
.040	.00649944	30	.18557
.050	.00806342	35	.18739
.060	.00960373	40	.18883
.080	.0126147	60	.19228
.100	.0155351	80	.19410
.200	.0288698	100	.19523
.300	.0403211	125	.19617
.400	.0501766	150	.19683
.500	.0586905	175	.19732
.600	.0660824	200	.19771
.800	.0782135	250	.19828
1.000	.0877128	300	.19867
1.250	.0970400	400	.19915
1.500	.104422	500	.19942
1.750	.110459	600	.19958
2.000	.115529	800	.19975
2.500	.123675	1000	.19984
3.000	.130043	1500	.19992
3.500	.135235	2000	.19995
4.000	.139592	3000	.19998
4.500	.143327	4000	.19999
5.000	.146580	5000	.19999
6.000	.152000	8000	.19999
7.000	.156363	10000	.19999

Table D.17 Normal flux at τ_z=0 for a diffuse wall radiating in a cosine fashion into a semi-infinite medium

β	$F_\beta(0)$	β	$F_\beta(0)$
.000	.00000000	8.0	.93999
.001	.00133214	9.0	.94642
.002	.00266188	10.0	.95161
.004	.00531422	12.5	.96103
.008	.0105904	15.0	.96735
.010	.0132143	17.5	.97193
.020	.0261931	20.0	.97539
.030	.0389405	25.0	.98025
.040	.0514604	30	.98350
.050	.0637566	35	.98584
.060	.0758331	40	.98754
.080	.0993421	60	.99168
.100	.122017	80	.99375
.200	.223892	100	.99499
.300	.309028	125	.99595
.400	.380372	150	.99654
.500	.440419	175	.99693
.600	.491239	200	.99718
.800	.571649	250	.99747
1.000	.631596	300	.99763
1.250	.687354	400	.99783
1.500	.728898	500	.99798
1.750	.760896	600	.99813
2.000	.786235	800	.99838
2.500	.823727	1000	.99858
3.000	.850083	1500	.99894
3.500	.869602	2000	.99915
4.000	.884632	3000	.99940
4.500	.896559	4000	.99954
5.000	.906253	5000	.99962
6.000	.921052	8000	.99976
7.000	.931816	10000	.99980

Table D.18 Normal flux at $\tau_z=0$ and $\tau_y=0$ for a semi-infinite medium bounded by a strip illuminated by a uniform collimated flux of magnitude F_o from directions σ = 1, 2, and 5

	Q(0,0)		
τ_a	σ = 1.0	σ = 2.0	σ = 5.0
.00	1.00000	.50000	.20000
.01	.98191	.48479	.18825
.02	.96820	.47393	.18072
.05	.93488	.44888	.16500
.10	.89101	.41805	.14796
.20	.82328	.37404	.12685
.50	.68580	.29438	.09472
1.00	.54403	.22176	.06910
2.00	.38368	.14789	.04477
5.00	.19563	.07057	.02068
10.00	.10415	.03655	.01058
20.00	.05308	.01845	.00532
50.00	.02135	.00740	.00213
100.00	.01070	.00371	.00106
∞	.00000	.00000	.00000

Table D.19 Normal flux at $\tau_z=0$ for a semi-infinite medium bounded by a strip illuminated by a uniform collimated flux of magnitude F_0 from direction $\sigma=1$

	$Q(\tau_y,0)$				
τ_y/τ_a	$\tau_a=.01$	$\tau_a=.10$	$\tau_a=1.0$	$\tau_a=10.0$	$\tau_a=100.0$
0.00	.98191	.89101	.54403	.10415	.01070
.20	.98198	.89160	.54770	.10796	.01113
.40	.98221	.89341	.55917	.12111	.01272
.60	.98263	.89664	.58025	.15071	.01668
.80	.98328	.90181	.61574	.22129	.02951
1.00	.98410	.91164	.69184	.52654	.50267
1.02	-.01584	-.08684	-.29341	-.38536	-.18919
1.04	-.01576	-.08545	-.28301	-.33635	-.11503
1.06	-.01567	-.08426	-.27419	-.29991	-.08086
1.08	-.01558	-.08320	-.26638	-.27083	-.06166
1.10	-.01549	-.08224	-.25930	-.24673	-.04952
1.12	-.01540	-.08135	-.25279	-.22628	-.04119
1.14	-.01531	-.08051	-.24675	-.20866	-.03515
1.16	-.01522	-.07972	-.24111	-.19327	-.03057
1.18	-.01513	-.07897	-.23579	-.17972	-.02698
1.20	-.01504	-.07825	-.23077	-.16768	-.02410
1.40	-.01430	-.07227	-.19137	-.09550	-.01111
1.60	-.01373	-.06766	-.16362	-.06297	-.00684
1.80	-.01326	-.06387	-.14240	-.04521	-.00476
2.00	-.01288	-.06064	-.12546	-.03431	-.00356
3.00	-.01153	-.04926	-.07418	-.01319	-.00133
4.00	-.01063	-.04196	-.04874	-.00708	-.00071
5.00	-.00994	-.03668	-.03420	-.00443	-.00044

Table D.20 Normal flux at $\tau_z=0$ for a semi-infinite medium bounded by a strip illuminated by a uniform collimated flux of magnitude F_o from direction $\sigma=2$

	$Q(\tau_y,0)$				
τ_y/τ_a	$\tau_a=.01$	$\tau_a=.10$	$\tau_a=1.0$	$\tau_a=10.0$	$\tau_a=100.0$
0.00	.48479	.41805	.22176	.03655	.00371
.20	.48487	.41857	.22388	.03798	.00386
.40	.48509	.42019	.23064	.04296	.00441
.60	.48549	.42309	.24344	.05454	.00578
.80	.48611	.42779	.26636	.08418	.01026
1.00	.48696	.43702	.32394	.25922	.25091
1.02	-.01296	-.06148	-.16352	-.17789	-.07303
1.04	-.01286	-.06019	-.15526	-.14889	-.04212
1.06	-.01277	-.05908	-.14850	-.12905	-.02892
1.08	-.01267	-.05809	-.14268	-.11404	-.02179
1.10	-.01258	-.05719	-.13753	-.10210	-.01739
1.12	-.01249	-.05636	-.13290	-.09228	-.01441
1.14	-.01240	-.05559	-.12868	-.08402	-.01226
1.16	-.01231	-.05487	-.12479	-.07697	-.01064
1.18	-.01223	-.05418	-.12119	-.07088	-.00939
1.20	-.01215	-.05353	-.11784	-.06555	-.00838
1.40	-.01144	-.04816	-.09298	-.03534	-.00385
1.60	-.01088	-.04413	-.07683	-.02271	-.00237
1.80	-.01043	-.04089	-.06513	-.01609	-.00165
2.00	-.01005	-.03818	-.05617	-.01211	-.00123
3.00	-.00875	-.02908	-.03091	-.00459	-.00046
4.00	-.00789	-.02364	-.01942	-.00245	-.00024
5.00	-.00724	-.01993	-.01321	-.00153	-.00015

Table D.21 Normal flux at $\tau_z=0$ for a semi-infinite medium bounded by a strip illuminated by a uniform collimated flux of magnitude F_o from direction $\sigma=5$

	$Q(\tau_y,0)$				
τ_y/τ_a	$\tau_a=.01$	$\tau_a=.10$	$\tau_a=1.0$	$\tau_a=10.0$	$\tau_a=100.0$
0.00	.18825	.14796	.06910	.01058	.00106
.20	.18832	.14835	.06990	.01100	.00111
.40	.18854	.14956	.07247	.01249	.00127
.60	.18892	.15179	.07754	.01601	.00166
.80	.18951	.15551	.08755	.02534	.00295
1.00	.19036	.16342	.12238	.10266	.10026
1.02	-.00954	-.03521	-.06813	-.06079	-.02212
1.04	-.00945	-.03407	-.06269	-.04880	-.01243
1.06	-.00935	-.03311	-.05856	-.04142	-.00844
1.08	-.00926	-.03226	-.05521	-.03611	-.00633
1.10	-.00917	-.03150	-.05238	-.03202	-.00503
1.12	-.00909	-.03082	-.04993	-.02871	-.00416
1.14	-.00900	-.03018	-.04778	-.02597	-.00354
1.16	-.00892	-.02959	-.04586	-.02366	-.00307
1.18	-.00884	-.02851	-.04413	-.01996	-.00271
1.20	-.00876	-.02851	-.04256	-.01996	-.00241
1.40	-.00809	-.02438	-.03189	-.01047	-.00111
1.60	-.00756	-.02146	-.02567	-.00665	-.00068
1.80	-.00713	-.01923	-.02141	-.00468	-.00047
2.00	-.00678	-.01745	-.01825	-.00351	-.00035
3.00	-.00559	-.01201	-.00969	-.00132	-.00013
4.00	-.00484	-.00917	-.00596	-.00071	-.00007
5.00	-.00428	-.00741	-.00399	-.00044	-.00004

Table D.22 Normal flux at $\tau_z=0$ and $\tau_y=0$ for a semi-infinite medium bounded by a constant temperature strip

τ_a	F(0,0)	τ_a	F(0,0)	τ_a	F(0,0)
.00	1.00000	.20	.80972	10.0	.08402
.01	.98112	.50	.65932	20.0	.04235
.02	.96660	1.00	.50663	50.0	.01698
.05	.93094	2.00	.34108	100.0	.00850
.10	.88356	5.00	.16270	∞	.00000

Table D.23 Normal flux at $\tau_z=0$ for a semi-infinite medium bounded by a constant temperature strip

	$F(\tau_y,0)$				
τ_y/τ_a	$\tau_a=.01$	$\tau_a=.10$	$\tau_a=1.0$	$\tau_a=10.0$	$\tau_a=100.0$
0.00	.98112	.88356	.50663	.08402	.00850
.20	.98116	.88417	.51080	.08733	.00885
.40	.98129	.88606	.52387	.09886	.01012
.60	.98153	.88941	.54778	.12572	.01327
.80	.98196	.89479	.58772	.19405	.02354
1.00	.98330	.90486	.67054	.52117	.50210
1.02	-.01637	-.09307	-.31391	-.38389	-.16844
1.04	-.01615	-.09186	-.30271	-.33016	-.09721
1.06	-.01601	-.09082	-.29315	-.29039	-.06663
1.08	-.01587	-.08984	-.28463	-.25893	-.05016
1.10	-.01574	-.08890	-.27685	-.23315	-.03998
1.12	-.01565	-.08800	-.26968	-.21154	-.03311
1.14	-.01556	-.08714	-.26300	-.19313	-.02817
1.16	-.01547	-.08632	-.25673	-.17725	-.02445
1.18	-.01540	-.08553	-.25083	-.16342	-.02155
1.20	-.01533	-.08478	-.24522	-.15128	-.01923
1.40	-.01479	-.07852	-.20100	-.08163	-.00883
1.60	-.01439	-.07369	-.16973	-.05239	-.00544
1.80	-.01403	-.06968	-.14590	-.03706	-.00379
2.00	-.01370	-.06624	-.12700	-.02788	-.00283
3.00	-.01233	-.05394	-.07125	-.01056	-.00106
4.00	-.01139	-.04587	-.04496	-.00564	-.00056
5.00	-.01068	-.03996	-.03060	-.00353	-.00035

APPENDIX E

TABLES OF RESULTS FOR THE FINITE MEDIUM

Table E.1 The functions $X(\sqrt{1+\beta^2}/\sigma,\tau_0,\beta)$ and $Y(\sqrt{1+\beta^2}/\sigma,\tau_0,\beta)$ for various values of σ and τ_0 for $\beta=0$

	$X(\sqrt{1+\beta^2}/\sigma,\tau_0,\beta)$				$Y(\sqrt{1+\beta^2}/\sigma,\tau_0,\beta)$			
τ_0	σ=1.0	σ=2.0	σ=5.0	σ=10.0	σ=1.0	σ=2.0	σ=5.0	σ=10.0
.00	1.0000	1.0000	1.0000	1.0000	1.0000	1.0000	1.0000	1.0000
.01	1.0248	1.0246	1.0243	1.0237	1.0148	1.0048	.9755	.9285
.02	1.0453	1.0449	1.0437	1.0417	1.0254	1.0055	.9482	.8598
.03	1.0631	1.0623	1.0598	1.0561	1.0334	1.0037	.9197	.7953
.04	1.0791	1.0778	1.0738	1.0679	1.0396	1.0002	.8909	.7352
.05	1.0940	1.0920	1.0863	1.0780	1.0446	.9957	.8625	.6798
.06	1.1080	1.1053	1.0977	1.0867	1.0489	.9905	.8346	.6289
.07	1.1213	1.1178	1.1081	1.0944	1.0525	.9849	.8076	.5822
.08	1.1342	1.1298	1.1178	1.1012	1.0557	.9789	.7814	.5395
.09	1.1466	1.1412	1.1268	1.1073	1.0585	.9727	.7561	.5005
.10	1.1586	1.1522	1.1352	1.1128	1.0610	.9663	.7318	.4648
.12	1.1817	1.1731	1.1506	1.1222	1.0652	.9532	.6858	.4026
.14	1.2037	1.1926	1.1643	1.1300	1.0684	.9397	.6432	.3506
.16	1.2247	1.2110	1.1766	1.1364	1.0709	.9261	.6039	.3072
.18	1.2449	1.2283	1.1876	1.1419	1.0728	.9123	.5676	.2710
.20	1.2644	1.2447	1.1976	1.1465	1.0740	.8984	.5341	.2406
.25	1.3101	1.2821	1.2188	1.1555	1.0750	.8640	.4614	.1843
.30	1.3523	1.3155	1.2357	1.1620	1.0736	.8304	.4020	.1475
.35	1.3917	1.3454	1.2496	1.1669	1.0704	.7979	.3534	.1231
.40	1.4287	1.3725	1.2611	1.1709	1.0659	.7668	.3137	.1064
.45	1.4637	1.3972	1.2709	1.1742	1.0602	.7371	.2811	.0948
.50	1.4968	1.4199	1.2792	1.1770	1.0537	.7089	.2542	.0864

Table E.2 The functions $X(\sqrt{1+\beta^2}/\sigma,\tau_0,\beta)$ and $Y(\sqrt{1+\beta^2}/\sigma,\tau_0,\beta)$ for various values at σ and τ_0 for $\beta=0$

	$X(\sqrt{1+\beta^2}/\sigma,\tau_0,\beta)$				$Y(\sqrt{1+\beta^2}/\sigma,\tau_0,\beta)$			
τ_0	σ=1.0	σ=2.0	σ=5.0	σ=10.0	σ=1.0	σ=2.0	σ=5.0	σ=10.0
.55	1.5283	1.4407	1.2865	1.1795	1.0466	.6822	.2319	.0801
.60	1.5583	1.4600	1.2929	1.1817	1.0388	.6570	.2134	.0753
.65	1.5869	1.4778	1.2986	1.1838	1.0306	.6331	.1979	.0714
.70	1.6143	1.4944	1.3037	1.1856	1.0220	.6106	.1848	.0681
.75	1.6406	1.5099	1.3083	1.1873	1.0131	.5894	.1738	.0654
.80	1.6658	1.5244	1.3126	1.1889	1.0040	.5694	.1643	.0630
.85	1.6900	1.5379	1.3164	1.1904	.9947	.5505	.1561	.0608
.90	1.7133	1.5507	1.3200	1.1919	.9852	.5327	.1490	.0589
.95	1.7357	1.5627	1.3234	1.1932	.9757	.5159	.1428	.0572
1.00	1.7573	1.5740	1.3265	1.1944	.9660	.5000	.1373	.0555
1.20	1.8366	1.6135	1.3372	1.1989	.9271	.4448	.1204	.0501
1.40	1.9060	1.6457	1.3460	1.2025	.8885	.4006	.1086	.0459
1.60	1.9672	1.6727	1.3533	1.2056	.8510	.3647	.0997	.0424
1.80	2.0218	1.6956	1.3596	1.2083	.8150	.3351	.0925	.0395
2.00	2.0706	1.7153	1.3651	1.2107	.7807	.3105	.0864	.0370
2.20	2.1146	1.7326	1.3699	1.2127	.7482	.2897	.0812	.0348
2.40	2.1543	1.7478	1.3742	1.2146	.7175	.2719	.0767	.0329
2.60	2.1905	1.7614	1.3780	1.2162	.6885	.2564	.0727	.0312
2.80	2.2234	1.7735	1.3815	1.2177	.6613	.2429	.0691	.0297
3.00	2.2535	1.7846	1.3846	1.2191	.6357	.2309	.0659	.0283
∞	2.9078	2.0127	1.4503	1.2473	.0000	.0000	.0000	.0000

Table E.3 The functions $X(\sqrt{1+\beta^2}/\sigma,\tau_0,\beta)$ and $Y(\sqrt{1+\beta^2}/\sigma,\tau_0,\beta)$ for various values of σ and τ_0 for $\beta=.1$

	$X(\sqrt{1+\beta^2}/\sigma,\tau_0,\beta)$				$Y(\sqrt{1+\beta^2}/\sigma,\tau_0,\beta)$			
τ_0	σ=1.0	σ=2.0	σ=5.0	σ=10.0	σ=1.0	σ=2.0	σ=5.0	σ=10.0
.00	1.0000	1.0000	1.0000	1.0000	1.0000	1.0000	1.0000	1.0000
.01	1.0248	1.0246	1.0243	1.0237	1.0148	1.0048	.9755	.9285
.02	1.0453	1.0449	1.0436	1.0417	1.0254	1.0055	.9482	.8598
.03	1.0631	1.0622	1.0598	1.0560	1.0333	1.0036	.9196	.7952
.04	1.0791	1.0777	1.0738	1.0679	1.0395	1.0001	.8909	.7352
.05	1.0939	1.0919	1.0863	1.0779	1.0446	.9956	.8624	.6797
.06	1.1079	1.1052	1.0976	1.0866	1.0488	.9904	.8345	.6288
.07	1.1212	1.1177	1.1080	1.0943	1.0524	.9847	.8075	.5821
.08	1.1340	1.1296	1.1177	1.1011	1.0556	.9788	.7813	.5394
.09	1.1464	1.1411	1.1267	1.1072	1.0584	.9726	.7560	.5004
.10	1.1584	1.1521	1.1351	1.1127	1.0608	.9662	.7316	.4647
.12	1.1815	1.1729	1.1505	1.1221	1.0650	.9530	.6856	.4024
.14	1.2035	1.1924	1.1642	1.1298	1.0682	.9395	.6430	.3505
.16	1.2245	1.2107	1.1764	1.1363	1.0706	.9258	.6037	.3071
.18	1.2446	1.2280	1.1874	1.1417	1.0724	.9120	.5674	.2708
.20	1.2640	1.2443	1.1973	1.1463	1.0736	.8981	.5339	.2404
.25	1.3096	1.2817	1.2184	1.1553	1.0745	.8636	.4611	.1841
.30	1.3517	1.3149	1.2353	1.1617	1.0730	.8298	.4016	.1473
.35	1.3909	1.3447	1.2491	1.1666	1.0696	.7972	.3530	.1228
.40	1.4278	1.3717	1.2606	1.1706	1.0649	.7660	.3132	.1062
.45	1.4626	1.3963	1.2703	1.1739	1.0591	.7362	.2805	.0945
.50	1.4955	1.4188	1.2786	1.1767	1.0525	.7079	.2536	.0861

Table E.4 The functions $X(\sqrt{1+\beta^2}/\sigma,\tau_o,\beta)$ and $Y(\sqrt{1+\beta^2}/\sigma,\tau_o,\beta)$ for various values of σ and τ_o for $\beta=.1$

	$X(\sqrt{1+\beta^2}/\sigma,\tau_o,\beta)$				$Y(\sqrt{1+\beta^2}/\sigma,\tau_o,\beta)$			
τ_o	σ=1.0	σ=2.0	σ=5.0	σ=10.0	σ=1.0	σ=2.0	σ=5.0	σ=10.0
.55	1.5268	1.4395	1.2859	1.1791	1.0451	.6811	.2313	.0798
.60	1.5566	1.4586	1.2922	1.1814	1.0372	.6557	.2128	.0749
.65	1.5850	1.4764	1.2978	1.1834	1.0288	.6318	.1972	.0710
.70	1.6122	1.4928	1.3029	1.1852	1.0200	.6091	.1841	.0678
.75	1.6383	1.5082	1.3075	1.1869	1.0109	.5878	.1730	.0650
.80	1.6632	1.5225	1.3117	1.1885	1.0016	.5676	.1634	.0626
.85	1.6872	1.5360	1.3155	1.1900	.9920	.5486	.1552	.0604
.90	1.7103	1.5486	1.3190	1.1914	.9823	.5307	.1481	.0585
.95	1.7325	1.5604	1.3223	1.1927	.9725	.5138	.1418	.0567
1.00	1.7539	1.5716	1.3254	1.1939	.9627	.4978	.1363	.0551
1.20	1.8320	1.6105	1.3360	1.1983	.9228	.4421	.1193	.0497
1.40	1.9003	1.6422	1.3445	1.2018	.8832	.3974	.1075	.0454
1.60	1.9604	1.6685	1.3517	1.2049	.8447	.3611	.0984	.0418
1.80	2.0136	1.6908	1.3578	1.2075	.8076	.3311	.0911	.0389
2.00	2.0612	1.7100	1.3631	1.2097	.7722	.3061	.0849	.0363
2.20	2.1037	1.7266	1.3677	1.2117	.7385	.2849	.0796	.0341
2.40	2.1421	1.7413	1.3718	1.2135	.7067	.2668	.0750	.0321
2.60	2.1768	1.7542	1.3755	1.2151	.6766	.2508	.0709	.0304
2.80	2.2082	1.7658	1.3787	1.2165	.6483	.2369	.0672	.0288
3.00	2.2368	1.7762	1.3817	1.2177	.6215	.2245	.0639	.0274
∞	2.6476	1.9190	1.4227	1.2353	.0000	.0000	.0000	.0000

Table E.5 The functions $X(\sqrt{1+\beta^2}/\sigma,\tau_0,\beta)$ and $Y(\sqrt{1+\beta^2}/\sigma,\tau_0,\beta)$ for various values of σ and τ_0 for $\beta=.5$

	$X(\sqrt{1+\beta^2}/\sigma,\tau_0,\beta)$				$Y(\sqrt{1+\beta^2}/\sigma,\tau_0,\beta)$			
τ_0	σ=1.0	σ=2.0	σ=5.0	σ=10.0	σ=1.0	σ=2.0	σ=5.0	σ=10.0
.00	1.0000	1.0000	1.0000	1.0000	1.0000	1.0000	1.0000	1.0000
.01	1.0247	1.0246	1.0242	1.0237	1.0147	1.0048	.9754	.9284
.02	1.0448	1.0444	1.0432	1.0413	1.0249	1.0051	.9477	.8594
.03	1.0621	1.0613	1.0589	1.0552	1.0324	1.0027	.9187	.7944
.04	1.0777	1.0764	1.0725	1.0667	1.0381	.9988	.8896	.7340
.05	1.0921	1.0902	1.0847	1.0765	1.0428	.9938	.8608	.6782
.06	1.1057	1.1031	1.0957	1.0850	1.0466	.9883	.8326	.6271
.07	1.1187	1.1153	1.1058	1.0925	1.0499	.9823	.8053	.5802
.08	1.1311	1.1269	1.1152	1.0991	1.0527	.9760	.7788	.5373
.09	1.1431	1.1379	1.1239	1.1050	1.0551	.9694	.7533	.4981
.10	1.1548	1.1486	1.1321	1.1103	1.0572	.9627	.7286	.4623
.12	1.1770	1.1687	1.1469	1.1193	1.0605	.9488	.6821	.3997
.14	1.1981	1.1874	1.1600	1.1267	1.0629	.9345	.6390	.3475
.16	1.2182	1.2049	1.1717	1.1329	1.0644	.9200	.5991	.3038
.18	1.2373	1.2213	1.1821	1.1380	1.0652	.9053	.5622	.2672
.20	1.2557	1.2367	1.1915	1.1423	1.0653	.8906	.5281	.2365
.25	1.2985	1.2718	1.2112	1.1506	1.0634	.8538	.4540	.1796
.30	1.3376	1.3026	1.2268	1.1565	1.0590	.8177	.3933	.1423
.35	1.3737	1.3300	1.2394	1.1609	1.0525	.7827	.3435	.1174
.40	1.4072	1.3545	1.2497	1.1644	1.0445	.7490	.3027	.1003
.45	1.4385	1.3765	1.2583	1.1672	1.0353	.7167	.2690	.0883
.50	1.4677	1.3964	1.2655	1.1696	1.0250	.6860	.2412	.0796

Table E.6 The functions $X(\sqrt{1+\beta^2}/\sigma,\tau_0,\beta)$ and $Y(\sqrt{1+\beta^2}/\sigma,\tau_0,\beta)$ for various values of σ and τ_0 for $\beta=.5$

	$X(\sqrt{1+\beta^2}/\sigma,\tau_0,\beta)$				$Y(\sqrt{1+\beta^2}/\sigma,\tau_0,\beta)$			
τ_0	σ=1.0	σ=2.0	σ=5.0	σ=10.0	σ=1.0	σ=2.0	σ=5.0	σ=10.0
.55	1.4952	1.4145	1.2717	1.1717	1.0140	.6567	.2180	.0730
.60	1.5210	1.4310	1.2771	1.1735	1.0022	.6289	.1987	.0679
.65	1.5454	1.4460	1.2817	1.1751	.9899	.6025	.1824	.0637
.70	1.5684	1.4598	1.2858	1.1765	.9771	.5775	.1685	.0602
.75	1.5901	1.4725	1.2894	1.1779	.9639	.5538	.1567	.0572
.80	1.6107	1.4841	1.2927	1.1791	.9504	.5313	.1466	.0546
.85	1.6301	1.4949	1.2956	1.1802	.9367	.5099	.1377	.0522
.90	1.6486	1.5048	1.2983	1.1812	.9227	.4897	.1300	.0500
.95	1.6661	1.5140	1.3007	1.1821	.9086	.4705	.1232	.0481
1.00	1.6827	1.5225	1.3029	1.1830	.8943	.4523	.1171	.0462
1.20	1.7412	1.5508	1.3102	1.1859	.8368	.3884	.0982	.0401
1.40	1.7890	1.5722	1.3156	1.1881	.7795	.3361	.0847	.0351
1.60	1.8282	1.5886	1.3197	1.1898	.7236	.2930	.0742	.0310
1.80	1.8605	1.6013	1.3229	1.1912	.6697	.2571	.0656	.0276
2.00	1.8871	1.6113	1.3255	1.1923	.6183	.2268	.0583	.0246
2.20	1.9090	1.6192	1.3275	1.1931	.5696	.2010	.0521	.0220
2.40	1.9271	1.6255	1.3292	1.1938	.5238	.1788	.0467	.0197
2.60	1.9420	1.6305	1.3305	1.1944	.4808	.1596	.0419	.0177
2.80	1.9544	1.6346	1.3316	1.1948	.4408	.1428	.0377	.0159
3.00	1.9645	1.6378	1.3324	1.1952	.4035	.1280	.0339	.0143
∞	2.0119	1.6520	1.3362	1.1968	.0000	.0000	.0000	.0000

Table E.7 The functions $X(\sqrt{1+\beta^2}/\sigma,\tau_0,\beta)$ and $Y(\sqrt{1+\beta^2}/\sigma,\tau_0,\beta)$ for various values of σ and τ_0 for $\beta=1$

	$X(\sqrt{1+\beta^2}/\sigma,\tau_0,\beta)$				$Y(\sqrt{1+\beta^2}/\sigma,\tau_0,\beta)$			
τ_0	σ=1.0	σ=2.0	σ=5.0	σ=10.0	σ=1.0	σ=2.0	σ=5.0	σ=10.0
.00	1.0000	1.0000	1.0000	1.0000	1.0000	1.0000	1.0000	1.0000
.01	1.0244	1.0243	1.0240	1.0234	1.0145	1.0045	.9751	.9281
.02	1.0436	1.0432	1.0420	1.0402	1.0237	1.0038	.9465	.8582
.03	1.0598	1.0591	1.0568	1.0533	1.0301	1.0004	.9165	.7923
.04	1.0745	1.0732	1.0696	1.0641	1.0349	.9955	.8865	.7312
.05	1.0880	1.0862	1.0809	1.0733	1.0386	.9898	.8570	.6748
.06	1.1007	1.0982	1.0913	1.0812	1.0416	.9834	.8281	.6232
.07	1.1129	1.1109	1.1007	1.0882	1.0441	.9767	.8002	.5759
.08	1.1245	1.1204	1.1095	1.0943	1.0460	.9696	.7731	.5326
.09	1.1356	1.1307	1.1176	1.0998	1.0476	.9622	.7470	.4930
.10	1.1463	1.1405	1.1251	1.1046	1.0488	.9547	.7217	.4568
.12	1.1666	1.1588	1.1386	1.1129	1.0502	.9391	.6739	.3934
.14	1.1856	1.1757	1.1504	1.1195	1.0504	.9229	.6294	.3404
.16	1.2035	1.1913	1.1607	1.1249	1.0498	.9065	.5882	.2960
.18	1.2204	1.2057	1.1699	1.1293	1.0483	.8898	.5501	.2587
.20	1.2364	1.2192	1.1780	1.1331	1.0461	.8731	.5148	.2275
.25	1.2730	1.2491	1.1947	1.1400	1.0381	.8312	.4377	.1692
.30	1.3057	1.2748	1.2075	1.1447	1.0272	.7901	.3744	.1309
.35	1.3350	1.2969	1.2175	1.1481	1.0141	.7500	.3224	.1052
.40	1.3615	1.3162	1.2255	1.1506	.9992	.7114	.2795	.0875
.45	1.3856	1.3330	1.2318	1.1526	.9830	.6743	.2440	.0750
.50	1.4075	1.3477	1.2370	1.1541	.9657	.6388	.2145	.0658

Table E.8 The functions $X(\sqrt{1+\beta^2}/\sigma,\tau_0,\beta)$ and $Y(\sqrt{1+\beta^2}/\sigma,\tau_0,\beta)$ for various values of σ and τ_0 for $\beta=1$

	$X(\sqrt{1+\beta^2}/\sigma,\tau_0,\beta)$				$Y(\sqrt{1+\beta^2}/\sigma,\tau_0,\beta)$			
τ_0	σ=1.0	σ=2.0	σ=5.0	σ=10.0	σ=1.0	σ=2.0	σ=5.0	σ=10.0
.55	1.4275	1.3607	1.2412	1.1554	.9475	.6049	.1899	.0588
.60	1.4457	1.3722	1.2447	1.1565	.9285	.5726	.1693	.0533
.65	1.4625	1.3823	1.2476	1.1575	.9090	.5419	.1519	.0488
.70	1.4778	1.3913	1.2500	1.1583	.8891	.5128	.1370	.0451
.75	1.4918	1.3993	1.2521	1.1590	.8688	.4852	.1244	.0418
.80	1.5047	1.4063	1.2539	1.1596	.8484	.4590	.1134	.0390
.85	1.5165	1.4126	1.2554	1.1601	.8278	.4342	.1040	.0365
.90	1.5273	1.4182	1.2568	1.1606	.8071	.4108	.0957	.0342
.95	1.5373	1.4232	1.2579	1.1610	.7864	.3886	.0884	.0321
1.00	1.5464	1.4277	1.2589	1.1613	.7657	.3676	.0819	.0302
1.20	1.5762	1.4413	1.2619	1.1625	.6847	.2944	.0621	.0239
1.40	1.5974	1.4499	1.2637	1.1632	.6075	.2361	.0485	.0191
1.60	1.6125	1.4556	1.2648	1.1636	.5356	.1896	.0385	.0154
1.80	1.6232	1.4592	1.2656	1.1639	.4697	.1525	.0309	.0124
2.00	1.6308	1.4616	1.2660	1.1641	.4099	.1229	.0249	.0101
2.20	1.6362	1.4631	1.2664	1.1642	.3563	.0992	.0202	.0082
2.40	1.6400	1.4642	1.2666	1.1643	.3086	.0801	.0164	.0066
2.60	1.6427	1.4648	1.2667	1.1644	.2665	.0649	.0133	.0054
2.80	1.6446	1.4653	1.2668	1.1644	.2294	.0526	.0109	.0044
3.00	1.6459	1.4656	1.2669	1.1644	.1970	.0427	.0088	.0036
∞	1.6489	1.4662	1.2670	1.1645	.0000	.0000	.0000	.0000

Table E.9 The functions $X(\sqrt{1+\beta^2}/\sigma,\tau_0,\beta)$ and $Y(\sqrt{1+\beta^2}/\sigma,\tau_0,\beta)$ for various values of σ and τ_0 for $\beta=2$

	$X(\sqrt{1+\beta^2}/\sigma,\tau_0,\beta)$				$Y(\sqrt{1+\beta^2}/\sigma,\tau_0,\beta)$			
τ_0	σ=1.0	σ=2.0	σ=5.0	σ=10.0	σ=1.0	σ=2.0	σ=5.0	σ=10.0
.00	1.0000	1.0000	1.0000	1.0000	1.0000	1.0000	1.0000	1.0000
.01	1.0233	1.0232	1.0229	1.0224	1.0134	1.0034	.9740	.9270
.02	1.0403	1.0399	1.0389	1.0373	1.0204	1.0006	.9433	.8552
.03	1.0546	1.0539	1.0519	1.0488	1.0248	.9952	.9115	.7876
.04	1.0674	1.0663	1.0631	1.0582	1.0278	.9887	.8800	.7252
.05	1.0793	1.0776	1.0730	1.0662	1.0299	.9813	.8490	.6678
.06	1.0903	1.0881	1.0819	1.0731	1.0311	.9733	.8188	.6151
.07	1.1006	1.0978	1.0900	1.0790	1.0318	.9648	.7895	.5668
.08	1.1103	1.1068	1.0973	1.0841	1.0319	.9560	.7610	.5225
.09	1.1194	1.1152	1.1039	1.0886	1.0314	.9468	.7334	.4820
.10	1.1281	1.1232	1.1100	1.0925	1.0306	.9374	.7067	.4448
.12	1.1442	1.1377	1.1206	1.0989	1.0278	.9180	.6561	.3797
.14	1.1589	1.1507	1.1297	1.1039	1.0237	.8980	.6089	.3251
.16	1.1723	1.1623	1.1374	1.1079	1.0186	.8777	.5651	.2793
.18	1.1847	1.1729	1.1440	1.1111	1.0126	.8572	.5245	.2409
.20	1.1961	1.1825	1.1497	1.1136	1.0059	.8366	.4870	.2086
.25	1.2211	1.2029	1.1609	1.1181	.9865	.7855	.4049	.1484
.30	1.2421	1.2192	1.1689	1.1208	.9641	.7355	.3374	.1088
.35	1.2598	1.2324	1.1746	1.1226	.9398	.6871	.2819	.0823
.40	1.2748	1.2432	1.1788	1.1238	.9139	.6407	.2363	.0641
.45	1.2875	1.2519	1.1819	1.1246	.8870	.5965	.1988	.0513
.50	1.2984	1.2591	1.1842	1.1251	.8594	.5546	.1678	.0421

Table E.10 The functions $X(\sqrt{1+\beta^2}/\sigma,\tau_o,\beta)$ and $Y(\sqrt{1+\beta^2}/\sigma,\tau_o,\beta)$ for various values of σ and τ_o for $\beta=2$

	$X(\sqrt{1+\beta^2}/\sigma,\tau_o,\beta)$				$Y(\sqrt{1+\beta^2}/\sigma,\tau_o,\beta)$			
τ_o	σ=1.0	σ=2.0	σ=5.0	σ=10.0	σ=1.0	σ=2.0	σ=5.0	σ=10.0
.55	1.3077	1.2650	1.1859	1.1256	.8315	.5150	.1422	.0352
.60	1.3156	1.2698	1.1872	1.1259	.8033	.4777	.1209	.0299
.65	1.3224	1.2738	1.1881	1.1261	.7753	.4427	.1032	.0257
.70	1.3283	1.2770	1.1889	1.1263	.7474	.4099	.0884	.0224
.75	1.3333	1.2797	1.1894	1.1265	.7198	.3792	.0760	.0196
.80	1.3376	1.2820	1.1899	1.1266	.6926	.3505	.0656	.0172
.85	1.3413	1.2838	1.1902	1.1267	.6660	.3238	.0568	.0152
.90	1.3445	1.2853	1.1905	1.1267	.6399	.2989	.0494	.0135
.95	1.3472	1.2866	1.1907	1.1268	.6144	.2758	.0430	.0120
1.00	1.3496	1.2876	1.1908	1.1268	.5896	.2544	.0376	.0107
1.20	1.3561	1.2903	1.1912	1.1269	.4973	.1830	.0225	.0069
1.40	1.3597	1.2915	1.1913	1.1270	.4167	.1309	.0139	.0044
1.60	1.3617	1.2921	1.1914	1.1270	.3474	.0931	.0088	.0029
1.80	1.3628	1.2923	1.1914	1.1270	.2886	.0659	.0057	.0019
2.00	1.3634	1.2925	1.1914	1.1270	.2390	.0465	.0037	.0012
2.20	1.3637	1.2925	1.1914	1.1270	.1975	.0327	.0024	.0008
2.40	1.3639	1.2925	1.1914	1.1270	.1629	.0229	.0016	.0005
2.60	1.3640	1.2926	1.1914	1.1270	.1341	.0160	.0010	.0003
2.80	1.3640	1.2926	1.1914	1.1270	.1103	.0112	.0007	.0002
3.00	1.3640	1.2926	1.1914	1.1270	.0907	.0078	.0004	.0001
∞	1.3641	1.2926	1.1914	1.1270	.0000	.0000	.0000	.0000

Table E.11 The functions $X(\sqrt{1+\beta^2}/\sigma,\tau_o,\beta)$ and $Y(\sqrt{1+\beta^2}/\sigma,\tau_o,\beta)$ for various values of σ and τ_o for $\beta=5$

	$X(\sqrt{1+\beta^2}/\sigma,\tau_o,\beta)$				$Y(\sqrt{1+\beta^2}/\sigma,\tau_o,\beta)$			
τ_o	σ=1.0	σ=2.0	σ=5.0	σ=10.0	σ=1.0	σ=2.0	σ=5.0	σ=10.0
.00	1.0000	1.0000	1.0000	1.0000	1.0000	1.0000	1.0000	1.0000
.01	1.0200	1.0199	1.0197	1.0192	1.0100	1.0001	.9708	.9238
.02	1.0332	1.0329	1.0321	1.0308	1.0133	.9935	.9365	.8486
.03	1.0441	1.0436	1.0420	1.0396	1.0143	.9849	.9017	.7784
.04	1.0535	1.0526	1.0502	1.0464	1.0139	.9750	.8671	.7135
.05	1.0617	1.0604	1.0570	1.0520	1.0123	.9641	.8331	.6537
.06	1.0689	1.0673	1.0629	1.0565	1.0098	.9526	.7999	.5987
.07	1.0754	1.0735	1.0680	1.0602	1.0067	.9406	.7676	.5482
.08	1.0813	1.0789	1.0724	1.0633	1.0029	.9282	.7363	.5019
.09	1.0867	1.0839	1.0762	1.0658	.9987	.9155	.7059	.4596
.10	1.0915	1.0883	1.0796	1.0680	.9941	.9026	.6767	.4208
.12	1.1001	1.0960	1.0852	1.0713	.9838	.8765	.6211	.3529
.14	1.1073	1.1024	1.0896	1.0737	.9723	.8501	.5697	.2960
.16	1.1134	1.1077	1.0931	1.0754	.9601	.8236	.5220	.2485
.18	1.1187	1.1121	1.0958	1.0767	.9471	.7973	.4781	.2088
.20	1.1232	1.1159	1.0980	1.0776	.9337	.7713	.4376	.1756
.25	1.1320	1.1230	1.1018	1.0790	.8987	.7080	.3500	.1145
.30	1.1381	1.1277	1.1040	1.0797	.8625	.6481	.2793	.0752
.35	1.1424	1.1309	1.1053	1.0800	.8261	.5919	.2225	.0499
.40	1.1455	1.1330	1.1060	1.0801	.7900	.5396	.1769	.0334
.45	1.1477	1.1345	1.1065	1.0802	.7547	.4913	.1406	.0226
.50	1.1492	1.1355	1.1068	1.0803	.7203	.4468	.1115	.0155
∞	1.1534	1.1377	1.1072	1.0803	.0000	.0000	.0000	.0000

Table E.12 The functions $X(\sqrt{1+\beta^2}/\sigma,\tau_o,\beta)$ and $Y(\sqrt{1+\beta^2}/\sigma,\tau_o,\beta)$ for various values of σ and τ_o for $\beta=10$

	$X(\sqrt{1+\beta^2}/\sigma,\tau_o,\beta)$				$Y(\sqrt{1+\beta^2}/\sigma,\tau_o,\beta)$			
τ_o	σ=1.0	σ=2.0	σ=5.0	σ=10.0	σ=1.0	σ=2.0	σ=5.0	σ=10.0
.00	1.0000	1.0000	1.0000	1.0000	1.0000	1.0000	1.0000	1.0000
.01	1.0168	1.0168	1.0165	1.0162	1.0068	.9969	.9676	.9208
.02	1.0270	1.0268	1.0262	1.0251	1.0071	.9874	.9305	.8430
.03	1.0348	1.0344	1.0332	1.0314	1.0050	.9757	.8929	.7703
.04	1.0410	1.0404	1.0386	1.0359	1.0014	.9627	.8556	.7030
.05	1.0461	1.0452	1.0429	1.0394	.9967	.9489	.8190	.6412
.06	1.0503	1.0493	1.0463	1.0420	.9913	.9346	.7834	.5844
.07	1.0540	1.0527	1.0491	1.0440	.9852	.9199	.7490	.5324
.08	1.0570	1.0555	1.0514	1.0456	.9787	.9049	.7156	.4848
.09	1.0597	1.0579	1.0533	1.0469	.9718	.8898	.6835	.4414
.10	1.0619	1.0600	1.0549	1.0479	.9646	.8747	.6526	.4017
.12	1.0656	1.0633	1.0572	1.0493	.9495	.8443	.5943	.3325
.14	1.0683	1.0657	1.0589	1.0502	.9338	.8143	.5407	.2750
.16	1.0704	1.0675	1.0601	1.0507	.9177	.7847	.4915	.2273
.18	1.0720	1.0689	1.0609	1.0511	.9014	.7558	.4465	.1877
.20	1.0733	1.0699	1.0615	1.0513	.8850	.7276	.4054	.1550
.25	1.0753	1.0715	1.0623	1.0516	.8443	.6607	.3179	.0959
.30	1.0764	1.0724	1.0627	1.0517	.8045	.5992	.2487	.0592
.35	1.0769	1.0728	1.0629	1.0518	.7660	.5429	.1944	.0365
.40	1.0773	1.0730	1.0630	1.0518	.7291	.4916	.1518	.0224
.45	1.0774	1.0731	1.0630	1.0518	.6938	.4451	.1184	.0138
.50	1.0775	1.0732	1.0630	1.0518	.6601	.4029	.0924	.0085
∞	1.0777	1.0733	1.0630	1.0518	.0000	.0000	.0000	.0000

Table E.13 The functions $X(\sqrt{1+\beta^2}/\sigma,\tau_o,\beta)$ and $Y(\sqrt{1+\beta^2}/\sigma,\tau_o,\beta)$ for various values of σ and τ_o for $\beta=40$

	$X(\sqrt{1+\beta^2}/\sigma,\tau_o,\beta)$				$Y(\sqrt{1+\beta^2}/\sigma,\tau_o,\beta)$			
τ_o	σ=1.0	σ=2.0	σ=5.0	σ=10.0	σ=1.0	σ=2.0	σ=5.0	σ=10.0
.000	1.0000	1.0000	1.0000	1.0000	1.0000	1.0000	1.0000	1.0000
.005	1.0068	1.0068	1.0067	1.0066	1.0018	.9968	.9820	.9578
.010	1.0103	1.0102	1.0101	1.0099	1.0003	.9904	.9612	.9145
.015	1.0126	1.0125	1.0123	1.0120	.9976	.9828	.9398	.8722
.020	1.0142	1.0141	1.0139	1.0134	.9943	.9747	.9183	.8313
.025	1.0155	1.0153	1.0150	1.0144	.9906	.9663	.8968	.7920
.030	1.0164	1.0162	1.0158	1.0151	.9866	.9576	.8756	.7543
.035	1.0171	1.0169	1.0164	1.0156	.9824	.9488	.8547	.7182
.040	1.0176	1.0174	1.0169	1.0160	.9781	.9399	.8341	.6837
.045	1.0180	1.0178	1.0172	1.0163	.9736	.9310	.8140	.6507
.050	1.0183	1.0181	1.0175	1.0165	.9691	.9220	.7942	.6193
.055	1.0186	1.0183	1.0177	1.0167	.9645	.9131	.7748	.5894
.060	1.0188	1.0185	1.0178	1.0168	.9599	.9042	.7559	.5608
.065	1.0189	1.0187	1.0180	1.0169	.9553	.8954	.7374	.5336
.070	1.0190	1.0188	1.0180	1.0169	.9507	.8866	.7193	.5077
.075	1.0191	1.0189	1.0181	1.0170	.9460	.8779	.7017	.4831
.080	1.0192	1.0189	1.0182	1.0170	.9414	.8693	.6844	.4596
.085	1.0193	1.0190	1.0182	1.0171	.9367	.8607	.6676	.4372
.090	1.0193	1.0190	1.0182	1.0171	.9321	.8522	.6511	.4160
.095	1.0194	1.0191	1.0183	1.0171	.9275	.8437	.6351	.3957
.100	1.0194	1.0191	1.0183	1.0171	.9229	.8354	.6195	.3764
∞	1.0195	1.0192	1.0184	1.0172	.0000	.0000	.0000	.0000

Table E.14 The functions $X(\sqrt{1+\beta^2}/\sigma,\tau_o,\beta)$ and $Y(\sqrt{1+\beta^2}/\sigma,\tau_o,\beta)$ for various values of σ and τ_o for β=100

	$X(\sqrt{1+\beta^2}/\sigma,\tau_o,\beta)$				$Y(\sqrt{1+\beta^2}/\sigma,\tau_o,\beta)$			
τ_o	σ=1.0	σ=2.0	σ=5.0	σ=10.0	σ=1.0	σ=2.0	σ=5.0	σ=10.0
.000	1.0000	1.0000	1.0000	1.0000	1.0000	1.0000	1.0000	1.0000
.001	1.0017	1.0017	1.0017	1.0017	1.0007	.9997	.9967	.9917
.002	1.0027	1.0027	1.0027	1.0027	1.0007	.9987	.9927	.9828
.003	1.0035	1.0034	1.0034	1.0034	1.0005	.9975	.9885	.9738
.004	1.0041	1.0041	1.0040	1.0040	1.0001	.9961	.9842	.9648
.005	1.0046	1.0046	1.0045	1.0045	.9996	.9946	.9798	.9557
.006	1.0050	1.0050	1.0050	1.0049	.9990	.9930	.9754	.9466
.007	1.0054	1.0053	1.0053	1.0052	.9984	.9914	.9708	.9375
.008	1.0057	1.0056	1.0056	1.0055	.9977	.9897	.9663	.9285
.009	1.0059	1.0059	1.0058	1.0058	.9969	.9880	.9617	.9195
.010	1.0061	1.0061	1.0061	1.0060	.9962	.9863	.9572	.9106
.012	1.0065	1.0065	1.0064	1.0063	.9945	.9827	.9480	.8929
.014	1.0068	1.0068	1.0067	1.0065	.9928	.9791	.9389	.8755
.016	1.0070	1.0070	1.0069	1.0067	.9911	.9754	.9297	.8584
.018	1.0072	1.0071	1.0070	1.0069	.9893	.9716	.9207	.8416
.020	1.0073	1.0072	1.0071	1.0070	.9874	.9679	.9116	.8250
.022	1.0074	1.0073	1.0072	1.0071	.9855	.9641	.9026	.8088
.024	1.0075	1.0074	1.0073	1.0071	.9836	.9604	.8937	.7928
.026	1.0075	1.0075	1.0074	1.0072	.9817	.9566	.8849	.7772
.028	1.0076	1.0075	1.0074	1.0072	.9798	.9528	.8762	.7619
.030	1.0076	1.0076	1.0074	1.0072	.9779	.9490	.8675	.7468
∞	1.0078	1.0077	1.0076	1.0074	.0000	.0000	.0000	.0000

Table E.15 Emissive power at $\tau_z=0$ and $\tau_z=\tau_o$ for a diffuse wall radiating in a cosine fashion into a finite medium

	$\phi_\beta(0,\tau_o)$				$\phi_\beta(\tau_o,\tau_o)$			
τ_o	β=0.0	β=.10	β=.50	β=1.0	β=0.0	β=.10	β=.50	β=1.0
.00	.50000	.50000	.50000	.50000	.50000	.50000	.50000	.50000
.01	.51216	.51216	.51212	.51196	.48783	.48781	.48728	.48593
.02	.52187	.52186	.52163	.52099	.47812	.47808	.47715	.47478
.03	.53007	.53005	.52959	.52844	.46992	.46986	.46857	.46518
.04	.53729	.53726	.53659	.53496	.46270	.46263	.46096	.45651
.05	.54383	.54380	.54292	.54087	.45616	.45607	.45399	.44845
.06	.54989	.54984	.54879	.54632	.45010	.44999	.44750	.44084
.07	.55557	.55551	.55428	.55141	.44442	.44429	.44138	.43360
.08	.56095	.56088	.55947	.55618	.43904	.43890	.43555	.42667
.09	.56607	.56600	.56440	.56068	.43392	.43376	.42998	.42001
.10	.57097	.57089	.56911	.56494	.42902	.42884	.42464	.41360
.12	.58019	.58009	.57793	.57283	.41980	.41958	.41454	.40142
.14	.58876	.58864	.58607	.57999	.41123	.41097	.40512	.38999
.16	.59677	.59663	.59362	.58654	.40322	.40293	.39627	.37920
.18	.60430	.60414	.60068	.59255	.39570	.39537	.38793	.36898
.20	.61139	.61121	.60729	.59811	.38860	.38823	.38003	.35925
.25	.62757	.62734	.62220	.61034	.37242	.37197	.36190	.33676
.30	.64193	.64164	.63524	.62066	.35806	.35753	.34565	.31644
.35	.65485	.65450	.64680	.62949	.34514	.34452	.33090	.29789
.40	.66661	.66619	.65716	.63711	.33338	.33269	.31737	.28084
.45	.67738	.67690	.66651	.64374	.32261	.32183	.30487	.26507
.50	.68733	.68678	.67500	.64953	.31266	.31181	.29326	.25043

Table E.16 Emissive power at $\tau_z=0$ and $\tau_z=\tau_o$ for a diffuse wall radiating in a cosine fashion into a finite medium

	$\phi_\beta(0,\tau_o)$				$\phi_\beta(\tau_o,\tau_o)$			
τ_o	β=0.0	β=.10	β=.50	β=1.0	β=0.0	β=.10	β=.50	β=1.0
.55	.69656	.69594	.68276	.65462	.30343	.30251	.28242	.23680
.60	.70516	.70447	.68986	.65911	.29483	.29383	.27225	.22406
.65	.71321	.71245	.69640	.66308	.28678	.28571	.26268	.21213
.70	.72077	.71993	.70244	.66659	.27922	.27808	.25365	.20094
.75	.72788	.72697	.70802	.66971	.27211	.27090	.24511	.19042
.80	.73460	.73361	.71320	.67249	.26539	.26411	.23701	.18052
.85	.74095	.73989	.71800	.67497	.25904	.25769	.22931	.17120
.90	.74697	.74584	.72248	.67719	.25302	.25160	.22198	.16240
.95	.75270	.75149	.72665	.67916	.24729	.24581	.21499	.15410
1.00	.75814	.75685	.73055	.68093	.24185	.24030	.20831	.14626
1.20	.77756	.77595	.74380	.68636	.22243	.22063	.18431	.11890
1.40	.79392	.79198	.75409	.68990	.20607	.20402	.16387	.09736
1.60	.80794	.80567	.76218	.69221	.19205	.18977	.14623	.07903
1.80	.82011	.81750	.76859	.69374	.17988	.17737	.13085	.06454
2.00	.83079	.82784	.77372	.69476	.16921	.16647	.11735	.05274
2.20	.84024	.83695	.77783	.69543	.15975	.15679	.10543	.04312
2.40	.84868	.84504	.78114	.69588	.15131	.14814	.09485	.03526
2.60	.85626	.85226	.78382	.69618	.14373	.14036	.08542	.02885
2.80	.86310	.85876	.78599	.69638	.13689	.13330	.07700	.02360
3.00	.86932	.86463	.78775	.69651	.13067	.12688	.06945	.01931
∞	1.00000	.94620	.79555	.69675	.00000	.00000	.00000	.00000

Table E.17 Emissive power at $\tau_z=0$ and $\tau_z=\tau_0$ for a diffuse wall radiating in a cosine fashion into a finite medium

	$\phi_\beta(0,\tau_0)$			$\phi_\beta(\tau_0,\tau_0)$		
τ_0	β=2.0	β=5.0	β=10.0	β=2.0	β=5.0	β=10.0
.00	.50000	.50000	.50000	.50000	.50000	.50000
.01	.51140	.50969	.50801	.48236	.47001	.44838
.02	.51933	.51566	.51233	.46819	.44439	.40406
.03	.52579	.52031	.51530	.45551	.42081	.36458
.04	.53142	.52409	.51745	.44371	.39884	.32920
.05	.53645	.52723	.51905	.43256	.37826	.29737
.06	.54101	.52988	.52026	.42193	.35890	.26870
.07	.54518	.53214	.52119	.41176	.34065	.24284
.08	.54900	.53409	.52192	.40200	.32342	.21951
.09	.55253	.53577	.52248	.39260	.30712	.19844
.10	.55580	.53724	.52292	.38353	.29170	.17942
.12	.56167	.53963	.52354	.36630	.26324	.14670
.14	.56678	.54148	.52394	.35013	.23766	.11997
.16	.57128	.54292	.52418	.33488	.21464	.09813
.18	.57527	.54405	.52434	.32046	.19389	.08028
.20	.57882	.54493	.52444	.30679	.17518	.06568
.25	.58614	.54642	.52457	.27551	.13603	.03978
.30	.59176	.54726	.52461	.24781	.10569	.02410
.35	.59613	.54774	.52462	.22314	.08216	.01460
.40	.59956	.54802	.52463	.20109	.06388	.00885
.45	.60227	.54818	.52463	.18134	.04968	.00536
.50	.60442	.54827	.52463	.16361	.03865	.00325
∞	.61315	.54840	.52465	.00000	.00000	.00000

Table E.18 Emissive power at $\tau_z=0$ and $\tau_z=\tau_o$ for a diffuse wall radiating in a cosine fashion into a finite medium

	$\phi_\beta(0,\tau_o)$		$\phi_\beta(\tau_o,\tau_o)$	
τ_o	β=40.0	β=100.0	β=40.0	β=100.0
.000	.50000	.50000	.50000	.50000
.001	.50106	.50081	.47977	.45201
.002	.50175	.50125	.46064	.40882
.003	.50229	.50155	.44235	.36981
.004	.50274	.50177	.42483	.33455
.005	.50314	.50193	.40802	.30266
.006	.50346	.50205	.39190	.27381
.007	.50375	.50214	.37643	.24773
.008	.50401	.50222	.36158	.22413
.009	.50423	.50227	.34732	.20278
.010	.50443	.50232	.33364	.18346
.012	.50476	.50238	.30788	.15018
.014	.50502	.50242	.28412	.12294
.016	.50523	.50244	.26220	.10065
.018	.50541	.50245	.24199	.08239
.020	.50555	.50246	.22333	.06745
.022	.50566	.50247	.20612	.05522
.024	.50576	.50248	.19024	.04521
.026	.50584	.50248	.17558	.03701
.028	.50590	.50248	.16206	.03030
.030	.50593	.50248	.14958	.02480
∞	.50620	.50250	.00000	.00000

Table E.19 Normal flux at $\tau_z=0$ and $\tau_z=\tau_o$ for a finite medium illuminated by a collimated flux of cosine magnitude for $\beta=0$

	$\mathcal{F}_A(0,\sigma,\tau_o)$				$\mathcal{F}_A(\tau_o,\sigma,\tau_o)$			
τ_o	σ=1.0	σ=2.0	σ=5.0	σ=10.0	σ=1.0	σ=2.0	σ=5.0	σ=10.0
.00	1.00000	.50000	.20000	.10000	1.00000	.50000	.20000	.10000
.01	.99502	.49504	.19512	.09523	.99502	.49504	.19512	.09523
.02	.99009	.49019	.19047	.09092	.99009	.49019	.19047	.09092
.03	.98521	.48543	.18605	.08700	.98521	.48543	.18605	.08700
.04	.98038	.48076	.18182	.08343	.98038	.48076	.18182	.08343
.05	.97559	.47617	.17780	.08018	.97559	.47617	.17780	.08018
.06	.97085	.47167	.17395	.07722	.97085	.47167	.17395	.07722
.07	.96615	.46725	.17028	.07451	.96615	.46725	.17028	.07451
.08	.96149	.46292	.16677	.07203	.96149	.46292	.16677	.07203
.09	.95688	.45866	.16341	.06977	.95688	.45866	.16341	.06977
.10	.95231	.45447	.16020	.06768	.95231	.45447	.16020	.06768
.12	.94328	.44633	.15419	.06401	.94328	.44633	.15419	.06401
.14	.93442	.43846	.14867	.06089	.93442	.43846	.14867	.06089
.16	.92571	.43086	.14359	.05821	.92571	.43086	.14359	.05821
.18	.91714	.42352	.13892	.05591	.91714	.42352	.13892	.05591
.20	.90872	.41642	.13460	.05390	.90872	.41642	.13460	.05390
.25	.88828	.39966	.12515	.04990	.88828	.39966	.12515	.04990
.30	.86867	.38419	.11728	.04689	.86867	.38419	.11728	.04689
.35	.84983	.36988	.11065	.04452	.84983	.36988	.11065	.04452
.40	.83171	.35661	.10501	.04258	.83171	.35661	.10501	.04258
.45	.81428	.34428	.10014	.04094	.81428	.34428	.10014	.04094
.50	.79749	.33280	.09589	.03950	.79749	.33280	.09589	.03950

Table E.20 Normal flux at $\tau_z=0$ and $\tau_z=\tau_o$ for a finite medium illuminated by a collimated flux of cosine magnitude for $\beta=0$

	$\mathcal{F}_A(0,\sigma,\tau_o)$				$\mathcal{F}_A(\tau_o,\sigma,\tau_o)$			
τ_o	σ=1.0	σ=2.0	σ=5.0	σ=10.0	σ=1.0	σ=2.0	σ=5.0	σ=10.0
.55	.78131	.32209	.09215	.03822	.78128	.32209	.09215	.03822
.60	.76572	.31208	.08882	.03706	.76568	.31208	.08882	.03706
.65	.75068	.30270	.08584	.03599	.75064	.30270	.08584	.03599
.70	.73615	.29390	.08313	.03501	.73612	.29390	.08313	.03501
.75	.72213	.28563	.08066	.03409	.72210	.28564	.08066	.03409
.80	.70858	.27785	.07839	.03322	.70855	.27785	.07839	.03322
.85	.69547	.27051	.07629	.03241	.69545	.27051	.07629	.03241
.90	.68280	.26358	.07434	.03164	.68278	.26358	.07434	.03164
.95	.67054	.25702	.07251	.03092	.67051	.25702	.07251	.03092
1.00	.65867	.25081	.07080	.03023	.65864	.25081	.07080	.03023
1.20	.61476	.22893	.06485	.02778	.61474	.22893	.06485	.02778
1.40	.57589	.21085	.05995	.02572	.57587	.21086	.05995	.02572
1.60	.54128	.19565	.05581	.02397	.54126	.19565	.05581	.02397
1.80	.51032	.18265	.05224	.02244	.51030	.18265	.05224	.02244
2.00	.48248	.17140	.04912	.02111	.48247	.17140	.04912	.02111
2.20	.45734	.16153	.04636	.01993	.45733	.16153	.04636	.01993
2.40	.43456	.15281	.04391	.01887	.43455	.15281	.04391	.01887
2.60	.41383	.14502	.04170	.01793	.41382	.14502	.04170	.01793
2.80	.39489	.13802	.03971	.01707	.39489	.13802	.03971	.01707
3.00	.37755	.13168	.03790	.01630	.37755	.13168	.03791	.01630
∞	.00000	.00000	.00000	.00000	.00000	.00000	.00000	.00000

Table E.21 Normal flux at $\tau_z=0$ and $\tau_z=\tau_o$ for a finite medium illuminated by a collimated flux of cosine magnitude for $\beta=.1$

	$\mathcal{F}_A(0,\sigma,\tau_o)$				$\mathcal{F}_A(\tau_o,\sigma,\tau_o)$			
τ_o	σ=1.0	σ=2.0	σ=5.0	σ=10.0	σ=1.0	σ=2.0	σ=5.0	σ=10.0
.00	1.00000	.50000	.20000	.10000	1.00000	.50000	.20000	.10000
.01	.99502	.49504	.19512	.09524	.99502	.49504	.19512	.09524
.02	.99009	.49019	.19047	.09092	.99009	.49019	.19047	.09092
.03	.98522	.48543	.18605	.08700	.98521	.48543	.18604	.08700
.04	.98038	.48076	.18183	.08343	.98038	.48075	.18182	.08343
.05	.97560	.47617	.17780	.08018	.97559	.47617	.17779	.08018
.06	.97085	.47168	.17396	.07722	.97084	.47167	.17395	.07721
.07	.96616	.46726	.17029	.07452	.96614	.46725	.17027	.07451
.08	.96150	.46292	.16678	.07204	.96149	.46291	.16676	.07203
.09	.95689	.45867	.16342	.06977	.95687	.45865	.16341	.06976
.10	.95232	.45449	.16022	.06769	.95229	.45446	.16019	.06768
.12	.94330	.44634	.15421	.06402	.94326	.44631	.15417	.06400
.14	.93444	.43849	.14869	.06090	.93439	.43844	.14865	.06087
.16	.92574	.43089	.14362	.05823	.92567	.43083	.14357	.05819
.18	.91719	.42356	.13895	.05593	.91710	.42348	.13888	.05588
.20	.90878	.41647	.13463	.05393	.90867	.41637	.13456	.05387
.25	.88837	.39973	.12520	.04993	.88820	.39958	.12509	.04986
.30	.86879	.38429	.11735	.04693	.86854	.38408	.11720	.04684
.35	.84999	.37002	.11074	.04457	.84966	.36974	.11055	.04446
.40	.83192	.35679	.10511	.04264	.83149	.35643	.10488	.04251
.45	.81455	.34450	.10026	.04100	.81400	.34405	.09999	.04086
.50	.79782	.33307	.09604	.03957	.79715	.33253	.09573	.03941

Table E.22 Normal flux at $\tau_z=0$ and $\tau_z=\tau_0$ for a finite medium illuminated by a collimated flux of cosine magnitude for $\beta=.1$

	$\mathcal{F}_A(0,\sigma,\tau_0)$				$\mathcal{F}_A(\tau_0,\sigma,\tau_0)$			
τ_0	σ=1.0	σ=2.0	σ=5.0	σ=10.0	σ=1.0	σ=2.0	σ=5.0	σ=10.0
.55	.78171	.32240	.09232	.03830	.78090	.32176	.09196	.03812
.60	.76619	.31244	.08901	.03715	.76523	.31170	.08861	.03695
.65	.75123	.30311	.08604	.03609	.75011	.30227	.08560	.03587
.70	.73679	.29437	.08336	.03511	.73550	.29341	.08287	.03488
.75	.72286	.28616	.08091	.03420	.72139	.28508	.08038	.03395
.80	.70940	.27843	.07866	.03335	.70744	.27724	.07809	.03308
.85	.69639	.27115	.07658	.03255	.69453	.26983	.07597	.03226
.90	.68383	.26428	.07465	.03179	.68176	.26284	.07400	.03148
.95	.67167	.25779	.07285	.03107	.66938	.25622	.07215	.03075
1.00	.65991	.25164	.07116	.03039	.65740	.24994	.07042	.03005
1.20	.61650	.23004	.06529	.02798	.61300	.22780	.06438	.02757
1.40	.57818	.21225	.06049	.02597	.57360	.20947	.05941	.02548
1.60	.54418	.19734	.05644	.02425	.53842	.19400	.05520	.02369
1.80	.51387	.18465	.05297	.02277	.50685	.18074	.05156	.02214
2.00	.48673	.17371	.04994	.02147	.47839	.16923	.04837	.02078
2.20	.46232	.16417	.04728	.02034	.45262	.15912	.04555	.01957
2.40	.44029	.15577	.04493	.01933	.42919	.15015	.04303	.01849
2.60	.42035	.14831	.04282	.01842	.40780	.14213	.04076	.01751
2.80	.40223	.14164	.04093	.01761	.38820	.13490	.03871	.01663
3.00	.38571	.13564	.03923	.01688	.37020	.12833	.03684	.01583
∞	.14811	.05306	.01553	.00670	.00000	.00000	.00000	.00000

Table E.23 Normal flux at $\tau_z=0$ and $\tau_z=\tau_o$ for a finite medium illuminated by a collimated flux of cosine magnitude for $\beta=.5$

	$\mathcal{F}_A(0,\sigma,\tau_o)$				$\mathcal{F}_A(\tau_o,\sigma,\tau_o)$			
τ_o	σ=1.0	σ=2.0	σ=5.0	σ=10.0	σ=1.0	σ=2.0	σ=5.0	σ=10.0
.00	1.00000	.50000	.20000	.10000	1.00000	.50000	.20000	.10000
.01	.99502	.49505	.19512	.09524	.99502	.49504	.19511	.09523
.02	.99011	.49020	.19048	.09093	.99008	.49018	.19046	.09091
.03	.98524	.48545	.18607	.08702	.98519	.48540	.18602	.08697
.04	.98043	.48080	.18187	.08347	.98033	.48071	.18178	.08339
.05	.97567	.47625	.17787	.08024	.97552	.47610	.17773	.08012
.06	.97096	.47178	.17405	.07730	.97074	.47156	.17385	.07713
.07	.96630	.46740	.17041	.07462	.96600	.46711	.17014	.07439
.08	.96169	.46311	.16694	.07217	.96129	.46272	.16660	.07189
.09	.95713	.45890	.16362	.06993	.95662	.45841	.16320	.06958
.10	.95262	.45477	.16046	.06788	.95199	.45417	.15994	.06746
.12	.94373	.44675	.15454	.06427	.94283	.44589	.15382	.06371
.14	.93503	.43903	.14913	.06121	.93379	.43787	.14818	.06050
.16	.92651	.43160	.14417	.05861	.92489	.43010	.14296	.05774
.18	.91816	.42444	.13962	.05637	.91611	.42256	.13814	.05534
.20	.90998	.41754	.13543	.05444	.90744	.41524	.13367	.05324
.25	.89024	.40137	.12634	.05062	.88628	.39786	.12380	.04899
.30	.87147	.38659	.11886	.04779	.86579	.38166	.11548	.04574
.35	.85361	.37306	.11265	.04561	.84593	.36652	.10837	.04314
.40	.83662	.36065	.10742	.04385	.82665	.35233	.10223	.04096
.45	.82045	.34925	.10298	.04239	.80791	.33901	.09686	.03909
.50	.80504	.33877	.09917	.04113	.78970	.32647	.09212	.03743

Table E.24 Normal flux at $\tau_z=0$ and $\tau_z=\tau_o$ for a finite medium illuminated by a collimated flux of cosine magnitude for $\beta=.5$

	$\mathcal{F}_A(0,\sigma,\tau_o)$				$\mathcal{F}_A(\tau_o,\sigma,\tau_o)$			
τ_o	σ=1.0	σ=2.0	σ=5.0	σ=10.0	σ=1.0	σ=2.0	σ=5.0	σ=10.0
.55	.79037	.32911	.09587	.04004	.77198	.31465	.08788	.03594
.60	.77639	.32020	.09298	.03906	.75472	.30347	.08406	.03457
.65	.76308	.31196	.09044	.03818	.73791	.29289	.08060	.03331
.70	.75038	.30435	.08817	.03738	.72152	.28286	.07742	.03213
.75	.73828	.29730	.08615	.03665	.70554	.27334	.07449	.03102
.80	.72674	.29076	.08432	.03597	.68994	.26428	.07177	.02997
.85	.71574	.28469	.08266	.03535	.67471	.25565	.06923	.02898
.90	.70525	.27905	.08115	.03477	.65985	.24742	.06685	.02805
.95	.69525	.27381	.07977	.03424	.64532	.23956	.06462	.02715
1.00	.68571	.26892	.07850	.03374	.63113	.23205	.06250	.02630
1.20	.65176	.25246	.07429	.03205	.57746	.20503	.05506	.02325
1.40	.62364	.23988	.07112	.03074	.52833	.18203	.04884	.02066
1.60	.60036	.23014	.06866	.02972	.48326	.16222	.04353	.01843
1.80	.58107	.22254	.06673	.02890	.44185	.14500	.03892	.01649
2.00	.56509	.21654	.06519	.02826	.40380	.12991	.03489	.01479
2.20	.55187	.21178	.06396	.02774	.36883	.11661	.03133	.01328
2.40	.54092	.20798	.06297	.02732	.33670	.10483	.02818	.01195
2.60	.53187	.20494	.06217	.02698	.30720	.09435	.02538	.01076
2.80	.52439	.20249	.06153	.02671	.28012	.08501	.02287	.00970
3.00	.51821	.20050	.06100	.02648	.25529	.07665	.02063	.00875
∞	.48933	.19184	.05869	.02550	.00000	.00000	.00000	.00000

Table E.25 Normal flux at $\tau_z=0$ and $\tau_z=\tau_o$ for a finite medium illuminated by a collimated flux of cosine magnitude for $\beta=1$

	$\mathcal{F}_A(0,\sigma,\tau_o)$				$\mathcal{F}_A(\tau_o,\sigma,\tau_o)$			
τ_o	σ=1.0	σ=2.0	σ=5.0	σ=10.0	σ=1.0	σ=2.0	σ=5.0	σ=10.0
.00	1.00000	.50000	.20000	.10000	1.00000	.50000	.20000	.10000
.01	.99503	.49506	.19513	.09524	.99501	.49503	.19511	.09522
.02	.99014	.49023	.19051	.09096	.99005	.49015	.19043	.09088
.03	.98531	.48552	.18613	.08708	.98512	.48533	.18595	.08691
.04	.98055	.48092	.18198	.08357	.98021	.48059	.18166	.08328
.05	.97586	.47643	.17804	.08039	.97532	.47591	.17755	.07996
.06	.97124	.47204	.17429	.07751	.97046	.47129	.17360	.07691
.07	.96668	.46776	.17073	.07489	.96562	.46674	.16981	.07410
.08	.96218	.46357	.16735	.07250	.96080	.46225	.16616	.07152
.09	.95775	.45948	.16413	.07033	.95600	.45781	.16266	.06913
.10	.95338	.45549	.16107	.06836	.95122	.45343	.15928	.06692
.12	.94483	.44777	.15538	.06490	.94171	.44484	.15290	.06298
.14	.93651	.44040	.15023	.06200	.93228	.43645	.14697	.05956
.16	.92844	.43337	.14555	.05956	.92292	.42826	.14144	.05659
.18	.92059	.42665	.14129	.05748	.91362	.42025	.13627	.05397
.20	.91296	.42023	.13741	.05572	.90439	.41243	.13144	.05165
.25	.89483	.40540	.12914	.05230	.88156	.39360	.12060	.04684
.30	.87798	.39217	.12253	.04986	.85909	.37575	.11126	.04305
.35	.86230	.38035	.11719	.04806	.83697	.35877	.10310	.03993
.40	.84774	.36978	.11284	.04667	.81517	.34261	.09591	.03727
.45	.83422	.36032	.10927	.04557	.79369	.32719	.08951	.03494
.50	.82166	.35186	.10632	.04466	.77253	.31249	.08377	.03286

Table E.26 Normal flux at $\tau_z=0$ and $\tau_z=\tau_0$ for a finite medium illuminated by a collimated flux of cosine magnitude for $\beta=1$

	$\mathcal{Z}_A(0,\sigma,\tau_0)$				$\mathcal{Z}_A(\tau_0,\sigma,\tau_0)$			
τ_0	σ=1.0	σ=2.0	σ=5.0	σ=10.0	σ=1.0	σ=2.0	σ=5.0	σ=10.0
.55	.81001	.34429	.10386	.04390	.75168	.29843	.07857	.03097
.60	.79920	.33751	.10180	.04326	.73116	.28501	.07385	.02924
.65	.78918	.33143	.10005	.04270	.71096	.27217	.06952	.02763
.70	.77990	.32599	.09856	.04222	.69109	.25989	.06553	.02615
.75	.77130	.32111	.09728	.04179	.67155	.24814	.06185	.02475
.80	.76334	.31673	.09618	.04142	.65235	.23690	.05844	.02345
.85	.75597	.31280	.09522	.04108	.63348	.22614	.05526	.02223
.90	.74915	.30928	.09439	.04079	.61496	.21585	.05229	.02108
.95	.74285	.30612	.09366	.04053	.59679	.20600	.04952	.01999
1.00	.73702	.30328	.09302	.04029	.57897	.19657	.04691	.01897
1.20	.71783	.29454	.09113	.03958	.51130	.16280	.03795	.01541
1.40	.70392	.28884	.08994	.03912	.44944	.13458	.03084	.01255
1.60	.69389	.28511	.08918	.03881	.39339	.11106	.02512	.01023
1.80	.68669	.28266	.08868	.03861	.34299	.09152	.02049	.00835
2.00	.68154	.28105	.08835	.03848	.29800	.07532	.01673	.00682
2.20	.67788	.27999	.08814	.03839	.25808	.06193	.01368	.00558
2.40	.67528	.27929	.08799	.03834	.22286	.05087	.01118	.00456
2.60	.67344	.27882	.08790	.03830	.19194	.04176	.00914	.00373
2.80	.67214	.27852	.08784	.03827	.16490	.03426	.00748	.00305
3.00	.67123	.27831	.08779	.03825	.14137	.02810	.00612	.00249
∞	.66910	.27791	.08771	.03822	.00000	.00000	.00000	.00000

Table E.27 Normal flux at $\tau_z=0$ and $\tau_z=\tau_o$ for a finite medium illuminated by a collimated flux of cosine magnitude for $\beta=2$

	$\mathcal{F}_A(0,\sigma,\tau_o)$				$\mathcal{F}_A(\tau_o,\sigma,\tau_o)$			
τ_o	σ=1.0	σ=2.0	σ=5.0	σ=10.0	σ=1.0	σ=2.0	σ=5.0	σ=10.0
.00	1.00000	.50000	.20000	.10000	1.00000	.50000	.20000	.10000
.01	.99505	.49508	.19515	.09526	.99499	.49501	.19509	.09520
.02	.99022	.49031	.19059	.09103	.98997	.49007	.19035	.09080
.03	.98550	.48570	.18631	.08724	.98493	.48515	.18578	.08674
.04	.98088	.48124	.18228	.08384	.97988	.48026	.18135	.08300
.05	.97637	.47693	.17849	.08079	.97481	.47540	.17707	.07953
.06	.97197	.47275	.17493	.07805	.96972	.47057	.17293	.07631
.07	.96767	.46871	.17158	.07559	.96461	.46576	.16891	.07331
.08	.96347	.46481	.16842	.07337	.95949	.46098	.16501	.07052
.09	.95937	.46103	.16546	.07138	.95435	.45622	.16123	.06792
.10	.95537	.45737	.16266	.06958	.94919	.45149	.15755	.06548
.12	.94766	.45041	.15755	.06649	.93883	.44209	.15051	.06105
.14	.94031	.44391	.15302	.06397	.92841	.43279	.14386	.05713
.16	.93331	.43783	.14900	.06191	.91793	.42358	.13755	.05363
.18	.92666	.43214	.14543	.06021	.90740	.41447	.13157	.05049
.20	.92033	.42683	.14226	.05880	.89682	.40546	.12590	.04766
.25	.90583	.41503	.13579	.05622	.87022	.38337	.11288	.04162
.30	.89308	.40509	.13094	.05456	.84348	.36194	.10136	.03671
.35	.88188	.39672	.12730	.05344	.81669	.34121	.09111	.03260
.40	.87206	.38968	.12456	.05267	.78995	.32121	.08196	.02910
.45	.86345	.38377	.12249	.05212	.76336	.30197	.07379	.02606
.50	.85593	.37881	.12091	.05172	.73699	.28352	.06647	.02340

Table E.28 Normal flux at $\tau_z=0$ and $\tau_z=\tau_o$ for a finite medium illuminated by a collimated flux of cosine magnitude for $\beta=2$

	$\mathcal{F}_A(0,\sigma,\tau_o)$				$\mathcal{F}_A(\tau_o,\sigma,\tau_o)$			
τ_o	σ=1.0	σ=2.0	σ=5.0	σ=10.0	σ=1.0	σ=2.0	σ=5.0	σ=10.0
.55	.84935	.37465	.11970	.05142	.71092	.26587	.05990	.02105
.60	.84361	.37116	.11878	.05119	.68523	.24903	.05400	.01896
.65	.83861	.36824	.11807	.05101	.65996	.23300	.04870	.01709
.70	.83425	.36580	.11752	.05087	.63517	.21777	.04394	.01541
.75	.83045	.36376	.11710	.05077	.61091	.20333	.03965	.01391
.80	.82715	.36206	.11677	.05068	.58720	.18967	.03578	.01256
.85	.82428	.36063	.11651	.05061	.56407	.17677	.03230	.01135
.90	.82179	.35944	.11631	.05056	.54156	.16461	.02917	.01025
.95	.81962	.35845	.11615	.05051	.51967	.15316	.02634	.00926
1.00	.81774	.35762	.11602	.05048	.49843	.14241	.02379	.00837
1.20	.81242	.35549	.11573	.05039	.41996	.10568	.01585	.00559
1.40	.80943	.35446	.11561	.05035	.35181	.07769	.01058	.00373
1.60	.80776	.35397	.11556	.05034	.29338	.05666	.00707	.00250
1.80	.80682	.35374	.11554	.05033	.24378	.04105	.00472	.00167
2.00	.80631	.35363	.11553	.05033	.20199	.02957	.00316	.00112
2.20	.80602	.35357	.11553	.05032	.11698	.02119	.00211	.00074
2.40	.80586	.35355	.11553	.05032	.13779	.01513	.00141	.00050
2.60	.80577	.35354	.11553	.05032	.11353	.01076	.00094	.00033
2.80	.80573	.35353	.11553	.05032	.09343	.00762	.00063	.00022
3.00	.80570	.35353	.11553	.05032	.07682	.00538	.00042	.00015
∞	.80567	.35353	.11552	.05032	.00000	.00000	.00000	.00000

Table E.29 Normal flux at $\tau_z=0$ and $\tau_z=\tau_o$ for a finite medium illuminated by a collimated flux of cosine magnitude for $\beta=5$

	$\mathcal{F}_A(0,\sigma,\tau_o)$				$\mathcal{F}_A(\tau_o,\sigma,\tau_o)$			
τ_o	σ=1.0	σ=2.0	σ=5.0	σ=10.0	σ=1.0	σ=2.0	σ=5.0	σ=10.0
.00	1.00000	.50000	.20000	.10000	1.00000	.50000	.20000	.10000
.01	.99512	.49515	.19522	.09533	.99492	.49494	.19502	.09514
.02	.99050	.49059	.19086	.09128	.98969	.48979	.19008	.09054
.03	.98611	.48631	.18688	.08776	.98431	.48453	.18518	.08618
.04	.98196	.48230	.18326	.08471	.97879	.47919	.18033	.08205
.05	.97802	.47853	.17966	.08205	.97314	.47377	.17553	.07811
.06	.97430	.47500	.17695	.07975	.96736	.46827	.17078	.07438
.07	.97077	.47169	.17421	.07774	.96147	.46270	.16608	.07082
.08	.96743	.46858	.17171	.07600	.95546	.45707	.16145	.06743
.09	.96428	.46568	.16944	.07448	.94936	.45140	.15687	.06421
.10	.96130	.46296	.16737	.07317	.94315	.44568	.15237	.06113
.12	.95581	.45802	.16377	.07102	.93049	.43414	.14358	.05542
.14	.95092	.45370	.16079	.06940	.91753	.42250	.13509	.05023
.16	.94655	.44992	.15832	.06817	.90433	.41083	.12692	.04552
.18	.94266	.44661	.15628	.06724	.89094	.39916	.11909	.04124
.20	.93919	.44372	.15459	.06653	.87739	.38754	.11160	.03736
.25	.93209	.43798	.15154	.06542	.84310	.35888	.09441	.02916
.30	.92679	.43390	.14965	.06485	.80863	.33116	.07936	.02273
.35	.92284	.43100	.14847	.06456	.77438	.30465	.06635	.01772
.40	.91991	.42894	.14775	.06441	.74066	.27956	.05520	.01380
.45	.91772	.42749	.14730	.06433	.70770	.25600	.04574	.01074
.50	.91610	.42645	.14702	.06429	.67564	.23401	.03776	.00836
∞	.91145	.42397	.14658	.06424	.00000	.00000	.00000	.00000

Table E.30 Normal flux at $\tau_z=0$ and $\tau_z=\tau_o$ for a finite medium illuminated by a collimated flux of cosine magnitude for $\beta\equiv 10$

	$\mathcal{Z}_A(0,\sigma,\tau_o)$				$\mathcal{Z}_A(\tau_o,\sigma,\tau_o)$			
τ_o	σ=1.0	σ=2.0	σ=5.0	σ=10.0	σ=1.0	σ=2.0	σ=5.0	σ=10.0
.00	1.00000	.50000	.20000	.10000	1.00000	.50000	.20000	.10000
.01	.99526	.49528	.19535	.09546	.99478	.49481	.19488	.09501
.02	.99098	.49107	.19132	.09172	.98920	.48930	.18960	.09008
.03	.98713	.48731	.18783	.08863	.98328	.48352	.18420	.08525
.04	.98367	.48396	.18481	.08608	.97706	.47749	.17870	.08053
.05	.98055	.48098	.18220	.08399	.97058	.47125	.17315	.07595
.06	.97775	.47833	.17994	.08226	.96386	.46484	.16758	.07151
.07	.97523	.47597	.17799	.08084	.95694	.45829	.16201	.06723
.08	.97297	.47387	.17630	.07967	.94983	.45162	.15646	.06312
.09	.97094	.47200	.17485	.07870	.94257	.44485	.15097	.05918
.10	.96912	.47034	.17359	.07791	.93518	.43801	.14554	.05542
.12	.96602	.46756	.17157	.07672	.92007	.42420	.13493	.04844
.14	.96353	.46536	.17007	.07592	.90465	.41033	.12475	.04217
.16	.96152	.46363	.16895	.07537	.88902	.39651	.11506	.03658
.18	.95991	.46226	.16812	.07501	.87330	.38281	.10590	.03163
.20	.95862	.46119	.16750	.07476	.85754	.36932	.09728	.02727
.25	.95639	.45939	.16656	.07444	.81841	.33678	.07815	.01862
.30	.95510	.45841	.16612	.07431	.78013	.30632	.06231	.01256
.35	.95436	.45787	.16591	.07427	.74307	.27813	.04941	.00838
.40	.95393	.45757	.16581	.07425	.70743	.25224	.03901	.00554
.45	.95368	.45741	.16576	.07425	.67329	.22859	.03070	.00364
.50	.95354	.45732	.16574	.07424	.64068	.20705	.02411	.00238
∞	.95317	.45705	.16559	.07424	.00000	.00000	.00000	.00000

Table E.31 Normal flux at $\tau_z=0$ and $\tau_z=\tau_o$ for a finite medium illuminated by a collimated flux of cosine magnitude for $\beta=40$

	$\mathcal{F}_A(0,\sigma,\tau_o)$				$\mathcal{F}_A(\tau_o,\sigma,\tau_o)$			
τ_o	σ=1.0	σ=2.0	σ=5.0	σ=10.0	σ=1.0	σ=2.0	σ=5.0	σ=10.0
.000	1.00000	.50000	.20000	.10000	1.00000	.50000	.20000	.10000
.005	.99822	.49822	.19823	.09825	.99679	.49680	.19682	.09686
.010	.99677	.49678	.19682	.09690	.99327	.49331	.19340	.09356
.015	.99558	.49561	.19570	.09584	.98951	.48959	.18981	.09016
.020	.99462	.49467	.19480	.09501	.98556	.48569	.18609	.08672
.025	.99383	.49390	.19408	.09437	.98144	.48166	.18229	.08327
.030	.99319	.49328	.19351	.09387	.97720	.47752	.17843	.07985
.035	.99267	.49277	.19305	.09348	.97286	.47330	.17456	.07648
.040	.99225	.49236	.19269	.09318	.96845	.46903	.17068	.07317
.045	.99191	.49203	.19239	.09294	.96398	.46472	.16682	.06996
.050	.99162	.49176	.19216	.09276	.95946	.46039	.16299	.06683
.055	.99140	.49155	.19198	.09262	.95492	.45605	.15921	.06380
.060	.99121	.49137	.19183	.09250	.95035	.45171	.15547	.06088
.065	.99106	.49123	.19171	.09242	.94578	.44737	.15179	.05807
.070	.99093	.49111	.19161	.09235	.94119	.44305	.14817	.05537
.075	.99083	.49102	.19154	.09230	.93660	.43875	.14462	.05277
.080	.99075	.49094	.19148	.09226	.93202	.43447	.14114	.05028
.085	.99068	.49088	.19143	.09222	.92744	.43022	.13773	.04790
.090	.99063	.49083	.19139	.09220	.92288	.42600	.13438	.04562
.095	.99059	.49079	.19136	.09218	.91832	.42181	.13111	.04345
.100	.99055	.49076	.19134	.09216	.91378	.41765	.12791	.04136
∞	.98774	.48803	.18883	.08992	.00000	.00000	.00000	.00000

Table E.32 Normal flux at $\tau_z=0$ and $\tau_z=\tau_0$ for a finite medium illuminated by a collimated flux of cosine magnitude for $\beta=100$

	$\mathcal{F}_A(0,\sigma,\tau_0)$				$\mathcal{F}_A(\tau_0,\sigma,\tau_0)$			
τ_0	σ=1.0	σ=2.0	σ=5.0	σ=10.0	σ=1.0	σ=2.0	σ=5.0	σ=10.0
.000	1.00000	.50000	.20000	.10000	1.00000	.50000	.20000	.10000
.001	.99981	.49981	.19981	.09981	.99918	.49918	.19919	.09919
.002	.99964	.49964	.19964	.09964	.99835	.49836	.19836	.09837
.003	.99949	.49949	.19949	.09949	.99751	.49751	.19752	.09754
.004	.99935	.49935	.19935	.09936	.99665	.49966	.19668	.09671
.005	.99922	.49922	.19923	.09924	.99578	.49579	.19582	.09587
.006	.99911	.49911	.19912	.09913	.99490	.49491	.19496	.09503
.007	.99901	.49901	.19902	.09903	.99401	.49403	.19409	.09419
.008	.99892	.49892	.19893	.09895	.99310	.49313	.19321	.09334
.009	.99883	.49884	.19885	.09887	.99220	.49223	.19233	.09250
.010	.99876	.49876	.19878	.09880	.99128	.49132	.19145	.09165
.012	.99863	.49864	.19866	.09869	.98493	.48949	.18967	.08996
.014	.99853	.49853	.19856	.09859	.98756	.48764	.18789	.08829
.016	.99844	.49845	.19848	.09852	.98567	.48578	.18611	.08663
.018	.99837	.49838	.19841	.09846	.98377	.48391	.18433	.08498
.020	.99831	.49832	.19836	.09841	.98187	.48204	.18255	.08335
.022	.99827	.49828	.19832	.09837	.97995	.48016	.18078	.08175
.024	.99823	.49824	.19828	.09834	.97803	.47828	.17902	.08017
.026	.99820	.49821	.19825	.09832	.97611	.47641	.17727	.07861
.028	.99817	.49819	.19823	.09830	.97419	.47453	.17553	.07708
.030	.99815	.49817	.19821	.09828	.97226	.47266	.17381	.07558
∞	.99504	.49509	.19523	.09815	.00000	.00000	.00000	.00000

Table E.33 Normal flux at $\tau_z=0$ and $\tau_z=\tau_o$ for a diffuse wall radiating in a cosine fashion into a finite medium

	$\mathcal{F}_c(0,\tau_o)$				$\mathcal{F}_c(\tau_o,\tau_o)$			
τ_o	β=0	β=.10	β=.50	β=1.0	β=0	β=.10	β=.50	β=1.0
.00	1.00000	1.00000	1.00000	1.00000	1.00000	1.00000	1.00000	1.00000
.01	.99025	.99025	.99026	.99029	.99029	.99028	.99023	.99007
.02	.98093	.98094	.98097	.98107	.98097	.98096	.98078	.98026
.03	.97195	.97196	.97203	.97224	.97196	.97195	.97160	.97058
.04	.96325	.96326	.96339	.96374	.96325	.96322	.96266	.96101
.05	.95481	.95482	.95502	.95555	.95478	.95475	.95394	.95157
.06	.94659	.94660	.94689	.94764	.94656	.94651	.94543	.94224
.07	.93858	.93860	.93898	.93999	.93855	.93849	.93710	.93302
.08	.93078	.93080	.93129	.93259	.93075	.93067	.92894	.92390
.09	.92315	.92318	.92380	.92542	.92313	.92304	.92095	.91489
.10	.91570	.91574	.91649	.91848	.91569	.91558	.91311	.90598
.12	.90130	.90134	.90241	.90520	.90129	.90115	.89787	.88845
.14	.88749	.88755	.88898	.89267	.88750	.88732	.88315	.87129
.16	.87423	.87431	.87614	.88084	.87424	.87403	.86892	.85450
.18	.86147	.86157	.86385	.86965	.86148	.86123	.85514	.83807
.20	.84917	.84929	.85206	.85905	.84919	.84889	.84177	.82197
.25	.82024	.82042	.82456	.83484	.82025	.81986	.81002	.78316
.30	.79357	.79383	.79954	.81352	.79358	.79309	.78037	.74628
.35	.76886	.76920	.77666	.79466	.76886	.76828	.75256	.71119
.40	.74585	.74627	.75566	.77792	.74584	.74518	.72637	.67779
.45	.72434	.72486	.73630	.76303	.72433	.72359	.70164	.64599
.50	.70416	.70479	.71842	.74975	.70416	.70333	.67821	.61569

Table E.34 Normal flux at $\tau_z=0$ and $\tau_z=\tau_o$ for a diffuse wall radiating in a cosine fashion into a finite medium

	$\mathcal{Z}_c(0,\tau_o)$				$\mathcal{Z}_c(\tau_o,\tau_o)$			
τ_o	β=0	β=.10	β=.50	β=1.0	β=0	β=.10	β=.50	β=1.0
.55	.68519	.68593	.70185	.73788	.68519	.68427	.65597	.58681
.60	.66730	.66815	.68647	.72726	.66730	.66628	.63482	.55929
.65	.65039	.65136	.67217	.71775	.65039	.64927	.61466	.53305
.70	.63437	.63547	.65884	.70923	.63437	.63314	.59542	.50802
.75	.61918	.62040	.64641	.70157	.61918	.61781	.57702	.48416
.80	.60474	.60609	.63479	.69469	.60474	.60320	.55941	.46141
.85	.59099	.59248	.62392	.68851	.59099	.58927	.54254	.43970
.90	.57788	.57952	.61374	.68294	.57788	.57595	.52635	.41900
.95	.56536	.56715	.60419	.67794	.56536	.56319	.51081	.39926
1.00	.55340	.55533	.59523	.67343	.55340	.55095	.49586	.38044
1.20	.51037	.51292	.56447	.65942	.51037	.50645	.44144	.31345
1.40	.47370	.47691	.54027	.65014	.47370	.46779	.39430	.25807
1.60	.44204	.44594	.52107	.64398	.44204	.43390	.35310	.21233
1.80	.41441	.41901	.50573	.63987	.41441	.40437	.31684	.17458
2.00	.39006	.39539	.49343	.63713	.39006	.37932	.28475	.14345
2.20	.36843	.37451	.48351	.63530	.36843	.35928	.25623	.11782
2.40	.34909	.35592	.47550	.63407	.34909	.34505	.23079	.09673
2.60	.33169	.33928	.46900	.63325	.33169	.33766	.20804	.07938
2.80	.31595	.32431	.46373	.63270	.31595	--	.18764	.06512
3.00	.30164	.31078	.45945	.63234	.30164	--	.16932	.05341
∞	.00000	.12207	.44041	.63159	.00000	.00000	.00000	.00000

Table E.35 Normal flux at $\tau_z=0$ and $\tau_z=\tau_o$ for a diffuse wall radiating in a cosine fashion into a finite medium

	$\mathcal{F}_c(0,\tau_o)$			$\mathcal{F}_c(\tau_o,\tau_o)$		
τ_o	β=2.0	β=5.0	β=10.0	β=2.0	β=5.0	β=10.0
.00	1.00000	1.00000	1.00000	1.00000	1.00000	1.00000
.01	.99036	.99061	.99078	.98950	.98613	.97642
.02	.98133	.98225	.98356	.97839	.96781	.93913
.03	.97280	.97477	.97768	.96691	.94679	.89514
.04	.96472	.96805	.97290	.95517	.92395	.84776
.05	.95704	.96202	.96900	.94322	.89988	.79898
.06	.94974	.95658	.96581	.93113	.87498	.75008
.07	.94279	.95169	.96321	.91893	.84956	.70195
.08	.93617	.94728	.96109	.90666	.82386	.65516
.09	.92986	.94331	.95935	.89435	.79807	.61010
.10	.92383	.93972	.95793	.88202	.77234	.56704
.12	.91259	.93357	.95582	.85738	.72154	.48743
.14	.90233	.92856	.95441	.83285	.67217	.41676
.16	.89295	.92447	.95347	.80854	.62469	.35480
.18	.88436	.92113	.95284	.78452	.57939	.30099
.20	.87649	.91841	.95242	.76086	.53643	.25459
.25	.85956	.91360	.95188	.70348	.43970	.16580
.30	.84588	.91069	.95168	.64899	.35786	.10677
.35	.83480	.90893	.95160	.59763	.28967	.06820
.40	.82581	.90787	.95158	.54949	.23346	.04328
.45	.81851	.90723	.95157	.50455	.18749	.02733
.50	.81256	.90684	.95156	.46276	.15014	.01719
∞	.78623	.90625	.95161	.00000	.00000	.00000